



**UNIVERSITA' DEGLI STUDI DI PADOVA**

Sede Amministrativa: Università degli Studi di Padova

Dipartimento di Scienze Chimiche

DOTTORATO DI RICERCA IN SCIENZE MOLECOLARI INDIRIZZO CHIMICO  
CICLO XX

**FUNCTION-STRUCTURE RELATIONSHIP OF  
PTH(1-11) ANALOGUES**

**Coordinatore** : Ch.mo Prof. Maurizio CASARIN

**Supervisore** : Ch.mo Prof. Evaristo PEGGION

**Dottorando** : Andrea CAPORALE

DATA CONSEGNA TESI  
31 gennaio 2008



Con infinito affetto e assenza incolmabile  
a Maria Magno  
e  
a Enrico Ficini

.....che ti sia sempre concesso quotidianamente  
di fare qualcosa che ti piaccia.....





# Abstract

Parathyroid hormone (PTH) is an 84 amino acid peptide hormone produced in the parathyroid glands. It acts primarily on bone and kidney to maintain extracellular calcium levels within normal limits. It has been shown that the 1-34 N-terminal fragment of PTH is sufficient to bind and activate the PTH type I receptor (PTH1R). The study of reduced-size PTH agonist and antagonist analogues has been the subject of extensive research for the development of bone anabolic drugs. Recent investigations focusing on the interaction of N-terminal fragments of PTH with PTH1R showed that some modifications can increase signalling potency in peptides as short as 11 amino acid residues (e.g.  $S^3 \rightarrow A^3$ ,  $N^{10} \rightarrow Q^{10}$ ,  $L^{11} \rightarrow R^{11}$ ).

This work of PhD thesis represents our effort to investigate the role of side chains and structural characteristics of N-terminal domain of PTH(1-11). We applied the hierarchical approach and some peptidomimetics concepts to synthesize specific libraries of peptide to obtain information about hormone/receptor interaction.

With these information, we have been able to project a first example of peptidomimetic of PTH. The strategical role of  $Val^2$  in the interaction with the PTH1R receptor was demonstrated and confirmed. We have observed that guanidine group in C-terminus has a specific role in the binding to the receptor for the shortest PTH(1-11) fragment. We have shown that substitutions with  $\alpha MeNle$  at positions 8 can increase helix stability which can be also stabilized and promoted through a bridge between 6 and 10 positions. We synthesized a group of active analogues which are characterized by a stable  $\alpha$ -helix in all peptide sequences and have the correct orientation of essential residues 2, 5, 8 and 11.

# Riassunto

L'ormone paratiroideo (PTH) è un ormone peptidico di 84 residui ammino acidici. Esso è prodotto dalle ghiandole paratiroidee ed agisce principalmente sulle ossa e sui reni per mantenere nella normalità i livelli di calcio extracellulare. Si è dimostrato come i primi 34 residui del PTH siano sufficienti a legarsi al recettore PTH di tipo I (PTH1R) ed ad attivarlo. Gli analoghi agonisti ed antagonisti di frammenti di PTH di piccole dimensioni sono stati oggetto di intensi studi per lo sviluppo di possibili farmaci con effetto anabolico sull'osso. Recenti lavori finalizzati allo studio della interazione tra i frammenti N-terminali del PTH con il recettore PTH1R hanno mostrato che certe modifiche possono aumentare l'attività in peptidi brevi con solo 11 residui (ad esempio,  $S^3 \rightarrow A^3$ ,  $N^{10} \rightarrow Q^{10}$ ,  $L^{11} \rightarrow R^{11}$ ).

Questo lavoro di dottorato rappresenta il nostro sforzo di comprendere il ruolo delle catene laterali e le caratteristiche strutturali del dominio N-terminale del PTH(1-11). Abbiamo applicato l'approccio gerarchico e alcuni concetti della peptidomimetica per sintetizzare serie di peptidi specifici per provare ad ottenere delle informazioni sulla interazione tra ormone e recettore.

Con queste informazioni, abbiamo potuto progettare un primo esempio di peptidomimetico del PTH. Il ruolo strategico della Val<sup>2</sup> nella interazione con il recettore PTH1R è stato dimostrato e confermato. Abbiamo osservato che il gruppo guanidinio in posizione C-terminale svolge uno specifico ruolo nel *binding* al recettore per i frammenti più corti del PTH(1-11). Abbiamo anche mostrato che la sostituzione della  $\alpha$ MeNle in posizione 8 può aumentare la stabilità dell'elica che può essere ulteriormente stabilizzata attraverso un ponte tra le posizioni 6 e 10. Abbiamo sintetizzato un gruppo di analoghi attivi che sono caratterizzati da una  $\alpha$ -elica stabile lungo tutto il peptide e che hanno una corretta orientazione dei residui essenziali 2, 5, 8 e 11.

# Index

ABSTRACT/RIASSUNTO.....	5
INDEX.....	7
INTRODUCTION: 1- Biological State of Art.....	9
2- Peptidomimetic: a way to produce peptide drugs.....	25
DISCUSSION and CONCLUSION.....	37
METHODS.....	87
EXPERIMENTAL PART.....	109
APPENDIX A.....	163
APPENDIX B.....	175
APPENDIX C.....	205



# 1 – INTRODUCTION

## Biological State of Art

### 1 – INTRODUCTION

Biological State of Art .....	9
1.1. Parathyroid hormone.....	10
1.2. Parathyroid hormone-related protein .....	11
1.3. Structure-Activity Relations in PTH and PTHrP .....	12
1.4. Receptor for PTH and PTHrP .....	13
1.4.1. PTH1R Signaling and Ligand Interactions .....	14
1.4.2.1 <i>Chimeras Analysis</i> .....	16
1.4.2.2 <i>Photoaffinity Cross-Linking</i> .....	16
1.5. The two-site model of PTH–PTHrP interaction.....	18
1.5.1. Ligands determinants of receptor signalling .....	19
1.6. PTH-based pharmaceutical agents .....	20
REFERENCES .....	22

## 1.1. Parathyroid hormone

In mammals, parathyroid hormone (PTH) is the most important regulator of calcium ion homeostasis<sup>1; 2</sup>. The peptide hormone is synthesized as a precursor protein containing a pre-sequence of 25 amino acids and a pro-sequence of 6 amino acids, which are both cleaved during the synthesis and secretion process to yield the mature form of 84 amino acids.

Parathyroid hormone (PTH) is almost exclusively produced in the parathyroid glands and acts primarily on bone and kidney to maintain extra-cellular calcium levels within normal limits. PTH is a true hormone in that it is produced by a gland and then travels through the bloodstream to act at its target tissues. PTH synthesis and secretion are largely regulated by the extra-cellular concentration of calcium, which is monitored by the calcium-sensing receptor of the parathyroid glands<sup>3</sup>. PTH is secreted from the chief cells of the parathyroid glands primarily in response to low extra-cellular calcium, but also in response to elevated extra-cellular phosphate. In response to high extra-cellular calcium, the release of PTH from parathyroid gland is inhibited, which is an unusual property for an endocrine tissue. It acts primarily on kidney and bone, where it binds to cells expressing the type 1 PTH/PTHrP receptor (PTH1R). The ensuing direct and indirect responses of these target cells help to maintain blood calcium concentrations to within narrow limits. In the kidney, PTH reduces calcium excretion by increasing calcium re-absorption in the distal convoluted tubule and it stimulates the activity of  $1\alpha$ -hydroxylase and thereby increases the 1, 25-dihydroxyvitamin D<sub>3</sub> [1,25(OH)<sub>2</sub>D<sub>3</sub>]-dependent absorption of calcium from the intestine. It furthermore prevents phosphate re-absorption primarily by affecting the expression levels of two different sodium-phosphate co-transporters, NPT-2a and NPT-2c, both of which are localized in the brush border membrane of the proximal tubules<sup>4; 5; 6</sup>. In bone, PTH can induce a rapid release of calcium from the matrix, but it also mediates longer-term changes in calcium metabolism by acting directly on osteoblasts and indirectly on osteoclasts, the bone-resorbing cells. PTH action on osteoblasts leads to changes in the synthesis and/or

activity of several proteins, including osteoclast differentiating factor, also known as TRANCE, RANKL, or osteoprotegerin ligand<sup>7; 8</sup>.

## 1.2. Parathyroid hormone-related protein

PTH-related protein (PTHrP) was first discovered in patients with various tumors who had increased levels of serum calcium and elevated urinary cAMP excretion, despite of low levels of PTH<sup>9</sup>. It was established that this condition, named the humoral hypercalcemia of malignancy syndrome, was the result of increased PTHrP secretion by the tumors<sup>10, 11, 12, 13</sup>. In humans, the PTHrP sequence is either 141 amino acids, or due to alternative mRNA splicing, 139 or 173 amino acids<sup>14</sup>. PTHrP shares significant N-terminal amino acid sequence homology with PTH, particularly within the first 13 residues (Fig. 1).

	1	10	20	30																																			
PTH	S	V	E	I	Q	L	M	H	N	L	G	K	H	L	N	S	M	E	R	V	E	W	L	R	K	K	L	Q	D	V	H	N	F	V	A	L			
PTHrP	A	V	E	I	Q	L	L	H	D	K	G	K	S	I	Q	D	L	R	R	R	F	F	L	H	H	L	I	A	E	I	H	T	A	E	I	R			
TIP	S	L	A	L	A	D	D	R	R	F	R	E	R	A	R	L	L	A	A	L	E	R	R	H	W	L	N	S	Y	M	H	K	L	L	V	L	D	A	F

Fig. 1. Sequence alignment of the amino-terminal portions of human parathyroid hormone (PTH) and parathyroid-related protein (PTHrP) and the entire sequence of human TIP39, a hypothalamic peptide that selectively activates the type 2 PTH receptor. Homologous residues are in blue<sup>15</sup>.

PTHrP acts as a paracrine or autocrine factor, and has several important physiological roles, including the regulation of chondrocyte growth and differentiation in the growth plates of developing long bones<sup>16</sup>. In this tissue, PTHrP slows chondrocyte differentiation and maintains the columnar organization of the proliferating chondrocytes<sup>16</sup>. PTHrP also plays important roles in other tissues. For example, PTHrP has a critical role in branching morphogenesis of the mammary gland; it is also produced by the lactating breast and is abundant in breast milk<sup>17, 18</sup>. Plasma PTHrP levels are elevated during lactation when the peptide serves to promote calcium mobilization from bone<sup>17</sup> and to regulate calcium transport from blood into the breast milk<sup>18</sup>.

**TABLE 1. SITES AND PROPOSED ACTIONS OF PARATHYROID HORMONE-RELATED PROTEIN.**

SITE	PROPOSED ACTIONS
Mesenchymal tissues	
Cartilage	Promotes proliferation of chondrocytes; inhibits terminal differentiation and apoptosis of chondrocytes
Bone	Stimulates or inhibits bone resorption
Smooth muscle	Released in response to stretching; relaxes smooth muscle
Vascular system	
Myometrium	
Urinary bladder	
Cardiac muscle	Positive chronotropic stimulus; indirect positive inotropic stimulus
Skeletal muscle	Unknown
Epithelial tissues	
Mammary	Induces branching morphogenesis; secreted in milk; possible roles in lactation
Epidermis	Unknown
Hair follicle	Inhibits anagen
Intestine	Unknown
Tooth enamel	Induces osteoclastic resorption of overlying bone
Endocrine tissues	
Parathyroid glands	Stimulates placental transport of calcium?
Pancreatic islets	Stimulates insulin secretion and somatic growth
Pituitary	Unknown
Placenta	Calcium transport?
Central nervous system	Released from cerebellar granular neurons in response to activation of L-type calcium channels; receptors in cerebellum, hippocampus, hypothalamus

PTHrP is also produced by the placenta, where it regulates the fetus-directed transport of maternal calcium across the placental membrane<sup>19, 20</sup>.

The size of the biologic actions of parathyroid hormone-related protein is impressive (Table 1), but several principles are evident. Parathyroid hormone-related protein has evolved to regulate local tissue functions, in contrast to the systemic hormonal function of parathyroid hormone. These local functions fall into several classes: in mesenchymal tissues

such as cartilage, the protein functions in

local feedback loops to control rates of proliferation and differentiation, thus allowing local tissue organization. It is expressed by several epithelia and participates in epithelial-mesenchymal interactions by activating the receptor for parathyroid hormone and parathyroid hormone-related protein in the underlying mesenchyme. To carry out its diverse biologic roles, parathyroid hormone-related protein functions as a polyhormone. It gives rise to several biologically active peptides, each of which presumably has its own receptor. To broaden its repertoire even further, it appears to have intracrine effects in the nucleus of cells that produce it in addition to having juxtacrine, paracrine, and possibly, endocrine effects after secretion<sup>21</sup>.

### 1.3. Structure-Activity Relations in PTH and PTHrP

PTH and PTHrP show significant sequence homology within the first 13 amino acid residues (Fig. 1), and this sequence conservation reflects the functional importance of the amino-terminal residues in receptor signalling<sup>22, 23, 24, 25, 26</sup>. The sequence homology of PTH and PTHrP decreases markedly in the 14-34 region, where only three amino acids are identical, and beyond residue 34 there is no recognizable similarity. For both PTH and PTHrP, the 15-34 region functions as the principal PTH1R binding domain,

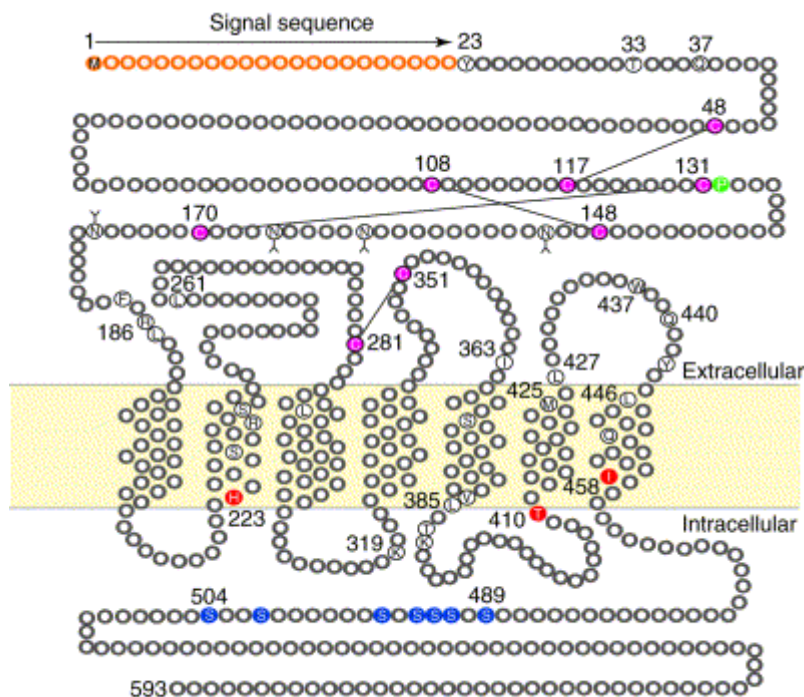


and these portions of the two peptides probably interact with overlapping regions of the receptor, as the two fragments compete equally for binding with radiolabeled PTH-(1–34) or PTHrP-(1–36) to the PTH1R<sup>27, 28</sup>. These data also suggest that the two divergent receptor binding domains of PTH and PTHrP adopt similar conformations. The three-dimensional crystal structures of PTH or PTHrP are not known, but the peptides have been analyzed extensively by nuclear magnetic resonance (NMR) methods. In general, these studies indicate that, under proper solvent conditions, PTH-(1–34) and PTHrP-(1–36) analogs contain defined segments of secondary structure, including a relatively stable  $\alpha$ -helix in the carboxy-terminal receptor-binding domain, a shorter less stable helix near the amino-terminal activation domain, and a flexible hinge or bend region connecting the two domains<sup>29, 30, 31</sup>.

Although most NMR solution studies gave evidence for peptide flexibility, the question of whether the conformations of PTH and PTHrP recognized by the receptor are folded with tertiary interactions, as suggested by some studies<sup>32, 33, 34</sup>, or extended, as suggested by other analyses<sup>31</sup>, remains unanswered.

#### **1.4. Receptor for PTH and PTHrP**

The PTH1R is part of a distinct family of GPCRs that exhibit none of the amino acid sequence motifs found in the other subgroups of the superfamily of heptahelical receptors<sup>35, 36, 37</sup>. These peptide hormone receptors, called class II or family B receptors, can be distinguished from other GPCRs by their large (150 amino acid) amino-terminal extracellular domain containing six conserved cysteine residues, as well as by several other conserved amino acids that are dispersed throughout the NH<sub>2</sub>-terminal domain, the membrane-embedded helices, and the connecting loops (Fig. 2).



TRENDS in Endocrinology & Metabolism

Fig. 2. The human parathyroid hormone type 1 (PTH-1) receptor (593 amino acids), showing its predicted domain organization (the locations of the seven transmembrane  $\alpha$ -helical domains in the sequence were predicted by the Protein-Predict computer program<sup>38</sup>). The Cys disulfide linkages (indicated by connecting lines) were determined from studies on the N-terminal PTH-1 receptor fragment produced in *Escherichia coli*<sup>39</sup>. N-Linked glycosyl groups are indicated by the forked symbols. Other key residues referred to in the text are indicated by single amino acid code within the open circles, some of which are labeled with sequence position number for reference. The human skeletal diseases of Blomstrand's chondrodysplasia (receptor inactivity) and Jansen's chondrodysplasia (receptor constitutive activity) result from mutations in green and red residues, respectively. Abbreviations: C, Cys; F, Phe; H, His; I, Ile; K, Lys; L, Leu; M, Met; N, Asn; P, Pro; Q, Gln; R, Arg; S, Ser; T, Thr; V, Val; W, Trp; Y, Tyr.<sup>12</sup>

#### 1.4.1. PTH1R Signaling and Ligand Interactions

The PTH1R is considered to be a potentially important target for pharmacological drugs aimed to treat disorders of mineral ion homeostasis in the skeleton, such as hyperparathyroidism, humoral hypercalcemia of malignancy, and osteoporosis. Studies on ligand interactions with the PTH1R have been largely focused on amino-terminal peptide hormone analogs, such as PTH-(1–34) and PTHrP-(1–34), as there is no evidence to suggest that midregional or carboxyterminal portions of the intact ligands interact with this receptor<sup>40, 41, 42</sup>. Stimulation of cells expressing the PTH1R by PTH-(1–34) or PTHrP-(1–34) agonist ligands can activate at least two second messenger signaling systems: the adenylyl cyclase/protein kinase A (AC/PKA) pathway (Fig. 3)

and the phospholipase C/protein kinase C (PLC/PKC) pathway<sup>43, 44</sup>. The classic PTH1R-mediated cAMP/PKA pathway has been widely studied in a variety of cellular settings and typically elicits a strong and sensitive response to agonist ligands. In comparison, agonist efficacy and potency profiles observed in assays of the PLC/PKC pathway are generally lower than those of the AC/PKA pathway<sup>45, 46</sup>. The roles of these two signaling pathways in mediating the downstream physiological effects of PTH and PTHrP are still poorly understood, but some progress has been made to establish the mechanisms by which the two signals are transduced at the membrane level. It has been well established that the determinants of cAMP/PKA signaling in the ligands PTH and PTHrP are located within the amino-terminal residues<sup>22, 23, 25, 26</sup>; however, the ligand determinants of PLC/PKC activation have been more difficult to define.

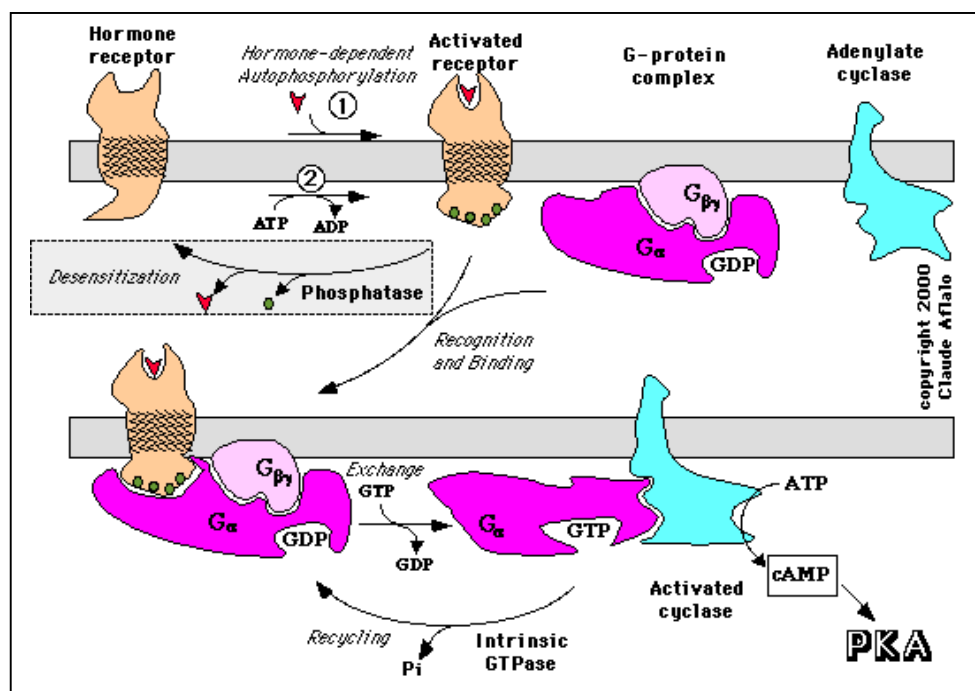


Figure 3: Binding of a ligand (or agonist) to a G protein-coupled receptor (GPCR) leads to activation of heterotrimeric G proteins ( $G_{\alpha}$ ,  $G_{\beta\gamma}$ ) and the stimulation of adenylyl cyclase (AC), which increases production of the second messenger molecule cAMP. An increase in cAMP promotes activation of the cAMP-dependent protein kinase (PKA), which activates various downstream effector molecules (active effectors).

#### ***1.4.2.1 Chimeras Analysis***

The mechanisms by which PTH and PTHrP bind to the PTH1R and then induce the conformational changes that lead to G protein coupling have been explored through the use of receptor mutants and receptor chimeras. Structurally altered PTH or PTHrP analogues have been proven to be useful in these studies by serving as functional probes of ligand interaction sites in the receptor. For example, the antagonist PTH-(7–34) bound to the human PTH1R with, 30-fold higher affinity than that for the rat PTH1R. Reciprocal pairs of rat/human and human/rat receptor chimeras were used to identify receptor regions involved in this binding selectivity, and the results identified the amino-terminal extracellular domain as the major determinant<sup>47</sup>. Similarly, studies on the analogue [Arg2 ]PTH-(1–34), which is an agonist with the opossum PTH1R and an antagonist with the rat PTH1R, revealed clues as to receptor residues involved in recognizing the side chain of position 2 in the ligand. Thus rat/opossum PTH1R chimeras and subsequent point mutational analysis identified three divergent residues near the extracellular ends of transmembrane helix 5 (TM5; Ser370 and Val371 , rat PTH1R) and TM6 (Leu427 , rat PTH1R) that determine [Arg2 ]PTH-(1–34) signaling specificity<sup>48</sup> (Fig. 4). The above functional studies on PTH1R mutants suggested a simple scheme for the ligand-receptor interaction in which the carboxy-terminal region of PTH-(1—34) interacts with the amino-terminal extracellular domain of the receptor and that the amino-terminal portion of the ligand interacts with the receptor region comprising the membrane-spanning helixes and extracellular loops. As summarized below, subsequent functional studies with other receptor variants that have been evaluated with different PTH or PTHrP analogs, as well as recent photoaffinity cross-linking studies, have supported this scheme.

#### ***1.4.2.2. Photoaffinity Cross-Linking***

The use of photoreactive PTH and PTHrP analogs as chemical cross-linking probes is providing a complementary approach to the mapping of ligand-receptor interactions by mutational methods. The peptide analogs that have been used most successfully for this purpose contain the photoreactive benzophenone moiety at sites tolerant to the modification. For example, Chorev and coworkers<sup>49</sup> showed that a PTH-(1–34) analog having the benzophenone functional group attached to the  $\epsilon$ -amino group of lysine-13

cross-linked to an eight amino acid receptor fragment located just amino-terminal of transmembrane domain (TM) 1, and mutation of Arg186 in this segment prevented the formation of the cross-link (Fig. 4).

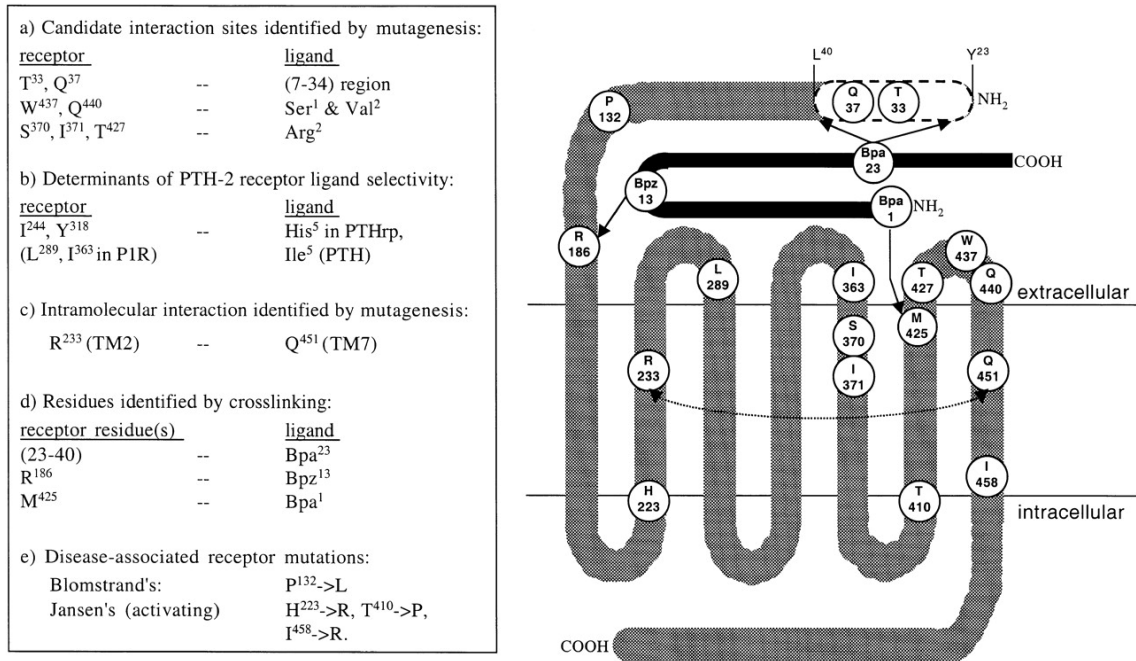


Fig. 4. Key sites in the PTH receptor and PTH or PTHrP ligand. Schematic shows some of the sites in the PTH-1 receptor (thick gray-shaded line) and PTH (or PTHrP) ligand (narrower solid line) that have been found by mutagenesis or photochemical cross-linking methods to have potentially important roles in ligand binding or receptor function. Receptor amino acids and position number correspond to the human PTH-1 receptor sequence. The three positions in the ligand at which photoreactive benzophenone groups have been introduced for cross-linking analyses are indicated. Corresponding receptor amino acids or region (Tyr23 –Met41 for the benzoylphenylalanine-23 analogue) that were identified as probable sites of cross-linking are indicated by the connecting arrows.<sup>50</sup>

These results suggest that the side chains of Lys13 and Arg186 are separated by a few angstroms from each other<sup>49</sup>. In another study by the same group, a PTH-(1–34) analog containing benzoylphenylalanine (Bpa) in place of alanine-1 was covalently cross-linked to a receptor segment in the COOH-terminal portion of TM6 containing Met414 and Met425, and mutation at Met425 abolished the cross-link<sup>51</sup>. Interestingly, Met425 is close to the residues that were previously shown to determine selectivity for [Arg2]PTH-(1–34)<sup>48</sup>(Fig. 4).

A third cross-linking site has been identified by Gardella's group using an analog of PTHrP-(1–36) containing Bpa at position 23, in place of the native phenylalanine. In this case, the reactive site was mapped to an 18-amino acid segment at the amino

terminus of the receptor (residues 23–40)<sup>52</sup> (Fig. 1). Subsequent alanine-scanning mutagenesis of this region revealed two amino acid residues, Thr33 and Gln37, that contribute functional binding interactions to the (7–34) portion of PTH<sup>52</sup>. So far, there is good correlation between the mutational analyses performed on the PTH receptors and the cross-linking data.

A ligand-induced conformational shift in the portion of the receptor containing the seven membrane spanning helices and connecting loops is thought to be the bases of the signal transduction mechanism<sup>53</sup>. However, for most GPCRs, this process is still poorly understood.

Scanning mutagenesis of the PTH1R identified functionally important segments in each of the three extracellular loops, and point mutational analysis of the third extracellular loop showed that changes at Trp437 and Gln440 weakened binding of PTH-(1–34), but not of PTH-(3–34)<sup>54</sup>. Similar defects in PTH-(1–34) binding but not PTH-(3–34) binding occurred with point mutations at Arg233 near the middle of TM2 and at Gln451 in the middle of TM7 (Fig. 4). These results imply that the membrane-spanning helices and the connecting extracellular loops form a part of the ligand binding pocket that recognizes residues 1 and 2 of the ligand. Interestingly, with combined mutations at Arg233 and Gln451, binding of PTH-(1–34) was restored, but cAMP signaling was greatly reduced<sup>55</sup>. This result suggests there is an interaction between helix 2 and helix 7 may interact, which is consistent with topological models derived from sequence alignment data<sup>56</sup>, and that these interactions play a role in transmembrane signaling.

### **1.5. The two-site model of PTH–PTHr interaction**

The combined functional and crosslinking data are consistent with a mechanism for PTH–PTHr interaction that involves two principal components:

- (1) an interaction between the C-terminal domain of the ligand and the N-terminal domain of the receptor, which contributes predominantly to binding affinity;
- (2) an interaction between the N-terminal portion of the ligand and the juxtamembrane region of the receptor, which contributes to signaling (Fig. 5).

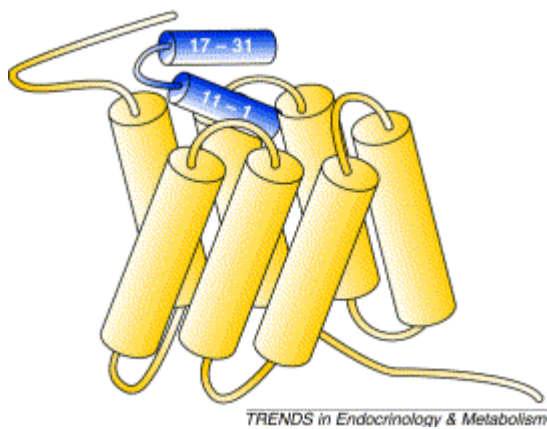


Fig. 5. The two domain hypothesis. The interaction between parathyroid hormone [PTH(1–34)] and its receptor involves two principal mechanistic components: (1) an interaction between the C-terminal domain of PTH(1–34), represented by residues 17–31, and the N-terminal extracellular domain of the receptor; and (2) an interaction between the N-terminal domain of PTH, represented by residues 1–11, and the juxtamembrane region of the receptor. These two components of the interaction are postulated to contribute predominantly to binding affinity and receptor activation, respectively. This hypothesis has been inferred from, and supported by, results of numerous mutational and crosslinking studies<sup>15</sup>.

This general interaction model probably applies to at least some of the other class II receptors, including those for CRF, calcitonin, secretin and glucagon<sup>57, 58, 59, 60</sup>. It is also possible that interactions at the two receptor domains occur in a cooperative or sequential manner<sup>61, 62</sup> and that a higher order of folding is involved. In support to this hypothesis there is a recent crosslinking study showing that a PTH(1–34) agonist analog with a benzophenone group attached to Lys27 contacts the first extracellular loop of the PTH-1R (Fig. 4)<sup>63</sup>; thus, the N-terminal extracellular domain of the receptor (and the 15–34 portion of the ligand) is probably close to the juxtamembrane region of the receptor, at least in the agonist-bound state<sup>64</sup>.

One possibility is that ligand-induced PTH-1R activation requires multiple ligand contacts to a large and diffuse surface of the receptor, including the N-terminal extracellular domain. However, the finding that a peptide sequence as short as PTH(1–9) can activate a receptor lacking most of the N-terminal domain (as is shown by the constitutive activity of the tethered receptor constructs<sup>65</sup>), suggests that it should be possible for a small nonpeptide molecule that interacts only with the juxtamembrane region of the receptor to function as a potent PTH-1R agonist.

### 1.5.1. Ligands determinants of receptor signalling

N-terminally truncated PTH or PTHrP analogs, such as PTH(3–34), PTH(7–34) and PTHrP(7–34), bind to PTH-1R with high affinity and elicit little or no increase in cAMP accumulation. Such fragments yield potent PTH-1R competitive antagonists. Bulky

amino acid modifications within the N-terminal portion of 1–34 analogues (at positions 2, 3 and 6) also confer antagonistic properties to the peptides<sup>33, 66, 67, 68</sup>. Peptides consisting only of the N-terminal residues of PTH have substantially diminished receptor-binding affinity and cAMP-signaling potency. The shortest N-terminal peptide of native sequence that retains full PTH-1R-binding affinity and cAMP signaling potency is PTH(1–31)<sup>69</sup>, but PTH(1–14) was recently shown to be the shortest native N-terminal PTH peptide for which some cAMP agonist activity could be detected (EC50 ~200  $\mu$ M)<sup>70</sup>. Structure–activity studies on the PTH(1–14) scaffold revealed that residues 1–9 form a crucial receptor-activation domain, and also that amino acid substitutions at several positions in PTH(1–14) improved potency, thus leading to multi-substituted analogs, such as [Ala3,12,Gln10,Arg11,Trp14] PTH(1–14), which is 250 times more potent in stimulating cAMP accumulation than is native PTH(1–14). Furthermore, the same substitutions conferred activity to the otherwise inactive PTH(1–11) fragment<sup>71</sup>. Recent data indicate that important determinants of PLC activation reside at the N-terminus of PTH. Thus, minor N-terminal truncation, as in [desNH2 -Gly1]PTH(1–34), PTH(2–34) and PTH(3–34), severely diminished the capacity of the peptide to stimulate inositol phosphate (IP) production via PLC in porcine kidney LLC-PK1 cells transfected with human PTH-1R<sup>72</sup>. In addition, the modified PTH(1–14) analogs stimulated IP production in transfected COS-7 cells, indicating that residues in this N-terminal portion of the ligand are sufficient for PLC signaling<sup>71</sup>.

## 1.6. PTH-based pharmaceutical agents<sup>73</sup>

While sustained elevation of PTH levels leads to bone erosion, it has long been known that pulsatile administration of PTH results in increased bone formation<sup>74</sup>. This anabolic effect of PTH is now the basis for the clinical use of PTH(1–34) in the treatment of osteoporosis<sup>75, 76</sup>. Unfortunately, like most short bioactive peptides, PTH shows no efficacy after oral administration; its anabolic effect thus depends on administration of daily injections. The discovery of a minimal-length PTH-based peptide or a small non-peptide compound, which efficiently activates the PTH/PTHrP receptor after oral administration, is therefore an important objective of current pharmaceutical research. PTH antagonists could potentially be used to treat hyperparathyroidism or the humoral



hypercalcemia of malignancy syndrome. However, most of the PTH- or PTHrP-based antagonist peptides are highly modified and may thus lead to antibody generation. Furthermore, in vivo half-lives are currently unknown and in vivo efficacy has not been demonstrated for the peptide antagonists.

# REFERENCES

- <sup>1</sup> Kronenberg, H. M., F. R. Bringhurst, S. Nussbaum, H. Jüppner, A. B. Abou-Samra, G. V. Segre, and J. T. Potts, Jr. Parathyroid hormone: biosynthesis, secretion, chemistry, and action. In: *Handbook of Experimental Pharmacology: Physiology and Pharmacology of Bone*, edited by G. R. Mundy and T. J. Martin. Heidelberg: Springer-Verlag, 1993, p. 185–201.
- <sup>2</sup> Potts, J. T., Jr., and H. Jüppner. Parathyroid hormone and parathyroid hormone-related peptide in calcium homeostasis, bone metabolism, and bone development: the proteins, their genes, and receptors. In: *Metabolic Bone Disease*, edited by L. V. Avioli and S. M. Krane. New York: Academic, 1997, p. 51–94.
- <sup>3</sup> Brown, E. M., G. Gamba, D. Riccardi, M. Lombardi, R. Butters, O. Kifor, A. Sun, M. A. Hediger, J. Lytton, and S. C. Hebert. *Nature* 1993, 366: 575–580.
- <sup>4</sup> H. Murer, I. Forster, J. Biber, *Pflugers Arch.* 2004, 447 (5), 763–767.
- <sup>5</sup> Pfister MF, Ruf I, Stange G, Ziegler U, Lederer E, Biber J, Murer H, *Proc. Natl. Acad. Sci. USA*, 1998, 95 (4), 1909–1914.
- <sup>6</sup> Segawa H, Kaneko I, Takahashi A, Kuwahata M, Ito M, Ohkido I, Tatsumi S, Miyamoto K., *J. Biol. Chem.* 2002, 277 (22), 19665–19672.
- <sup>7</sup> Quinn, J. M., J. Elliott, M. T. Gillespie, and T. J. Martin. *Endocrinology*, 1998, 139: 4424–4427.
- <sup>8</sup> Yasuda, H., N. Shima, N. Nakagawa, K. Yamaguchi, M. Kinosaki, S. I. Mochizuki, A. Tomoyasu, K. Yano, M. Goto, A. Murakami, E. Tsuda, T. Morinaga, K. Higashio, N. Udagawa, N. Takahashi, and T. Suda. *Proc. Natl. Acad. Sci. USA*, 1998, 95: 3597–3602.
- <sup>9</sup> Stewart AF, Horst R, Deftos LJ, Cadman EC, Lang R, Broadus AE., *N. Engl. J. Med.* 1980, 303 (24), 1377–1383.
- <sup>10</sup> Moseley JM, Kubota M, Diefenbach-Jagger H, Wettenhall RE, Kemp BE, Suva LJ, Rodda CP, Ebeling PR, Hudson PJ, Zajac JD, et al.. *Proc. Natl. Acad. Sci. USA*, 1987, 84 (14) 5048–5052.
- <sup>11</sup> Burtis WJ, Wu T, Bunch C, Wysolmerski JJ, Insogna KL, Weir EC, Broadus AE, Stewart AF., *J. Biol. Chem.*, 1987, 262 (15), 7151–7156.
- <sup>12</sup> Strewler GJ, Stern PH, Jacobs JW, Eveloff J, Klein RF, Leung SC, Rosenblatt M, Nissenson RA., *J. Clin. Invest.* , 1987, 80 (6), 1803–1807.
- <sup>13</sup> Suva LJ, Winslow GA, Wettenhall RE, Hammonds RG, Moseley JM, Diefenbach-Jagger H, Rodda CP, Kemp BE, Rodriguez H, Chen EY, et al., *Science*, 1987, 237 (4817) 893–896.
- <sup>14</sup> D.W. Brandt, W. Wachsman, L.J. Deftos, *Cancer Res.* 1994, 54 (3), 850–853.
- <sup>15</sup> Gardella T. J., Jüppner H., *TRENDS in Endocrinology & Metabolism* 2001, Vol.12 No.5, 210-7
- <sup>16</sup> H.M. Kronenberg, *Nature* 2003, 423 (6937), 332–336.
- <sup>17</sup> M.C. Neville, T.B. McFadden, I. Forsyth, *J. Mammary Gland Biol. Neoplasia*, 2002, 7 (1), 49–66.
- <sup>18</sup> J. Van Houten et al., The calcium-sensing receptor regulates mammary gland parathyroid hormone-related protein production and calcium transport, *J. Clin. Invest.*, 2004, 113 (4) (2004) 598–608.
- <sup>19</sup> Rodda CP, Kubota M, Heath JA, Ebeling PR, Moseley JM, Care AD, Caple IW, Martin TJ., *J. Endocrinol.* 1988, 117 (2), 261–271.
- <sup>20</sup> Kovacs CS, Lanske B, Hunzelman JL, Guo J, Karaplis AC, Kronenberg HM., *Proc. Natl. Acad. Sci. USA*, 1996, 93 (26), 15233–15238.
- <sup>21</sup> Strewler G. J., *The New England Journal of Medicine, The Physiology of Parathyroid Hormone-related Protein*; (2000) Vol. 342; N. 3.
- <sup>22</sup> Goltzman, D., A. Peytremann, E. Callahan, G. W. Tregear, and J. T. Potts, Jr., *J. Biol. Chem.* 1975. 250, 3199–3203.
- <sup>23</sup> Horiuchi, N., M. P. Caulfield, J. E. Fisher, M. E. Goldman, R. L. McKee, J. E. Reagan, J. J. Levy, R. F. Nutt, S. B. Rodan, T. L. Schofield, T. L. Clemens, and M. Rosenblatt, *Science* 1987, 238, 1566–1568.
- <sup>24</sup> Horiuchi, N., M. F. Holick, J. T. Potts, Jr., and M. Rosenblatt. *Science* 1983, 220, 1053–1055.
- <sup>25</sup> Kemp, B. E., J. M. Mosely, C. P. Rodda, P. R. Ebeling, R. E. H. Wettenhall, D. Stapleton, H. Diefenbach-Jagger, F. Ure, V. P. Michelangali, H. A. Simmons, L. G. Raisz, and T. J. Martin. *Science* 1987, 238: 1568–1570.
- <sup>26</sup> Tregear, G. W., J. Van Rietschoten, E. Greene, H. T. Keutmann, H. D. Niall, B. Reit, J. A. Parsons, and J. T. Potts, Jr. *Endocrinology* 1973, 93, 1349–1353.
- <sup>27</sup> Abou-Samra, A.-B., S. Uneno, H. Jüppner, H. Keutmann, J. T. Potts, Jr., G. V. Segre, and S. R. Nussbaum. *Endocrinology*, 1989, 125, 2215–2217.
- <sup>28</sup> Caulfield, M. P., and M. Rosenblatt. *Trends Endocrinol. Metab.* 1990, 2, 164–168.

- <sup>29</sup>Barden, J., R. Cuthbertson, W. Jia-Zhen, J. Moseley, and B. Kemp. *J. Biol. Chem.* 1997, 273 29572–29578.
- <sup>30</sup>Marx, U., S. Austermann, P. Bayer, K. Adermann, A. Ejchart, H. Sticht, S. Walters, F. Schmid, R. Jaenicke, W. Forssmann, and P. Rosch. *J. Biol. Chem.* 1995, 270: 15194–15202.
- <sup>31</sup>Pellegrini, M., M. Royo, M. Rosenblatt, M. Chorev, and D. Mierke. *J. Biol. Chem.* 1998, 273, 10420–10427.
- <sup>32</sup>Barden, J. A., and B. E. Kemp. *Biochim. Biophys. Acta*, 1994, 1208: 256–262.
- <sup>33</sup>Cohen, F. E., G. J. Strewler, M. S. Bradley, M. Carlquist, M. Nilsson, M. Ericsson, T. L. Ciardelli, and R. A. Nissenson. *J. Biol. Chem.* 1991, 266, 1997–2004.
- <sup>34</sup>Gardella, T. J., M. D. Luck, A. K. Wilson, H. T. Keutmann, S. R. Nussbaum, J. T. Potts, Jr., and H. M. Kronenberg. *J. Biol. Chem.* 1995, 270, 6584–6588.
- <sup>35</sup>L.F. Kolakowski Jr., GCRDb: a G-protein-coupled receptor database. *Receptor Channels* 2(1) 1–7.
- <sup>36</sup>Ji, T. H., M. Grossmann, and I. Ji. *J. Biol. Chem.* 1998, 273, 17299–17302.
- <sup>37</sup>Segre, G. V., and S. R. Goldring. *Trends Endocrinol. Metab.* 1993, 4, 309–314.
- <sup>38</sup>Rost B, Fariselli P, Casadio R. *Protein Sci.*, 1995, 4, 521–533
- <sup>39</sup>Grauschopf, U.; Lilie, H.; Honold, K.; Wozny, M.; Reusch, D.; Esswein, A.; Schafer, W.; Rucknagel, K. P.; Rudolph, R. *Biochemistry*, 2000, 39, 8878– 8887
- <sup>40</sup>Inomata, N., M. Akiyama, N. Kubota, and H. Jüppner. *Endocrinology* 1995, 136, 4732–4740.
- <sup>41</sup>Pines, M., A. E. Adams, S. Stueckle, R. Bessalle, V. Rashti-Behar, M. Chorev, M. Rosenblatt, and L. J. Suva. *Endocrinology* 1994, 135, 1713–1716.
- <sup>42</sup>Takasu, H., H. Baba, N. Inomata, Y. Uchiyama, N. Kubota, K. Kumaki, A. Matsumoto, K. Nakajima, T. Kimura, S. Sakakibara, T. Fujita, K. Chihara, and I. Nagai. *Endocrinology* 1996, 137, 5537–5543.
- <sup>43</sup>Potts, J. T., Jr., and H. Jüppner. Parathyroid hormone and parathyroid hormone-related peptide in calcium homeostasis, bone metabolism, and bone development: the proteins, their genes, and receptors. In: *Metabolic Bone Disease*, edited by L. V. Avioli and S. M. Krane. New York: Academic, 1997, p. 51–94.
- <sup>44</sup>Segre, G. V. Receptors for parathyroid hormone and parathyroid hormone-related protein. In: *Principles in Bone Biology*, edited by J. P. Bilezikian, L. G. Raisz, and G. A. Rodan. New York: Academic, 1996, p. 377–403.
- <sup>45</sup>Guo, J., A. Iida-Klein, X. Huang, A. B. Abou-Samra, G. V. Segre, and F. R. Bringhurst. *Endocrinology* 1995, 136, 3884–3891.
- <sup>46</sup>Iida-Klein, A., J. Guo, L. Y. Xie, H. Jüppner, J. T. Potts, Jr., H. M. Kronenberg, F. R. Bringhurst, A. B. Abou-Samra, and G. V. Segre. *J. Biol. Chem.* 1995, 270, 8458–8465.
- <sup>47</sup>Jüppner, H., E. Schipani, F. R. Bringhurst, I. McClure, H. T. Keutmann, J. T. Potts, Jr., H. M. Kronenberg, A. B. Abou-Samra, G. V. Segre, and T. J. Gardella. *Endocrinology* 1994, 134, 879–884.
- <sup>48</sup>Gardella, T. J., H. Jüppner, A. K. Wilson, H. T. Keutmann, A. B. Abou-Samra, G. V. Segre, F. R. Bringhurst, J. T. Potts, Jr., S. R. Nussbaum, and H. M. Kronenberg. *Endocrinology* 1994, 135, 1186–1194.
- <sup>49</sup>Adams, A., A. Bisello, M. Chorev, M. Rosenblatt, and L. Suva. *Mol. Endocrinol.* 1998, 12, 1673–1683.
- <sup>50</sup>Michael Mannstadt, Harald Jüppner and Thomas J. Gardella, *Am J Physiol Renal Physiol*, 1999, 277, 665-675.
- <sup>51</sup>Bisello, A., A. E. Adams, D. F. Mierke, M. Pellegrini, M. Rosenblatt, L. J. Suva, and M. Chorev. *J. Biol. Chem.* 1998, 273, 22498–22505.
- <sup>52</sup>Mannstadt, M., M. Luck, T. J. Gardella, and H. Jüppner. *J. Biol. Chem.* 1998, 273, 16890–16896.
- <sup>53</sup>Farrens, D. L., C. Altenbach, K. Yang, W. L. Hubbell, and H. G. Khorana. *Science* 1996, 274: 768–770.
- <sup>54</sup>Lee, C., M. D. Luck, H. Jüppner, J. T. Potts, Jr., H. M. Kronenberg, and T. J. Gardella. *Mol. Endocrinol.* 1995, 9; 1269–1278.
- <sup>55</sup>Gardella, T. J., M. D. Luck, M.-H. Fan, and C. W. Lee. *J. Biol. Chem.* 1996, 271, 12820–12825.
- <sup>56</sup>Donnelly, D.. *FEBS Lett.* 1997, 409: 431–436..
- <sup>57</sup>Bergwitz C, Gardella TJ, Flannery MR, Potts JT Jr, Kronenberg HM, Goldring SR, Jüppner H. *J. Biol. Chem.* 1996, 271, 26469–26472
- <sup>58</sup>Turner PR, Mefford S, Bambino T, Nissenson RA. *J. Biol. Chem.* 1998, 273, 3830–3837
- <sup>59</sup>Nielsen SM, Nielsen LZ, Hjorth SA, Perrin MH, Vale WW. *Proc. Natl. Acad. Sci. U.S.A.*, 2000, 97, 10277–10281
- <sup>60</sup>Stroop SD, Kuestner RE, Serwold TF, Chen L, Moore EE. *Biochemistry* 34, 1995, 1050–1057
- <sup>61</sup>Hoare SR, Gardella TJ, Usdin TB. *J. Biol. Chem.* 2001, 276, 7741–7753

- 
- <sup>62</sup>Ji TH, Grossmann M, Ji I. *J. Biol. Chem.* 1998, 273, 17299–17302
- <sup>63</sup>Greenberg Z, Bisello A, Mierke DF, Rosenblatt M, Chorev M. *Biochemistry*, 2000, 39, 8142–8152
- <sup>64</sup>Piserchio A, Bisello A, Rosenblatt M, Chorev M, Mierke DF. *Biochemistry*, 2000, 39, 8153–8160
- <sup>65</sup>Shimizu M, Carter PH, Gardella TJ. *J. Biol. Chem.* 2000, 275, 19456–19460
- <sup>66</sup>Carter PH, Jüppner H, Gardella TJ. *Endocrinology*, 1999, 140, 4972–4981
- <sup>67</sup>Behar V, Bisello A, Rosenblatt M, Chorev M. *J. Biol. Chem.*, 1999, 275, 9–17
- <sup>68</sup>Gardella TJ, Axelrod D, Rubin D, Keutmann HT, Potts JT Jr, Kronenberg HM, Nussbaum SR. *J. Biol. Chem.*, 1991, 266, 13141–13146
- <sup>69</sup>Whitfield, J.F. and Morley, P. *Trends Pharmacol. Sci.*, 1995, 16, 382–386
- <sup>70</sup>Luck MD, Carter PH, Gardella TJ. *Mol. Endocrinol.*, 1999, 13, 670–680
- <sup>71</sup>Shimizu M, Potts JT Jr, Gardella TJ. *J. Biol. Chem.*, 2000, 275, 21836–21843
- <sup>72</sup>Takasu H, Gardella TJ, Luck MD, Potts JT Jr, Bringhurst FR. *Biochemistry*, 1999, 38, 13453–13460
- <sup>73</sup>Gensure RC, Gardella TJ, Jüppner H. *Biochemical and Biophysical Research Communications*, 2005, 328, 666–678
- <sup>74</sup>Reeve J, Meunier PJ, Parsons JA, Bernat M, Bijvoet OL, Courpron P, Edouard C, Klenerman L, Neer RM, Renier JC, Slovik D, Vismans FJ, Potts JT Jr., *Br. Med. J.* 1980, 280 (6228), 1340–1344.
- <sup>75</sup>Neer RM, Arnaud CD, Zanchetta JR, Prince R, Gaich GA, Reginster JY, Hodsmann AB, Eriksen EF, Ish-Shalom S, Genant HK, Wang O, Mitlak BH. *N. Engl. J. Med.*, 2001, 344 (19), 1434–1441.
- <sup>76</sup>Orwoll ES, Scheele WH, Paul S, Adami S, Syversen U, Diez-Perez A, Kaufman JM, Clancy AD, Gaich GA., *J. Bone Miner. Res.*, 2003, 18 (1), 9–17

# 2 – INTRODUCTION

## Peptidomimetic: a way to produce peptide drugs

### 2 – INTRODUCTION

Peptidomimetic: a way to produce peptide drugs .....	25
2.1 A rational approach to obtain an active peptide derivative .....	27
2.1.1 <i>The hierarchical approach</i> .....	28
2.1.2 <i>Approch to Peptidomimetics</i> .....	31
2.3 Aim of the thesis .....	34
REFERENCES .....	36

The discovery<sup>1</sup> of peptide hormones, growth factors and neuropeptides involved in vital biological functions of our organism has increased interest in therapeutic use of peptides. The elucidation of the human genome revitalized the interest in using proteins or protein fragments for the treatment of presently incurable diseases. The discovery of diverse peptides with physiological activity in peripheral tissues and in the CNS\* increased the interest in exploiting peptides, peptide analogues and peptide mimetics as therapeutic drugs.

In the last three decades, natural polypeptides have been widely studied in order to further understand their molecular mechanisms of action. In general, it appears that limited degradation steps occur physiologically in the release of the bioactive molecules from their precursors. The biotransformation of some hormones such as corticotrophin (ACTH) and oxytocin and of neuropeptides such as bradykinin and enkephalin is well documented<sup>2</sup>. Physiological degradation is also involved in the inactivation of the peptides after their biological function. In tissue or cellular compartments, the inactivation involves specific endopeptidases, and in the systemic circulation and peripheral organs it involves less specific exopeptidases (amino- and carboxypeptidases). Although peptide degradation by peptidases is important for producing bioactive molecules and for inactivating them after their function has been performed, this very efficient metabolic process represents a major challenge to the use of peptides as drugs. Moreover, because drugs are usually administered far from their sites of action, a drug must be able to reach its target site, which usually involves penetration of several biological barriers. Unmodified peptides do not circulate in the blood for more than a few minutes because of enzymatic degradation, and have generally poor bioavailability in tissues and organs, which limits their usefulness as therapeutic agents. The task of the medicinal chemist is therefore to perform chemical modifications that maximize enzymatic stability and bioavailability, preserving or even enhancing the potency and selectivity of the bioactive peptide. Therefore, the rational design of such peptide drugs requires evaluation of biological parameters such as metabolism, absorption and transport, not only through the systemic circulation but into specific organs and through membrane barriers. It is also necessary to obtain structural data and to identify the portion(s) of the molecule responsible for its biological activity. These

---

\* Central Nervous System

findings can then be exploited to design pharmacologically improved molecules that retain the chemical groups essential for biological activity. Advances in the field of peptide synthesis and drug design will allow the engineering of new generations of more stable and potent peptide drugs.

Peptide derivatives can be classified into three main groups according to the importance of the chemical modifications to the original sequence, going from relatively conservative substitutions to more drastic modifications (Table 1)<sup>1</sup>. Generally, the optimization of peptide drugs follows each of these steps in a sequence, beginning with relatively small chemical modifications of the natural structure that do not affect the peptide backbone (modified peptide), then transforming the peptide into a pseudopeptide and finally developing peptide mimetic molecules. The aim of this step-by-step approach is to enhance both pharmacological and pharmacokinetic profiles of the unmodified peptide in order to increase its stability, potency and specificity and to improve delivery to the site of action.

<i>Name</i>	<i>Definition</i>	<i>Example</i>
<b>Modified peptides</b>	Peptide derivatives containing relatively small modifications that do not alter the peptide bond. These derivatives can be considered as peptides in chemical nature.	End modifications, cyclization, chirality changes, non-coded amino acids, N-amide nitrogen alkylation
<b>Pseudopeptides</b>	Peptide derivatives containing peptide bond modifications consisting of the replacement of some chemical groups. These derivatives are only partially peptide in chemical nature.	Amide bond surrogates Peptoids Azapeptides
<b>Peptide mimetics</b>	Organic molecules that no longer contain any peptide bonds but mimic the pharmacological activity of peptides.	Rationally-designed peptide mimetics Rationally-identified mimetics

Table 1. Different types of Peptide Derivatives Classified According to Degree of Modification

## 2.1 A rational approach to obtain an active peptide derivative

Peptides are known to influence essentially all vital physiological processes via inter- and intra-cellular communication, and signal transduction mediated through various classes of receptors<sup>3, 4</sup>. Thus, a major goal of peptide research has been to elucidate or

understand the relationships between a peptide three-dimensional (3D) structure and its biological activity to develop suitable therapeutic agents controlling human health, disease and dysfunction. The initial event that is essential for eliciting (or blocking) a biological response is interaction often is referred to as the pharmacophore, and may involve either a continuous sequence of amino acids (sychnologic organization) or amino acid residues far from each other in the primary structure (rhegnylogic organization)<sup>5</sup> but close on a surface in the 3D structure of the polypeptide<sup>6</sup>. In either case, the peptide backbone is the scaffold for the key side chain groups involved in the interaction, and in some cases, also may act as a hydrogen bond donor and/or acceptor in molecular recognition (binding). In all cases, the side chain moieties involved directly in the binding are critical for the interaction, and their 3D architecture and stereoelectronic properties provide the critical complementary shape and chemical properties for efficient molecular recognition. Although native biologically active peptides have a great potential for medical applications, they often need to be modified to overcome certain problems molecular recognition. In the case of peptides, this means interaction of a portion of the surface formed by the 3D structure of the ligand with a complementary surface of the acceptor/receptor molecule. In the case of the ligand, the portion of the 3D surface is involved in current drug-delivery strategies. The desired properties often not present or optimized in the native ligand include: receptor/acceptor selectivity; high potency; stability against proteolytic breakdown; and appropriate biodistribution and bioavailability.

### ***2.1.1 The hierarchical approach***

Peptidomimetic research in the last two decades was a hierarchical approach to the rational design of peptidomimetics<sup>7</sup>. Once the natural peptide structure is known, the first step in this approach involves the identification of the key amino acid residues necessary for receptor recognition by single amino acid modifications in the peptide ligand. Simultaneously, local constraints are built into the ligand to constrain the local backbone conformation to the most appropriate local minima compatible with molecular recognition. Two of the widely used methods are novel  $\alpha$ -substituted amino acids and/or amide bond replacements. Alternatively, more global constraints are



incorporated via cyclization to make an appropriate template for all structural elements that make up pharmacophore.

Peptide mimetics can be discovered by either rational design or random screening. The rational design of peptide mimetics requires detailed structural information of the peptide and knowledge of the chemical groups responsible for its activity<sup>8, 9</sup>. Structural characterization of peptide is essential in order to define the positions of the relevant chemical groups. The objective is to reconstruct the position of the active groups based on the structural data, using an organic template to fix them. The third phase is a careful analysis of the 3D arrangement of critical side chain groups and backbone functionalities that are essential for bioactivity. These biophysical studies include state-of-the-art NMR spectroscopy, X-ray crystallography if possible, circular dichroism measurements, and computational methods (molecular mechanics and molecular dynamics calculations) utilizing the biophysical structural parameters as key constraints. In many cases such studies can lead to highly potent, selective and efficacious drug candidates, and provide the starting point for the non-peptide mimetics. The goal is to produce a fairly rigid molecule that can adopt only one major conformation, with the key chemical groups in spatial orientations similar to those of the parent peptide. A binary mimetic is the simplest model, in which two pharmacophores are linked on a template. More complex models can be constructed, such as ternary and quaternary mimetics in which three and four pharmacophores are linked to a template.

Compounds with rigid or semi-rigid conformations are synthesized, and the most active structures selected by studying conformation-activity relationships. The major effort was find other organic moieties which can replace the peptide scaffold and position the crucial recognition elements correctly. This approach provides a systematic framework for the de novo design of peptidomimetics as outlined in Fig. (1).

The limiting factor for the rational design of peptide mimetics is usually the availability of a precise conformational model on which the entire construct can be based. The quality of the data obtained by NMR spectroscopy or X-ray diffraction analysis of the parent peptide is crucial. It is also very important that the medium for spectroscopic measurement uses a folding of the peptide similar to that at the target site. Peptide mimetic libraries have been generated, restricted to compounds containing the chemical

groups responsible for the activity of the parent peptide. These libraries are screened against the biological target using a simple, quickly in vitro assay<sup>1</sup>.

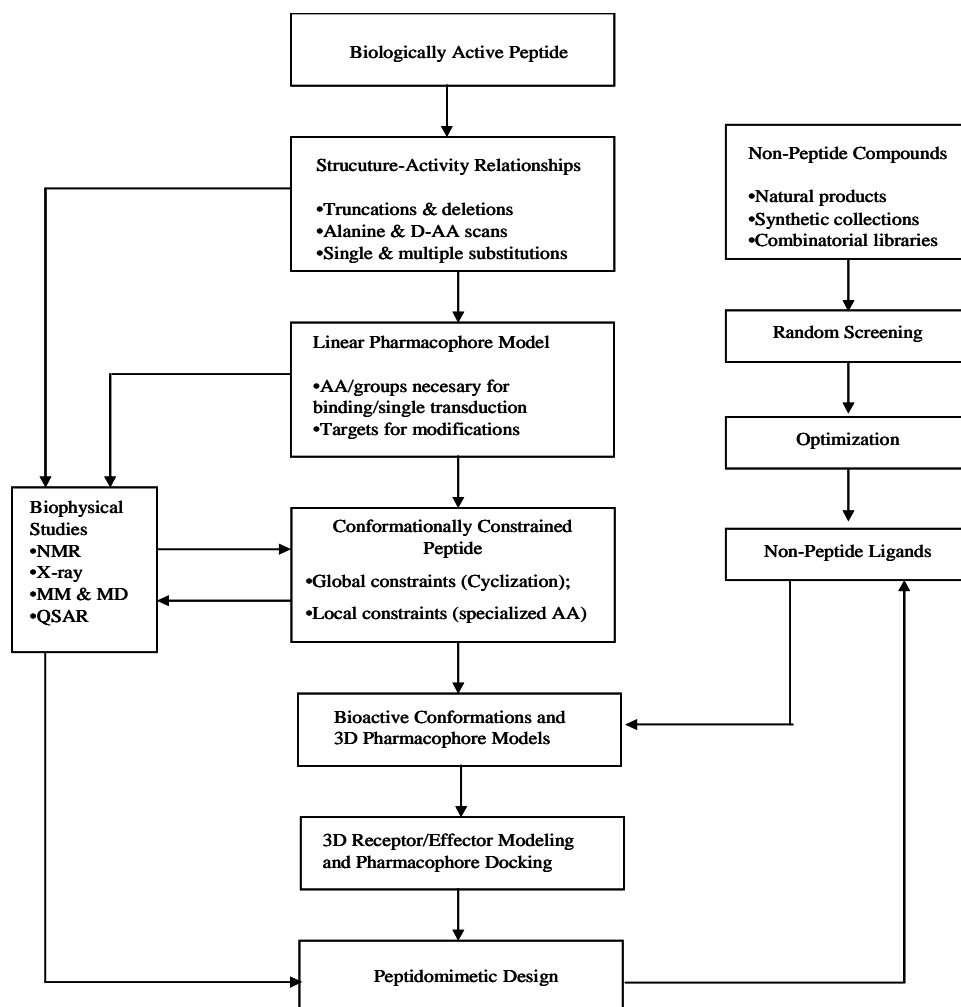


Fig. 1: A de novo approach for peptidomimetic design<sup>7</sup>.

It is worth mentioning here that peptidomimetic design is a multidisciplinary area that often relies on: 1) new asymmetric synthesis and methodologies for the preparation of novel molecules; 2) high-throughput screening of ligands and libraries of ligands using multiple in vitro and in vivo biological assays; 3) computational methods; and 4) state-of-the-art biophysical methods for determining the structural, conformational, topographical and dynamic properties of designed ligands<sup>7</sup>.

## ***2.1.2. Approach to Peptidomimetics***

### *2.1.2.1 D-Amino Acids*

One simple approach to stabilizing a peptide against proteolysis is to modify the side-chains of some of the amino acid residues. So, the incorporation of non-coded amino acids into the sequence has become a widespread approach in engineering peptide drugs<sup>10, 11</sup>. It is possible to modify some natural amino acids which are often methylated or halogenated. A possible change is to modify chirality. The stereochemical specificity of natural proteins, which contain only L-enantiomer amino acids, is important to recognition and interaction. Replacing some or even all the L-amino acids of a peptide sequence with their corresponding D-amino acids confer resistance to proteolytic degradation. Another important advantage for peptide drug development is that D-amino acid analogues have been found to be significantly less immunogenic than the L-amino acid counterparts<sup>12, 13</sup>.

One drawback common to the use of D-analogues is the loss of activity due to conformational changes. To address this problem, Schumacher et al.<sup>14</sup> proposed an elegant approach based on mirror-image phage display. They identified active D-peptide ligands by screening libraries of natural L-peptides on a protein target synthesized with D-amino acids. The assumption was that the L-peptide would interact with the D-protein in a way similar to that in which the D-peptide would interact with the natural L-protein target. Another promising strategy for using D-amino acids to improve enzymatic stability while maintaining biological activity consists of designing what is called a retro-inverse peptide. The idea is to simultaneously invert the sequence and change the chirality of the peptide<sup>15, 16</sup>. Structurally, the retro-inverse peptide is much more similar to the original peptide than the simple D-analogue.

### *2.1.2.2 Non-natural Amino Acids*

The introduction of non-natural amino acids generates modifications in the secondary and tertiary structures of a peptide, and is used to further enhance the stability and activity of peptide sequences. An impressive variety of molecules can be introduced<sup>11, 17</sup>. However, unusual modifications are often associated with problems with chemical synthesis, such as very low coupling yields. To overcome the limits of classical solid phase synthesis, semi-synthetic and biological systems have been developed<sup>18</sup>.

Because of their own conformational features, some non-natural amino acids introduce backbone rigidity that may confer a great potential for improvement of the compound. The two most commonly used conformationally-constrained residues are  $\alpha$ -aminoisobutyric acid (Aib, also known as 2-methylalanine; Fig. (2)) and its analogue  $\alpha, \alpha$ -dialkylated glycine, Fig. (2). The hallmark feature of the Aib residue is the high degree of local stereo-chemical rigidity that accompanies its incorporation into peptide chains, stabilizing local secondary structure<sup>19</sup>.

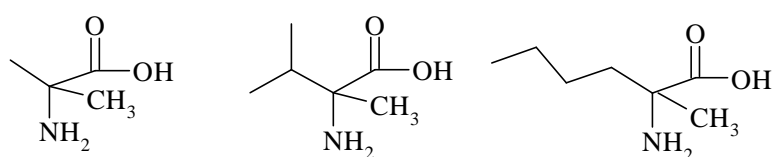


Fig 2: Aib and some  $\alpha, \alpha$ -dialkylated glycines used in our work

### 2.1.2.3 Peptoids

The concept and synthesis of peptoids as active molecules were first described by Simon and coworkers<sup>20</sup>. The side-chain linked to the  $\alpha$ -carbon in peptide structure is “switched” by one position to the amide nitrogen. Therefore, peptoids can be considered as N-substituted oligoglycines. This particular structure provides a higher metabolic stability to the molecule, because the natural proteases do not recognize the N-substituted amide bonds. Peptoids exhibit more structural flexibility than peptides; this property has been used to determine molecular recognition properties between the parent peptide and the molecular target<sup>21</sup>. The wide variety of conformational states available from peptoids has been used to generate very diverse libraries of novel molecules<sup>20</sup>. Zuckermann et al.<sup>22</sup> identified novel ligands with high affinity for 7-transmembrane G-protein complex receptors, screening of a 5000-peptoid library. The absence of amide hydrogens in peptoids inhibits the formation of hydrogen bonds, reducing the possibility that peptoids will adopt regular motifs of secondary structure.

This feature further increases the conformational space available to peptoids, but may reduce their biological activity when a ordered structure is needed.

#### *2.1.2.4 Cyclization*

The design of cyclic analogues represents another widely used strategy to increase peptide stability and potency. The structural constraint induced by cyclization reduces conformational flexibility and may enhance potency, selectivity, stability and bioavailability as well as membrane barrier permeability. For example, oral administration of cyclic peptides has been investigated for vasopressin and opioid analogues<sup>23, 24</sup>. Cyclic peptides are called homodetic if in the ring there is a peptide bond and heterodetic if the cyclization includes other bridges such as disulfide, ester (lactone), ether or thioether bridges. Several chemical strategies have been developed to convert a linear peptide to a cyclic structure<sup>25, 26, 27</sup>. The most common approach to synthesizing a heterodetic cyclic peptide involves forming a disulfide bridge between two cysteine residues. This strategy implies the incorporation of cysteines when they are not present in the original sequence, resulting in the modification of the peptide sequence, which may affect activity. The modification of the sequence of a bioactive peptide by removing or introducing new residues may lead to a loss of activity. Therefore, synthesis of homodetic cyclic peptides is often preferred. A ring may be formed via cyclization of the amino- and carboxy-groups of the N- and C-termini, forming a head-to-tail cyclic peptide linked by an amide bond. The coupling of side-chain to side-chain and of side-chain to head are also interesting approaches, because they allow selection of the amino acid used to perform the cyclization. Generally the two residues important for activity are selected to make the bridge. This strategy has been used in the synthesis of a cyclic analogue of a myelin basic protein epitope<sup>28, 29</sup>. The possibility of synthesizing a cyclic analogue of a linear peptide depends on the sequence, amino acid composition and length of the peptide.

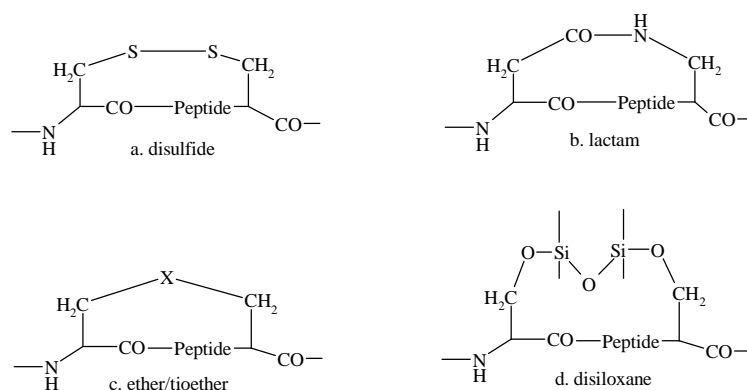


Fig.3: type of cyclization

### 2.1.2.5 Peptide Mimetics

We have just explained that a peptide mimetic is a small molecule that mimics the biological activity of a peptide, but it does not contain any peptide bonds and does not have a modular structure with amino acids or their derivatives as building blocks. Peptide mimetics usually have a molecular weight lower than 700 Da, and usually exhibit good bioavailability and sufficient metabolic stability to allow oral administration. However, they often have greater problems of toxicity, solubility and specificity than natural or modified peptides. For these reasons, some investigators use the term peptide mimetic to refer to any type of chemically modified peptides, including peptides which have a modification or replacement of some of the atoms presents in backbone, and even modified peptides<sup>26, 30, 31</sup>.

## 2.3 Aim of the thesis

Peptides are very diverse and versatile molecules that offer wide therapeutic potential. However, only a few peptide drugs have been approved for the treatment of human diseases<sup>†</sup>. This is largely due to the inherent enzymatic instability of unmodified peptides and their relatively poor bioavailability. In compensation, peptide drugs are usually less toxic, more soluble and easier to identify and synthesize than small organic molecules.

No high resolution structures have been provided yet for the PTH1R nor the hormone-receptor complex, due to the difficulty in producing and purifying significant quantities

<sup>†</sup> An example is FORTEO®(Teriparatide) produced by Eli-Lilly. It is a first anti-osteoporosis drug produced by recombinant human PTH(1-34) approved by FDA.

of recombinant protein, and in applying the NMR and X-ray diffraction techniques to transmembrane proteins. The first goal of this research was to try to obtain information about hormone/receptor through a synthetic approach. This approach generates peptide mimetic libraries which have a few restricted modified compounds containing the chemical groups responsible for the activity of the parent peptide. These libraries are screened against the biological target using a simple, fast and potent in vitro assay. In this way, the first step is to study amino acid residues of the most active minimal sequence of PTH(1-11) in order to obtain structural information and to better understand the mechanisms responsible for ligand selectivity.

The main goal of peptide medicinal chemistry is to transform a prototype peptide into a pharmacologically useful drug that is metabolically stable and is able to reach its target organ. Thus, a second (ambitious!) goal of the research was to synthesise a first example of peptidomimetic of PTH using the information collected in the first part of this thesis. Nevertheless, the rational design of ideally bioactive, stable and bioavailable peptide drugs remains an extremely difficult task.

# REFERENCES

- <sup>1</sup> Adessi C., Soto C. *Current Medicinal Chemistry*, 2002, 9, 963-978
- <sup>2</sup> Strand, F. L. In *Neuropeptides. Regulators of physiological Process*. Strand, F. L., Ed.; The MIT Press: Cambridge, 1999; Vol. 3, pp. 43-64.
- <sup>3</sup> Bonner, G.G.; Davis, P.; Stropova, D.; Ferguson, R.; Yamamura, H.I.; Porreca, F.; Hruby, V.J. *Peptides* 1997, 18, 93.
- <sup>4</sup> Hruby, V.J.; Hadley, M.E. In *Design and Synthesis of Organic Molecules Based on Molecular Recognition*; G. VanBinst, Ed.; Springer-Verlog: Heidelberg, 1986; pp. 269-289.
- <sup>5</sup> Schwyzer, R. *Ann. N.Y. Acad. Sci.* 1977, 297, 3.
- <sup>6</sup> Hruby, V.J. *Drug Discovery Today* 1997, 2, 165.
- <sup>7</sup> V. J. Hruby, P. M. Balse *Current Medicinal Chemistry*, 2000, 7, 945-970
- <sup>8</sup> Moore, G. J. *Trends Pharmacol. Sci.*, 1994, 15, 124.
- <sup>9</sup> Nikiforovich, G. V. *Int. J. Pept. Protein Res.*, 1994, 44, 513.
- <sup>10</sup> Mendel, D.; Ellman, J. A.; Chang, Z.; Veenstra, D. L.; Kollman, P. A.; Schultz, P. G. *Science*, 1992, 256, 1798.
- <sup>11</sup> Balaram, P. *Curr. Opinion Struct. Biol.*, 1992, 2, 845.
- <sup>12</sup> Gill, T. J.; Hanna, J. G.; Doty, P. *Nature*, 1963, 197, 746.
- <sup>13</sup> Borek, F.; Stupp, Y.; Fuchs, S.; Sela, M. *Biochem. J.*, 1965, 96, 577.
- <sup>14</sup> Schumacher, T. N.; Mayr, L. M.; Minor, D. L., Jr.; Milhollen, M. A.; Burgess, M. W.; Kim, P. S. *Science*, 1996, 271, 1854.
- <sup>15</sup> Chorev, M.; Goodman, M. *Trends Biotechnol.*, 1995, 13, 438.
- <sup>16</sup> Chorev, M.; Goodman, M. *Acc. Chem. Res.*, 1993, 26, 266.
- <sup>17</sup> Spatola, A. F. In *Chemistry and Biochemistry of Peptides and Proteins*; Weinstein, B., Ed.; Marcel Dekker: New York, 1983; Vol. 7, pp. 267-357.
- <sup>18</sup> Lesley, S. A. In *Peptide and Protein Drug Analysis*; reid, R. E., Ed.; Marcel Decker, Inc: New York, 2000; Vol. 6, pp. 191-205.
- <sup>19</sup> Nagaraj, R.; Balaram, P. *FEBS Lett.*, 1978, 96, 273.
- <sup>20</sup> Simon, R. J.; Kania, R. S.; Zuckermann, R. N.; Huebner, V. D.; Jewell, D. A.; Banville, S.; Ng, S.; Wang, L.; Rosenberg, S.; Marlowe, C. K. *Proc. Natl. Acad. Sci. U.S A.*, 1992, 89, 9367.
- <sup>21</sup> Kessler, H. *Angew. Chem. Int. Ed. Engl.*, 1993, 32, 543.
- <sup>22</sup> Zuckermann, R. N.; Martin, E. J.; Spellmeyer, D. C.; Stauber, G. B.; Shoemaker, K. R.; Kerr, J. M.; Figliozzi, G. M.; Goff, D. A.; Siani, M. A.; Simon, R. J.; *J. Med. Chem.*, 1994, 37, 2678.
- <sup>23</sup> Saffran, M.; Franco-Saenz, R.; Kong, A.; Papahadjopoulos, D.; Szoka, F. *Can. J. Biochem*, 1979, 57, 548.
- <sup>24</sup> Borhardt, R. T. *J. Control Release*, 1999, 62, 231.
- <sup>25</sup> Kates, S. A.; Solé, N. A.; Albericio, F.;Barany, G. In *Peptides: Design, synthesis, and biological activity*; Basava, C. and Anantharamaiah, G. M., Ed.; Birkhäuser: Boston, 1994; Vol. 4, pp. 39-58.
- <sup>26</sup> Wiley, R. A.; Rich, D. H. *Med. Res. reviews*, 1993, 13, 327.
- <sup>27</sup> Goodman, M.;Ro, S. In *Burger's Medicinal Chemistry and Drug Discovery*; Wolff, M. E., Ed.; John Wiley and Sons, Inc: New York, 1995; Vol. 20, pp. 803-861.
- <sup>28</sup> Tselios, T.; Probert, L.; Daliani, I.; Matsoukas, E.; Troganis, A.; Gerothanassis, I. P.; Mavromoustakos, T.; Moore, G. J.; Matsoukas, J. M. *J. Med. Chem.*, 1999, 42, 1170.
- <sup>29</sup> Tselios, T.; Daliani, I.; Deraos, S.; Thymianou, S.; Matsoukas, E.; Troganis, A.; Gerothanassis, I.; Mouzaki, A.; Mavromoustakos, T.; Probert, L.; Matsoukas, J. *Bioorg. Med. Chem. Lett.*, 2000, 10, 2713.
- <sup>30</sup> al Obeidi, F.; Hruby, V. J.; Sawyer, T. K. *Mol. Biotechnol.*, 1998, 9, 205.
- <sup>31</sup> Sawyer, T. K. In *Peptide and Protein Drug Analysis*; reid, R. E., Ed.; Marcel Decker, Inc: New York, 2000; Vol. 16, pp. 81-114.



# 3 – DISCUSSION and CONCLUSION

3 – DISCUSSION and CONCLUSION.....	37
3.1 D-Scan .....	40
3.2 Retro-Inverse Analogues .....	46
3.3 Diamine analogues.....	49
3.4 Peptoids.....	53
3.5 C <sup>α,α</sup> -tetra-substituted amino acid analogues .....	57
3.5.1 PTH(1-11) analogues containing αMeVal.....	57
3.5.2 PTH(1-11) analogues containing αMeNle.....	63
3.6. Ciclopeptides .....	69
3.7. Peptidomimetic .....	77
3.8 CONCLUSION.....	82
REFERENCES .....	84

Peptides are the primary means of intercellular communication in many diverse biological systems, but lack appropriate physical chemical properties and metabolic stability to be ideally suited as therapeutics. As a result of major advances in organic chemistry and in molecular biology<sup>1</sup> most bioactive peptides have been prepared in larger quantities and made available for pharmacological and clinical experiments. Similarly, the development of combinatorial possibilities in peptide and organic synthesis offer considerable potential to design new lead products. Thus, in the last few years new methods have been established for the treatment and therapy of a series of diseases, and hopes have also been raised for the therapy of other illnesses in which peptides have been implicated. However, the use of peptides as drugs is limited by the following factors: a) their low metabolic stability towards proteolysis in the gastrointestinal tract and in serum; b) their poor absorption after oral ingestion, in particular due to their relatively high molecular mass or the lack of specific transport systems or both; c) their rapid excretion through liver and kidneys; and d) their undesired effects caused by interaction of the conformationally flexible peptides with various receptors. In addition, a bioactive peptide can cause effects in several types of cells and organ systems<sup>2</sup>. This has led to the concept of peptidomimetics, as we have just explained in chapter 2. In other words, they are a compound which tries to highly modify the backbone, but retains essential chemical functionalities and the ability to display them in a characteristic three-dimensional pattern which is complementary to peptide receptor. We have just defined the hierarchical approach, which is based on probing the conformational and side chain-functionality requirements of the receptor by single amino acid modifications. In our work of thesis, we apply this schematic approach to study a minimal active sequence of PTH(1-11).

Gardella's and co-workers' efforts to understand better the PTH/P1R interaction mechanism have sought to define the minimum components of the ligand that enable receptor activation. The native PTH(1-14) peptide is only weakly active, with a potency (EC<sub>50</sub>) for stimulation of cAMP formation in the hundred-micromolar range compared with a potency in the low nanomolar range for PTH(1-34)<sup>3</sup>, but they identified a number of substitutions that markedly improve signaling potency of the PTH(1-14) peptide. The analogue [Ala<sup>3,12</sup>,Gln<sup>10</sup>,Har<sup>11</sup>,Trp<sup>14</sup>]PTH(1-14)NH<sub>2</sub>, containing the combined substitutions of Ser<sup>3</sup>→Ala, Asn<sup>10</sup>→Ala, Leu<sup>11</sup>→homoarginine (Har), Gly<sup>12</sup>→Ala, and His<sup>14</sup>→Trp,

exhibits a cAMP-stimulating potency in PTH1R expressing cells that is 1000-fold higher than that of native PTH(1-14)<sup>4</sup>. Competition binding studies show that these PTH(1-14) analogues interact predominantly, if not exclusively, with the region of the receptor containing the extracellular loops and transmembrane domain helices (i.e., the J domain)<sup>5,6,7,8,9,10,11</sup>. The most potent PTH(1-14) analogue is conformationally constrained near the N terminus by the Aib(1,3) substitutions, which together provide for an additional ~100-fold improvement in analogue binding affinity and signaling potency<sup>10</sup>. Studies on other model oligo-peptide systems have shown that Aib stabilizes  $\alpha$ -helical structures; an effect caused by the restrictions on peptide bond rotations imposed by the extra C <sup>$\alpha$</sup>  methyl group of Aib<sup>12</sup>. Consistent with this, the Aib modified PTH(1-14) analogues were found by circular dichroism spectroscopy methods to be more helical than their alanine-containing counterpart peptides<sup>10</sup>. These findings thus lend support the hypothesis that the amino-terminal domain of PTH is  $\alpha$ -helical when bound to the receptor.

Newest investigations focusing on the interaction of N-terminal fragments of PTH with PTH1R showed that certain modifications can increase signalling potency in peptides as short as 11 amino acids. Thus, it is possible to apply the principles and concepts of hierarchical approach of peptidomimetics directly on a minimal active modified sequence PTH(1-11) used as model:



Initially, to understand the role of the side-chains of all amino acid residues of this peptide every L-AA were substituted by the correspondent D-AA, obtaining a library of PTH(1-11) analogues which were tested as agonists.

### 3.1 D-Scan

Replacement of each residue by its optical isomer provides useful information on possible turn positions since only certain turn types can contain both L and D-residues and still place the amino acid side chain in the same relative position to the peptide. The D-scan technique allows to analyze and study the effect of substitution of D amino acids in the sequence of PTH(1-11) and to investigate how the side chains of every residues are responsible of the binding to the receptor. This is the preliminary step to understand the possibility to modify the backbone or structures.

A drawback to the use of D-analogues is the loss of activity due to conformational changes. To study this problem, Schumacher et al.<sup>13</sup> proposed an interesting approach based on mirror-image phage display. They identified active D-peptide ligands by screening libraries of natural L-peptides on a protein target synthesized with D-amino acids. The assumption was that the L-peptide would interact with the D-protein in a way similar to that in which the D-peptide would interact with the natural L-protein target. So, initially, we thought to adopt the same approach to synthesize all-D-PTH(1-34). Unfortunately, this peptide didn't exhibit any activity. A CD analysis showed approximately the same structure of all-L-PTH(1-34) but with a left  $\alpha$ -helix (fig. 1).

The stereochemical specificity of natural proteins, which contain only L-enantiomer amino acids, is important to recognition and interaction between molecules.

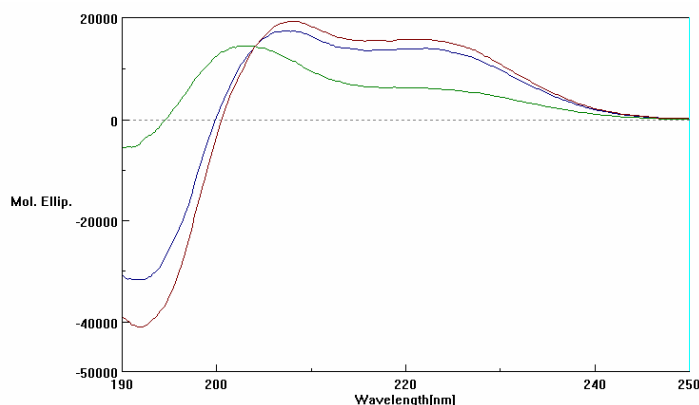


Fig. 1 CD spectra of All-D-PTH(1-34) in phosphate buffer at different pH value (from 2 to 8). Light Green line is at low pH value. It is interesting to observe that the peptide assumes an ordered structure at physiological conditions. CD spectra are completely symmetrical to L-PTH(1-34)

We thought that the loss of activity was caused by a change of orientation of all structure, and decided to investigate the effect of substitution of every residues with corresponding D-AA on fragment PTH(1-11). Replacing some or even all the L-amino acids of a peptide sequence with their corresponding D-amino acids will confer resistance to proteolytic degradation. A further important advantage for peptide drugs development is that D-amino acid analogues have been found to be significantly less immunogenic than the native sequence<sup>14, 15</sup>.

Name	Peptide sequence	EC50 (M)
RP	Aib-Val-Aib-Glu-Ile-Gln-Leu-Nle-His-Gln-Har-NH <sub>2</sub>	1E-09
D2	Aib- <b>D-Val</b> -Aib-Glu-Ile-Gln-Leu-Nle-His-Gln-Har-NH <sub>2</sub>	7E-06
D4	Aib-Val-Aib- <b>D-Glu</b> -Ile-Gln-Leu-Nle-His-Gln-Har-NH <sub>2</sub>	2E-06
D5	Aib-Val-Aib-Glu- <b>D-Ile</b> -Gln-Leu-Nle-His-Gln-Har-NH <sub>2</sub>	4E-07
DA5	Aib-Val-Aib-Glu- <b>D-Allo-Ile</b> -Gln-Leu-Nle-His-Gln-Har-NH <sub>2</sub>	4.5E-07
D6	Aib-Val-Aib-Glu-Ile- <b>D-Gln</b> -Leu-Nle-His-Gln-Har-NH <sub>2</sub>	4E-06
D7	Aib-Val-Aib-Glu-Ile-Gln- <b>D-Leu</b> -Nle-His-Gln-Har-NH <sub>2</sub>	3E-06
D8	Aib-Val-Aib-Glu-Ile-Gln-Leu- <b>D-Nle</b> -His-Gln-Har-NH <sub>2</sub>	2E-06
D9	Aib-Val-Aib-Glu-Ile-Gln-Leu-Nle- <b>D-His</b> -Gln-Har-NH <sub>2</sub>	2E-06
D10	Aib-Val-Aib-Glu-Ile-Gln-Leu-Nle-His- <b>D-Gln</b> -Har-NH <sub>2</sub>	1E-07
D11	Aib-Val-Aib-Glu-Ile-Gln-Leu-Nle-His-Gln- <b>D-Har</b> -NH <sub>2</sub>	7.5E-08

Tab. 1 Library of D-Scan analogues. All peptides were tested at Tuft University by Dr Angela Wittelsberger. The experimental error on the biological tests is of 15%.

The library was synthesized by SPPS, employing the Fmoc protocol. The only exception was the synthesis of the analogue containing homoarginine, where last amino acid was added manually.

The D-homoarginine was prepared by direct guanilation of the lysine. Typically, the synthesis of guanidines involves the reaction of amines with an electrophilic species. We applied a convenient preparation of fully protected homoarginine (Har) that involves the reaction of N- $\alpha$ -Fmoc-lysine with diBoc-triflyl guanidine, prepared according to reported method<sup>16</sup>, in presence of trimethylsilyl chloride (TMS-Cl) as a silylating agent in DCM solvent to obtain N- $\alpha$ -Fmoc-diBoc urethane protected homoarginine. Since N- $\alpha$ -Fmoc-

Lysine was not completely soluble in DCM, it was first converted into soluble derivative by silylation with TMS-Cl in refluxing DCM under anhydrous condition. The guanylation was then performed with *in situ* silylated amino acid in presence of a base. After completion of the reaction, silyl deprotection of the carboxyl group was achieved with methanol. The fully protected homoarginine so obtained was incorporated in the synthesis of peptide of interest.

We hypothesized that the silylating reagent helped the action of guanylation reagent to protect carboxylic group and to activate the amine group. In fact the bulky TMS group at the amine nitrogen appears to enhance the nucleophilicity for attack at  $sp^2$  carbon site<sup>17</sup>. To prove this hypothesis we decided to guanylate a mimetic substrate of Lys, ZNH-(CH<sub>2</sub>)<sub>5</sub>-NHBoc. Initially we tested the substrate with a common guanylation reagent Bis-Boc-S-methylisothiourea<sup>18</sup>. After Boc cleaving, the reaction without silylating agent yielded the desired product in a good yield. The same reaction carried out on Fmoc-L-Lys-OH didn't give any product, except the starting material. DMF was used instead of DCM as a solvent, and even in this case, only the starting material was found. The mimetic substrate ZNH-(CH<sub>2</sub>)<sub>5</sub>-NH<sub>2</sub> was tested in a guanylation reaction with Bis-Boc-triflyl guanidine and in presence of silylating TMS-Cl and a white precipitate was formed, which wasn't identifiable and in the liquid phase no product was found. We think that the different behaviour of the two reagents is due to the use of silylating agents which were important in presence of a free carboxylic group. The use of TMS-Cl with Fmoc-Cl to protect amino group in presence of the free carboxylic group is a normal method of peptide synthesis<sup>19</sup>. Probably TMS-Cl had to be used since the formation of N-trimethylsilyl amino acid trimethylsilyl esters leads to temporary protection of the carboxyl group, whereas the amino group was further activated due to the polarity of N-Si-Bond. This was confirmed by the use of Bis-Boc-triflyl guanidine on Lysine and on ZNH-(CH<sub>2</sub>)<sub>5</sub>-NH<sub>2</sub> with silylating reagent. In the first case we obtained guanylated product in good yield; in the second case we did not obtain any product.

The conformational properties of the D-AA scan library were initially investigated by CD in TFE 20% in water, as in our previous experiments on potentially bioactive PTH-derived peptides<sup>20</sup>. The addition of TFE<sup>21</sup>, as co-solvent to aqueous solutions of peptides, induces stabilize the  $\alpha$ -helix conformation. This "TFE effect" has been extensively applied to the

study of structure and conformation in model peptides and protein fragments<sup>22</sup>. Since short peptides form quite unstable secondary structures in aqueous solutions, the addition of TFE to the solution is often necessary to study ordered conformations. Despite the widespread use of TFE as a helix-stabilizing agent, the mechanism of its action is still widely debated. While mechanisms in which TFE binds to residues in the helical conformation and stabilizes the structure have been proposed, there is no evidence for direct interactions between TFE and hydrophobic side chains<sup>23</sup>. However, recent molecular dynamics simulations<sup>24</sup> and NMR studies<sup>25, 26</sup> suggest that TFE molecules may preferentially cluster around peptides in solution, reducing the hydration sphere around the peptide backbone. In pure water, there is a greater order of the solvent shell around the helix compared to the random coil conformation, resulting in an unfavorable entropic change upon helix formation. By disruption of hydrogen bonding between the helical peptide backbone and solvent, TFE reduces the solvent ordering which occurs upon helix formation, stabilizing the helix respect to the coil state<sup>27</sup>.

The spectra in the far-UV region were collected at room temperature. The CD spectra showed a low helix-content for analogues D4, D5, D7, D8 and D9. The CD spectra of D10, D6 and D2 seemed to present a more ordered structure. For these analogues, the presence of some contribution of  $3_{10}$ -helix or  $\beta$ -turn cannot be excluded. Finally, the spectrum of analogue D11 exhibits the typical shape of the  $\alpha$ -helical conformation, with two negative bands of comparable magnitude near 222 and 208 nm and a stronger positive band near 190 nm (fig. 2).

NMR studies were performed on all analogues. The secondary chemical shifts of the  $C^\alpha$  protons are shown in Fig.3. We observe a small effect on the structure of the peptide when a D-AA is introduced in positions 2 and 8-11. Peptide D2 maintains a relatively high helix-content possibly because of the influence of the  $C^{\alpha,\alpha}$  tetra-substituted amino acids lose to D-Val<sup>2</sup> (Aib in position 1 and 3).

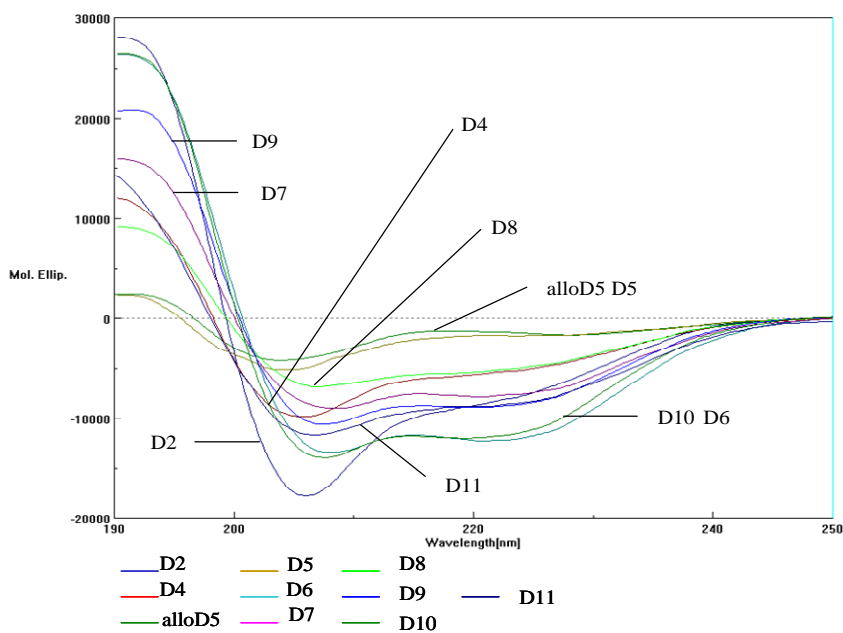


Fig.2 CD spectra of D-scan analogues of PTH(1-11).

We find a less ordered structure for the analogues modified with D-Glu<sup>4</sup>, D-Ile<sup>5</sup>, D-Leu<sup>7</sup>, D-Nle<sup>8</sup> and D-His<sup>9</sup>. This effect is maximized for D5, possible because this is the only  $\beta$ -

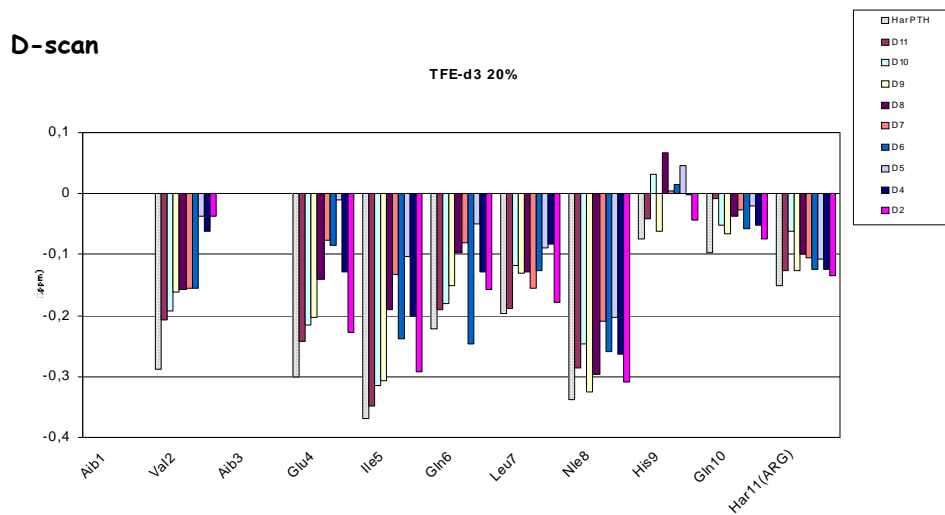


Fig.3: Secondary Chemical Shifts of PTH(1-11) analogues.  $\delta\Delta = \delta$  measured -  $\delta$  random coil



branched AA in the sequence, which is with the Aib, the most hindered amino acid. The CD analysis results and NMR studies confirm that the D-AA substitution in the D11 analogue has no effect on the  $\alpha$ -helical conformation.

The results of biological tests showed that the activity of the D-Har<sup>11</sup> analogue is of the same order of magnitude as the most active modified PTH(1-11) analogue. This behaviour is supported by our conformational analysis, where we have observed a major  $\alpha$ -helical structure only for D11. This is in agreement with previous works where a correlation between activity and helix content has been demonstrated<sup>4,20</sup>.

In general, these studies confirm the importance of residues in the (1-9) region of PTH(1-34) for biological activity. This correlation between the effects of NH<sub>2</sub>-terminal substitutions on the activities of PTH(1-14) and PTH(1-34) suggests that the shorter peptides interact with the same site in the receptor of PTH(1-34). This study also points to the importance of other residues in the N-terminal region of PTH that contribute to bioactivity. The results of biological tests showed that the activity of D11 analogue is of the same order of magnitude of the most active modified PTH(1-11). The importance of a basic, guanidine group in the C-terminal position has been shown to be independent of the configuration of C <sup>$\alpha$</sup> -carbon. In fact, studies on hormone-receptor complex, reveal the presence of H-bond between Arg11 of hormone analogue and Glu444 of receptor. This type of bond is not necessary for PTH(1-34) in which a major number of residues are present and responsible of the interaction with the receptor. In particular, the 1000-fold reduction in affinity and potency observed by the removal of Har<sup>11</sup> highlights the important role that this residue (which replaces leucine of native PTH) plays in receptor binding<sup>4</sup>. Molecular modeling suggests that this role might involve the insertion of the guanidinium side-chain group between the extracellular ends of TM1 and TM7<sup>7</sup>. In this way, in the PTH(1-11) the stabilization of this position could be critic for activity of the analogue. Recent functional<sup>28</sup> and structural<sup>29</sup> studies on PTH(1-14) analogues suggest that Gln<sup>10</sup> participates in an intramolecular side chain-side chain interaction with Gln<sup>6</sup> and thereby stabilizes local  $\alpha$ -helical structure. The loss of this putative stabilizing interaction may thus account for the lack of activity in the PTH(1-9) and other shorter analogues examined thus far.

The network of interactions that occur between the N-terminal portion of PTH and the J domain of the PTH1R is likely to be highly complex. Minimum-length PTH ligands that interact specifically with this region of the receptor, such as those described herein, should help to simplify the problem of mapping and characterizing these interactions.

### 3.2 Retro-Inverse Analogues

To investigate the properties of the N-terminal PTH pharmacophore changing only the peptide backbone, a further approach is the use of retro-inverso modifications<sup>30</sup>. In this method the L-amino acids of a peptide are exchanged with D-amino acids, and simultaneously the direction of the peptide is reversed. The topology of the side chains, with the exception of proline group, is largely maintained, and such structures are no longer substrates for proteases. The retro-inverso modification itself does not contain conformational restrictions compared with those of the native peptide. The small number of retro-inverso derivatives that actually show activity comparable to that of the original compounds indicates that the peptide backbone plays also an important role for recognition by the receptor or that there are indeed differences in the topology<sup>31</sup> of both classes of compound. Anyway, at this step of our study, we were interested to observe all possible modifications on peptide structure which are compatible with biological activity. Thus, a new micro-library was synthesized:

Name	Peptide Sequence	EC50(M)
RI	H-Har-Gln-His-Nle-Leu-Gln-Ile-Glu-Aib-Val-Aib-NH <sub>2</sub>	No Active
RII	H-Abu-Gln-His-Nle-Leu-Gln-Ile-Glu-Aib-Val-Aib-NH <sub>2</sub>	No Active
RIII	H-Amc-Gln-His-Nle-Leu-Gln-Ile-Glu-Aib-Val-Aib-NH <sub>2</sub>	No Active

Tab. 2 List of retro-inverse analogues of PTH(1-11)

The synthesis of retro-inverso series presented a problem of hindered amino acid near the solid support. The aggregation phenomena of the growing peptide chain are a problem which may complicate the synthesis. In the first step of the synthesis a C<sup>α</sup>-tetra-substituted

amino acid was coupled to the resin and the following one was Val which is also hindered and lipophilic amino acids<sup>32</sup>.

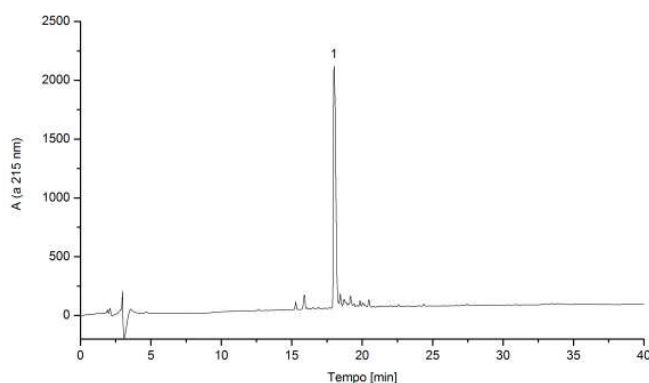


Fig. 3:  
Chromatogram  
of one of three  
analogues  
retroinverse of  
PTH(1-11) at  
215 nm

In order to test the loading of the resin after the first coupling we followed the reaction using Fmoc Absorbance test. A known amount of resin is cleaved directly in the cell and then the absorbance of Fluorenyl group, cleaved from the resin, is measured at 290 nm. The concentration of free Fluorenyl group is directly proportional to Aib coupled to resin. We observed that a double coupling of Aib with HATU and HOAt in presence of 2, 4, 6, collidine as base, the more efficient coupling reagents for SPPS, introduced by L. Carpino<sup>33</sup>, yielded a good loading of resin. For reasons not clear, 2,4,6-collidine as a base appears to be particularly suitable for systems derived from HOAt<sup>34</sup>. However, we observed that a third coupling was able to remove partially the Fmoc protective group on the first Aib. This event was observed by MS analysis where the signal of FmocAibAibNH<sub>2</sub> was detectable. To have a better coupling yield a double coupling and intermediate acetylation to block deleted growing chains were performed.

From the HPLC analysis of crude peptide, it was possible to detect a good yield and an efficient synthesis of the retro-inverse peptides (fig. 3).

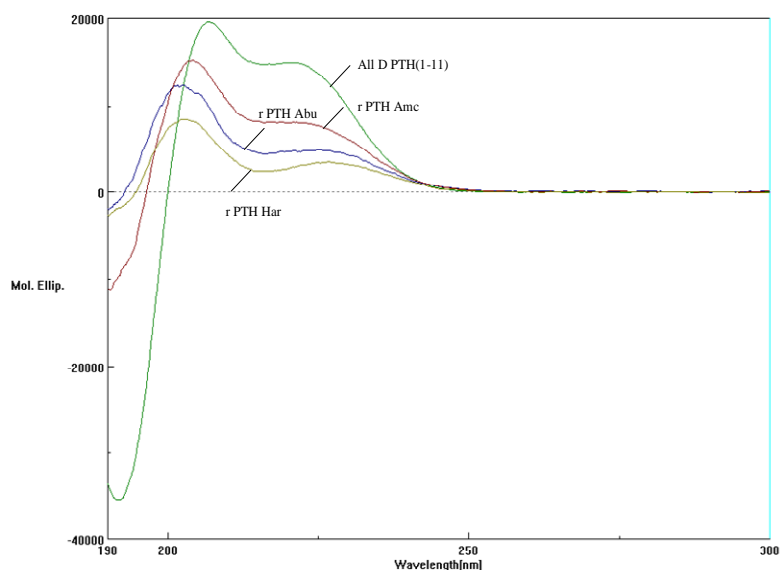


Fig. 4 series of retro-inverse analogues of PTH(1-11).

After purification of the crude peptides by HPLC, CD spectra were recorded to determine the conformation. We used as reference the CD spectrum of peptide H-Aib-Val-Aib-Glu-Ile-Gln-Leu-Nle-His-Gln-Har-NH<sub>2</sub> with inverted sign (fig. 4).

Retro-inverse peptides exhibited an ordered structure but no  $\alpha$ -helix structure, which is a requirement to activate the receptor. The biological tests confirmed the low activity of these analogues (fig. 5).

The lack of  $\alpha$ -helix structure could be due to the absence of C <sup>$\alpha$</sup> -tetra-substituted amino acids in N-terminal position. The Aib and analogues of its family are well known to be the most effective peptide 3<sub>10</sub>/ $\alpha$ -helix formers and stabilizers<sup>35</sup>.

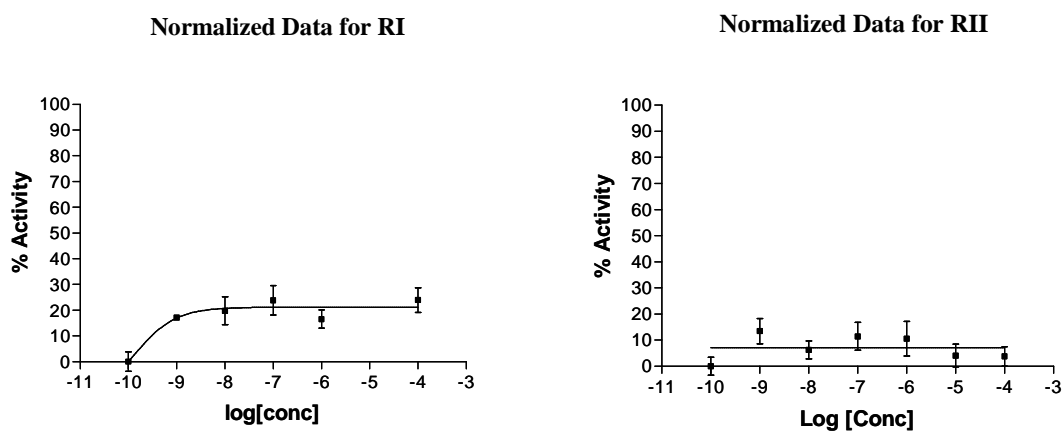
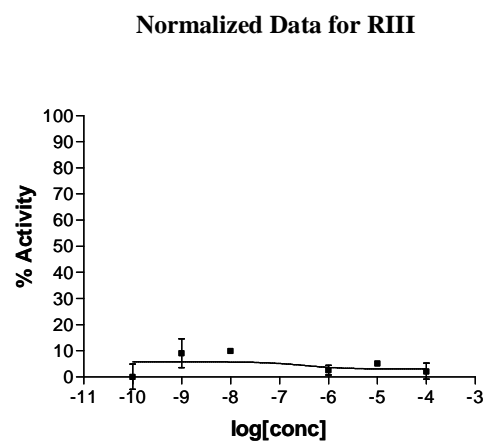


Fig. 5 Full Dose Response of Retro-inverse analogues of PTH(1-11). It is possible to observe that the activity value versus concentration is very low.



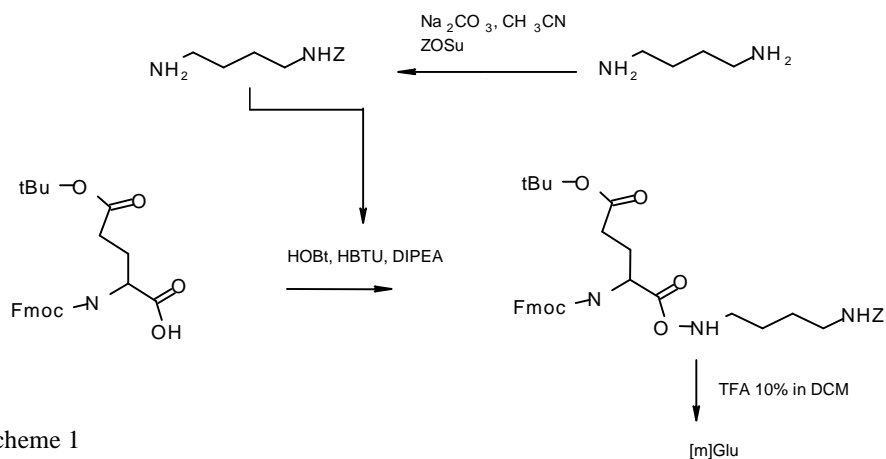
### 3.3 Diamine analogues

From biological and CD data of D-Scan, we can hypothesize that guanidine group at the C-terminal position has an important role in bioactivity. In order to investigate the role of positive charge at the C-terminus and the effective role of Aib in N-terminal position to form the helix of the peptides we synthesized another series of analogues which presented in C-terminal position a first example of peptidomimetics for homoarginine:

Name	Peptide Sequence	EC50(M)
RP	H-Aib-Val-Aib-Glu-Ile-Gln-Leu-Nle-His-Gln-Har-NH <sub>2</sub>	1E-09
K	H-Aib-Val-Aib-Glu-Ile-Gln-Leu-Nle-His-Gln-Lys-NH <sub>2</sub>	5E-08
n=4	H-Aib-Val-Aib-Glu-Ile-Gln-Leu-Nle-His-Gln NH(CH <sub>2</sub> ) <sub>4</sub> NH <sub>2</sub>	No Active
n=5	H-Aib-Val-Aib-Glu-Ile-Gln-Leu-Nle-His-Gln NH(CH <sub>2</sub> ) <sub>5</sub> NH <sub>2</sub>	1E-07
n=6	H-Aib-Val-Aib-Glu-Ile-Gln-Leu-Nle-His-Gln NH(CH <sub>2</sub> ) <sub>6</sub> NH <sub>2</sub>	2E-07

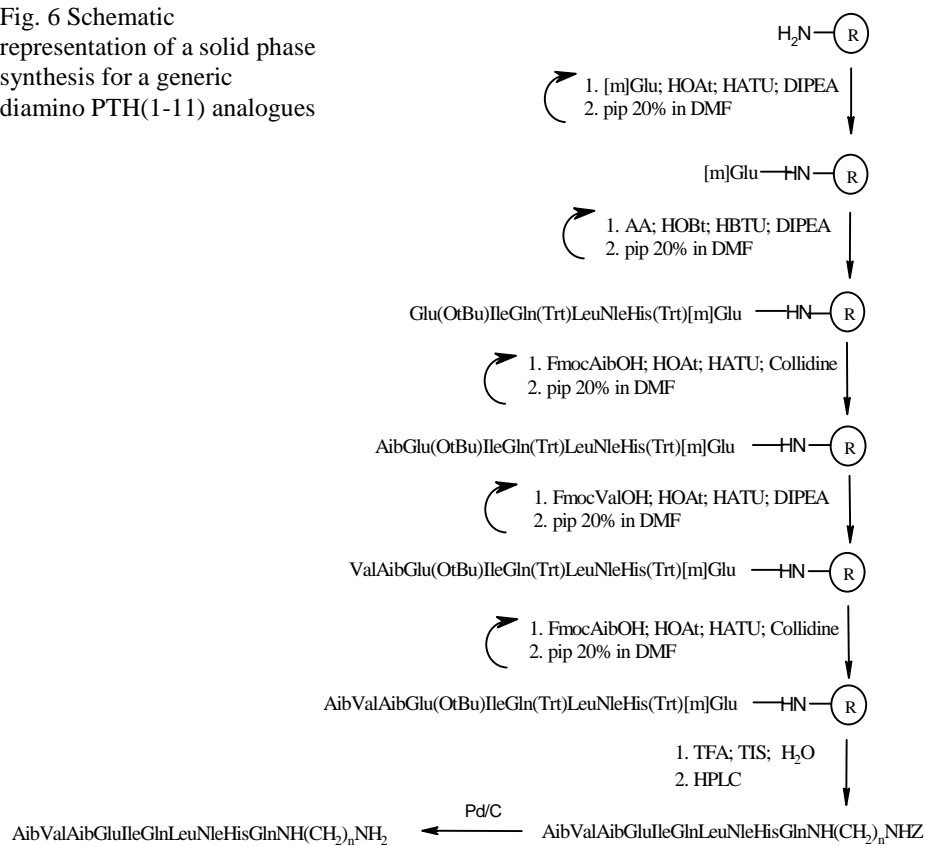
Tab. 3 it is shown diamine analogues. All peptides were tested at Tuft University by Dr Angela Wittelsberger. The experimental error on the measurement is 15%.

The PTH(1-11) analogue containing Lys was synthesized as internal reference in the series. In the literature it was reported that an analogue of PTH(1-14) was active a very similarly to the arginine analogue<sup>11</sup>. The synthesis of mimetic of Homoarginine was carried out in solution modifying Glu to obtain a new functionalized amino acid orthogonally protected to use in solid phase synthesis. We started from the bi-functional properties of Glu, which has two Carboxylic groups that can be use to anchor the amino acid and the growing chain to the solid support. Thus, the synthetic approach followed was report in Scheme 1. One carboxylic function of Glu could be used to bind a diamine chain, and  $\epsilon$ -COOH could used to anchor the amino acid to resin. In this way, a little library can be synthesized to explore the length of carbonic chain which separates the peptide backbone from positive charge. The lengths were n=4, 5 and 6. The first diamine was the mimetic of side chain of Ornitine, the second one of Arginine and the third of homoarginine, without the guanidine group. The diamine was protected with an orthogonal group which was compatible with both acidic and basic conditions of the synthesis of analogues.



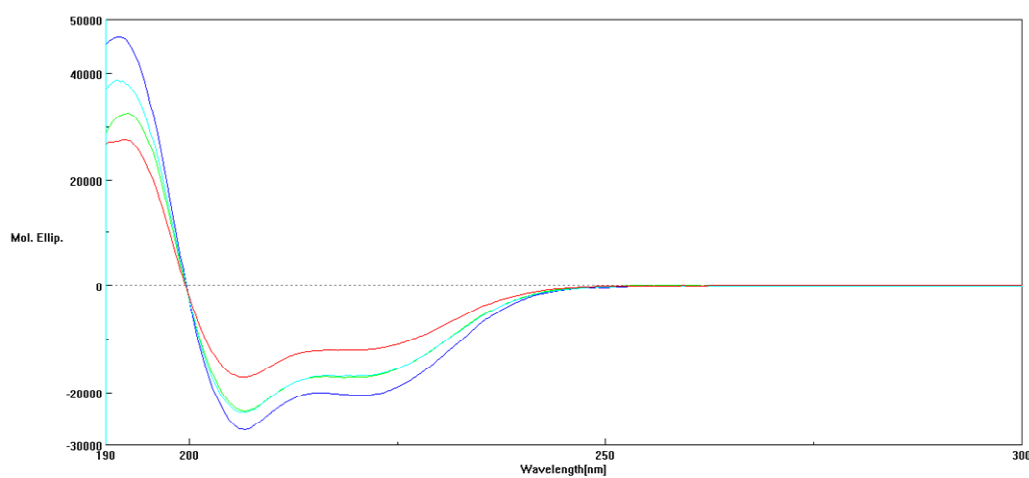
The protective group was carbobenzoxy group (Z). It allows a complete protection and an easy cleavage in very bland condition at the end of the synthesis.

Fig. 6 Schematic representation of a solid phase synthesis for a generic diamino PTH(1-11) analogues



The amine was coupled to the  $\alpha$ -COOH of Glu in solution with normal peptide coupling reagents. Then the modified amino acid was coupled to the resin and the synthesis was carried out on the solid support, in normal condition of SPPS.

After HPLC purification, a CD study with biological tests was made. From the CD spectra it was possible to observe a presence of  $\alpha$ -helix.



- Aib Val Aib Glu Ile Gln Leu Nle His Gln Lys-NH<sub>2</sub>
- Aib Val Aib Glu Ile Gln Leu Nle His Gln NH(CH<sub>2</sub>)<sub>4</sub>NH<sub>2</sub>
- Aib Val Aib Glu Ile Gln Leu Nle His Gln NH(CH<sub>2</sub>)<sub>5</sub>NH<sub>2</sub>
- Aib Val Aib Glu Ile Gln Leu Nle His Gln NH(CH<sub>2</sub>)<sub>6</sub>NH<sub>2</sub>

Fig. 7 CD spectra of diamino analogues of PTH(1-11)

A complete comparison of the CD spectra of direct peptides versus retro-inverso peptide confirmed that the lack of helix structure was caused by the absence in N-terminal position of Aib residue (fig. 7).

For the diamine analogues, it is possible to observe that there is a residual activity. The structure is an ordered one similar to  $\alpha$ -helix, with typical minimum at 208 and 222 nm. The minor activity could be related to the absence of amide C-terminal group of peptides or the absence of chirality of the C-terminal residue. The arginine mimetics are not chiral.



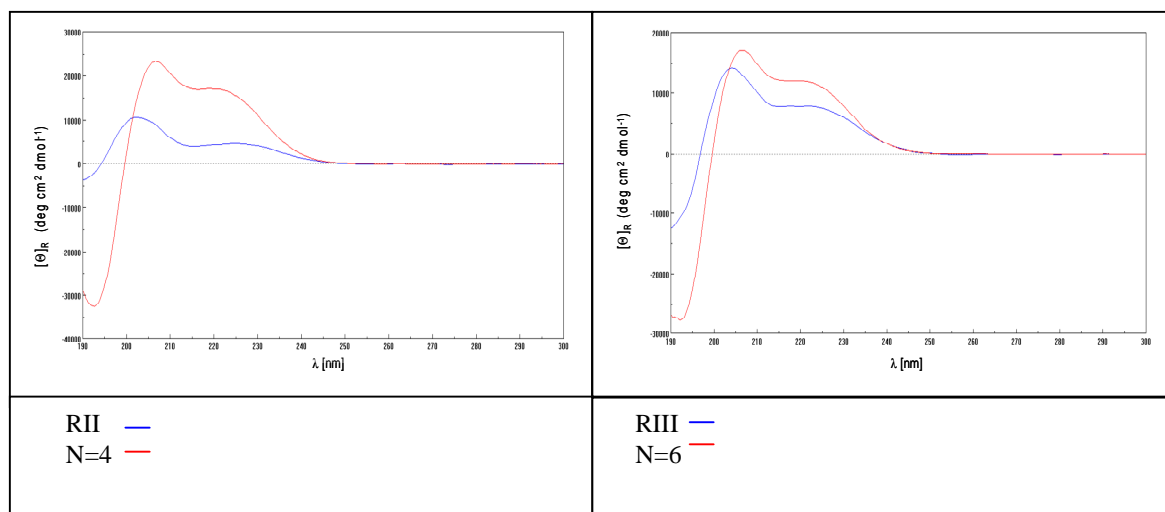


Fig. 8 CD spectra of retro-inverso analogues vs linear analogues of PTH(1-11)

### 3.4 Peptoids

The peptoids<sup>2</sup>, which are oligomeric peptides analogues, are compounds containing N-alkylated glycines connected together in a peptide-like manner, in which the  $\alpha$ -CHR side chains have been moved on NR units, consequently the NH groups (of the peptide bond) become tertiary amines. The positions of the side chains and carbonyl groups of the original peptide chain (**I**) remain unchanged, as can be seen from the comparison with the peptoid chain (**II**) (Fig. 9).

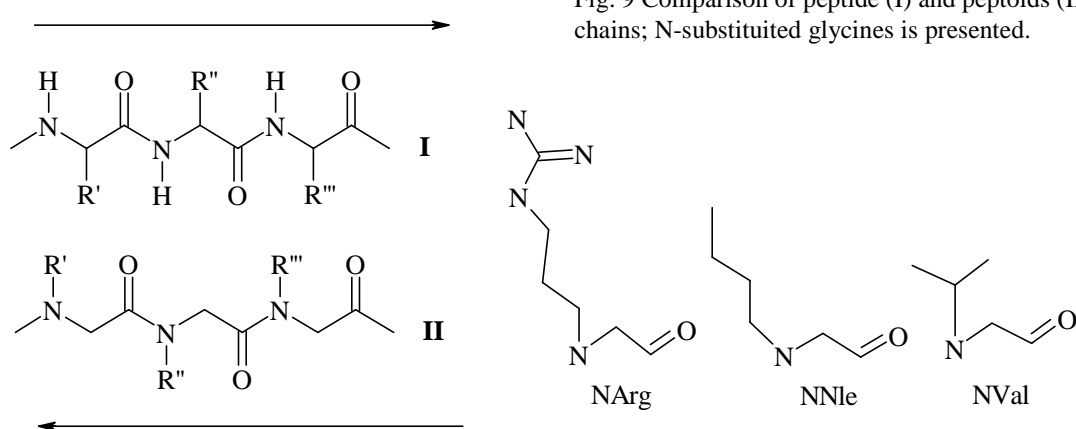


Fig. 9 Comparison of peptide (**I**) and peptoids (**II**) chains; N-substituted glycines is presented.

We synthesized three hybrids (table 4) where only one amino acid was replaced by the corresponding N-substituted amino acids. In these peptoid-peptide hybrids the identity of the side chain was preserved. These compounds might be considered a combination of backbone and side chain modifications. We started to investigate the role of the side chain of Val at position 2, of Nle at position 8, and we used the peptoid residue to define role of Arg at position 11 in the interaction of short PTH fragments with PTH1R.

Name	Peptide Sequence	EC50(M)
NVal	H-Ala- <b>NVal</b> -Aib-Glu-Ile-Gln-Leu-Nle-His-Gln-HarNH <sub>2</sub>	No Active
NNle	H-Aib-Val-Aib-Glu-Ile-Gln-Leu- <b>NNle</b> -His-Gln-HarNH <sub>2</sub>	No Active
NArg	H-Aib-Val-Aib-Glu-Ile-Gln-Leu-Nle-His-Gln- <b>NArg</b> NH <sub>2</sub>	2.0E-6

Tab. 4

For peptide with NVal in position 2, we replaced Aib in position 1 with Ala due to steric hindrance caused by N-alkylglycine. All peptides were tested at Tuft University by Dr Angela Wittelsberger. The experimental error is 15%.

Peptide-peptoid hybrids were synthesized using a combination of standard Fmoc solid-phase peptide synthesis for amino acid residues<sup>33, 34, 36</sup> and of the submonomer approach for N-substitute glycine residues. The required N-substituted glycine residues, NVal, NNle and NArg, were obtained by Prof.ssa L. Biondi, and were synthesized according to the procedure reported in literature<sup>37, 38</sup>.

The CD spectra of hybrids are shown in figure 10. Peptide-peptoid hybrid **NArg** shows a typical  $\alpha$ -helix CD spectrum, similar to the CD spectrum of the reference peptide (fig. 10 B), with the helix content increasing at increasing concentrations of TFE (fig. 11).

This was consistent with the presence of biological activity for NArg<sup>11</sup>, even if lower by 3 orders of magnitude, which could be related to a wrong length of carbonic chain. Hybrid **NVal** (fig. 10 A) was not biologically active. It is possible to observe an ordered structure which doesn't exclude the presence of some contribution of  $3_{10}$ -helix or  $\beta$ -turn. The introduction of NVal<sup>2</sup> at the N-terminal position might forbid initial organization of helix, and it is possible that the side chain of Val was not pointed to the correct direction to interact with the receptor. Peptide-peptoid hybrid **NNle** showed a CD spectrum typical of a

flexible and extended structure. The introduction of this peptoid disrupted the helix structure and also canceled the biological activity (fig. 10 C).

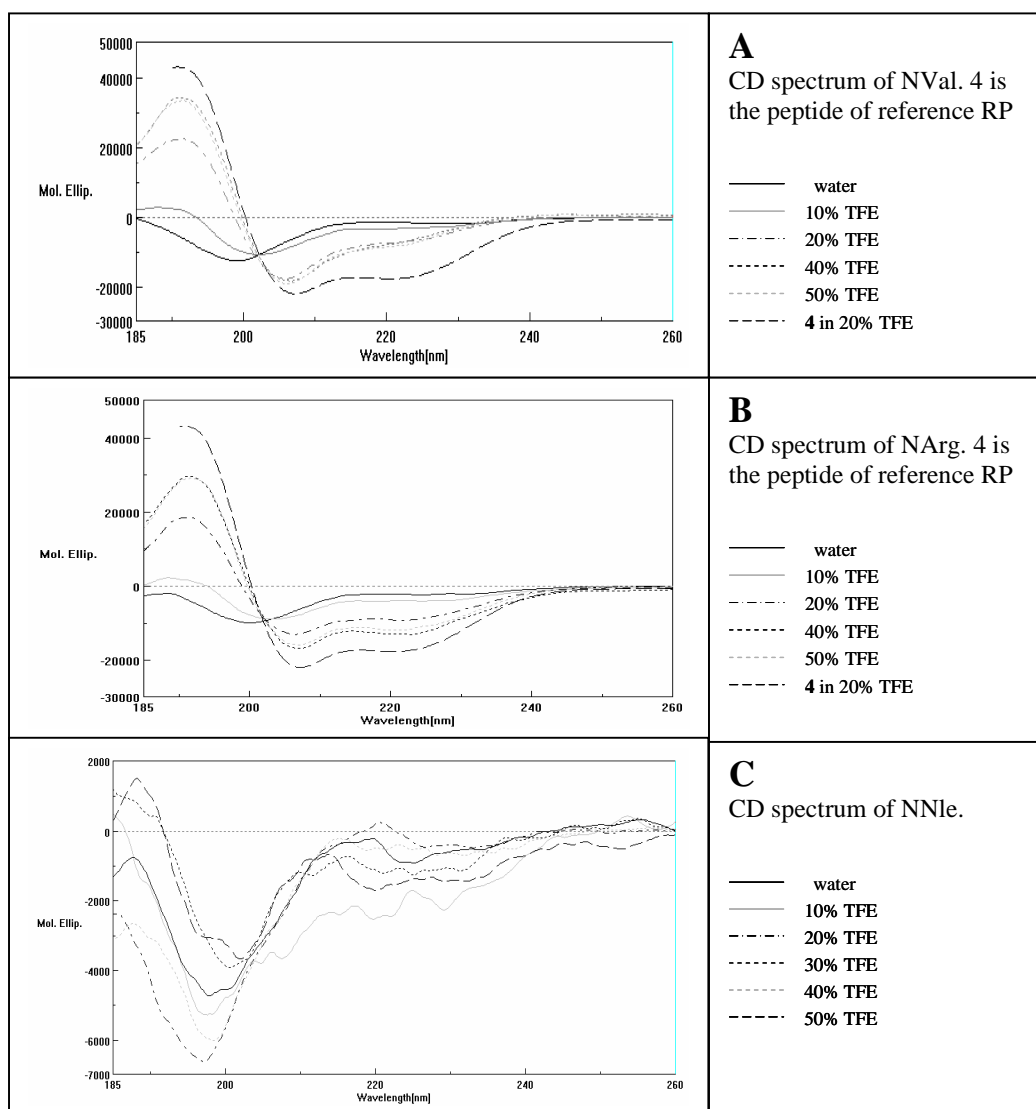


Fig. 10. CD spectra of Peptoid-peptide hybrids at various TFE concentrations.

Shifting the side chain to the amide nitrogen creates a tertiary amide, thus favoring *cis-trans* isomerism. This shift results in increased flexibility, proteolytic stability, and lipophilicity of an oligomer but also reduces the H-bonding capacity, all of which may affect biological activity and bioavailability of a peptoid ligand as compared to peptides of similar structure<sup>39</sup>.

The side-chains shift in peptide-peptoid hybrids could change the placement of the N-substituted glycine side chain by approximately 30° in three-dimensional space, as compared with the analogous amino acid side chain<sup>40</sup>. For the peptide-peptoid hybrids, the side-chains shift may also perturb the topological orientation of the adjacent amino acid side chains, thus placing both the N-substituted glycine side chain and the adjacent amino acid side chain in a three-dimensional arrangement unfavourable for receptor activation<sup>41</sup>.

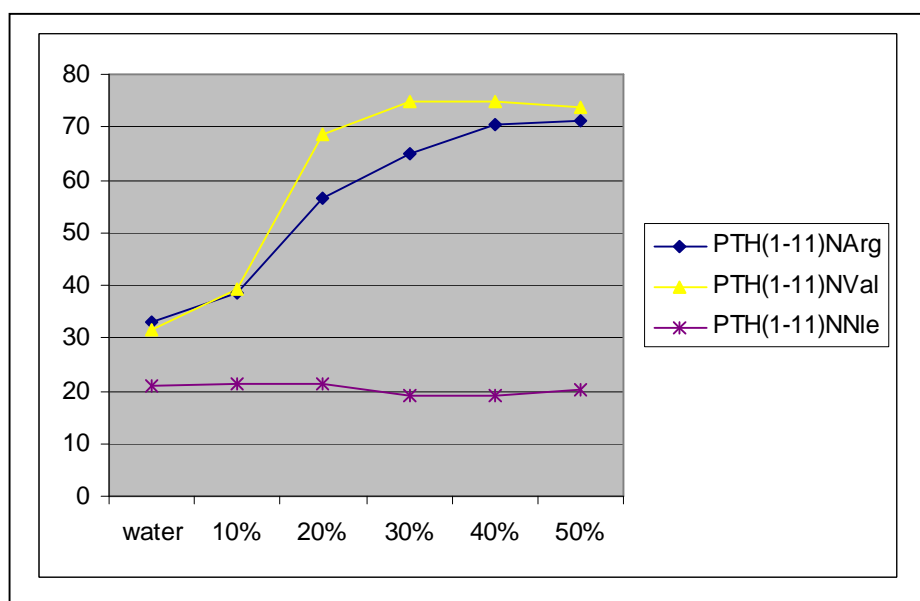


Fig. 11 Effect of percentage of  $\alpha$ -helix versus concentration of TFE

The low activity of the hybrids might result from the decrease in hydrogen binding ability of the peptoid compounds. The reduced ability of peptoid residues to form intramolecular hydrogen bonds also decreases their capability to form regular structural motifs. Secondary structures, such as helices, are known to be stabilized by intramolecular H-bonds<sup>42</sup>. Additionally, the activity of the peptoid oligomers may be explained by considering that shifting the side chain from the  $\alpha$ -carbon to the amide nitrogen allocates the side chain in an unfavourable topological position<sup>36</sup>.

The present work confirms the result<sup>4, 10, 11</sup> of preliminary hierarchical approach carried out by Gardella and co-workers. There is a functional intolerance of the residues in the (1-9)

region, especially for Val<sup>2</sup>, Ile<sup>5</sup>, and Met<sup>8\*</sup>, consistent with the hypothesis that NH<sub>2</sub>-terminal residues of PTH interact with the transmembrane helices and/or extracellular loops of the receptor. But some of substitutions, such as Nle→Met<sup>8</sup> or Har→Leu<sup>11</sup>, might induce a more favourable peptide conformation or other ones might introduce more favourable side chain interactions with the receptor.

### 3.5 C<sup>α,α</sup>-tetra-substituted amino acid analogues

#### 3.5.1 PTH(1-11) analogues containing αMeVal

From computer simulation studies carried out in our laboratory<sup>7</sup>, the interaction in proposed mechanism involves the binding of PTH N-terminus residue to the receptors. Since the N-terminal residues from first to sixth of the short length PTH(1-14) analogues were found to be very critical for receptor activation, we tried to rigidify the structure. Our previous works<sup>20</sup>, present literature results<sup>4, 10, 11, 43</sup> suggested that the α-helical structure was a prerequisite for proper binding and activation of the PTH/PTH1R.

C<sup>α,α</sup>-tetra-substituted amino acids are known as a effective peptide 3<sub>10</sub>/α-helix formers and stabilizers<sup>34</sup>, because of the Thorpe-Ingold effect<sup>44, 45, 46</sup>. Recently, it was demonstrated that the presence of a single C<sup>α</sup>-tri-substituted residue close to the N-terminus favoured the formation of α-helical structure in the central region<sup>35</sup>. In the same work, it was demonstrated that even in the case of a very high percentage of C<sup>α</sup>-tetra-substituted amino acids, the precise positioning of the single C<sup>α</sup>-tri-substituted residue in the sequence may have a dramatic effect on the helical structure of peptide backbone. More specifically, incorporation of the guest residue near the N-terminus seems to be critical for the conformational transition<sup>34</sup>. We<sup>20</sup> and other researchers<sup>43</sup> have demonstrated that wild type sequence of PTH(1-11) showed clearly in solution a stable α-helix formed from Ser<sup>3</sup> to Leu<sup>11</sup> residue.

In order to stabilize helical structure from the first residue and to understand completely the role of the Val in position 2 in the interaction of short PTH fragments with PTH1R, we synthesized a new series of analogues of the most active modified PTH(1-11), H-Aib-Val-

---

\* The only substitution well tolerated is Nle instead of Met, probably because of isosteric proprieties of Met toward Nle residue.

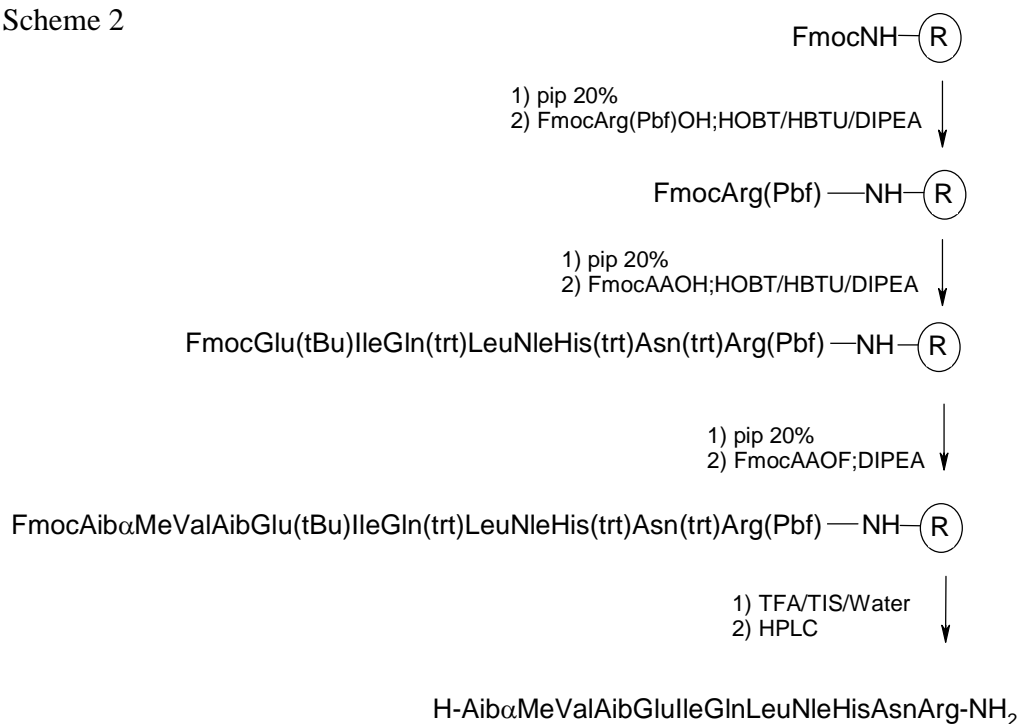
Aib-Glu-Ile-Gln-Leu-Nle-His-Asn/Gln-Arg/Har-NH<sub>2</sub>, containing sterically hindered and helix-promoting C<sup>α</sup>-tetra-substituted amino acids, Aib and αMeVal.

Name	Peptide Sequence	EC50(M)
AMEVAL1	Aib- <b>αMeVal</b> -Aib-Glu-Ile-Gln-Leu-Nle-His-Gln-Har-NH <sub>2</sub>	1E-05
AMEVAL2	Ac5c- <b>αMeVal</b> -Aib-Glu-Ile-Gln-Leu-Nle-His-Gln-Har-NH <sub>2</sub>	6E-06
9	Aib- <b>αMeVal</b> -Ser-Glu-Ile-Gln-Leu-Nle-His-Gln-Arg-NH <sub>2</sub>	No active
11	Ala- <b>αMeVal</b> -Ser-Aib-Ile-Gln-Leu-Nle-His-Gln-Arg-NH <sub>2</sub>	No active
12	Ala- <b>αMeVal</b> -Aib-Glu-Ile-Gln-Leu-Nle-His-Gln-Arg-NH <sub>2</sub>	No active
13	Aib- <b>αMeVal</b> -Aib-Glu-Ile-Gln-Leu-Nle-His-Gln-Arg-NH <sub>2</sub>	7E-05

Tab. 5 Library of PTH(1-11) analogues containing αMeVal. All peptides were tested at Tuft University by Dr Angela Wittelsberger. The experimental error is 15%.

The peptides have been synthesised by SPPS. To maximize the total yield, a combined HBTU/HOBt/DIPEA and acyl fluoride coupling method was used and a general solid-phase synthesis of PTH(1-11) containing αMeVal is outlined in Scheme 2. The analogues were prepared using Fmoc methodology with Rink Amide MHBA Resin (Novabiochem) (0.73 mmol/g loading) as a resin. The side-chain protecting groups were compatible with the Fmoc methodology. The αMeVal was prepared as Fmoc-αMeVal-OF. The first amino acid was anchored to the resin using the HBTU/HOBt/DIPEA protocol; the most common peptide coupling additive is HOBt, used either as a carbocation with another coupling agent or incorporated into a stand-alone reagent such as an uronium salt<sup>33, 35, 36</sup>. Such additions generally inhibit side reactions and reduce racemates. In this case, we used HOBt as an auxiliary nucleophile. Deprotection of amino groups was achieved under standard conditions, with 20% piperidine solution in NMP. The Fmoc-αMeVal-OF was used with an excess of 3 eq., with an eq. of DIEA<sup>47</sup>. The coupling time was 2h and repeated two times. The following amino acid was introduced on resin with the same protocol.

Scheme 2



The acid fluoride technique is frequently recommended in peptide coupling reactions of extremely hindered amino acids<sup>48</sup>. Since amino acid fluorides showed a better stability towards moisture and acid-labile functional groups than amino acid chlorides<sup>49</sup>, several acid fluorinating reagents were developed. Fmoc amino acid fluorides, shown to be rapidly acting species for peptide synthesis in solution or for the SPPS of simple peptides, were also expected to be useful for solid phase synthesis of more complicated, longer peptides and for coupling of sterically hindered units, such as C<sup>α</sup>-tetra-substituted amino acids<sup>50</sup>. Moreover for sterically hindered amino acids, such as MeAib or Iva, the acid fluoride method gave excellent yields in peptide coupling reactions<sup>51, 52</sup>.

The conformational properties of the series of peptides were initially investigated by CD in TFE 20% in water<sup>20</sup>. CD spectra in the far-UV region were collected at room temperature and are shown in Figure 12.

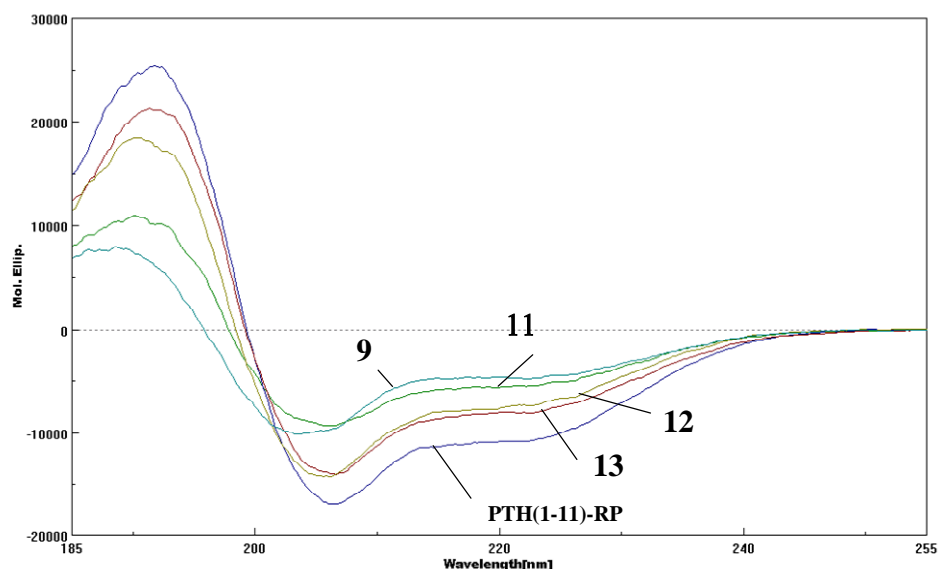


Fig. 12 The CD spectra of the five analogues in aqueous solution containing 20% TFE (v/v) show a clear correspondence between the number of substitutions with C<sup>α</sup>- tetra-substituted amino acids and helix content of the peptides. Peptides **9** - **13** exhibit a CD pattern of the helical conformation, and analogue **PTH(1-11)-RP** shows the highest helix content.

The spectrum of analogue PTH(1-11)-RP taken as reference peptide, exhibited the typical shape of the  $\alpha$ -helical conformation, with two negative bands of comparable magnitude near 222 and 208 nm and a stronger positive band near 190 nm. For analogue PTH(1-11)-RP, the  $\alpha$ -helix content was estimated at 68%.<sup>25</sup> Other analogues are characterised by negative bands at ~200 nm, showing a lower content of ordered structure with respect to reference peptide. Analogues **12** and **13** exhibit a similar band of reference peptide, but with lower intensity. However, the shape of these curves does not exclude the presence of some contribution of  $\alpha$ -helix or  $3_{10}$ -helix for these analogues, as well as the co-presence of two or more conformations. The right-handed  $3_{10}$ -helical peptide displays a negative CD band at 207 nm, accompanied by a shoulder centred near 222 nm. The ratio  $R = [\theta]_{222}/[\theta]_{207}$  is 0.4<sup>53</sup>.

NMR spectra were recorded at 298 K in a 2mM solution containing 20% TFE (v/v). In all analogues, collected even PTH(1-11) analogues containing D-Val and NVal, the chemical shifts differences<sup>54</sup> of  $\alpha$ CH protons with respect to the corresponding random coil values identify a helical segment spanning the sequence from residue Aib<sup>1</sup> to Nle<sup>8</sup>.



## Secondary Chemical Shifts ( $\Delta\delta = \delta_{\text{measured}} - \delta_{\text{random coil}}$ )

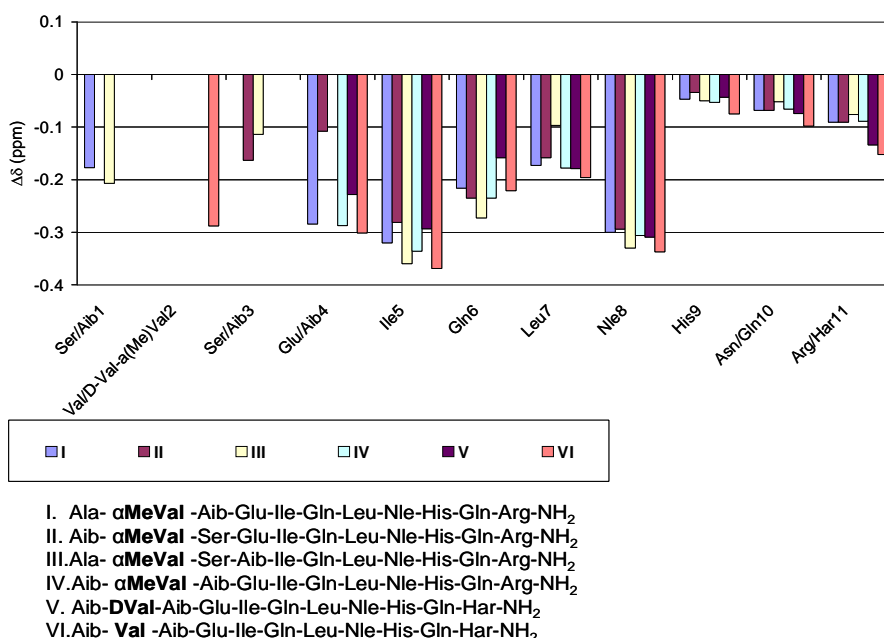


Fig. 13 In all analogues,  $\delta\Delta < -0.1$ ppm identify a helical segment spanning the sequence from residue Aib<sup>1</sup> to Nle<sup>8</sup>.

In the ROESY spectra, a number of  $\alpha\text{H}(i)\text{-HN}(i+3)$ ,  $\alpha\text{H}(i)\text{-}\beta\text{H}(i+3)$  and  $\alpha\text{H}(i)\text{-HN}(i+4)$  connectivities typical of the  $\alpha$ -helix were observed in all analogues (see Appendix C). For analogues **I** and **IV** even the first residue is comprised in the helical segment. Superimposition of the ensembles of the low energy structures resulting from distance geometry and molecular dynamics calculations indicated a clear higher convergence towards the helical structure of the analogues **I - IV**, compared to the native one. For the analogue **I** there was a reduction in angle dispersion even for residues 2 and 3. Analogue **IV** did not show the same behaviour, probably because of some critical overlapped connectivities.

The introduction of Aib at position 1 and 3 increased helix stability and consequently a best activity was detected. Analogues containing C <sup>$\alpha,\alpha$</sup>  tetra-substituted amino acid  $\alpha$ MeVal exhibited a very low activity even in the presence of an ordered structure compatible with  $\alpha$ -helix according to ROESY data.

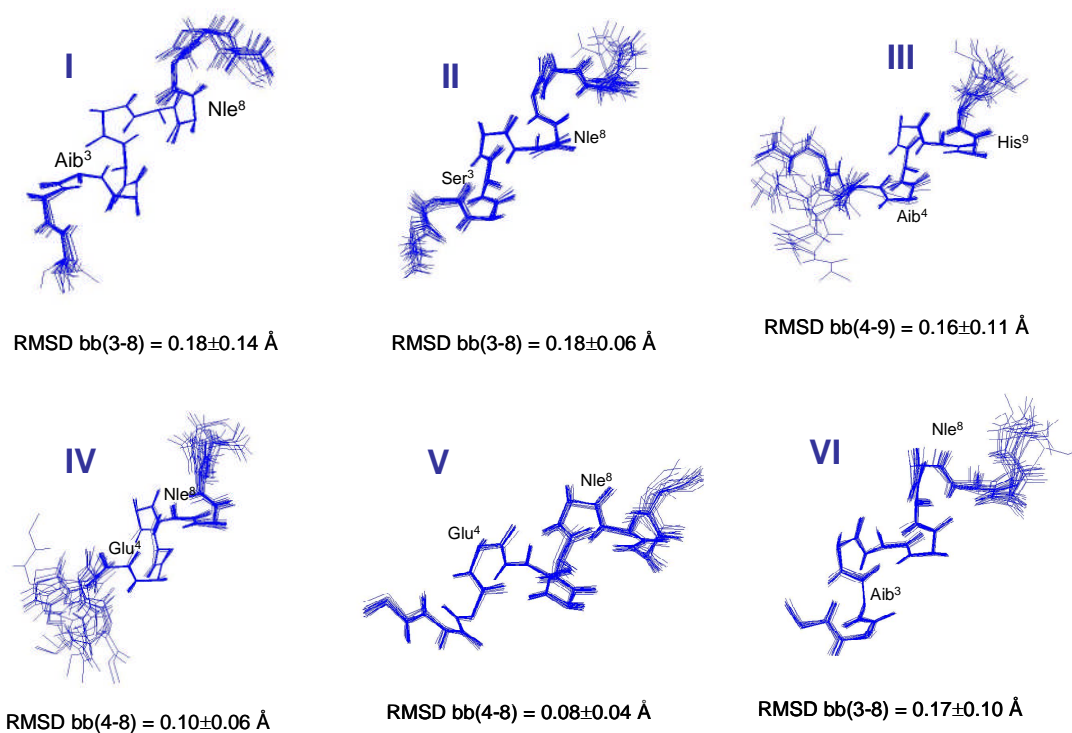


Fig. 14 Superimpositions of the lowest energy calculated structures of Analogues I-VI. It is interesting to observe how that D-Val (V) might orient  $\text{NH}_2$  terminus in a not correct direction.

From our studies, for these analogues it is not possible to exclude  $3_{10}$  helix presence in helical structure, according to CD spectra with a strong absorbance near to 200 nm, although in MD we observe a convergent helical structure for analogues from **I-IV**. But analogue **IV** shows a CD spectra where the contribution of  $\alpha$ -helix is very low (35 %) confirming the possibility that the structure might have a contribution of  $3_{10}$  helix.

The role of Val<sup>2</sup> is demonstrated fundamental in the activation of the receptor. In fact, the only change of chirality reduces of three orders of magnitude the activity, or the simple shifting of side chain on tertiary nitrogen transforms the peptide in no active one. In other words, if the structure is forced to assume a  $3_{10}$  helix in the first N-terminal segment, there is a loss or a reduction of activity. We can conclude that Val in position 2 is strategic and is not possible to modify this residue and its orientation.

### 3.5.2 PTH(1-11) analogues containing $\alpha$ MeNle

In order to investigate the role of  $\alpha$ -helicity in the interaction of short PTH fragments with PTH/PTH1R, a new series of PTH(1-11) analogues containing sterically hindered and helix-promoting C $^{\alpha}$ -tetra-substituted amino acids was synthesized. It has been demonstrated that the structural order of residues 1-4 plays a significant role in PTH action<sup>43</sup>; in order to stabilize the helical structure,  $\alpha$ (Me)Nle was inserted at position 8. It is known that replacement of Met<sup>8</sup> with Nle in PTH is well tolerated, with no loss of binding affinity.

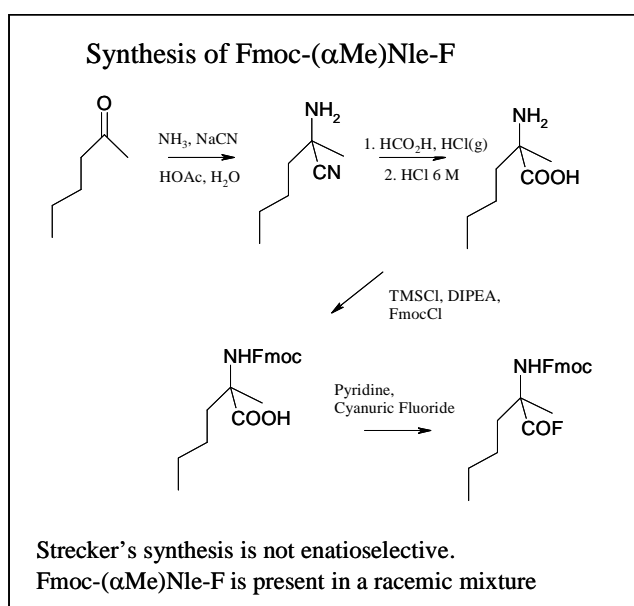
Name	Peptide sequence	EC50 (M)
<b>RP</b>	Aib-Val-Aib-Glu-Ile-Gln-Leu-Nle-His-Gln-Arg-NH2	1.0E-09
<b>AMeLAla3</b>	Aib-Val-Ala-Glu-Ile-Gln-Leu-L( $\alpha$ Me)Nle-His-Gln-Arg-NH2	//
<b>AMeDAla3</b>	Aib-Val-Ala-Glu-Ile-Gln-Leu-D( $\alpha$ Me)Nle-His-Gln-Arg-NH2	//
<b>AMeLAla1</b>	Ala-Val-Aib-Glu-Ile-Gln-Leu-L( $\alpha$ Me)Nle-His-Gln-Arg-NH2	//
<b>AMeDAla1</b>	Ala-Val-Aib-Glu-Ile-Gln-Leu-D( $\alpha$ Me)Nle-His-Gln-Arg-NH2	//
<b>AMeLAib1,3</b>	Aib-Val-Aib-Glu-Ile-Gln-Leu-L( $\alpha$ Me)Nle-His-Gln-Arg-NH2	2.0E-08
<b>AMeDAib1,3</b>	Aib-Val-Aib-Glu-Ile-Gln-Leu-D( $\alpha$ Me)Nle-His-Gln-Arg-NH2	2.7E-07

Tab. 6 Library of PTH(1-11) analogues containing  $\alpha$ MeNle. All peptides were tested at Tuft University by Dr Angela Wittelsberger. The experimental error is 15%.

The hydrophobic side chain of Nle<sup>8</sup> appears to be critical for the interaction with the receptor, and in the computer-based models for the PTH/PTH1R complex residue 8 is found in a deep hydrophobic cleft<sup>7</sup>.

The synthesis of  $\alpha$ MeNle was carried out following the Strecker's Amino Acids Synthesis Protocol, starting from the corresponding Ketone (fig. 15). Strecker's synthesis yields the racemic mixture. Thus, we studied the structural properties of PTH(1-11) analogues of analogues containing either L or D Nle.

Fig. 15



Attempts to resolve the racemic mixture failed, and we decided to insert the  $\alpha$ MeNle directly into sequence and resolve the diastereomeric mixture at the end of the peptide synthesis. Thus, the peptides were synthesised by SPPS employing Fmoc-protected amino acids. To maximize the total yield, we combined the HBTU/HOBt/DIPEA and the acyl fluoride coupling methods<sup>47</sup>. The latter was used to incorporate the C $^{\alpha}$ -tetra-substituted amino acids and the next amino acids in sequence.

The mixture of D/L  $\alpha$ MeNle analogues of PTH(1-11) was resolved by HPLC in good yield and purity (fig. 16). Unfortunately, because of the difficulty of couplings in SPPS, the total yield was low.

Scheme 4

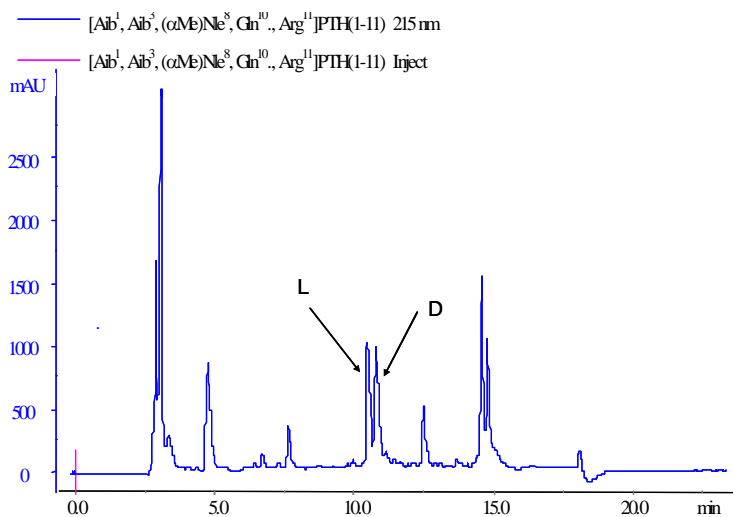
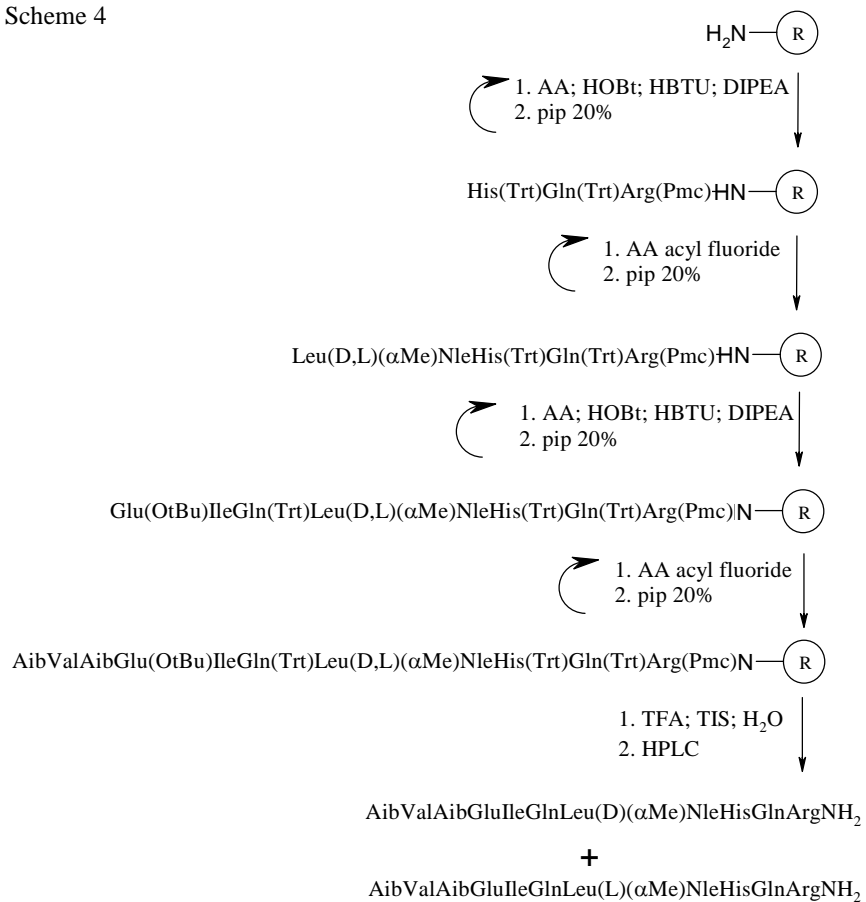


Fig. 16 HPLC of crude material of PTH(1-11) containing racemic αMeNle

The CD spectra of the all analogues of PTH(1-11) in aqueous solution containing 20% TFE (v/v) at peptide concentration of 1mM show the typical CD pattern of the  $\alpha$ -helical conformation (fig. 17 ), with a helix content in the range of 35-55% (calculated according to reference<sup>55</sup>). The helix contents are always higher than that of the native sequence.

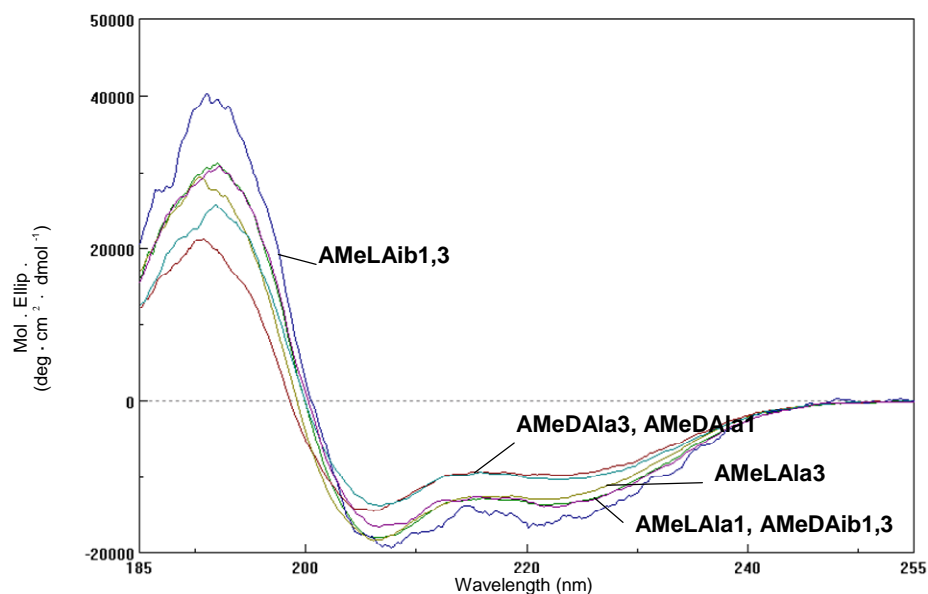


Fig. 17 CD spectra in aqueous solution containing 20% TFE(v/v) at ~1mM peptide concentration

NMR spectra were recorded at 298 K in a 1 mM solution containing 20% TFE (v/v). In general, the chemical shifts differences of the  $\alpha$ CH protons with respect to the corresponding random coil values confirm the higher tendency toward the helical ordered structure relative to PTH(1-11). Moreover, from analogue **I** to analogue **VI** there is an increasing tendency to stabilize the helical segment, especially for residues 2 and 4, indicating the presence of ordered structure even in the very first segment (Fig. 18). The same tendency can be observed in the CD spectra, where the characteristic minima of  $\alpha$ -helix (208 nm and 222 nm) are underlined. Moreover, in the ROESY spectra, a number of  $\alpha$ H(i)-NH(i+3),  $\alpha$ H(i)- $\beta$ H(i+3) and  $\alpha$ H(i)-NH(i+4) connectivities typical of the  $\alpha$ -helix were observed in all analogues. According to the ROE tables, the analogues of PTH(1-11) that differ only in the configuration of residue 8, adopt the same structure.

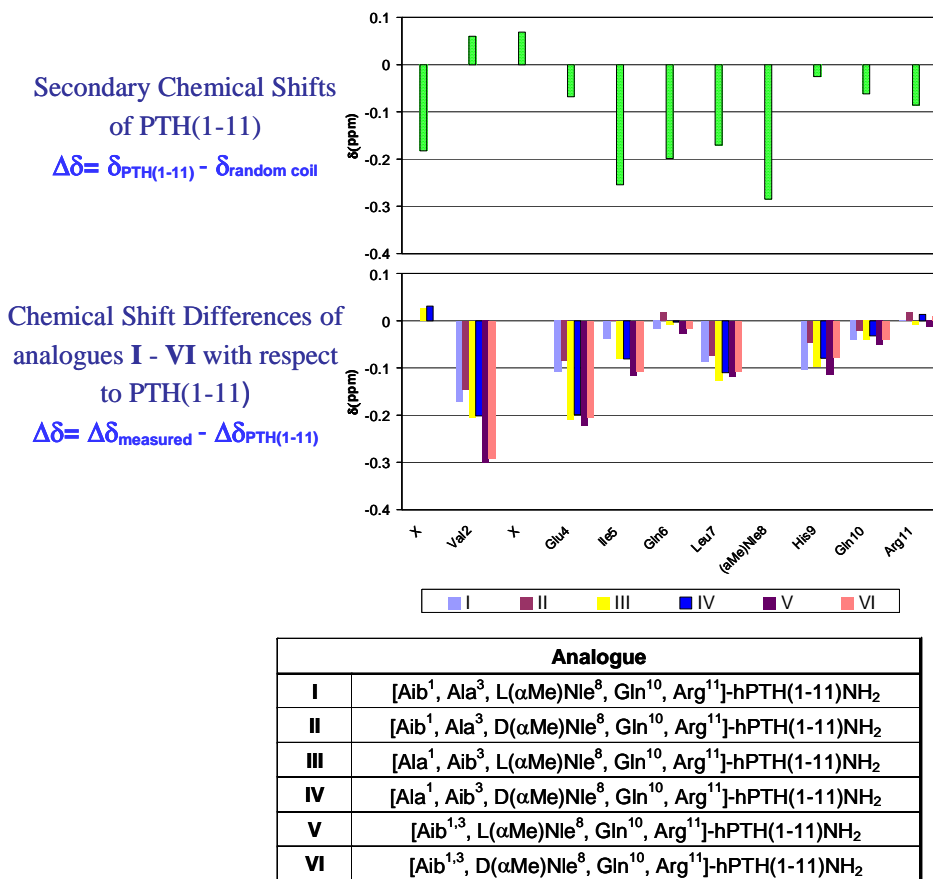


Fig. 18 From analogue **I** to analogue **VI** the figure shows an increasing tendency to stabilize the  $\alpha$ -helical segment, especially for residues 2 and 4.

Superimposition of the ensembles of the low energy structures resulting from distance geometry and molecular dynamics calculations clearly indicated a high convergence towards the helical structure for all analogues, and the atomic RMSD of the backbone atoms confirms an increasing convergence going from analogue **I** to analogue **VI**.

If we compare the chemical shifts differences between the  $\alpha$  protons for analogues containing  $\alpha$ MeVal and those containing  $\alpha$ MeNle in order to understand the tendency to  $\alpha$ -helix, we can observe that  $\Delta\delta$  values for analogues **I** - **X** show a spread tendency to an enhanced helicity in the region 1-4 residues. Moreover, we observe that the region 7-10 residues are more stabilized for analogues **V**-**X**, due to the presence of  $\alpha$ MeNle (fig. 19).

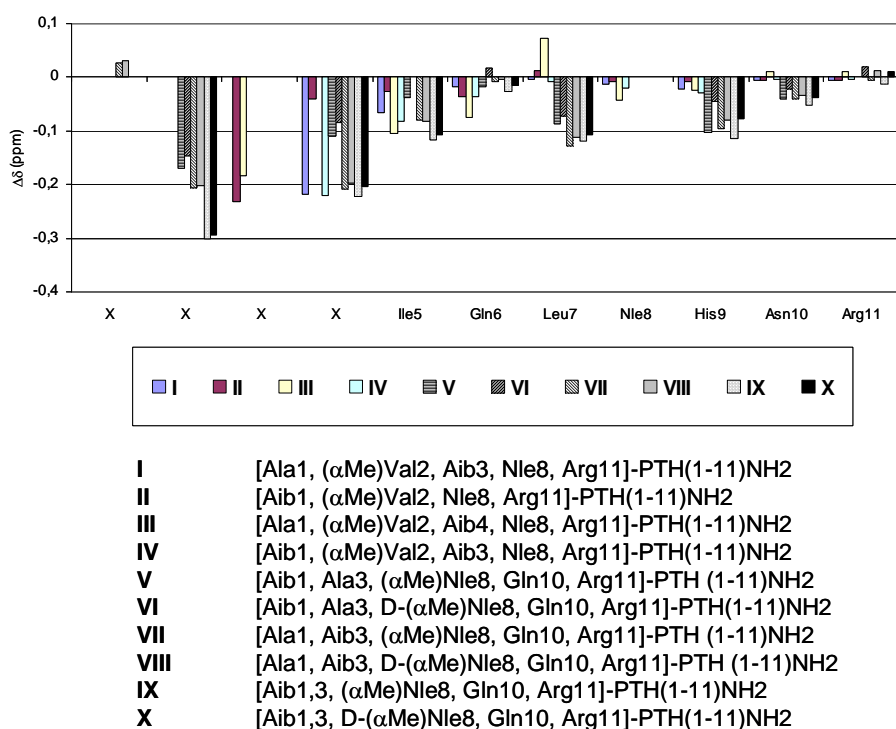


Fig. 19 Chemical Shift Differences of  $\alpha$  protons for analogues **I** - **X** with respect to analogue [Ala<sup>1</sup>, Nle<sup>8</sup>, Arg<sup>11</sup>]- PTH(1-11)NH<sub>2</sub> taken as reference.

$$\delta\Delta = \delta\Delta_{\text{measured}} - \delta\Delta_{\text{reference}}$$

All these observations confirm that helicity is important for biological activity. In fact, PTH(1-11) analogues containing Aib and  $\alpha$ MeNle in position 1, 3 and 8 respectively, exhibit a good biological activity similar to that of reference peptide. This result can be justified by the consideration that peptide containing  $\alpha$ MeNle have no signal in CD compatible to  $3_{10}$  helix. In other words, it is possible that the presence of  $\alpha$ MeVal in N-terminus of PTH(1-11) favours the structure in  $3_{10}$  helix, while  $\alpha$ MeNle in a position far from Aib in position 1 and 3 favours  $\alpha$ -helical structure. An interesting aspect is that the presence of D/L  $\alpha$ MeNle does not destroy the ordered structure, contrary to what occurs when D-Nle was introduced in reference peptide in D-scan.

The difference of helicity is possible to observe through a model of the most structural analogues of PTH(1-11) in the series analyzed (fig. 20).



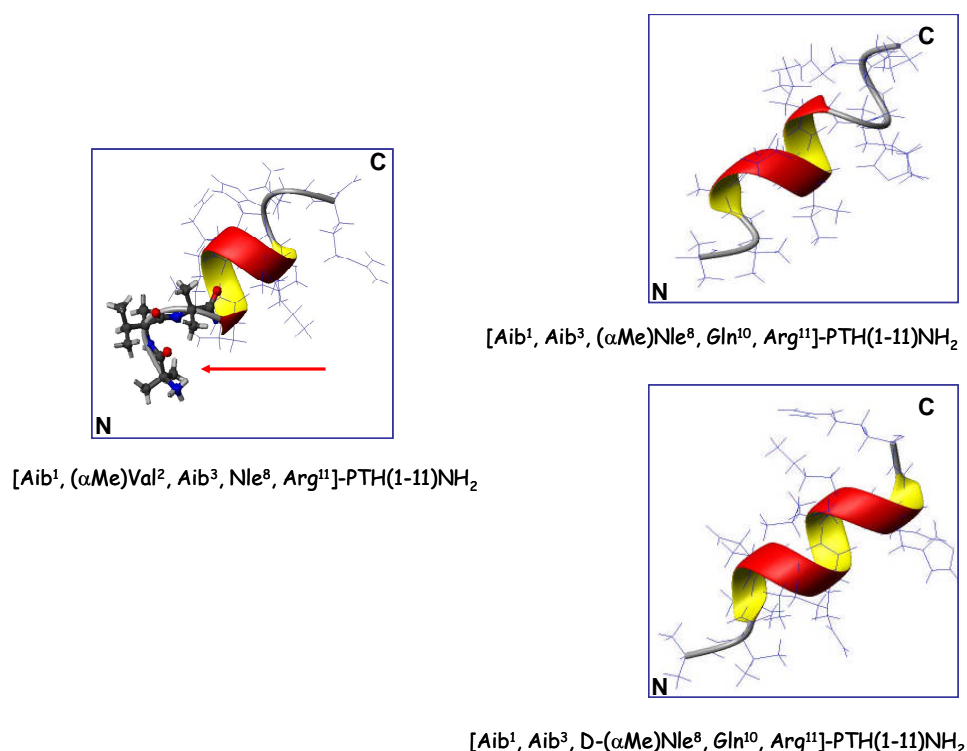


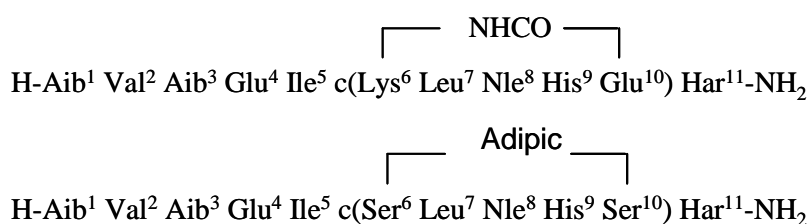
Fig. 20 Some analogues of PTH(1-11) containing C<sup>α</sup>-tetra-substituted amino acids. It is possible to observe a major 3<sub>10</sub> helix contribution for peptide containing αMeVal (arrow)

### 3.6. Ciclopeptides

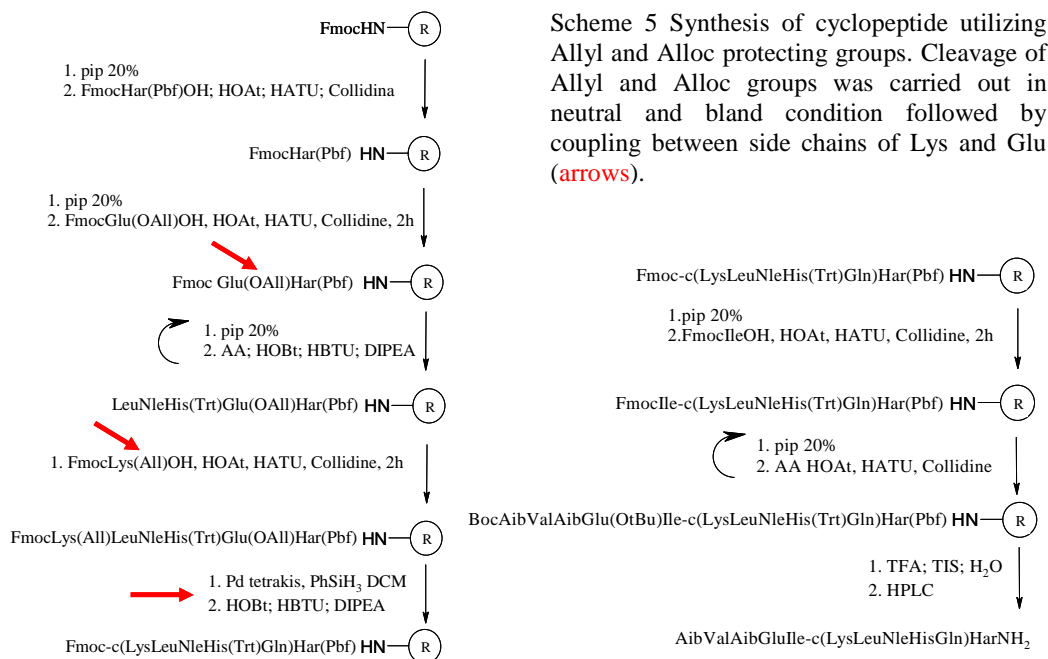
The best results on modification on PTH(1-11) to improve the activity were related to conformationally constrained peptides. Initially, the work was concentrated on local constrains such as the introduction of C<sup>α</sup>-tetra-substituted amino acids. Global restrictions in the conformation of a peptide are possible by limiting the flexibility of the peptide strand through cyclization. To this purpose, the amino acid side chains that are not involved in receptor recognition are connected together or the peptide backbone. This approach is used as a method to design bioactive peptides and peptidomimetics with high potency, receptor/acceptor selectivity, stability against proteolytic degradation and bioavailability and membrane permeability<sup>56</sup>. From CD spectra of the D-scan study, it appears that analogues which maintained better α-helical structure, contained D-Glu in position 6 and 10. Recently Gardella and co-workers reported that an analogues of PTH(1-11)<sup>28, 57</sup> cyclized between 6 and 10 residues exhibited almost the same activity of linear analogues.

In order to demonstrate that the hierarchical concept was a correct approach to discovery new biologically active products, we synthesized some peptide cyclized both between the side chains and directly in backbone. This part of the project was made in collaboration with Dr Chiara Cabrele at Regensburg University.

Two peptides with a cycle between side chains in position 6 and 10 were synthesized; the first one had a bridge between Lys<sup>6</sup> and Glu<sup>10</sup>; the second one had a bridge between two Serine residues inserted in position 6 and 10.



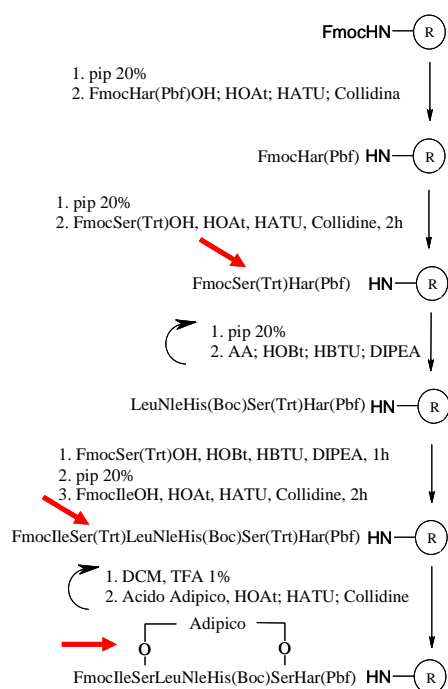
In the synthesis of cyclopeptides the crucial step is the cyclization. In fact the side reaction which often occurs is the intra-molecular polymerization. The side chain protective groups are chosen to be orthogonal with Fmoc-methodology. The synthesis of cyclic peptides remains a difficult task for SPPS and requires the use of multicomponent sets of orthogonal protecting groups. The Allyl and Alloc protecting groups are very useful for utilizing an orthogonal protection strategy in the synthesis of cyclic peptides because they have the advantage that can be removed with a specific reagent. The Allyl and Alloc groups are generally removed by treatment of the protected resin with tetrakis (triphenyl phosphine) palladium (0) [Pd(PPh<sub>3</sub>)<sub>4</sub>] in different mixtures of solvents and in presence of a nucleophile, which is the scavenger of Allyl groups released during deprotection. Recent methodology to remove Allyl and Alloc groups and to couple the free side chains was reported by P. Grieco and co-workers<sup>58</sup> under neutral condition.



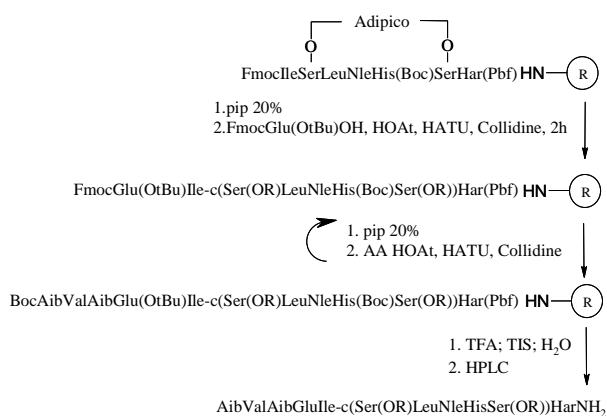
Scheme 5 Synthesis of cyclopeptide utilizing Allyl and Alloc protecting groups. Cleavage of Allyl and Alloc groups was carried out in neutral and bland condition followed by coupling between side chains of Lys and Glu (arrows).

After partial synthesis of peptide, the cyclization was introduced to avoid side reaction of inter-polymerization which was found during preliminary experiment of cyclization directly on SPPS (data not shown). Thus, to improve the optimal Allyl and Alloc deprotection conditions, cleavage step was carried out under inert Nitrogen atmosphere in order to prevent oxidation of Palladium (0). For this reason, during the synthesis it was critical to take particular care of removing all oxygen from the system. Moreover, a double cleavage was carried out, and a small total cleavage and mass analysis were taken. When the cyclization occurred, a second control through small total cleavage and mass analysis was made. SPPS was ended carried out following the normal protocol.

The second cyclopeptide have a bigger bridge between 6 and 10 positions. In this way it is possible to compare the effect of bridge dimension on the structure and the biological activity. Moreover, in the second peptide the chemical characteristics of bridge increase stability toward proteases.



Scheme 6 Synthesis of cyclopeptide utilizing Trt protecting group on Ser. After cleavage of Trt in very bland acidic condition, the coupling with adipic acid was carried out with ½ equivalents of acids and 6 equivalents of reagents (arrows).



The first attempt of the synthesis was stopped after cyclization because the coupling of Ile was failed. The possible reason might be due to the hindered effect of the bridge and the Ile residue, or due to aggregation effect of more hydrophobic characteristics of growing peptide after cyclization. For this reason, FmocIleOH was introduced before the cyclization step in order to minimize the hydrophobic and aggregation effects. The coupling of adipic acid was carried out with half equivalent of acid and 6 equivalent of coupling reagents, and controlled by mass analysis and HPLC analysis of crude material after small total cleavage. After total synthesis of cyclopeptide, the total cleavage was carried out and the crude material was controlled by HPLC, showing satisfied yield (fig. 21).

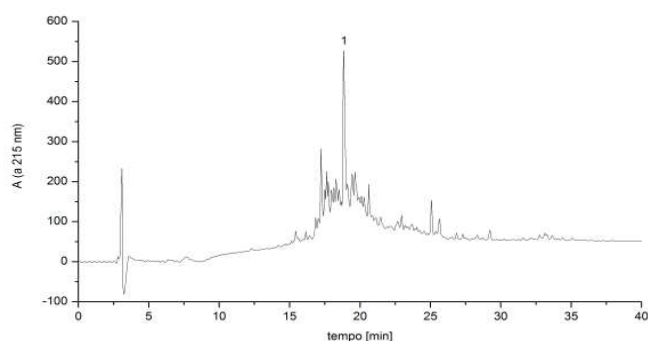


Fig. 21. Chromatogram of crude material after total cleavage ( $t_R = 18,8$  min).

The conformational properties of the cyclopeptides were initially investigated by CD in TFE 20% in water<sup>20</sup>. CD spectra in the far-UV region compared with that PTH(1-11) –RP at room temperature and are shown in Figure 22.

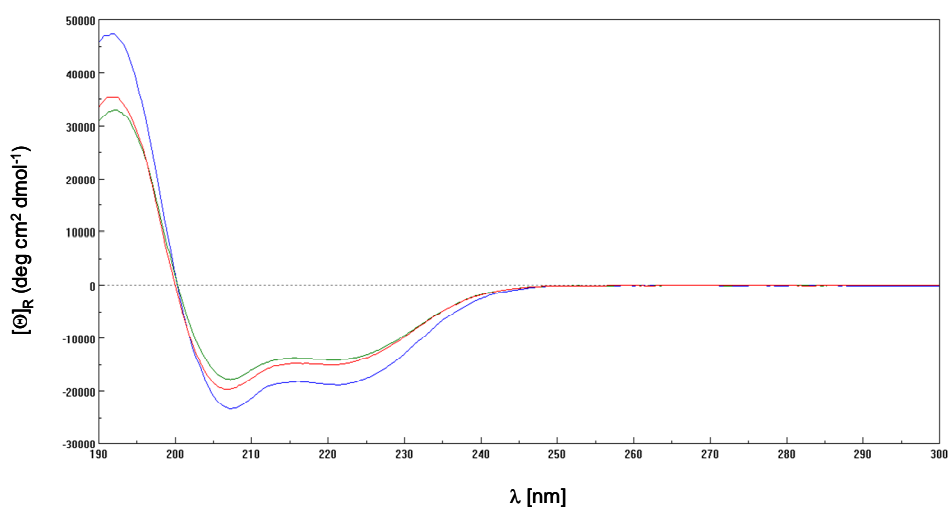
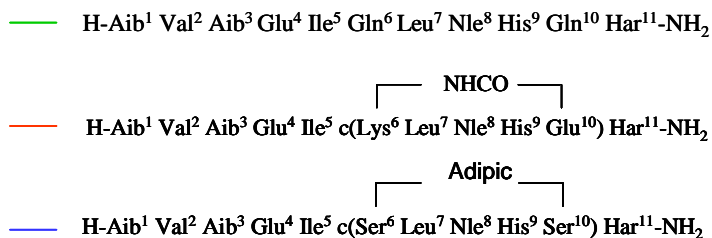


Fig 22



The spectrum of analogue cyclo[Lys<sup>6</sup>, Glu<sup>10</sup>]PTH(1-11) exhibited the typical shape usually of the  $\alpha$ -helical conformation, and the spectrum was very similar to that of reference peptide. For this analogue, the  $\alpha$ -helix content was estimated around 70%.<sup>25</sup> The second

analogue cyclo adipic[Ser<sup>6</sup>, Ser<sup>10</sup>]PTH(1-11) was characterized by a more negative band at ~222 nm, showing a higher content of ordered structure with respect to reference peptide. Unlucky, the NMR analysis is in progress. The biological tests gave a complete activity for cyclo adipic[Ser<sup>6</sup>, Ser<sup>10</sup>]PTH(1-11), confirming the hypothesis of  $\alpha$ -helicity is a prerequisite for activity (fig. 23).

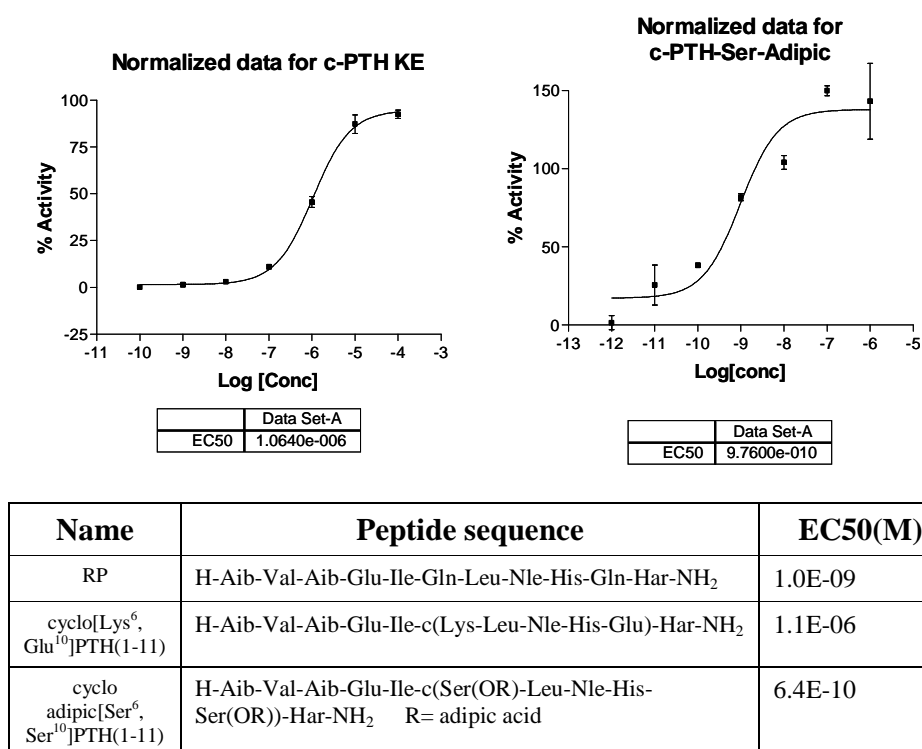


Fig .23 Series of cyclopeptides analogues of PTH(1-11) with reference peptide. All peptides were tested at Tuft University by Dr Angela Wittelsberger. The experimental error on the measurement is 15%.

It is interesting to notice that the peptide containing the KE bridge had a low activity. A very similar peptide was presented by Gardella and co-workers<sup>28, 55</sup>, cyclo(6,10)[Ala<sup>1, 3, 12</sup>, Lys<sup>6</sup>, Glu<sup>10</sup>, Har<sup>11</sup>, Trp<sup>14</sup>]PTH(1-14)NH<sub>2</sub>, which either maintained the “same potency or exhibited a 6-fold improvement in potency”<sup>28</sup>. In our case, the cyclopeptide containing the KE bridge, which presented all the modifications involved in the enhancement of activity, showed a lower activity than reference peptide which had the same  $\alpha$ -helical structure in CD spectrum. A hypothesis could be that the side chains of residues 6 and 10 interacted

directly to the receptor PTH1R. Nevertheless, cyclopeptide analogue of PTH(1-11) containing the adipic acid bridge exhibited an enhancement of activity. In this analogue, the 6 and 10 positions were substituted by two Ser, which didn't enhance the activity in linear substitution<sup>11</sup>. A reasonable hypothesis might be that the second bridge, which has 10 atoms instead of 8 like KE bridge, allows a higher flexibility of the peptide to fit better in the receptor pocket. Anyway the bridge maintained and stabilized the  $\alpha$ -helix structure of N-terminal PTH(1-11) better than in the analogues containing C $^{\alpha}$ -tetra-substituted amino acids in the sequence.

During the period spent in Regensburg University, we tried to synthesize a peptide cyclized directly in backbone, too. Some recent works of S. Arora reported the possibility to mimic the C=O - H-N hydrogen bond as a covalent bond of the type C=X-Y-N, where X and Y would be part of the *i* and the *i*+4 residues, respectively. The method proposed to form the covalent bond between the *i* and the *i*+4 residues was a carbon-carbon bond derived from a ring-closing metathesis reaction<sup>59, 60</sup> directly on resin. Initially, the amino acids involved in H-bond to be modified were identified in the sequence of PTH(1-11). The two amino acids were Ile and Nle, mainly because their side chains are without functional groups and they are positioned in the middle of PTH(1-11) sequence. The modified amino acids were synthesized according to literature<sup>58</sup> (fig. 24, 25). *o*Ns N-amine protective group was chosen for its property to make aminic proton acid to allow the allylation of N in a bland and rapid way. The two N-allyl amino acids were introduced in sequence with HOAt/HATU coupling reagents, with good yield and efficiency. When the peptide was ready, the ring-closing metathesis was tried either on refluxing dichloroethane temperature or in microwaves without good results. Probably in our synthesis, there were some problems connected up to the sequence and in our hands the resin lost its swelling properties. In fact, in sequence of PTH(1-11), Histidine is present and it is commonly protected either with Trt or with Boc, which are thermolabile. Histidine side chain is responsible to complex the Ruthenium of Hoveyda-Grubbs catalyst and in this way it might deactivate catalyst (scheme 7).

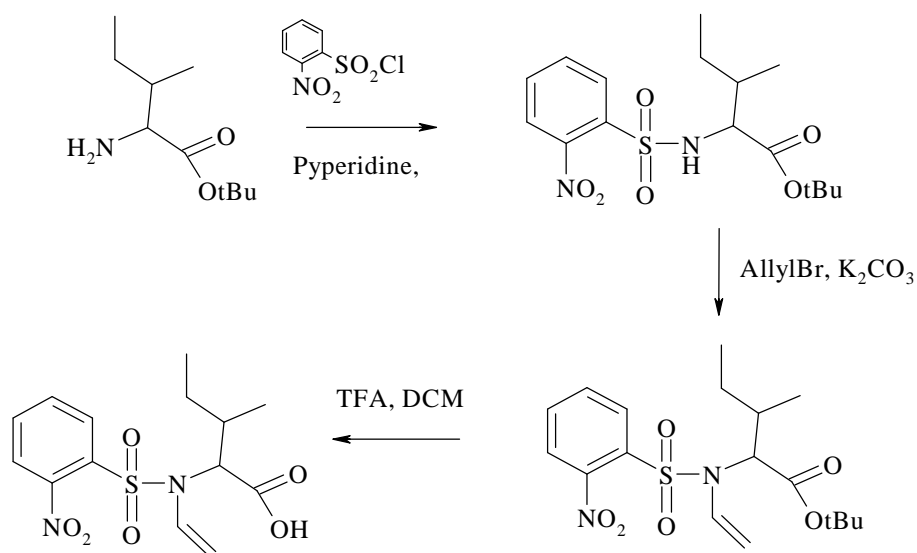


Fig. 24 Synthesis of oNsN(Allyl)IleOH. The synthesis was carried out in solution.

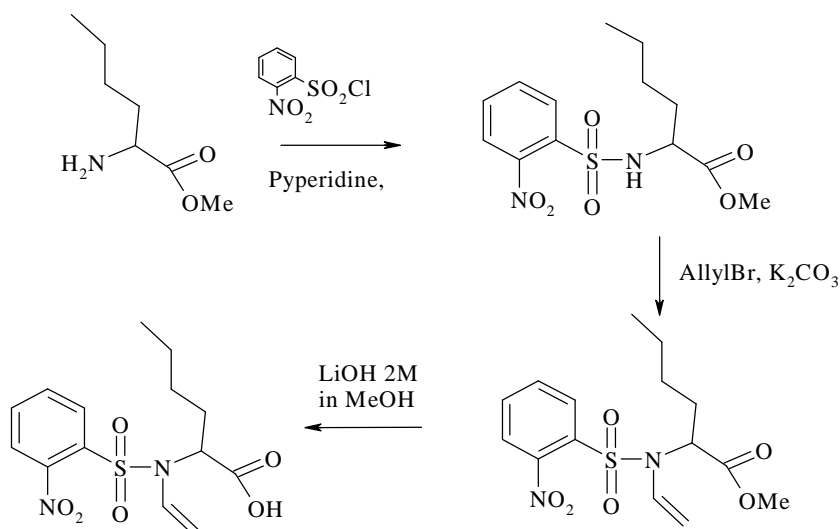
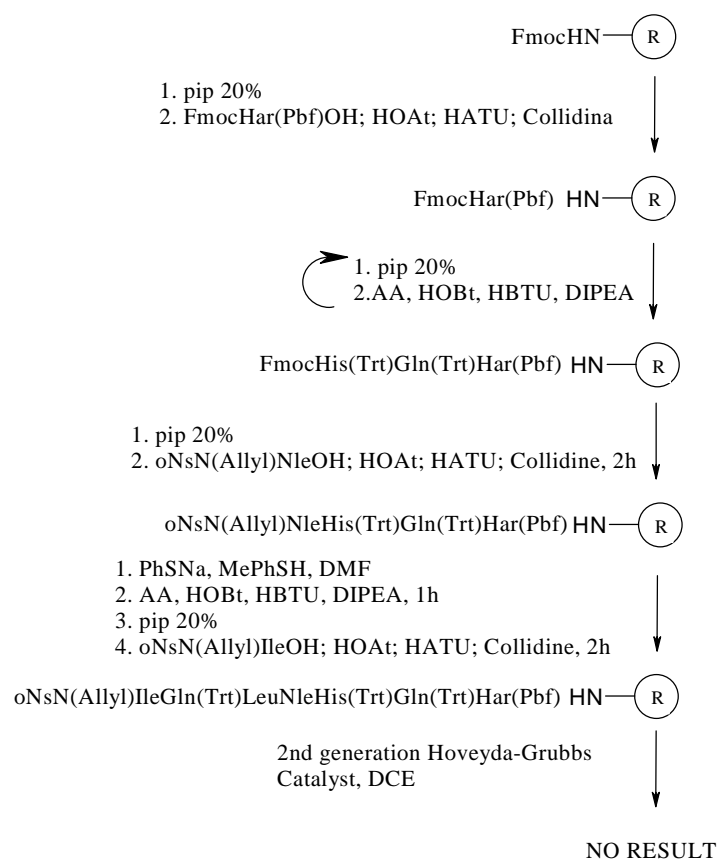


Fig. 25 Synthesis of oNsN(Allyl)NleOH. The synthesis was carried out in solution. The cleavage of Methyl ester gave the racemic mixture in every reaction condition. Attempts carried out with enzyme were unsuccessful.





Scheme 7 Synthesis SPPS of analogue of PTH(1-11) cyclized directly in backbone

Hoveyda-Grubbs was chosen following literature works<sup>59</sup>. Arora and coworkers tested a series of Grubbs Catalysts on a similar peptide linked to the same resin utilized in this work in order to find the most efficient catalyst for ring closing metathesis reaction.

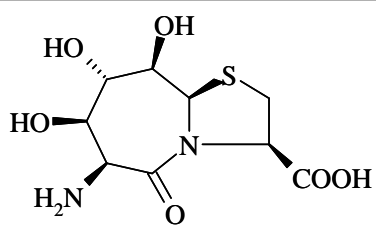
### 3.7. Peptidomimetic

In these years, our research group had an effective collaboration with Regensburg University. In this collaboration Prof. A. Geyer proposed to insert a dipeptide mimetic originated by his synthesis of a modified carbohydrate<sup>61, 62, 63</sup> in a biological active peptide. The dipeptide mimetic (Scheme. 8) was introduced in strategic positions, in order to leave the side chain of the essential residues 2, 5 and 8 unmodified.

Name	Peptide sequence	EC50(M)
I	[Ala <sup>1</sup> ,7,5-bTL <sup>3,4</sup> ,Nle <sup>8</sup> ,Arg <sup>11</sup> ]PTH(1-11)NH <sub>2</sub>	No Active
II	[Ala <sup>1</sup> ,7,5-bTL <sup>6,7</sup> ,Nle <sup>8</sup> ,Arg <sup>11</sup> ]PTH(1-11)NH <sub>2</sub>	No Active
III	[Ala <sup>1</sup> ,Nle <sup>8</sup> ,7,5-bTL <sup>9,10</sup> ,Arg <sup>11</sup> ]PTH(1-11)NH <sub>2</sub>	No Active

Scheme 8 Series of analogues of PTH(1-11) containing a dipeptidomimetic. All peptides were tested at Tuft University by Dr Angela Wittelsberger.



**7,5-bTL**

The analogues were prepared using Fmoc methodology with Rink Amide MHBA resin (Novabiochem) (0.73 mmol/g loading) as a solid support. The bicyclic lactam 7,5-bTL was prepared and protected at the free amino group as fluorenyl carbamate. The first amino acid was linked to the resin using the HBTU/HOBt/DIPEA protocol. The coupling of 7,5-bTL was accomplished with the more potent condensation reagent HATU/HOAt/2,4,6-collidine<sup>33, 34, 36</sup>. Since 7,5-bTL had a high synthetic value, it was used in a stoichiometric amount with respect to the resin, and with 4 equivalents of coupling reagents<sup>64</sup>, and a longer reaction time was used to improve the yield of incorporation. The next amino acid was introduced on the sterically hindered free amino group of the lactam using a double coupling procedure after preliminary acetylation.

The conformational properties of the three peptide mimetics were initially investigated by CD in TFE 20% in water at room temperature<sup>20</sup> (fig. 26). The spectrum of analogue I exhibits the typical shape usually associated with the  $\alpha$ -helical conformation, estimated at 66%. The presence of  $\beta$ -turns is not excluded, since their CD patterns qualitatively resemble that of a  $\alpha$ -helix<sup>65</sup>. Analogues II and III are characterized by negative bands at ~200 nm, showing a lower content of ordered structure with respect to analogue I. However, the shape of these curves does not exclude the presence of some contribution of  $\alpha$ -helix or  $\beta$ -turn for these analogues, as well as the co-presence of two or more conformations.

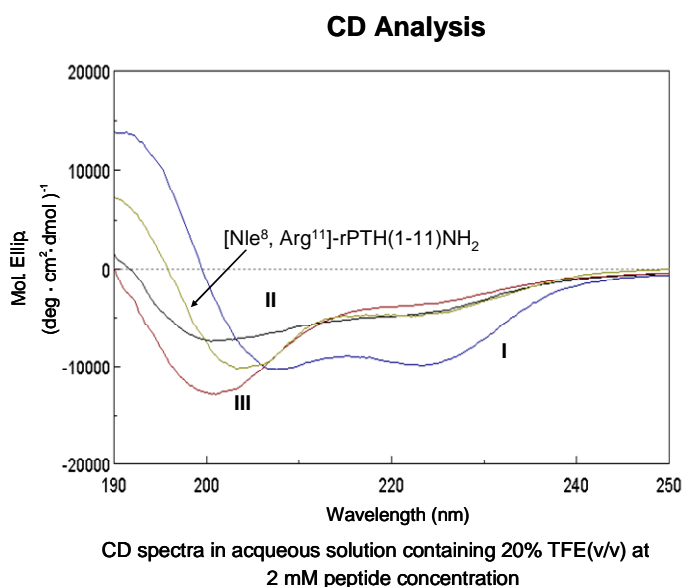


Fig. 26 CD spectra of analogues of PTH(1-11) containing 7,5 bTl

By NMR experiments, the sequential and medium range ROE connectivities were determined for analogues I–III in 20% v/v TFE- $d_3$ . For analogue I, in the ROESY spectra, a number of  $\alpha\text{H}(i)\text{-NH}(i+3)$ ,  $\alpha\text{H}(i)\text{-}\beta\text{H}(i+3)$  and  $\alpha\text{H}(i)\text{-NH}(i+4)$  connectivities typical of the  $\alpha$ -helix indicated the presence of an  $\alpha$ -helix spanning the sequence Ile<sup>5</sup>-Arg<sup>11</sup>.

Analogue II contained a smaller number of these ROE interactions, located only in the C-terminal portion, starting from Nle<sup>8</sup>. Analogue III showed only one  $\alpha\text{H}(i)\text{-NH}(i+1)$  interaction because of a large number of overlapped peaks. The small number of  $\alpha\text{H}(i)\text{-NH}(i+3)$ ,  $\alpha\text{H}(i)\text{-}\beta\text{H}(i+3)$  connectivities indicated the absence of significant secondary structure.

A table of the chemical shift differences of the  $\alpha\text{H}$  protons with respect to the values of the random coil conformation<sup>53</sup> showed a short helical segment in the sequence Ile<sup>5</sup>-Nle<sup>8</sup> for analogue I, according to CD spectra, while analogues II and III exhibit no helical structure (fig. 27).

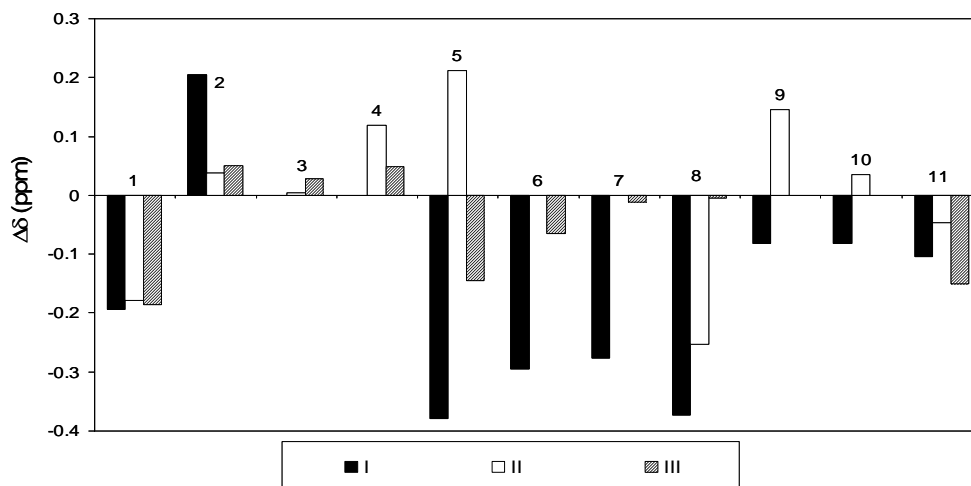


Fig. 27 Secondary Chemical Shifts ( $\Delta\delta = \delta_{\text{measured}} - \delta_{\text{random coil}}$ ). For analogue I, negative values  $\geq 0.1$  ppm identifies a short helical segment in the sequence Ile<sup>5</sup>-Nle<sup>8</sup>. Analogues II and III exhibit no preference for helical structure.

It has been shown that 7,5-bTL can occupy  $i$  to  $i + 1$  positions of type I and type II  $\beta$ -turns in cyclic hexapeptides<sup>63</sup>. In analogue I, we found a H-bond, indicated by a (CO<sup>4</sup>-NH<sup>7</sup>) H-bond involving the backbone, type immediately following the 7,5-bTL<sup>3,4</sup> residue. Furthermore, there are significant occurrences of (i, i+4) H-bonds with  $i=4, 5$  and  $6$ . This means that in analogue I 7,5-bTL was able to induce a  $3_{10}$  helix loop which developed into an  $\alpha$ -helical structure. This hypothesis was backed by the calculation of a secondary structure with the Kabsch and Sander algorithm<sup>66</sup>, which indicated for analogue I an  $\alpha$ -helical segment in the region Ile<sup>5</sup>-His<sup>9</sup>.

From Structural calculation and superimposition of the ensembles of calculated structures of analogues I-III, order parameters for analogues II and III showed that the dihedral angles  $\varphi$  and  $\psi$  were not very well defined for residues preceding the peptide-mimetic moiety, indicating that 7,5-bTL disrupted the tendency to form an ordered structure in the region immediately before its position. In fact, analogue III appeared to be completely random (fig. 28).

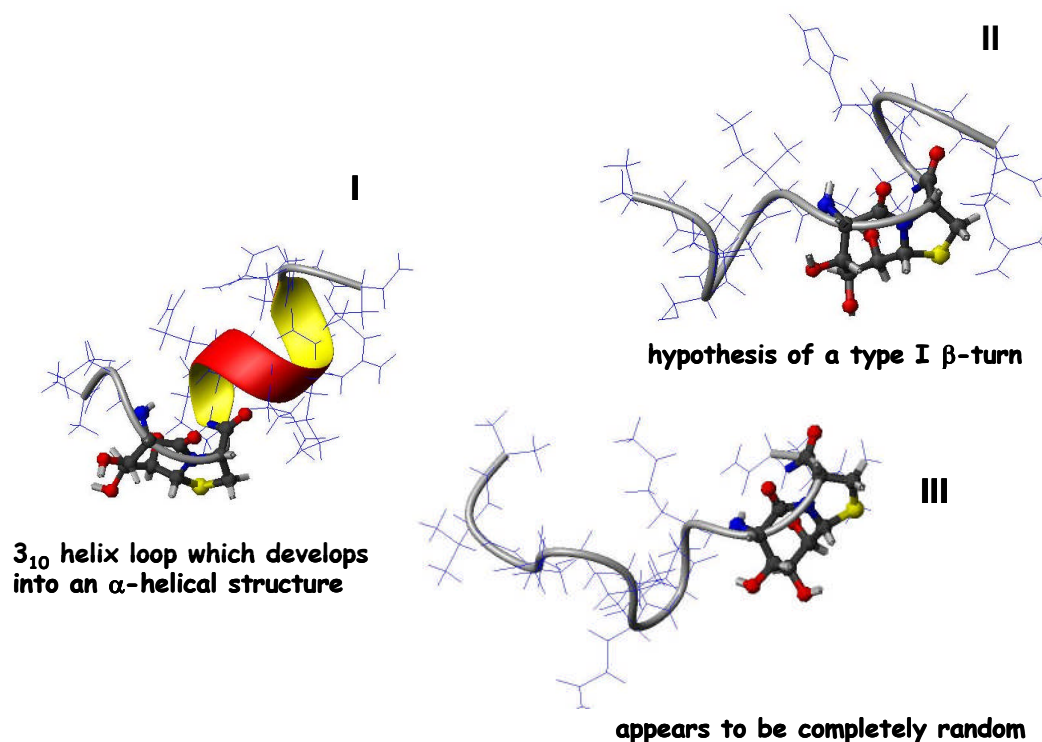


Fig. 28 Schematic representation of one of the lowest energy structures of Analogues I-III.

Biological tests showed that no analogues PTH(1-11) containing the dipeptidomimetic exhibited activity. These results underlined that stabilization of  $\alpha$  helical segment at the N-terminus of PTH(1-11) analogues, as observed in analogue I, might be necessary but not sufficient condition to generate a bioactive PTH-like compound. It is possible that the side chain of Glu<sup>4</sup> was not well mimicked by 7,5-bTL, or that substitution with the peptide mimetic between the residues Val<sup>2</sup> and Ile<sup>5</sup> constrained the side chains in an unfavourable interaction with the receptor. Analogue I exhibited a spatial orientation of the Val<sup>2</sup>, Ile<sup>5</sup> and Nle<sup>8</sup> side chains significantly different from that of PTH(1-11). Taken together, these results suggested that a very stable helix encompassing these residues appears to be fundamental, although not sufficient, for PTH-like ligand-PTH1R interaction<sup>67</sup>.

### 3.8 CONCLUSION

...” the structure of these flexible compounds do not allow conclusions about the receptor bound conformation, although knowledge of this conformation is necessary for rationally designing new bioactive compounds”...

Kessler et al., *Angew. Chem. Int. Ed. Engl.* **1997**, 36, 1374-1389

We have demonstrated that applying the principles and concepts of hierarchical approach of peptidomimetics directly on the shortest active modified PTH(1-11) sequence, **H-Aib-Val-Aib-Glu-Ile-Gln-Leu-Nle-His-Gln-Har-NH<sub>2</sub>**, it is possible to use peptides as very diverse and versatile molecules both like wide therapeutic potential and like means to study the hormone/receptor complex. During these years of PhD course we synthesized and characterized by CD and NMR a series of libraries of peptides to obtain information on pharmacophores properties and structure of PTH(1-11).

Our work was focused to understand which side chains of residues of PTH(1-11) are essential and peptide conformational space are available. Part of the synthesis of PTH(1-11), D-Scan analogues, allowed us to realize that almost all residues of N-terminus are useful to the binding. Mainly, Val<sup>2</sup> is determinant to activate the receptor, in fact peptides which presented few modifications in direction of its side chain resulted completely no-active, such as  $\alpha$ MeVal or NVal. This result suggests that the side chain orientation in the space plays determinant role in the receptor activity. In fact, only the presence of fragment of the  $3_{10}$  helix in N-terminus was enough to confer a low activity to the analogue. A higher conformational freedom can be observed for Nle in position 8. If on one side the substitution of D-Nle was enough to destroy of ordered structure of reference peptide, on the other side the introduction of  $\alpha$ MeNle in position 8, even if in D-configuration, induced a more ordered peptide and allowed to better preserve the activity. Thus, through a synthetic approach we justified the role of pharmacophore of residues 2 and 8 defining their importance in the binding. Moreover, with the same technique we were able to identify the role of homoarginine in position 11. Homoarginine plays a important role to anchor the PTH(1-11) to the receptor. In particular, the 1000-fold reduction in affinity and potency seen with the removal of Har<sup>11</sup> highlights the important role of this residue (which replaces

leucine of native PTH) in receptor binding<sup>4</sup>. Molecular modeling suggests that this role might involve the insertion of the guanidinium side-chain group between the extracellular ends of TM1 and TM7<sup>7</sup>. So, in the PTH(1-11) the stabilization of this position could be critical for the activity of the analogue. At the same time, it was demonstrated that the guanidine group in the C-terminal position would not be independent on the configuration of C<sup>α</sup>-carbon. In fact, analogues containing diamine in C-terminal position exhibited low activity, although they demonstrated that specific length of side chain is necessary for activity. The study carried out with diamine series showed that another prerequisite for guanidine group would be a correct orientation. In other words, the amide group in C-terminus might orient the guanidine group in correct way or the amide group might play some role in the binding with the trans-membrane region of the receptor. In any case, the network of interactions that occur between the N-terminal domain of PTH and the J domain of the PTH1R is very likely to be highly complex.

All our work suggested that a very stable helix encompassing these residues appears to be fundamental, although not sufficient, for PTH-like ligand-PTH1R interaction. Finally, it seems that the side chains of some hydrophilic residues are necessary for either stabilize the structure or binding to the J domain of PTH1R.

The concept of a totally synthetic approach to generate libraries of peptides for conformational study through NMR, CD and MD resulted difficult but successful to find new lead products to test as pro-drugs.

On the synthetic side, we demonstrated that the use of acylfluorides is a good way to bypass synthesis of hindered and difficult biological sequences, but also that the peptide synthesis, mainly the versatility of SPPS, is important in organic chemistry to explore and project new biological products.

## REFERENCES

- <sup>1</sup>G. Jung, A. G., Beck-Sickinger, *Angew. Chem. Int. Ed. Engl.* 1992, 31, 367.
- <sup>2</sup>Giannis A., Kolter T., *Angew. Chem. Int. Ed. Engl.* 1993, 32, 1244-1267
- <sup>3</sup>Luck M., Carter P., Gardella T. *Mol Endocrinol* 1999, 13:670-680.
- <sup>4</sup>Shimizu M., Carter P., Khatri A., Potts JJ, Gardella T. *Endocrinology* , 2001, 142: 3068-3074.
- <sup>5</sup>Rolz C., Pellegrini M., Mierke D., 1999. *Biochemistry* 38:6397-6405.
- <sup>6</sup>Jin L., Briggs S., Chandrasekhar S., Chirgadze N., Clawson D., Schevitz R., Smiley D., Tashjian A., Zhang F... *J Biol Chem.* 2000, 275:27238-27244
- <sup>7</sup>Monticelli L., Mammi S., Mierke D. *Biophys. Chem.*, 2002, 95; 165-172.
- <sup>8</sup>Hoare S., Gardella T., Usdin T. *J. Biol. Chem.*, 2001, 276:7741-7753;
- <sup>9</sup>Gardella T.J., Jüppner H. *Trends Endocrinol. Metab.*, 2001, 12; 210-217.
- <sup>10</sup>Shimizu N., Guo J., Gardella T. *J. Biol. Chem.* 2001, 276; 49003-49012.
- <sup>11</sup>Shimizu M., Potts J.J., Gardella T. *J. Biol. Chem.*, 2000, 275; 21836-21843
- <sup>12</sup>Kaul R., Balaram P., *Bioorg. Med. Chem.* 1999, 7;105-117.
- <sup>13</sup>Schumacher, T. N.; Mayr, L. M.; Minor, D. L., Jr.; Milhollen, M. A.; Burgess, M. W.; Kim, P. S. *Science*, 1996, 271, 1854.
- <sup>14</sup>Gill, T. J.; Hanna, J. G.; Doty, P. *Nature*, 1963, 197, 746.
- <sup>15</sup>Borek, F.; Stupp, Y.; Fuchs, S.; Sela, M. *Biochem. J.* 1965, 96, 577
- <sup>16</sup>Feichtinger K., Zapf C., Sings H. L., Goodman, M., *J. Org. Chem.*, 1998, 63, 3804-05.
- <sup>17</sup>Arrieta, A., Palomo, C. *Synthesis* 1982, 1050-1052
- <sup>18</sup>Gerz T., Kuncce D., Markowski P., Izdebki J., *Synthesis* 2004, 1, 37-42
- <sup>19</sup>Bolin, D. R.; Sytwu, I.-I.; Humiec, F., Meienhofer, Int. *J. Pept. Protein Res.* 1989, 33, 353-359.
- <sup>20</sup>Barazza, A; Wittelsberger, A; Fiori, N; Schievano, E; Mammi, S; Toniolo, C; Alexander, J. M.: Rosenblatt, M.; Peggion, E.; Chorev, M. *J Pept Res* 2005, 65(1), 23-35.
- <sup>21</sup>Goodman, M., and Listowsky, I., *J. Am. Chem. Soc.* 1962,84, 3770-3771.
- <sup>22</sup>Buck, M., *J. Rev. Biophys.*, 1998, 31, 297-355
- <sup>23</sup>Storrs, R. W., Truckses, D., and Wemmer, D. E., *Biopolymers*, 1992, 32, 1695- 1702.
- <sup>24</sup>Roccatano, D., Colombo, G., Fiorini, M., and Mark, A. E., *Proc. Natl. Acad. Sci. U.S.A.*, 2000, 99, 12179-12184
- <sup>25</sup>Fiorini, M., Diaz, M. D., Burger, K., and Berger, S., *J. Am. Chem. Soc.*, 2002 124, 7737-7744.
- <sup>26</sup>Diaz, M. D., Fiorini, M., Burger, K., and Berger, S., *Chem. Eur. J.*, 2002, 8, 1663-1669
- <sup>27</sup>Walgers, R., Lee, T. C., and Cammers-Goodwin, A., *J. Am. Chem. Soc.*, 1998, 120, 5073-5079.
- <sup>28</sup>Shimizu N., Petroni B., Khatri A., Gardella T., *Biochemistry* , 2003, 42:2282-2290.
- <sup>29</sup>Piserchio A., Shimizu N., Gardella T., Mierke D., *Biochemistry* , 2002, 41:13217-13223.
- <sup>30</sup>M. Goodman, M. Chorev. *Acc. Chem. Res.* 1979. 12, 1.
- <sup>31</sup>M. Cushman. J. Jurayj. J. D. Moyer. *J Org. Chem.* 1990, 55. 316, and references therein.
- <sup>32</sup>Martin L. Ivancich A., Vita C., Formaggio F., Toniolo C., *J. Peptide Res*, 2001, 58, 424-432.
- <sup>33</sup>Carpino L. A., *J. Am. Chem. Soc.*, 1993 115, 4397-4398
- <sup>34</sup>Carpino L. A., El-Faham A., *J. Org. Chem.*, Vol. 59, No. 4, 1994;
- <sup>35</sup>Crisma M. Bisson W., Formaggio F., Broxterman Q. B., Toniolo C., 2002. *Biopolymers*, 64, 236-245
- <sup>36</sup>Carpino L. A., El-Faham A., Albericio F. *J. Org. Chem.* 1995,60, 3561-3564;
- <sup>37</sup>Kruijtzter, J. A. W.; Hofmeyer, L. J. F.; Heerma, W.; Versluis, C.; Liskamp, R. M. J. *Chem. Eur. J.* 1998, 4, 1570
- <sup>38</sup>Uno T., Beausoleil E., Goldsmith R. A., Levine B. H., Zuckermann R. N., Teth. *Lett.* 1999, 40, 1475-1478
- <sup>39</sup>Simon, R. J.; Kania, R. S.; Zuckermann, R. N.; Huebner, V. D.; Jewell, D. A.; Banville, S.; Ng, S.; Wang, L.; Rosenberg, S.; Marlowe, C. K.; Spellmeyer, D. C.; Tan, R. Y.; Frankel, A. D.; Santi, D. V.; Cohen, F. E.; Bartlett, P. A., *Proc. Natl. Acad. Sci. U.S.A.* 1992, 89, 9367
- <sup>40</sup>de Haan, E. C.; Wauben, M. H. M.; Grosfeld-Stulemeyer, M. C.; Kruijtzter, J. A. W.; Liskamp, R. M. J.; Moret, E. E. *Bioorg. Med. Chem.* 2002, 10, 1939
- <sup>41</sup>Holder J.R., Bauzo R.M., Xiang Z., Scott J., Haskell-Luevano C., *Bioorg. Med. Chem. Lett.* 13 (2003) 4505-4509



- 
- <sup>42</sup>Richardson, J. S. *Adv. Protein Chem.* 1981, 34, 167
- <sup>43</sup>Lim S.-K., Lee E. J., Kim H.-Y., Lee W., 2004. *J. Peptide Res.*, 64, 25-32
- <sup>44</sup>Beesley R. M., Ingold C. K., Thorpe J. F., *J. Chem. Soc.*, 1915, 105, 1080-1087
- <sup>45</sup>Sammes P. G., Weller D. J., *Synthesis* 1995, 1205-1222
- <sup>46</sup>Toniolo C., Crisma M., Formaggio F., Peggion C., *Biopolymers* 2001; 396-419
- <sup>47</sup>Carpino L. A., Mansour E. M. E., Sadat-Aalae, D. *J. Org. Chem.*, 1991, 56, 2611-2614
- <sup>48</sup>Han S.-Y., Kim Y.-A. *Tetrahedron*, 2004, 60, 2447-2467
- <sup>49</sup>Carpino L. A., Ionescu D., El-Faham A., *Tetrahedron Letters*, 1998, 39, 241-244.
- <sup>50</sup>Wenschuh H., Beyermann M., Krause E., Brudel M., Winter R., Schümann M., Carpino L. A., Bienert M., *J. Org. Chem.* 1994, 59, 3275-3280
- <sup>51</sup>Carpino L. A., Beyermann M., Wenschuh H., Bienert M. *Acc. Chem. Res.* 1996, 29, 268-274;
- <sup>52</sup>Carpino L. A., Ionescu D., El-Faham A., Beyermann M., Henklein P., Hanay C., Wenschuh H., Bienert M. *Organic Letters* 2003, 5, 975-977
- <sup>53</sup>Toniolo C., Polese A., Formaggio F., Crisma M., Kamphuis J., *J. Am. Chem. Soc.*, 1996, 118, 2744-2745
- <sup>54</sup>Pastore A, Saudek V. *Magn. Reson.*, 1990, 90; 165-176.
- <sup>55</sup>Yang, J. T. Wu, C. S. Martinez, H. M., *Methods in Enzymol.*, 1986, 130, 208-269
- <sup>56</sup>Hruby V. J., Balse P. M., *Current Medicinal Chemistry*, 2000, 7, 945-970.
- <sup>57</sup>Tsomaia N., Pellegrini M., Hyde K., Gardella T. J., Mierke D. F., *Biochemistry*, 2004, 43, 690-9
- <sup>58</sup>Grieco P., Gitu P. M., Hruby V. J., *J. Peptide Res.* 2001, 57, 250-256
- <sup>59</sup>Chapman R. N.; Dimartino G., Arora P. S., *J. Am. Chem. Soc.*, 2004, 126, 12252
- <sup>60</sup>Dimartino G., Wang D., Chapman R. N., Arora P. S., *Org. Lett.*, 2005, 7, 2389
- <sup>61</sup>Geyer A., Moser F., *Eur. J. Org. Chem.*, 2000, 1113-1120.
- <sup>62</sup>Tremmel P., Brand J., Knapp V., Geyer A., *Eur J. Org. Chem.*, 2003, 878-884
- <sup>63</sup>Tremmel P., Geyer A., *Angew. Chem. Intl. Ed.*, 2004, 5789-5791
- <sup>64</sup>Belvisi L, Bernardi A, Checchia A, Manzoni L, Potenza D, Scolastico C, Castorina M, Cupelli A, Giannini G, Carminati P, Pisano C., *Org. Lett.*, 2001, 3, 1001-1004.
- <sup>65</sup>Rose G.D., Gierasch L.M., Smith J.A., *Adv. Protein Chem.*, 1985, 37, 1-109.
- <sup>66</sup>Kabsch W, Sander C., *Biopolymers*, 1983, 22, 2577-2637.
- <sup>67</sup>Fiori N., Caporale A., Schievano E., Mammi S., Geyer A., Tremmel P., Wittelsberger A., Woznica I., Chorev M., Peggion E., *J. Pept. Sci.* 2007, 13, 504-512



# 4-METHODS

4-METHODS .....	87
Solid Phase Peptide Synthesis SPPS.....	88
Circular Dichroism .....	91
NMR – Nuclear Magnetic Resonance Spectroscopy .....	95
2D-NMR .....	96
Sequential assignment.....	98
3D structure determination .....	101
Distance Geometry .....	102
Restrained Molecular Dynamic .....	103
Peptide content.....	104
Amino Acid Analysis.....	104
UV Methods.....	105
Biological tests.....	106
REFERENCES .....	108

## Solid Phase Peptide Synthesis SPPS<sup>1</sup>

The innovative idea of peptide synthesis on a solid support (SPPS) was developed by Robert Bruce Merrifield in 1963<sup>2</sup>, who got the Nobel Award in 1984, and provided a major development of peptide chemistry. Today, the original concept has been extended and generalized to organic synthesis on polymeric supports, which includes not only heterogeneous reactions involving an insoluble polymer, but also the application of soluble polymeric materials which allow homogeneous reactions (liquid-phase peptide synthesis).

SPPS is based commonly on sequential addition of  $\alpha$ -amino acids with side-chain protected amino acids residues to an insoluble polymeric support. In SPPS the peptide chain is assembled in the usual manner, starting from the C-terminus. The amazingly simple concept is that the first amino acid of the peptide to be synthesized is connected via its carboxy group to an insoluble polymer support (resin) that can be easily separated from either reagents or dissolved products by filtration. The general principle is shown in Fig 1.

A necessary prerequisite is that the resin is able to support amino acids, which are anchored through linkers previously in the polymeric material (Fig.1 , step 1). An amino acid N <sup>$\alpha$</sup>  protected is then reacted with the functional group of the linker (step 2). The acid-labile Boc group or base-labile Fmoc-group is used for N- $\alpha$ -protection. After removal of this protecting group (step 3), the next protected amino acid is coupled (step 4) using either a coupling reagent or pre-activated protected amino acid derivate. Steps 3 and 4 can be then repeated (step 5) until the required peptide sequence has been assembled. In this way, the resulting peptide is attached to the resin, by means of a linker, through its C-terminus which can be cleaved simultaneously detaching the peptide from the resin. In many cases the semi-permanent side chain-protecting groups may be simultaneously removed (step 6).

The mayor concept is that the insoluble resin with the linked peptide can be separated from the reagents by filtration and then, after cleavage, the peptide itself can be removed as dissolved product in the same way. When syntheses are carried out on resin tedious and time-consuming isolation and purification of all intermediates, as it occurs in solution synthesis, are not required.

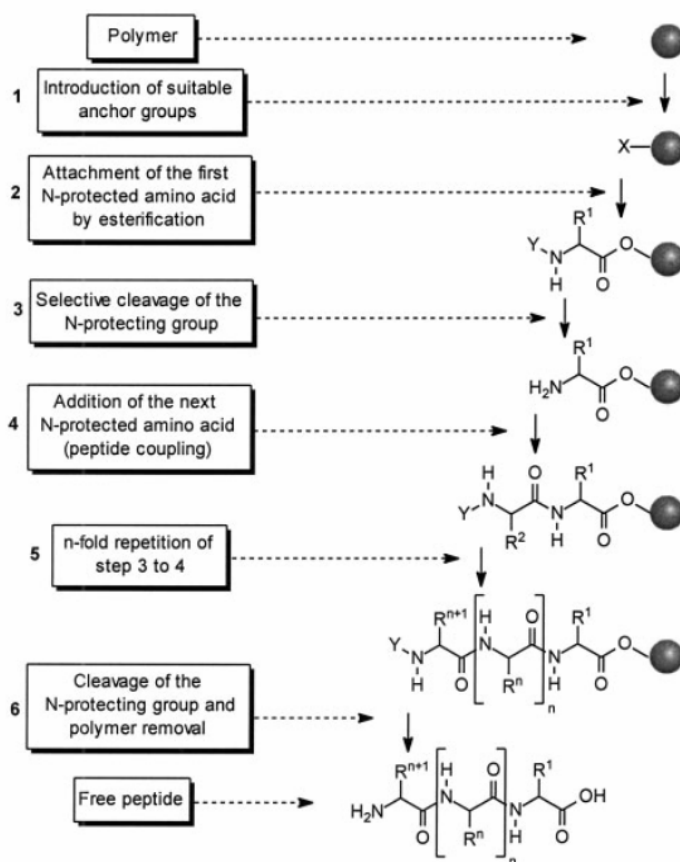


Fig.1: Process of solid-phase peptide synthesis. Y = temporary protecting group;  $R^1$ ,  $R^2$ ,  $R^n$ ,  $R^{n+1}$  = amino acid side chains, if necessary, protected with semipermanent protecting group<sup>1</sup>

Since the growing peptide chain remains bound to the support during steps 3 to 5, and excess reagents and by-products are removed by filtration, these simple technical operations can be automated.

Cleavage of the Boc protecting group is achieved by trifluoroacetic acid (TFA) and the Fmoc protecting group by piperidine. Final cleavage of the peptidyl resin and side-chain deprotection requires strong acid, such as hydrogen fluoride, in case of Boc Chemistry, and TFA in Fmoc Chemistry. Dichloromethane (DCM) and N, N dimethylformamide (DMF) or N-methylpyrrolidone (NMP) are the primary solvents used for resin deprotection, coupling and washing.

Fmoc chemistry is the only strategy which might be fully compatible with automatic flow method, because it allows in real time spectrophometric monitoring of the progress of coupling and the deprotection<sup>3, 4</sup>.

These are however some limitation in SPPS:

- The final product of a synthesis will be only a homogeneous compound, if all deprotection and coupling steps proceed quantitatively.
- A large excess of each amino acid and coupling reagents are required in the corresponding coupling reaction in order to achieve complete conversion.
- There is a permanent risk of undesirable side reactions during activation, coupling, and deprotection.
- Monitoring the reaction progress and analysis of complete conversion are difficult to perform in heterogeneous reaction systems, and are hampered by experimental error.
- Swelling properties of the polymeric resin and diffusion of the reagents are important parameters for the success of a solid-phase synthesis.
- Aggregation phenomena of the growing peptide chain may complicate the synthesis.
- Occasionally, drastic conditions required to cleave the peptide from the polymer may also damage the final product.

In any case the SPPS has many advantages in rapid synthesis and the possibility to work on parallel bulk allows the combinatorial synthetic approach.

In solid-phase combinatorial synthesis, reagents can be used in excess without separation problems in order to obtain complete conversion. Easy purification and automation of the process represent further advantages. However, reagents cannot usually be used in excess, and process automation might be much more difficult<sup>5</sup>. The choice of strategy and library size depends on the problem to be investigated: if nothing is known about a target, then maximum diversity is desirable, and the highest possible number of different compounds should be screened. The increasing knowledge of biochemical concepts and biopolymer structures also contributes considerably to lead to structure detection. So, structure-based molecular design, which can be employed to guide the main-finding process, and structural data on a target protein are applied in a rational approach using computational methods to identify potential low-molecular mass ligands. In such a case a smaller, focused library of single compounds may be prepared with a specific approach<sup>6</sup>. Once a main compound has been identified, the diversity requirements change fundamentally, and structure-activity relationships are performed by substituent variation to optimize the compound properties with the aim of

developing a drug candidate. Consequently, a sensible combination of different methodologies and technologies will eventually be considered<sup>7</sup>.

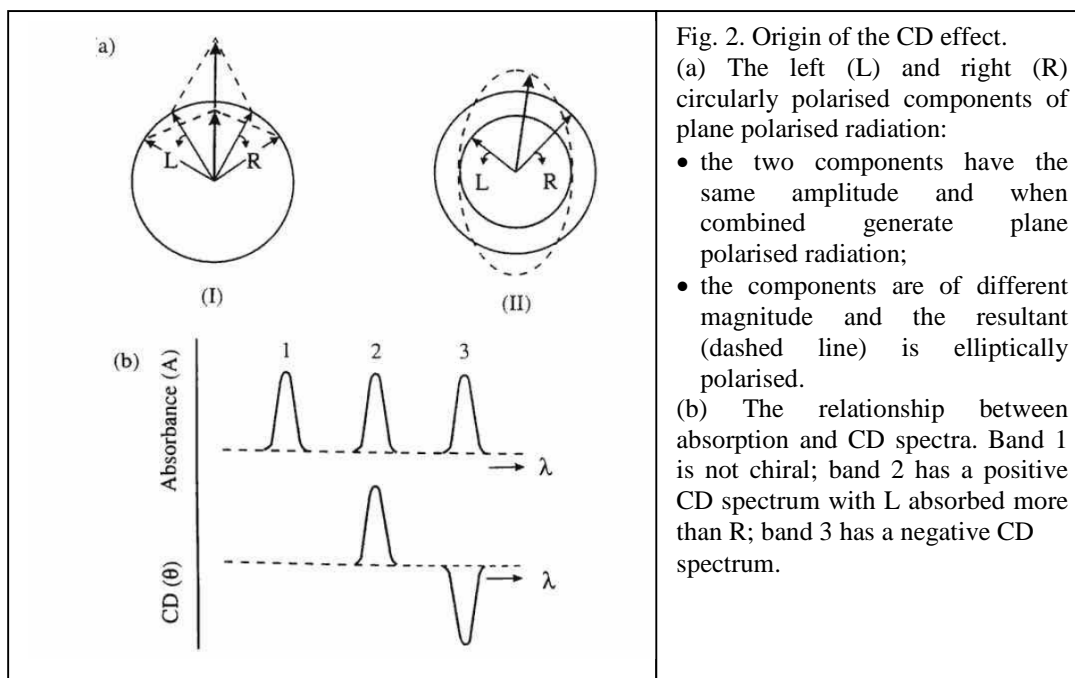
### **Circular Dichroism<sup>8</sup>**

A good level of knowledge of structure of peptides and protein can be obtained by the use of circular dichroism (CD). Since this spectroscopic technique has a great versatility, it might be used to determine the conformation of biological macromolecules in solution and to study processes that involve conformational transitions in solution and kinetic biochemical reactions.

CD refers to the differential absorption of the left and right handed circularly polarised components of plane-polarised radiation. This effect will occur when a chromophore is chiral (optically active) either (a) intrinsically by reason of its structure, or (b) by being covalently linked to a chiral centre, or (c) by being placed in an asymmetric environment. Practically the plane-polarised radiation is split into its two circularly polarised components through a modulator subjected to an alternating (50 kHz) electric field.

A linearly polarized ( $E_0$ ) electromagnetic radiation is the sum of two right (R) and left (L) hands polarized vectors rotating, which have the same size ( $E_{0R} = E_{0L}$ ), but in opposition of phase ( $\phi_R = -\phi_L$ ).

If the left and right circularly polarised components are not absorbed (or are absorbed to the same extent) by the sample, combination of the components would regenerate a polarised radiation in the original plane. However, if one of the components is absorbed by the sample to a greater extent, the resultant radiation (combined components) would now be elliptically polarised, as shown in Fig. 2.



Practically, the CD instrument (spectropolarimeter) does not recombine the components but detects separately the two components; it will then display the dichroism at a given wavelength of radiation expressed as either the difference in absorbance ( $A = \log \frac{I_0}{I}$ ) of the two components ( $\Delta A = A_L - A_R$ ) or as the ellipticity in degrees ( $\Theta$ ) ( $\Theta = \arctg\left(\frac{b}{a}\right)$ , where b and a are the minor and major axes of the resultant ellipse). There is a simple relationship between  $\Delta A$  and  $\Theta$  ( $\Theta$  in degrees), i.e.  $\Theta = 32.98 \Delta A$ . A CD spectrum is obtained when the dichroism is measured as a function of wavelength (Fig. 1). In the experiments CD the value of  $\Delta A$  is measured and the angle  $\Theta$  is obtained from the above relationship. The CD spectra of peptides and protein are plotted in terms of molar ellipticity for residue,  $[\Theta]_R$ :

$$[\Theta]_R = \frac{100 \cdot \Theta}{c \cdot l \cdot n} = \frac{3298}{n} (\epsilon_L - \epsilon_R) \quad (\text{degrees cm}^2 \text{ dmol}^{-1})$$

where n is the residues number in the molecules.

For Lambert-Beer's law, absorption A is given by:

$$A = \epsilon \cdot l \cdot c$$



where  $c$  is the concentration of the optical sample,  $\epsilon$  is the molar extinction coefficient and  $l$  is optical path. So, we can write for  $\epsilon_R$  and  $\epsilon_L$ :

$$\Delta\epsilon = \epsilon_L - \epsilon_R = \frac{A_L - A_R}{cl} \quad (\text{L}\cdot\text{cm}^{-1}\cdot\text{mol}^{-1})$$

In the far UV, the peptide bond is the main absorbing group; studies in this region can give information on the secondary structure of peptides. In the near UV, the aromatic amino acid side chains (phenylalanine, tyrosine and tryptophan) absorb in the range 250 to 290 nm. The tertiary folding of the polypeptide chain can provide chiral environments of these side chains, thus giving rise to CD spectra which are characteristic fingerprints of the native structure. In model compounds containing a disulphide bond, the dihedral angle of this bond can often be deduced from the appearance of the CD spectrum in the 240 to 290 nm region. In the case of extensively disulphide bonded proteins, the same difficulties in performing such analyses can appear because of the overlap of the disulphide signals with those from the aromatic side chains<sup>9, 10, 11</sup>. In addition, non-protein components or cofactors, such as added ligands may absorb in regions of the spectrum well separated from those of amino acids and peptide bonds. The CD signals in these regions can be used to provide detailed information on the environment of, and possible interactions between, these cofactors or ligands.

In the far UV region (typically 240 nm to 190 or 180 nm) the absorbing group is principally the peptide bond. There is a weak but broad  $n \rightarrow \pi^*$  transition centred around 210-220 nm and an intense  $\pi \rightarrow \pi^*$  transition about 190 nm<sup>3, 12</sup>. Studies of far UV CD can be used to assess quantitatively the overall secondary structure content of the protein and the peptide, since it has been known for many years that the different forms of regular secondary structure found in peptides and proteins exhibit distinct CD spectra (Fig. 3).

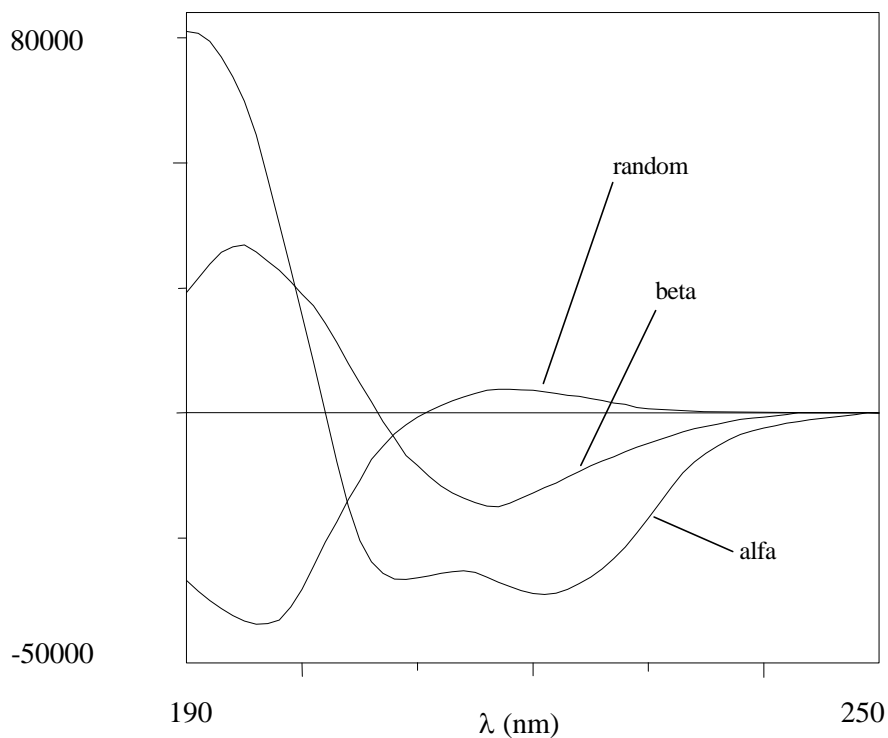


Fig.3: spectra CD of three typical conformations of poly-L-lysine which assumes in aqueous solution at different conditions of pH and temperature:  $\alpha$ -helix at pH>10.5 and R.T.,  $\beta$  structure at pH>10.5 and  $T \geq 50^\circ\text{C}$  and random coil at pH<10.5<sup>13</sup>

By linear combination of the three standard spectra, it is possible to calculate CD spectra corresponding to experimental structures where all three conformations are present in various ratios. The comparison between CD spectra calculated and spectra experimentally found can determine the content of  $\alpha$ -helix,  $\beta$  structure and random coil in the structure of peptides and proteins. While typical spectrum of  $\alpha$ -helix is rather invariant, the same behaviour cannot be observed for the spectra of the  $\beta$ -structure and random coil<sup>6</sup>. The  $\beta$ -structure and random coil of chains polypeptide originate different CD spectra both in intensity and in position of bands.

The major limit of Fasman's method<sup>6</sup> is the fact that, in protein structures, there are other structures such as  $3_{10}$ -helix and various kinds of  $\beta$  structures, with its own CD characteristics, not absolutely determined. Commonly valid standards are not indeed available<sup>14</sup>, because the dichroic profiles of all possible conformation are not yet been determined.  $\alpha$ -helix spectrum is independent from the nature of the solvent, until the solvent does not modify the amount of  $\alpha$ -helix present, and it is also independent from the nature of the side chains, except for peptides containing high percentage of aromatic

residues. In  $\beta$ -structures or random coil, there is a substantial variability of CD spectra according to variation of the experimental conditions. The content of  $\alpha$ -helix is calculated by the relationship between the value of molar ellipticity for residue at 222 nM for the peptide and  $[\Theta]_R^{222\text{nm}}$  for a standard compound totally in  $\alpha$ -helix.

CD spectroscopy provides information on the average conformation in solution of macro-molecules therefore it is not possible to determine whether the percentage of the secondary structure calculated is the result of a set of molecules which are partly structured or which are a portion of molecules completely structured and another one completely disordered.

The correct position of residues along the chain is determined by the use of NMR. In this work, the use of CD spectroscopy was limited to quantitative analysis of helix content and to determine of the experimental conditions in which peptides are mostly ordered.

### **NMR – Nuclear Magnetic Resonance Spectroscopy**

In biological chemistry, NMR spectroscopy appears to be a complementary technique, and sometimes even alternative, to the X-ray diffraction, since it allows the complete structural characterization of peptides and protein which are difficult to crystallize or are in the form of single crystal able to yield high-resolution. This is usually a characteristic of biomolecules with large conformational freedom.

Since the measurements are carried out in solution, it is possible to modify parameters such as solvent, ionic strength, pH and temperature, to create conditions to reproduce as closely as possible those native. The technique allows also to study dynamic processes occurring in solution (e. g. conformers' inter-conversion), provided that the time scale is compatible with that of NMR measurements.

The maximum limit of this technique is the need of rather concentrated solutions (about 1 to 2 mM) in absence of aggregation phenomena. Another limit is the molecular weight, in fact molecules greater than 15 KDa can not be analysed by this method: at high molecular weights, there is an enlargement of spectral lines caused by decreased times of relaxation and an increase of the overlapping of signals.

By enrichment of the samples with  $^{13}\text{C}$  or  $^{15}\text{N}$ , by heteronuclear experiments it is possible to use larger dispersion due to dimension of nuclei, and to study substances

with MW higher than 30-40 KDa. The X-ray crystallography provides an image of a molecule in three dimensions; instead, NMR spectroscopy allows the determination inter-nuclear distances, from which it is possible to identify the three-dimensional structure.

## 2D-NMR

2D experiments consist in appropriate sequence of pulses whose intensity of recorded signals is a function of two different ranges of time,  $t_1$  and  $t_2$ . All two dimensional sequences have the same basic format and can be divided into four stages: preparation, evolution, mixing and detection periods (fig. 5):

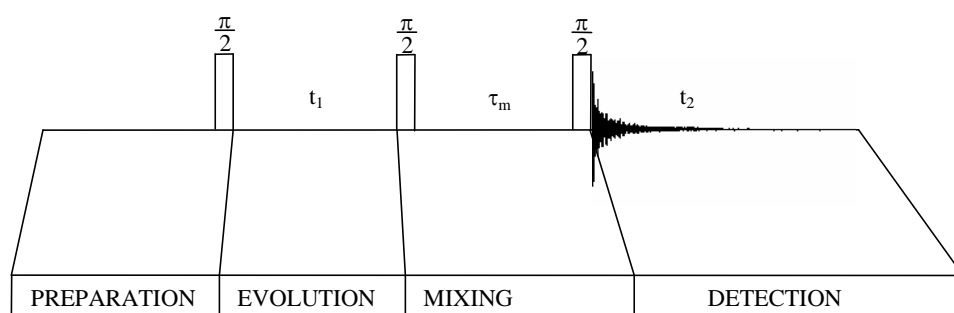


Fig 4: Units of NMR two dimensional experiment.

- Preparation: the sample, at the thermal equilibrium, is perturbed by a pulse of  $\pi/2$  that deflects magnetization on transversal plane
- Evolution allows the magnetization to evolve for a period of  $t_1$ , under the influence of factors such as coupled spin-spin and Larmor's precession;
- Mixing consists in a series of pulses at intervals of time,  $t_m$ , to permit the transfer of magnetization between the spins;
- Detection: in time  $t_2$ , free induction decay is recorded as in the mono-dimensional experiment.

This sequence of steps has not been a 2D-experiment yet. The final 2D-spectrum is obtained by repeating  $n$  times the described sequence in  $\Delta t_1$  increments (constant) of time  $t_1$ . In this way  $n$  FID are generated.

FID signals acquired during  $t_2$  and modified by Fourier's transform give a matrix  $S(t_1, \omega_2)$ , which can be seen as a collection of  $n$  1D-NMR spectra with signals in frequencies domain,  $\omega_2$ , modulated in size and/or in phase because of evolutions during

various  $t_1$ . The application of Fourier's transform long axis of times  $t_1$  of the matrix  $S(t_1, \omega_2)$  allows to obtain 2D-spectrum  $S(\omega_1, \omega_2)$ , where each signal is a function of two frequencies  $\omega_1$  and  $\omega_2$ . So, only  $t_2$  is a real temporal axis since during this period it is recorded an actual FID.

In a 2D-NMR spectrum peaks along diagonal  $(\omega_A, \omega_A)$  refer to nuclei whose magnetization doesn't transfer and precede with same frequency during both  $t_1$  and  $t_2$ . They are present in a 1D-NMR spectrum in a same way. Signals out of diagonal  $(\omega_A, \omega_B)$ , called *cross-peaks*, represent the correlation between nuclei A and B which undergo a transfer of magnetization during time  $t_m$ , under one between following two types of interactions:

- Scalar coupling allows transfer of magnetization between groups of nuclei separated by a limited number of chemical bonds through their electron shells polarization. The experiments used in this work are TOCSY and COSY with the purpose to determine Spin system of each amino acid residue;
- Dipolar coupling allows transfer of magnetization between nuclear spatial neighbours ( $d < 4.5\text{-}5.0 \text{ \AA}$ ) and is due by nuclear Overhauser effect (NOE). The experiments of dipolar correlation used in this work are ROESY and allow sequentially allocation and determination of inter-proton distances.

In 2D-NMR spectrum of a peptide some well defined zones are detectable which cross-peaks produced by specific resonances:

- A zone: *fingerprint* region (where there are resonances of NH-C $^{\alpha}$ H);
- B zone: NH-alifatic proton resonances region;
- C zone: amide and aromatic resonances region;
- D zone: Alifatic proton resonances region;
- E zone: water (solvent) resonance region.

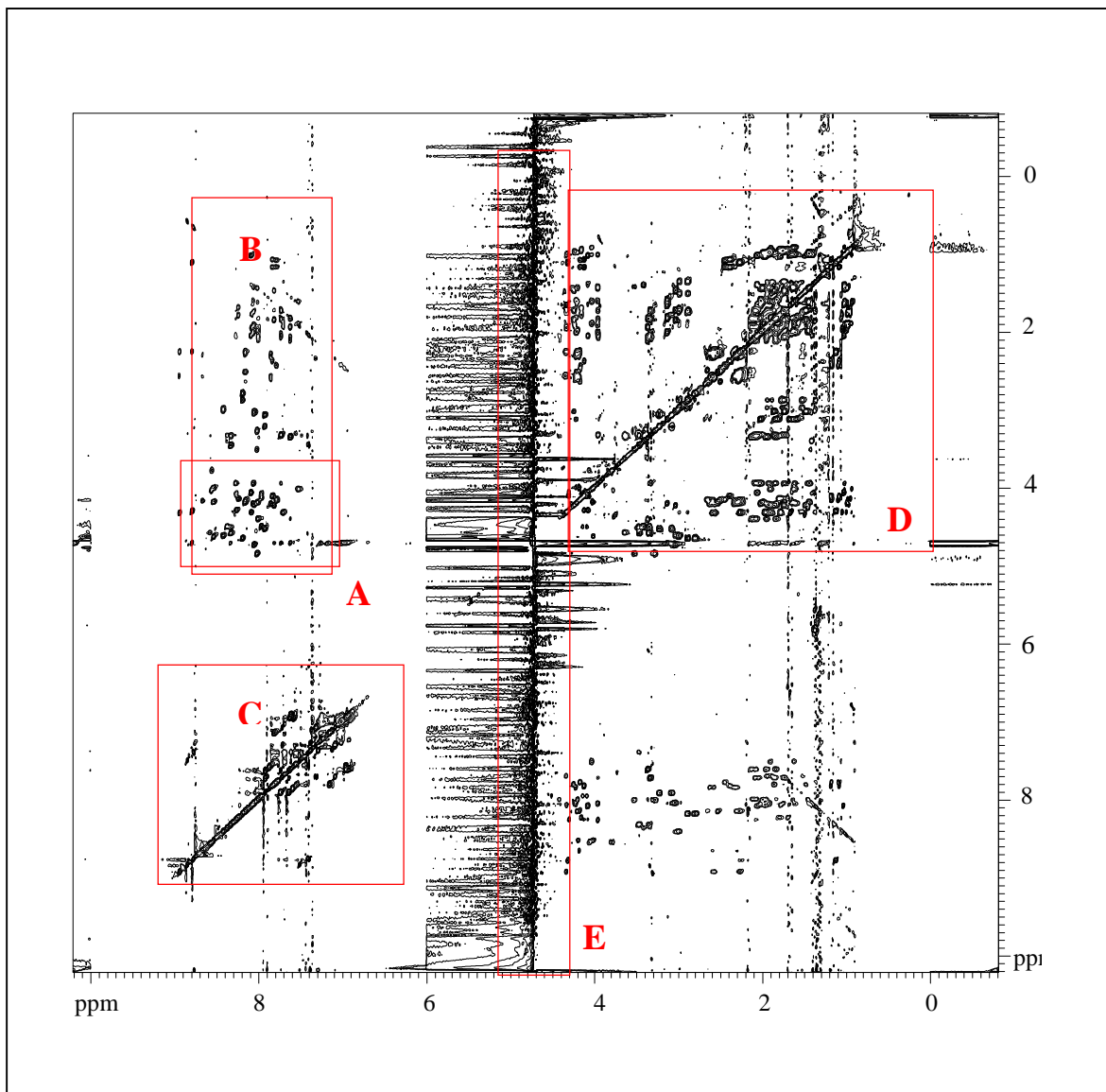


Fig. 5: general aspect of 2D-spectrum TOCSY of a peptide (squared zones are the region of spectrum of major interest).

### Sequential assignment

The primary structure of a peptide is the sequence of amino acid residues along the chain which is the first level of knowledge of a peptide.

Today the method commonly used for peptides and proteins is based on 2D-NMR spectra proposed by Wüthrich<sup>15</sup> in 1982.

The first step of sequential allocation consists in identifying single amino acids through COSY and TOCSY experiments. The regions of TOCSY spectrum which give the most

significant information are the fingerprint regions where  $\text{NH-C}^\alpha\text{H}$  peaks are present and aliphatic NH regions where NH proton correlate with spin system of side-chains.

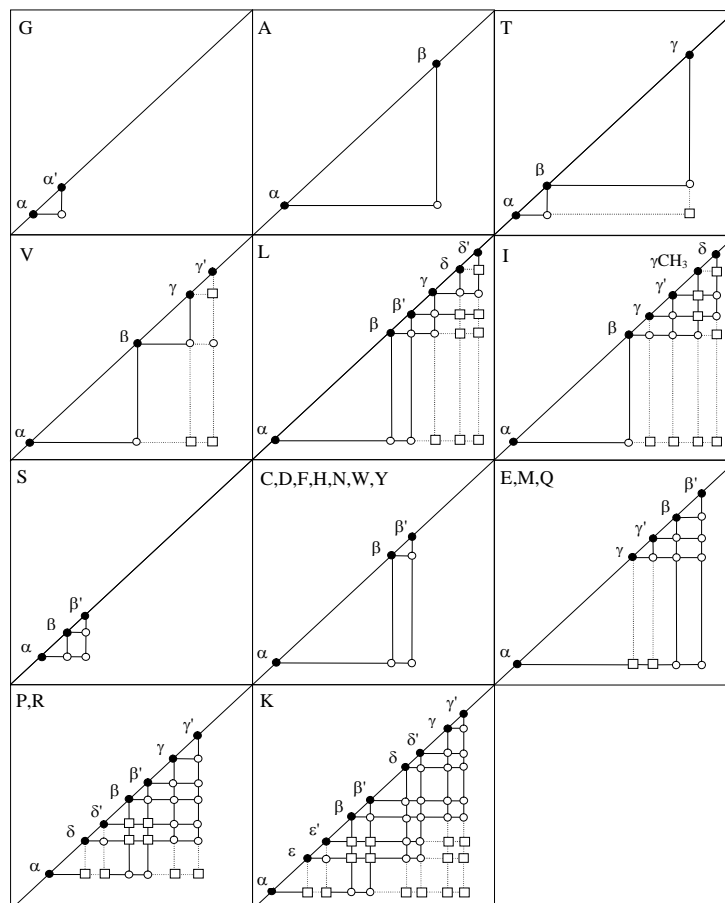


Fig. 6: Spin system of 20 amino acids. Peaks on diagonal are represented by (●); COSY peaks are represented by (○); the squares (□) represent other peaks TOCSY.

For a complete allocation of all residues it is necessary to use NOESY spectra. The second step of sequential allocation is to identify the fragment sequence by exploiting the dipolar connections between consecutive amino acid residues to identify completely the primary structure. From a NOESY spectrum the typical dipolar correlations are those of adjacent amino acids:  $\text{C}^\alpha\text{H-NH}$ ,  $\text{NH-NH}$  e  $\text{C}^\beta\text{H-NH}$  between  $i$  and  $i+1$  residues (fig. 7).

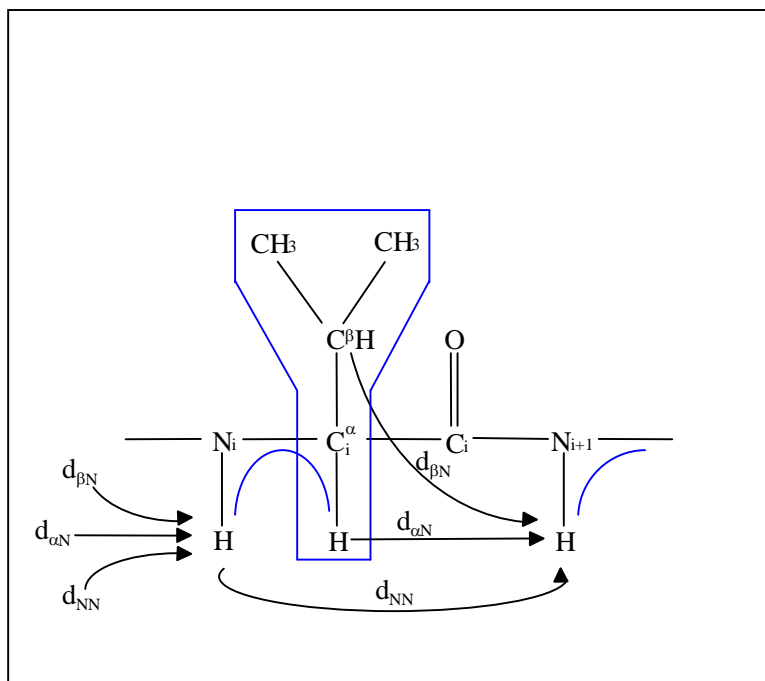


Fig. 7: a portion of peptide chain with indication of C<sup>α</sup>H-NH COSY correlations (lines) and NOESY correlations (arrows).

The NOESY spectra constitute also a good source of additional information useful for peptide secondary structure identification.

	$\alpha$ -helix	$3_{10}$ helix	Antiparallel structure $\beta$	parallel $\beta$ structure	I $\beta$ -turn	II $\beta$ -turn
$d_{\alpha N}(i, i+1)$	3.5	3.4	2.2	2.2	3.4/3.2	-
$d_{\alpha N}(i, i+2)$	4.4	3.8	-	-	3.6	3.3-2.2
$d_{\alpha N}(i, i+3)$	3.4	3.3	-	-	3.1-4.2	3.8-4.7
$d_{\alpha N}(i, i+4)$	4.2	-	-	-	-	-
$d_{NN}(i, i+1)$	2.8	2.6	4.0	3.3	2.6/2.4	4.5/2.4
$d_{NN}(i, i+2)$	4.2	4.6	-	-	3.8	4.3
$d_{\alpha\beta}(i, i+3)$	2.5-4.4	3.1-5.0	-	-	-	-

**Tab. 1:** inter-proton distances (Ångstrom) for some ordered conformations. Distances major of 5 Å are not reported. For distance  $d_{NN}(i, i+1)$  in the turns, the first one is referred to 2 and 3 residues, the second one to residues 3 e 4.



Different secondary structures are generated indeed by typical inter-residue signals which interrelated between nuclei distant in the sequence, but through dipolar coupling neighbours in the space. The inter-proton and middle range distances of secondary structures<sup>16</sup> are shown in table 1.

### 3D structure determination

From 2D NMR spectra it is possible to obtain some indirect informations on peptide 3D structure. These informations are mainly arrays of distances between neighbour nuclei ( $d \leq 5 \text{ \AA}$ ) since NOE acts only at short range and it can be used only to determine local conformations.

There is also the possibility that macromolecule in solution undergoes faster conformation transitions than the time scale NMR, so it cannot correlate each cross-peak to an inter-nuclear distance. Thus, NMR data reproduce an average situation of all fast inter-conversion of all conformations. Inter-nuclear distances are determined by integration of NOE peaks in the NOESY spectrum, as used constraints in molecular modelling experimental programs in order to determine accessible conformational space.

The NOE effect between two nuclei is inversely proportional to the sixth power of their distance:

$$\eta_{ij} \propto \frac{1}{r^6} f(\tau_c)$$

Integrating the cross-peaks of a NOESY and using the following equation, which correlates NOE effects with distances:

$$\frac{\eta_{ij}}{\eta_{kl}} = \frac{r_{kl}^6}{r_{ij}^6}$$

It is therefore possible to determine the inter-atomic distances, after calibration on a peak corresponding to a known distance (e.g. two protons in a CH<sub>2</sub> group).

In this thesis work, the inter-atomic distances have been used as constrains in calculations of molecular modelling in two ways:

- 1) distance geometry (DG)
- 2) restrained molecular dynamic (RMD)

## Distance Geometry

In this technique a number of rigid structures are obtained using multidimensional space projection (with  $N(N-1)/2$  dimensions, where  $N$  is the number of atoms present) into a Cartesian 3D space. Distance Geometry uses inter-atomic distance as internal coordinates system to identify the molecular geometry. Distances between atoms closer as three bounds are calculated on basis of simple geometric and trigonometric hypothesis/considerations, applied at theoretic data obtained from elementary knowledge of chemical structure of the molecule (distances and bond angles). For atoms not close in the molecule, we consider an average values which range in a defined range in order to explore the highest possible conformational space. The lower bounds of this space are calculated from the sum of Van der Waals radius; the upper bounds are put arbitrarily and are anyway higher enough in order to not limit conformational available space. The set of distances obtained is a squared metric matrix where generic element  $a_{ij}$  represents the distance between the atoms  $i$  and  $j$ . The upper bounds are at the top the diagonal of matrix, while the lower bounds are at bottom of diagonal. The program works on the matrix in order to eliminate these distance values which are not physically allowed, on the basis of geometric principle of triangular inequality (*bound smoothing*)<sup>17</sup>.

Inter-atomic distances determined by NMR experiments are used for the construction of a second squared matrix where higher and lower bounds are calculated by adding and subtracting 10% to experimental distances. The comparison between the matrix of covalent distances and experimental distances provides a third more restrictive matrix where the lowest distance, as upper limit, and the highest distance, as lower limit, are chosen between the two possible available distances. The following action is *random metrization*<sup>18</sup> generates a further inter-atomic distances correct matrix: each of them is randomly chosen in previous matrix between allowed distances for each pair of nuclei. *Bound smoothing* is applied to the remaining distances in order to impose a more restrictive constrains. This process leads to a final triangular matrix of correct distances that is converted into a set of Cartesian coordinates though a new procedure called *embedding*. This program of Distance Geometry, synthetically described here, allows to generate many structures, all compatible with experimental NOE data and with geometrical requirements but does not take into account energetic requirements. Each

DG structure obtained is therefore subjected to a *Restrained Molecular Dynamic* analysis to minimize the potential energy function.

### **Restrained Molecular Dynamic**

Molecular Dynamic programs allow to optimize energetically the structures proposed during the research of global energy minimum. After providing enough energy to the system, it is possible to try to overcome local energetic barriers, simulating molecular motions. The accessible conformational space, for peptide structures, is very wide and might have many points of relative energetic minimum. The exploration of this area is restricted by introduction of constraints which make unfavourable those conformations not compatible with experimental data during molecular simulation<sup>19</sup>.

Constraints on the inter-atomic distances, for example, are introduced by additional potential energy factor in the total energy expression. The only structures accepted are these which have deviations from NOE data not higher than 0.5 Å. Finally, we remember that the simulations are led in vacuum, since the presence of solvent will spend too much calculation time. In this thesis work, DG structures are used to explain the biological behaviour and structural analysis.

Distance geometry (DG) and molecular dynamics (MD) calculations were carried out using the simulated annealing (SA) protocol of the X-PLOR 3.0 program. For distances involving equivalent or non-stereo-assigned protons,  $r^{-6}$  averaging was used. The MD calculations involved a minimization step of 100 cycles, followed by SA and a refinement step. The SA consisted of 30 ps of dynamics at 1500 K (10000 cycles, in 3 fs steps) and of 30 ps of cooling from 1500 K to 100 K in 50 K decrements (15000 cycles, in 2 fs steps). The SA procedure, in which the weights of ROE and non-bonded terms were gradually increased, was followed by 200 cycles of energy minimization. In the SA refinement stage, the system was cooled down from 1000 K to 100 K in 50 K decrements (20000 cycles, in 1 fs steps). Finally, the calculations were completed with 200 cycles of energy minimization using a ROE force constant of 50 cal/(mole·Å). 150 structures were generated for each analogue, and the 20 minimum energy structures containing no distance constraint violation (<0.5 Å from the integration value) were chosen for conformational study, using the INSIGHT II and MOLMOL (version 2.6) programs with a SILICON GRAPHICS O2 R 10000 workstation. The secondary

structure was determined using H-bond analysis, dihedral angle calculations, and the Kabsch and Sander algorithm<sup>20</sup>.

## **Peptide content**

Peptide content means the percentage of total peptides present in the synthesized product containing also impurities, such as water, salts, etc. Peptide content can be determined by “Amino Acid Analysis” or AAA, and using UV method.

### **Amino Acid Analysis.**

Amino acid analysis is a process to determine the quantities of each individual amino acid in a protein. There are three steps in amino acid analysis:

- 1. Hydrolysis.*
- 2. Separation and Derivatization.*
- 3. Calculation.*

**1. Hydrolysis:** A known amount of norleucine, used as internal standard, which is present in the resin Novabiochem MBHA, is added to the sample. Since norleucine does not naturally occur in proteins, is stable to acid hydrolysis and can be chromatographically separated from other protein amino acids, it makes an excellent internal standard. The molar amount of internal standard should be approximately equal to that of most of the amino acids in the sample. The sample, containing at least 10 µg of peptide, is then transferred to a hydrolysis tube and dried under vacuum. The tube is placed in a vial containing 6 N HCl and a small amount of phenol and the protein is hydrolyzed by the HCl vapours under vacuum. The hydrolysis is carried out for 48 h<sup>1</sup> at 110°C. Then, the sample is dried under vacuum.

**2. Separation and Derivatization:** The amino acids are separated on an ion-exchange column and at the end of separation there is derivatization. Derivatization is performed automatically on the amino acid analyzer by reacting the free amino acids with ninhydrin, which is detected at 440 nm. A standard solution containing a known amount

---

<sup>1</sup> Commonly, the reaction is carried out 22 h when a hydrophobic-hydrophobic sequence is not present.

(500 pmol) of 17 common free amino acids is also loaded on a separate amino acid analyzer sample spot and derivatized. This will be used to generate a calibration file that can be used to determine amino acid content of the sample.

**3. Calculation:** Chromatographic peak areas are identified and quantitated using a data analysis system that is connected to the amino acid analyzer system. A calibration file is obtained from the average values of the retention times (in minutes) and areas (in (Au) of the amino acids in 10 standard runs. Since a known amount of each amino acid is loaded onto the analyzer, a response factor ((Au/pmol) can be calculated. This response factor is used to calculate the amount of amino acid (in pmols) in the sample. The amount of each amino acid in the sample is calculated by dividing the peak area of each amino acid (corrected for the differing molar absorptivities of the various amino acids) by the internal standard (norleucine) in the chromatogram and multiplying this by the total amount of internal standard added to the original sample.

### UV Methods

An ultraviolet light adsorption method has several advantages<sup>21</sup>: it can be performed directly on the sample without the addition of many reagents, it is very quickly since no incubation are required, and the relationship between peptide concentration and absorbance is linear. Use of the peptide bond absorption to determine peptide content has been employed frequently. In fact, it has high sensitivity and has the advantage of relatively little variability due to amino acids composition. The peptide bond absorbs below 210 nm. Although in this region some absorption by Trp and Tyr residues occurs, less variability between peptides is observed than at 280. The disadvantage of this region is that many chemicals also absorb. Moreover, measurement at the actual peak of absorption around 190 nm is difficult for several technical reasons, not least being the absorption of light by air. Tombs *et al.*<sup>22</sup> suggested that 205 nm might be the best wavelength for protein determination. We made a comparison between UV method and AAA, and we found a good agreement in a range of 15%. This is a good yield if we think that a lot of unnatural amino acids are used in our peptide analogues. So, we used UV method at 205 to determine peptide content for routine measurement. The side chain of amino acids, which contribute to total peptide absorption at 205 nm, are only of His and Har/Arg which can also have a moderate contribution.

## Biological tests

### ACTIVITY ASSAYS

*Cell Culture and CRE-Luc Transfection.* Human embryonic kidney (HEK 293) cells stably transfected with recombinant hPTH1-receptor (HEK293/C20 cell line)<sup>23</sup> were cultured at 37°C in Dulbecco's modified Eagle's medium supplemented with 10% fetal bovine serum in a humidified atmosphere of 95% air and 5% CO<sub>2</sub>. The cells were subcultured by treatment with Versene every week and the medium was changed every 3-4 days. Twenty-four hours before transfection, C20 HEK293 cells were seeded at 10<sup>5</sup> cells/well in 24 wells, Collagene coated plates. On the following day the cells were treated with FuGENE 6 Transfection Reagent (2µl/well), CRE-Luc plasmid (0.5µg/well) in 0.5 ml/well Opti-Mem I, serum free medium, according with the manufacturer's recommended procedure.

*Luciferase Assay.* Eighteen hours after transfection, the medium was replaced with 225 µl/well of Dulbecco's Modified Eagle Medium. 25 µl/well of a solution of peptide in PBS/0.1% BSA was added, and the cells were incubated for four hours at 37 °C, yielding maximal response to luciferase. Each peptide concentration was used in triplicate. The medium was aspirated and the cells were washed once with PBS pH 7.4 (250 µl/well). The cells were lysed by addition of 200 µl of Passive Lysis Buffer per well and gentle shaking for 5 min. The suspension was then transferred to labelled low binding eppendorf tubes, centrifuged for 2 min, and 80 µl of the supernatant was transferred into labelled glass tubes.

*Luciferase activity.* Luciferase activity was measured on a Lumat LB 9507 luminometer (EG&G Berthold). This instrument automatically injects pre-defined volumes of two solutions, A and B, with compositions described below. Initially, a Solution 0 was prepared, containing glycylglycine 25 mM, MgSO<sub>4</sub> 15 mM, and ethyleneglycol-bis(β-aminoethyl ether)-N,N,N',N'-tetraacetic acid (EGTA) 4 mM in deionized water. Solution A was 0.2 mM D-luciferin in Solution 0. Solution B was K<sub>3</sub>PO<sub>4</sub> 0.02 M, ATP 2.5 mM, and dithiothreitol 1 mM in Solution 0. The instrument was calibrated to add 100 µl of Solution A and 300 µl of Solution B to a sample tube, and performed the

measurement for 20 seconds. The mean read-out from three wells with identical peptide concentrations was used to present the data.

*Data Calculation.* Calculations and data analysis were performed using Microsoft Excel 2000 and GraphPad Prism, Version 3.0.

# REFERENCES

- <sup>1</sup> Norbert Sewald and Hans-Dieter Jakubke, Peptides: Chemistry and Biology, Wiley and Sons, N.Y. USA 209-211 (2002)
- <sup>2</sup> R. B. Merrifield, J. Am. Chem. Soc. 1963, 85, 2149
- <sup>3</sup> S. A. Salisbury, E. J. Tremeer, J. W. Davies, D. E. I. A. Owen, et al. J. Chem. Soc. Chem. Commun., 1990, 538.
- <sup>4</sup> Young SC, White PD, Davies JW, Owen DE, Salisbury SA, Tremeer EJ.. Biochem. Soc. Trans., 18, 131, 1990
- <sup>5</sup> F. Balkenhohl, C. von dem Bussche-Hünnefeld, A. Lansky, C. Zechel, Angew. Chem. Int. Ed. Engl. 1996, 35, 2288
- <sup>6</sup> J. C. Hogan, Jr., Nature Biotechnol. 1997, 15, 328
- <sup>7</sup> H.-J. Böhm, M. Stahl, Curr. Opin. Chem. Biol. 2000, 4, 283
- <sup>8</sup> Kelly S. M. and Price N. C. *Current Protein and Peptide Science*, 2000, Vol. 1, No. 4, 349-384
- <sup>9</sup> Woody, R.W. and Dunker, A.K. (1996) in Circular Dichroism and the Conformational Analysis of Biomolecules (Fasman, G.D., ed.). pp. 109-157, Plenum Press, New York.
- <sup>10</sup> Greenfield, N.J. (1999) Trends Analyt. Chem., 18, 236-244.
- <sup>11</sup> Chaffotte, A.F., Guillou, Y. and Goldberg, M.E. (1992) Biochemistry ,31, 9694-9702.
- <sup>12</sup> Venyaminov, S.Yu. and Yang, J.T. (1996) in Circular Dichroism and the Conformational Analysis of Biomolecules (Fasman, G.D., ed.). pp. 69-107, Plenum Press, New York.
- <sup>13</sup> Greenfield N., Fasman G. D. Biochem. 8 (10), 1969, 4108-4116
- <sup>14</sup> Toniolo C., Polese A., Formaggio F., Crisma M., Kamphuis J., 1996. J. Am. Chem. Soc., 118, 2744-2745
- <sup>15</sup> K. Würthrich, NMR of Proteins and Nucleic Acids, Wiley and Sons, N. Y., USA (1986)
- <sup>16</sup> K. Würthrich, M. Billiter, W. Braun, J. Mol. Biol. 180, 715-740 (1984)
- <sup>17</sup> J. M. Crippen, Distance Geometry and Conformational Calculation, Chemometrics Research Studies Press, Letchworth UK (1981)
- <sup>18</sup> J. M. Crippen, T. F. Havel, Distance Geometry and Molecular Conformation, Research Studies Press, Letchworth UK (1988)
- <sup>19</sup> A. T. Brunger, G. M. Clore, A. M. Gronenberg, M. Karplus, Proc. Natl. Acad. Sci. USA, 83, 3801-3805 (1986)
- <sup>20</sup> Kabsch, W.; Sander, C. Biopolymers 1983, 22, 2577-2637
- <sup>21</sup> Stoscheck C. M. Methods in Enzymology, 82, 50-68, 1990
- <sup>22</sup> Tombs, M. P., Souter F., MacLagan, N. F. Biochem. J. 73, 167, (1959)
- <sup>23</sup> Pines, M.; Adams, A. E.; Stueckle, S.; Bessalle, R.; Rashti-Behar, V. et al. *Endocrinology* **1994**, 135, 1713-1716.



# Experimental Part

Starting Materials and Reagents are commercial available.

Amino Acids: from Advanced ChemTech/GL Biochem (Shangai)

- FmocAbuOH (Fmoc amino- $\gamma$ -butyric acid, MW= 325,4 g/mol)
- BocAibOH (Boc  $\alpha$ -amino-isobutyric, MW: 203,2 g/mol)
- FmocAibOH (Fmoc  $\alpha$ -amino-isobutyric, MW: 325,4 g/mol)
- FmocAmcOH (Fmoc amino-capronic acid, MW: g/mol)
- FmocGln(Trt)OH (Fmoc(Trityl)Glutamin, MW: 610,7 g/mol)
- FmocGlu(OtBu)OH (Fmoc(tert butyl Ester)Glutamic acid, MW: 425,5 g/mol)
- FmocHar(Pbf)OH (Fmoc(Pentamethyl-Benzo-Furanyl)Homoarginine, MW: 648,8 g/mol)
- FmocHis(Trt)OH (Fmoc(Trityl)Histidine, MW: 619,7 g/mol)
- FmocHis(Boc)OPfp (Fmoc(Trityl)Histidine pentafluorophenol Ester, MW: 643,5 g/mol)
- FmocIleOH (Fmoc Isoleucine, MW: 353,4 g/mol)
- FmocD(allo)IleOH (Fmoc Allo Isoleucine, MW: 353,4 g/mol)
- FmocLeuOH (Fmoc Leucine, MW: 353,4 g/mol)
- FmocLeuOPfp (Fmoc Leucine, pentafluorophenol Ester, MW: 519,5 g/mol)
- FmocNleOH (Fmoc Norleucine, MW: 353,4 g/mol)
- FmocSer(OTrt)OH (Fmoc (Trityl) Serine, MW: 569,7 g/mol)
- FmocValOH (Fmoc Valine, MW: 339,4 g/mol)

Resin: Nova Biochem Rink Amide MHBA (Loading 0,073 mmol/g)

Coupling reagents:From GL Biochem (Shangai)

- HBTU: 2-(1H-benzotriazol-1-yl)-1,1,3,3-tetramethyluronium hexafluorophosphate
- HOBt: 1-hydroxybenzotriazole
- HATU:2-(1-aza-benzotriazol-1-yl)-1,1,3,3-tetramethyluronium hexafluorophosphate
- HOAt: 1-Aza-1-hydroxybenzotriazole

Acids, Bases, Solvents: From Carlo Erba and Fluka-Aldrich

- Acetonitrile (HPLC grade) – ACN/CH<sub>3</sub>CN
- Sodium Hydroxide - NaOH
- Trifluoroacetic Acid - TFA
- Trinitrobenzensulfonic Acid - TNBS
- Acetic Anhydride – Ac<sub>2</sub>O
- 2,4,6 Collidine
- Di-cloro methane – DCM/CH<sub>2</sub>Cl<sub>2</sub>
- diisopropylethylamine - DIPEA
- Dimethyl formamide - DMF
- Ethanol - EtOH

- Ethyl Ether – Et<sub>2</sub>O
  - Methanol - MeOH
  - N-methyl pyrrolidone - NMP
  - Piperidine - Pip
  - Trifluoroethanol - TFE
  - Triisopropyl silane - TIS
  - Triethyl amine - TEA
  - Trimethyl chloro silane – Me<sub>3</sub>SiCl
- mQ Water is obtained through “Reagent Grade System” by Millipore.

### **Thin Layer Chromatography (TLC)**

Solid support of TLC is commercial available by Merck (5 × 10 cm), silica gel 60 Kiesel gel UV254 with thickness of layer 0,25 mm and TLC by Fluka DC-Alufolien-Kiesel gel UV254 with thickness of layer 0,2 mm. The solvent used to run TLC was reported in experimental part. To detect it is used either Fluorescent reactivity of TLC or Ninhydrine reagent (1% in solution of n-Butanol) or KMnO<sub>4</sub> (1% in water solution).

### **High Pressure Liquid Chromatography (HPLC)**

The instrument is produced by Amersham Pharmacia Biotech (Acta Basic 10), with a UV three canals detector and an integrator connected to a PC. Common solvents include miscible combinations of water and organic liquid (acetonitrile). Water contains a percentage of trifluoroacetic acid which acts as an ion pairing agent in order to assist in the separation of the analyte components. It is used as reversed phase HPLC (RP-HPLC) which consists of a non-polar stationary phase and an aqueous, moderately polar mobile phase. The common stationary phase used is silica C18, a straight chain alkyl group such as C<sub>18</sub>H<sub>37</sub>. To analytical purpose it is used a analytic column Vydac C18 218TP54 (250 × 4,6 mm, d:5µm, Flow: 1ml/min); semi-preparative column Vydac C18 218TP510 (250 × 10.0 mm, d:10µm, Flow: 5 ml/min); and preparative column Water DeltaPAK C18 11799 (300 × 19.0 mm, d:15µm Spherical, Flow: 17 ml/min).

The preparative HPLC is produced by Shimadzu series LC-8°, with a UV detector Shimadzu SPD-6° and an integrator model 561 by Perkin Elmer.

The technique of separation is gradient elution, where the mobile phase changes its composition during a separation process. Standard gradient starts from 10 % solvent B and finishes up with 90 % solvent B in 30 min. The benefit of gradient elution is that it helps speed up elution by allowing components that elute more quickly to come off the

column under different conditions than components which are more readily retained by the column. By changing the composition of the solvent, components of a mixture can be resolved selectively because they stay instantly at equilibrium between mobile phase and stationary phase. Whether a component spends more time in the mobile phase and less in the stationary phase, therefore it elutes faster, and mixture can be separated. For preparative gradient, the composition of solvent was defined about crude peptide every time.

The miscible combinations are made using solvent:

- A = H<sub>2</sub>O milliQ + TFA 0.1%
- B = CH<sub>3</sub>CN 90% in water milliQ + TFA 0,1%

### **Mass Spectroscopy (MS)**

Mass Spectra were performed by a PerSeptive Biosystems Mariner - ESI-TOF. Ionization technique used in this instrument is electrospray ionization. In electrospray ionization, a solution of the sample (analyte) dissolved in a convenient solvent is pushed through a very small capillary, which is charged and usually in metal. The analyte exists as an ion in solution either in its anion or cation form. Because equal charges repel, the liquid pushes itself out of the capillary and forms an aerosol; at the same time an unchanged gas, such as nitrogen, is sometimes used to help for nebulizing the liquid and to help for evaporating the neutral solvent in the droplets. As the solvent evaporates, the analyte molecules are forced closer together, repel each other and break up the droplets. This process is called Coulombic fission because it is driven by repulsive Coulombic forces between charged molecules. The process takes the analyte to be free of solvent and a lone ion. Now, lone ion moves to the mass analyzer of a mass spectrometer. In electrospray processes, the ions observed may be quasi-molecular ions created by the addition of a proton (a hydrogen ion) and denoted  $[M+H]^+$ , or of another cation such as sodium ion,  $[M+Na]^+$  or potassium  $[M+K]^+$ .

Mass analyzers separate the ions according to their mass-to-charge ratio. The time of flight (TOF) is the method used to measure the time that it takes for the ion to reach a detector while traveling over a known distance. The ion is accelerated by an electrical field to the same kinetic energy with the velocity of the ion depending on the mass-to-charge ratio.

### **UV-VIS spectroscopy**

Absorbance measurements were performed with SHIMADZU UV-2501 interfaced with PC. All experiments were carried out at room temperature using HELLMA quartz cells with Suprasil windows and optical path-length of 1 cm. Spectra were taken on following parameters:

- Scan Speed: 60 nm/min;
- Shift Size: 2 nm;
- Spectrum: 190-350 nm.

This analysis was used to calculate peptide content using characteristic absorbance at 205 nm and following equation:

$$C(\text{mg/ml}) = A_{205}/31$$

### **Circular Dichroism**

CD measurements were carried out on a JASCO J-715 spectropolarimeter interfaced with a PC. The CD spectra were recorded and processed using the J-700 program for Windows. All experiments were carried out at room temperature using HELLMA quartz cells with Suprasil windows and optical path-length of 0.01 cm and 0.1 cm. All spectra were recorded using a bandwidth of 2 nm and a time constant of 8 sec at a scan speed of 20 nm/min. The signal to noise ratio was improved by accumulating 8 scans. Measurements were performed in the wavelength range 190-250 nm and the concentration of the peptides was in the range 0.07 – 1.07 mM. The peptides were analyzed in aqueous solution containing 2,2,2-trifluoroethanol (TFE) 20%(v/v). The spectra are reported in terms of mean residue molar ellipticity ( $\text{deg}\cdot\text{cm}^2\cdot\text{dmol}^{-1}$ ). The helical content for each peptide was estimated according to the literature.<sup>1</sup>

### **Nuclear Magnetic Resonance (NMR)**

NMR spectra were recorded at 298 K on a BRUKER AVANCE DMX-600 spectrometer. The experiments were carried out in  $\text{H}_2\text{O}/\text{TFE-d}_3$  (4:1)<sub>v/v</sub>. The sample concentration was approximately 1 mM in 600  $\mu\text{l}$  of solution. The water signal was

suppressed by pre-saturation during the relaxation delay. The spin systems of all amino acid residues were identified using standard DQF-COSY<sup>2</sup> and CLEAN-TOCSY<sup>3, 4</sup> spectra. In the latter case, the spin-lock pulse sequence was 70 ms long. The sequence-specific assignment was accomplished using the rotating-frame Overhauser enhancement spectroscopy (ROESY), using a mixing time of 150 ms. In all homonuclear experiments the spectra were acquired by collecting 400-512 experiments, each one consisting of 32-256 scans and 4K data points.

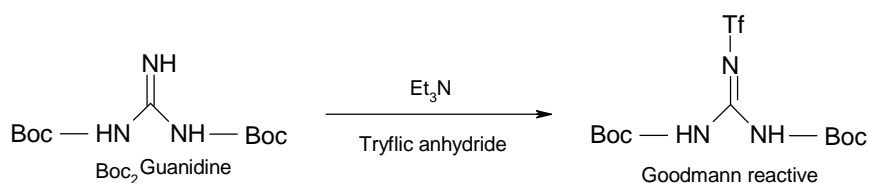
Spectral processing was carried out using XWINNMR. Spectra were calibrated against the TMS signal. Inter-proton distances were obtained by integration of the ROESY spectra using the AURELIA software package. The calibration was generally based on the geminal protons of Ile<sup>5</sup>, set to a distance of 1.78 Å.

## § Preparation of analogues for D-Scan

### Total synthesis of HomoArginine

*Preparation of N,N'-Bis-Boc-guanidine:* To a stirred solution of guanidine HCl (4.8g, 0.05 mole) in 100ml of 4 molar NaOH + Dioxane (1:1) at 0°C Boc-anhydride (24g, 0.11 mole, 2.2 eq.) was added and stirring was continued for 2 hours at 0°C and then for overnight at room temperature. After removal of dioxane from the mixture at low temperature (30-40°C), it was diluted with water (100ml) and was extracted with ethylacetate (3 x 50ml). The combined organic phase was washed with 0.25 N HCl, water, brine (3 times/each) and then dried over anhydrous sodium sulfate. It was filtered and evaporated to dryness in vacuo. The solid obtained was precipitated and filtered from hexane to yield bis Boc-guanidine in 40 to 58.5% yield (5.2g – 7.6g).

*Preparation of N,N'-Bis-Boc-N''-triflyl-guanidine:*<sup>5</sup>



<i>Specie</i>	<i>MW</i>	<i>[g/mL]</i>	<i>mmol</i>	<i>eq</i>	<i>amount</i>
<b>Boc<sub>2</sub>Guanidine</b>	<b>260</b>		<b>3,8</b>	<b>1</b>	<b>1 g</b>
<b>TEA (Et<sub>3</sub>N)</b>	<b>101,2</b>	<b>0,73</b>	<b>7,6</b>	<b>2</b>	<b>1,06 mL</b>
<b>Tryflic Anhydride</b>	<b>282,1</b>	<b>1,71</b>	<b>7,6</b>	<b>2</b>	<b>1,25 mL</b>
<b>DCM (dry)</b>					<b>20 mL</b>

To a stirred solution of Bis-Boc-guanidine (5.2g, 20mm) in 100ml of DCM (dried over molecular sieve) under nitrogen Et<sub>3</sub>N (2.9ml, 21mm, 1.05 eq.) was added. After stirring for 5-10 minutes at room temperature, it was stirred at or below -70 to -78°C and fresh triflic anhydride (3.5ml, 21mm, 1.05 eq.) was added dropwise over a period of 5 minutes. When the addition was complete, the reaction mixture temperature (-64°C) was left reach at room temperature (approximately 2-3 hours). The solution was washed with 2M Sodium bisulfate and water (2 times/each). The organic phase was dried over anhydrous Sodium Sulfate, filtered and evaporated to dryness in vacuo. The residue left was treated with hexane and the solid obtained was filtered, washed with hexane and dried to yield 70.5% (5.52g) of the desired product. The product was controlled by Esi-Tof: 392 [M+H<sup>+</sup>]. mp: 114-115 °C.

<sup>1</sup>H NMR (200 MHz, DMSO-d<sub>6</sub>): ppm 11.45 (br s, 2H), 1.45 (s, 18H).

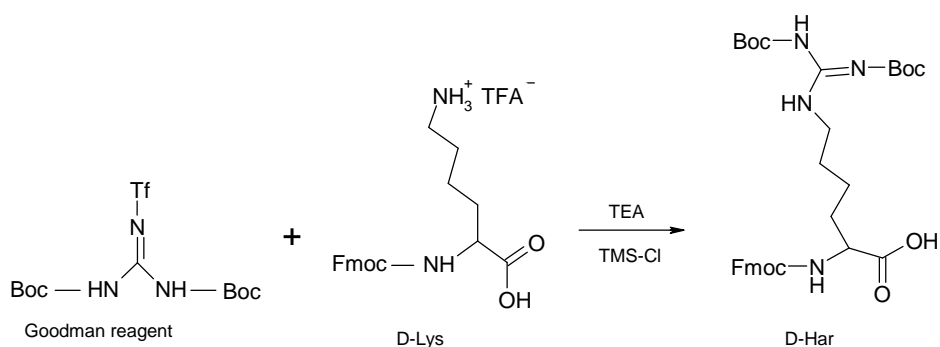
*Preparation of N,N'-Bis-Boc-S-methylisothiourea:*<sup>6</sup> S-Methylisourea sulfate (2.78 g, 10 mmol) was dissolved in a solution of water and dioxane 50/50 followed by addition of 1 M aq NaOH solution (20 mL, 20 mmol) and di-tert-butyl dicarbonate (11.62 g, 50 mmol, 1.3 equiv.). The reaction mixture was vigorously stirred overnight at r.t. The formed precipitate was filtrated and washed with a small amount of water. The filtrate was concentrated under reduced pressure to approximately half volume and the solid was separated by filtration. The solids were combined and suspended in water (200 mL) at approximately 50°C, shaken and filtrated again. It was then dried under vacuum at r.t. over phosphoric anhydride to give N,N'-Bis-Boc-S-methylisothiourea (5.57 g, 96%) as a white solid; mp 127°C (Lit. mp 122-123°C)

<sup>1</sup>H NMR (200 MHz, CDCl<sub>3</sub>): δ = 1,51 (s, 9H), 1,52 (s, 9H), 2,40 (s, 3H), 11,62 (br s, 1H).

## Preparation of N- $\alpha$ -Fmoc-bisBoc-Urethane-Homoarginine

*Use of Bis-Boc-triflyl-guanidine and MSTFA:* To a stirred suspension of N- $\alpha$ -Fmoc-L-Lysine (1.84g, 5mmol) in 30ml of dry DCM under nitrogen, N-methyl-N(trimethylsilyl) trifluoroacetamide (2.0ml, 11mmol, 2.2 eq.) was added dropwise over a period of 15-20 minutes until it became a homogenous solution. It was then refluxed for one hour and then brought to room temperature while a solution of Bis-Boc-triflyl-guanidine (2.35g, 6mmol, 1.2 eq.) in DCM was added followed by Et<sub>3</sub>N (0.84ml, 6mmol, 1.2 eq.). The mixture was stirred for one hour at room temperature, two hours at reflux temperature and then at room temperature overnight. The progress of the reaction was monitored by TLC. It was washed with 2M Sodium bisulfate, brine, water (2 times/each), dried over anhydrous Sodium Sulfate and was filtered. The filtrate was concentrated into a syrup (3.3g) in vacuo. According to HPLC (data not shown), it contained the product (Rt = 9.39 min, 56.4%), guanylated agent (Rt = 4.94 min, 25.4%) and starting amine (Rt = 7.30 min., 3%). When the reaction was carried out at room temperature for overnight (without reflux at any stage), the syrup contained the product (71.7%) with guanylated agent (9%) and with starting amine (7.8%). The crude product was purified by flash chromatography using DCM : MeOH 9 : 1 (v/v) with a yield of 66% of a white powder.

*Use of Bis-Boc-triflyl-guanidine and TMS-Cl:*



**Reagents:**

	<i>MW</i>	<i>[g/mL]</i>	<i>mmol</i>	<i>eq</i>	<i>amount</i>
<b>Fmoc-D-Lys-OH ·TFA</b>	<b>484</b>		<b>1,03</b>	<b>1</b>	<b>500 mg</b>
<b>TEA (Et<sub>3</sub>N)</b>	<b>101,2</b>	<b>0,73</b>	<b>2,47</b>	<b>3,6</b>	<b>0,51 mL</b>
<b>TMS-Cl</b>	<b>108,6</b>	<b>0,86</b>	<b>0,69</b>	<b>2</b>	<b>0,26 mL</b>
<b>Goodman reactive</b>	<b>391</b>		<b>1,24</b>	<b>1,2</b>	<b>483,3 mg</b>
<b>DCM (dry)</b>					<b>20 mL</b>

To a stirred suspension of N- $\alpha$ -Fmoc-L-Lysine (0.92g, 2.5mmol) in 30ml of dry DCM, Et<sub>3</sub>N (0.42ml, 3.0 mmol, 1.2 eq.) was added followed by TMS-Cl (0.32ml, 2.5mmol, 1 eq.) and the stirring was continued for 30 minutes at room temperature and 60 minutes at refluxing temperature and then it cooled to room temperature. It was then stirred at 0°C and Bis-Boc-triflyl-guanidine (1.18g, 3mmol, 1.2 eq.) was added followed by Et<sub>3</sub>N (0.42ml, 3mmol, 1.2 eq.) and was allowed to reach at room temperature on 1 hour. It was then stirred at refluxing temperature for 2 hours and at room temperature overnight and the progress of reaction was controlled by TLC. After stirring the solution with methanol (~10ml) for 20-30 minutes, the solvent was evaporated and the residue was dissolved in ethylacetate and washed with 2M Sodium bisulfate, brine and water (2 times/each). The product was dried over anhydrous Na<sub>2</sub>SO<sub>4</sub>, filtered, evaporated into a syrup which was solidified by drying under vacuum. The solid was collected using hexane to yield 1.4g (91.5%) of crude product. According to HPLC, the product (Rt = 9.37 min, 69.3%) was contaminated with starting amine (7.37 min., ~19%). The crude product was purified by flash chromatography using DCM : MeOH 9 : 1 (v/v) with a yield of 63% of a white powder.

*Use of Bis-Boc-S-methylisothiurea and TMS-Cl:* A stirred mixture of N- $\alpha$ -Fmoc-L-Lysine (1.84g, 5mmol) and Et<sub>3</sub>N (1.4ml, 10mmol, 2 eq.) in 60ml of DCM at 0°C was treated with TMS-Cl (1.3ml, 10mmol, 2 eq.) and stirring was continued for 1 hour at room temperature. The solution was then stirred at 0°C and Et<sub>3</sub>N (1.4ml, 2 eq.) was added followed by Bis-Boc-S-methylisothiurea (1.82g, 6.25mmol, 1.25 eq.); the initial fine suspension became homogenous solution. The solution was refluxed for 19 hours, and after cooling to room temperature, it was treated with MeOH (~ 10ml) and stirring was continued for 20-25 minutes. The mixture was evaporated to dryness and the residue was dissolved in H<sub>2</sub>O/EtOAc and acidified to pH = 4 with 3N HCl. The organic



layer was washed with brine, water, dried over  $\text{Na}_2\text{SO}_4$ , filtered and evaporated into a solid. The yield was 2.62g (85.6%). By HPLC analysis, the material contained only 24.2% of the desired product; the remaining product was guanylation agent Bis-Boc-S-methylisothiurea<sup>1</sup>.

*Use of Bis-Boc-S-methylisothiurea and MSTFA:* To a stirred suspension of N- $\alpha$ -Fmoc-L-Lysine (0.92g, 2.5mmol) in 30ml DCM under nitrogen MSTFA (1ml, 5.5mmol, 2.2 eq.) was added. The suspension became clear solution within 10 minutes. After stirring for 30 minutes at room temperature, the solution was refluxed for 1 hour and was then cooled to room temperature. It was now stirred at 0°C and Bis-Boc-S-methylisothiurea (0.87g, 3mmol, 1.2 eq.) was added followed by  $\text{Et}_3\text{N}$  (0.42ml, 3mmol, 1.2 eq.) and stirring was continued for 1 hour. It was again refluxed for 2 hours and then stirred for overnight at room temperature. The solution was diluted with DCM/ $\text{H}_2\text{O}$ , acidified to pH of 4 and then washed separated DCM phase with brine (2 times), dried it over  $\text{Na}_2\text{SO}_4$ , filtered and then dried to yield a solid residue. The yield was 1.4g (91.5%). The solid, analyzed by HPLC, it contained the desired product (14.5%) as the minor component and guanylation agent (67%) as the major component.

*Use of Bis-Boc-S-methylisothiurea:* To a solution of Bis-Boc-S-methylisothiurea (66 mg, 0.114 mmol) in 2 ml of dry DCM, Fmoc-Lys-OH-TFA (32 mg, 0.057 mmol) was added with few drops of DMF. After few minutes, DMAP (6 mg, 0.005 mmol) was added and the mixture was stirred at room temperature. The progress of the reaction was monitored by TLC (8:2 light petroleum ether/ethyl acetate). After three hours the reaction was stopped, the solvent was evaporated, and the residue was dissolved in EtOAc. The solution was then washed with  $\text{KHSO}_4$  5%, water and  $\text{NaHCO}_3$  10%. The organic phase was dried ( $\text{Na}_2\text{SO}_4$ ) and evaporated. The only final product found was the starting material.

---

<sup>1</sup> NOTE: When reflux period was reduced to 2 hours followed by overnight stirring at room temperature, the product yield was only 2.5% as evidenced by HPLC.

### Characterization of Fmoc-Homoarginine Bis Boc.

$^1\text{H}$  NMR (200 MHz,  $\text{CDCl}_3$ ): ppm 11.39 (s, 1H), 7.77-7.3 (8H Fmoc); 6.4 (mb, 1H  $\text{NH}(\text{amide})$ ); 4.4 (d, 2H  $\text{CH}_2(\text{Fmoc})$ ); 4.25-4.20 (t; mb, 2H  $H\alpha\text{-Har}$ ;  $H\text{-(Fmoc)}$ ); 3.15 (m, 2H), 1.82 (m, 4H), 1.49 (m, 2H), 1.49-1.41 (2 s, 18H).

### Synthesis of D-Homoarginine

*First Step: Preparation of Fmoc-D-Lys(NH<sub>2</sub>)-OH:* Fmoc-D-Lys(Boc)-OH (500 mg – 1.06 mmol) was cleaved with a solution of TFA 15% in DCM. After 2 hours, the solvent was evaporated under vacuum. HPLC  $R_t$  = 7,53 min.

*Second Step: Preparation of Fmoc-D-Har(Boc)<sub>2</sub>-OH:* To a stirred suspension of N- $\alpha$ -Fmoc-D-Lysine·TFA (500 mg, 1.05 mmol) in 15 ml of dry DCM,  $\text{Et}_3\text{N}$  (0.32 ml, 2.31 mmol) was added, followed by TMS-Cl (0.13 ml, 1.05 mmol). The stirring was continued for 30 min at r.t. and for 60 min at reflux temperature and then cooled to r.t. (to obtain a homogeneous solution, 1 eq. of TMS-Cl was added and the solution was stirred at reflux temperature for 30 min). The solution was then stirred at 0°C and Bis-Boc-triflyl-guanidine (0.39 g, 1 mmol) was added followed by  $\text{Et}_3\text{N}$  (0.16 ml, 1.15 mmol). The solution left to reach at room temperature in 1 hour period. It was then stirred at reflux temperature for 2 hours and at room temperature for two days. The progress of the reaction was controlled by TLC (DCM/MeOH 9:1). After stirring the solution with methanol (5 ml) for 25 min, the solvent was evaporated and the residue was extracted with ethyl-acetate and washed with  $\text{KHSO}_4$  5%, brine and water (2 times/each). It was dried over anhydrous  $\text{Na}_2\text{SO}_4$ , filtrated, evaporated. The crude material was purified by flash chromatography (DCM 95/ MeOH 5). The yield was 480 mg (63%) and M.W. determined by mass spectroscopy was 611.26.

### Synthesis of ZNH-(CH<sub>2</sub>)<sub>5</sub>-NHC(=NH)NH<sub>2</sub>

ZNH-(CH<sub>2</sub>)<sub>5</sub>-NHBoc (100 mg, 0.297 mmol) was deblocked with a solution of TFA 15% in DCM. After 1 hour, the solvent was evaporated under vacuum.

*Use of Bis-Boc-triflyl-guanidine and TMS-Cl:* To a stirred solution of ZNH-(CH<sub>2</sub>)<sub>5</sub>-NH<sub>2</sub>·TFA (100 mg, 0.297 mmol) in 5 ml of dry DCM,  $\text{Et}_3\text{N}$  (83.7 microliter, 0.6 mmol)

was added, followed by TMS-Cl (37.8 microliter, 0.3 mmol) and the stirring was continued for 30 min at r.t. and for 60 min at reflux temperature and it was then cooled to r.t. (to obtain a clear solution, 1 eq. of TMS-Cl was added and the solution was stirred at refluxing temperature for 30 min.). The solution was then stirred at 0°C and Bis-Boc-triflyl-guanidine (0.12 g, 0.3 mmol) was added followed by Et<sub>3</sub>N (0.16 ml, 1.15 mmol). It was left react at room temperature during 1 hour period. It was then stirred at refluxing temperature for 2 hours and at room temperature for two days. The course of reaction was followed by TLC (EtOAc/Etp 25:75). According to TLC (EtOAc/Etp 25:75), these was not desired product present except to starting materials.

*Use of Bis-Boc-S-methylisothiourea:* To a stirred solution of ZNH-(CH<sub>2</sub>)<sub>5</sub>-NH<sub>2</sub>·TFA (100 mg, 0.297 mmol) in 5 ml of dry DMF, DMAP (36.6 mg, 0.327 mmol) and Bis-Boc-S-methylisothiourea (170 mg, 0.297 mmol) were added. The reaction mixture was stirred at r.t. until TLC (EtOAc/Etp 25:75) showed the complete consumption of the amine. The solvent was then evaporated under reduced pressure, and the residue was dissolved in EtOAc. The solution was washed successively with KHSO<sub>4</sub> 5%, NaHCO<sub>3</sub> 10% and water and brine. The organic phase was then dried over Na<sub>2</sub>SO<sub>4</sub> and evaporated. The product was purified by flash chromatography in Ether petroleum and EtOAc 80:20. The yield was 67.4%, and the M.W. was 478 dalton.

<sup>1</sup>H NMR (200MHz, CDCl<sub>3</sub>): ppm 11.5 (m, b, 1 -HNC(=N-)NH); 8.3 (m, b, 1 -HNC(=N-)NH); 7.4 (m, 3H); 7.3 (m, 2H); 5.1 (d, 2H); 4.8 (m, 1 NH-) 3.4 (dd, 2H); 3.2 (dd, 2H); 1.6-1.4(m, 24H).

## § Synthesis of Series of D-Scan

All analogues of PTH(1–11)NH<sub>2</sub> were synthesized on automated peptide synthesizer (model 348 Ω Advanced ChemTech, Louisville,KY) using Fmoc (*N*-(9-fluorenyl)methoxycarbonyl) main chain protecting group chemistry, HBTU/HOBt/DIPEA (4:4:8 molar ratio) for coupling reactions and HATU/HOAt/Collidine for the coupling of Fmoc-Aib-OH and Fmoc-L/D-Val-OH, and trifluoroacetic acid-mediated cleavage/side chain deprotection. The solid support is Rink Amide MHBA Resin (Novabiochem) (0.73 mmol/g loading). (Table 1).

TABLE 1

Name	Peptide sequence	MW	Yields	p.c.(%)	Purity
RP	Aib-Val-Aib-Glu-Ile-Gln-Leu-Nle-His-Gln-Har-NH <sub>2</sub>	1318	33.5%	74	>97%
D2	Aib- <b>D-Val</b> -Aib-Glu-Ile-Gln-Leu-Nle-His-Gln-Har-NH <sub>2</sub>	1318	50.5%	47	>97%
D4	Aib-Val-Aib- <b>D-Glu</b> -Ile-Gln-Leu-Nle-His-Gln-Har-NH <sub>2</sub>	1318	61.2%	69	>97%
D5	Aib-Val-Aib-Glu- <b>D-Ile</b> -Gln-Leu-Nle-His-Gln-Har-NH <sub>2</sub>	1318	35.4%	65	>97%
DA5	Aib-Val-Aib-Glu- <b>D-Allo-Ile</b> -Gln-Leu-Nle-His-Gln-Har-NH <sub>2</sub>	1318	42.0%	70	>97%
D6	Aib-Val-Aib-Glu-Ile- <b>D-Gln</b> -Leu-Nle-His-Gln-Har-NH <sub>2</sub>	1318	34.5%	54	>97%
D7	Aib-Val-Aib-Glu-Ile-Gln- <b>D-Leu</b> -Nle-His-Gln-Har-NH <sub>2</sub>	1318	35.8%	72	>97%
D8	Aib-Val-Aib-Glu-Ile-Gln-Leu- <b>D-Nle</b> -His-Gln-Har-NH <sub>2</sub>	1318	39.0%	90	>97%
D9	Aib-Val-Aib-Glu-Ile-Gln-Leu-Nle- <b>D-His</b> -Gln-Har-NH <sub>2</sub>	1318	44.8%	72	>97%
D10	Aib-Val-Aib-Glu-Ile-Gln-Leu-Nle-His- <b>D-Gln</b> -Har-NH <sub>2</sub>	1318	34.4%	76	>97%
D11	Aib-Val-Aib-Glu-Ile-Gln-Leu-Nle-His-Gln- <b>D-Har</b> -NH <sub>2</sub>	1318	38.5%	68	>97%

**Note:** The peptides were analyzed by reverse phase high-performance liquid chromatography using a Vydac C18 218TP510 column with linear gradient (20-45% in 10 min) of 90% CH<sub>3</sub>CN and water containing 0.1% trifluoroacetic acid, and flow 1 ml/min. The peptides were purified by reverse phase high-performance liquid chromatography using Water Delta Pak C18 100Å with linear gradient (30-40% in 10 min) of 90% CH<sub>3</sub>CN and water containing 0.1% trifluoroacetic acid, and flow 17 ml/min. The purity was determined by analytical HPLC with linear gradient (10-90% in 30 min). Peptide content is determined by UV methodology.

### D-Val<sup>2</sup>-HarPTH

Chemical Shift for [Aib<sup>1,3</sup>, D-Val<sup>2</sup>, Nle<sup>8</sup>, Gln<sup>10</sup>, Har<sup>11</sup>]-PTH(1-11)NH<sub>2</sub>,  
conc: 1.39 mM, at T=298 K, in solution of water/TFE-d<sub>3</sub> 20%.

AA	δNH	δα	δβ	δ
1 Aib	-	-	1.715, 1.668	-
2 D-Val	7.801	4.147	2.198	γ <sub>CH3</sub> = 1.024
3 Aib	8.490	-	1.496	-
4 Glu	8.485	4.067	2.073	γ <sub>CH2</sub> = 2.461
5 Ile	7.990	3.931	2.003	γ <sub>CH2</sub> = 1.584, 1.367 γ <sub>CH3</sub> = 0.976 δ <sub>CH3</sub> = 0.923
6 Gln	7.743	4.215	2.217, 2.146	γ <sub>CH2</sub> = 2.446, 2.387 δ <sub>NH2</sub> = 7.286, 6.757
7 Leu	7.875	4.206	1.793, 1.667	γ <sub>CH</sub> = 1.667 δ <sub>CH3</sub> = 0.932, 0.896
8 Nle	7.948	4.076	1.810	γ <sub>CH2</sub> = 1.398, 1.296 δ <sub>CH2</sub> , ε <sub>CH3</sub> = 0.859
9 His	7.998	4.587	3.407, 3.295	H <sup>2</sup> = 8.603 H <sup>4</sup> = 7.377

10	Gln	8.103	4.299		$\gamma_{\text{CH}_2}$ = 2.441, 2.391 $\delta_{\text{NH}_2}$ = 7.445, 6.753
11	Har	8.074	4.262	1.907, 1.829	$\gamma_{\text{CH}_2}$ = 1.631 $\delta_{\text{CH}_2}$ = 1.525, 1.468 $\epsilon_{\text{CH}_2}$ = 3.194 $\delta_{\text{N}}$ = 7.150 $\omega_{\text{NH-term}}$ = 7.361, 7.040

### D-Glu<sup>4</sup>-HarPTH

Chemical Shift for [Aib<sup>1,3</sup>,D-Glu<sup>4</sup>, Nle<sup>8</sup>, Gln<sup>10</sup>, Har<sup>11</sup>]-PTH(1-11)NH<sub>2</sub>, conc:  
2.10 mM, at T=298 K, in solution of water/TFE-d<sub>3</sub> 20%.

AA	$\delta_{\text{NH}}$	$\delta_{\alpha}$	$\delta_{\beta}$	$\delta$
1 Aib	-	-	1.681	-
2 Val	7.833	4.122	2.141	$\gamma_{\text{CH}_3}$ = 1.002
3 Aib	8.411	-	1.512	-
4 D-Glu	8.128	4.166	2.251, 2.068	$\gamma_{\text{CH}_2}$ = 2.445
5 Ile	7.903	4.024	1.987	$\gamma_{\text{CH}_2}$ = 1.536, 1.282 $\gamma_{\text{CH}_3}$ = 0.950 $\delta_{\text{CH}_3}$ = 0.911
6 Gln	8.278	4.245	2.159, 2.094	$\gamma_{\text{CH}_2}$ = 2.452, 2.382 $\delta_{\text{NH}_2}$ = 7.409, 6.791
7 Leu	7.990	4.303	1.732, 1.673	$\gamma_{\text{CH}}$ = 1.673 $\delta_{\text{CH}_3}$ = 0.948, .896
8 Nle	7.928	4.122	1.780	$\gamma_{\text{CH}_2}$ = 1.362, 1.281 $\delta_{\text{CH}_2}$ , $\epsilon_{\text{CH}_3}$ =0.870
9 His	8.191	4.628	3.372, 3.266	$H^2$ = 8.617 $H^4$ = 7.350
10 Gln	8.177	4.322	2.194, 2.113	$\gamma_{\text{CH}_2}$ = 2.444 $\delta_{\text{NH}_2}$ = 7.472, 6.774
11 Har	8.155	4.272	1.897, 1.817	$\gamma_{\text{CH}_2}$ = 1.637 $\delta_{\text{CH}_2}$ = 1.506, 1.460 $\epsilon_{\text{CH}_2}$ = 3.198 $\delta_{\text{N}}$ = 7.153 $\omega_{\text{NH-term}}$ = 7.424, 7.042

### D-Ile<sup>5</sup>-HarPTH (D-Allo- Ile<sup>5</sup>-HarPTH)

Chemical Shift for [Aib<sup>1,3</sup>,D-Ile<sup>5</sup>, Nle<sup>8</sup>, Gln<sup>10</sup>, Har<sup>11</sup>]-PTH(1-11)NH<sub>2</sub>, conc:  
1.54 mM, at T=298 K, in solution water/TFE-d<sub>3</sub> 20%.

AA	$\delta_{\text{NH}}$	$\delta_{\alpha}$	$\delta_{\beta}$	$\delta$
1 Aib	-	-	1.684	-
2 Val	7.897	4.147	2.141	$\gamma_{\text{CH}_3}$ = 0.986
3 Aib	8.422	-	1.479	-
4 Glu	7.855	4.286	2.115, 2.008	$\gamma_{\text{CH}_2}$ = 2.444, 2.408
5 D-Ile	8.146	4.120	2.044	$\gamma_{\text{CH}_2}$ = 1.482, 1.246 $\gamma_{\text{CH}_3}$ = 0.967 $\delta_{\text{CH}_3}$ = 0.902
6 Gln	8.275	4.324	2.134, 2.026	$\gamma_{\text{CH}_2}$ = 2.371 $\delta_{\text{NH}_2}$ = 7.461, 6.787
7 Leu	8.133	4.296	1.679	$\gamma_{\text{CH}}$ = 1.596 $\delta_{\text{CH}_3}$ = 0.950, 0.890

8	Nle	7.936	4.183	1.713	$\gamma_{\text{CH}_2}= 1.279, 1.214$ $\delta_{\text{CH}_2}, \epsilon_{\text{CH}_3}= 0.866$
9	His	8.261	4.676	3.336, 3.219	$H^2= 8.627$ $H^4= 7.327$
10	Gln	8.299	4.353	2.155, 2.051	$\gamma_{\text{CH}_2}= 2.398$ $\delta_{\text{NH}_2}= 7.501, 6.795$
11	Har	8.238	4.288	1.869, 1.791	$\gamma_{\text{CH}_2}= 1.636$ $\delta_{\text{CH}_2}= 1.493, 1.445$ $\epsilon_{\text{CH}_2}= 3.197$ $\delta_{\text{N}}= 7.160$ $\omega_{\text{NH-term}}= 7.507, 7.043$

### D-Gln<sup>6</sup>-HarPTH

Chemical Shift for [Aib<sup>1,3</sup>, D-Gln<sup>6</sup>, Nle<sup>8</sup>, Gln<sup>10</sup>, Har<sup>11</sup>]-PTH(1-11)NH<sub>2</sub>, in conc: 1.70 mM, at T=298 K, in solution water/TFE-d<sub>3</sub> 20%.

AA	$\delta_{\text{NH}}$	$\delta_{\alpha}$	$\delta_{\beta}$	$\delta$	
1	Aib	-	-	1.693	-
2	Val	7.955	4.028	2.141	$\gamma_{\text{CH}_3}= 1.009$
3	Aib	8.462	-	1.474	-
4	Glu	8.11	4.211	2.074	$\gamma_{\text{CH}_2}= 2.481, 2.395$
5	Ile	7.832	3.986	1.983	$\gamma_{\text{CH}_2}= 1.591, 1.236$ $\gamma_{\text{CH}_3}= 0.927$ $\delta_{\text{CH}_3}= 0.878$
6	D-Gln	8.415	4.127	2.049, 2.346	$\gamma_{\text{CH}_2}= 2.215$ $\delta_{\text{NH}_2}= 7.349, 6.764$
7	Leu	8.104	4.259	1.708, 1.638	$\gamma_{\text{CH}}= 1.638$ $\delta_{\text{CH}_3}= 0.936, 0.893$
8	Nle	8.043	4.126	1.777	$\gamma_{\text{CH}_2}= 1.372, 1.284$ $\delta_{\text{CH}_2}, \epsilon_{\text{CH}_3}= 0.868$
9	His	8.265	4.644	3.364, 3.239	$H^2= 8.619$ $H^4= 7.334$
10	Gln	8.282	4.316	2.171, 2.085	$\gamma_{\text{CH}_2}= 2.426$ $\delta_{\text{NH}_2}= 7.463, 6.778$
11	Har	8.209	4.272	1.883, 1.803	$\gamma_{\text{CH}_2}= 1.630$ $\delta_{\text{CH}_2}= 1.496, 1.446$ $\epsilon_{\text{CH}_2}= 3.188$ $\delta_{\text{N}}= 7.157$ $\omega_{\text{NH-term}}= 7.442, 7.050$

### D-Leu<sup>7</sup>-HarPTH

Chemical Shift for [Aib<sup>1,3</sup>, D-Leu<sup>7</sup>, Nle<sup>8</sup>, Gln<sup>10</sup>, Har<sup>11</sup>]-PTH(1-11)NH<sub>2</sub>, in conc: 2.40 mM, at T=298 K, in solution water/TFE-d<sub>3</sub> 20%.

AA	$\delta_{\text{NH}}$	$\delta_{\alpha}$	$\delta_{\beta}$	$\delta$	
1	Aib	-	-	1.696	-
2	Val	7.935	4.029	2.131	$\gamma_{\text{CH}_3}= 1.013$
3	Aib	8.435	-	1.473	-
4	Glu	7.969	4.218	2.069	$\gamma_{\text{CH}_2}= 2.489, 2.403$
5	Ile	7.897	4.092	1.970	$\gamma_{\text{CH}_2}= 1.579, 1.238$ $\gamma_{\text{CH}_3}= 0.937$ $\delta_{\text{CH}_3}= 0.883$
6	Gln	8.186	4.292	2.152, 2.050	$\gamma_{\text{CH}_2}= 2.392$ $\delta_{\text{NH}_2}= 7.343, 6.752$

7	D-Leu	8.239	4.229	1.759, 1.618	$\gamma_{\text{CH}} = 1.618$ $\delta_{\text{CH}_3} = 0.961, 0.901$
8	Nle	8.137	4.175	1.767, 1.714	$\gamma_{\text{CH}_2} = 1.300, 1.254$ $\delta_{\text{CH}_2}, \epsilon_{\text{CH}_3} = 0.873$
9	His	8.315	4.635	3.344, 3.262	$\text{H}^2 = 8.617$ $\text{H}^4 = 7.361$
10	Gln	8.298	4.346	2.171, 2.056	$\delta_{\text{NH}_2} = 7.505, 6.784$ $\gamma_{\text{CH}_2} = 2.402$
11	Har	8.220	4.290	1.882, 1.796	$\gamma_{\text{CH}_2} = 1.635$ $\delta_{\text{CH}_2} = 1.491, 1.446$ $\epsilon_{\text{CH}_2} = 3.195$ $\delta_{\text{N}} = 7.158$ $\omega_{\text{NH-term}} = 7.488; 7.043$

### D-Nle<sup>8</sup>-HarPTH

Chemical Shift for [Aib<sup>1,3</sup>, D-Nle<sup>8</sup>, Gln<sup>10</sup>, Har<sup>11</sup>]-PTH(1-11)NH<sub>2</sub>, in conc: 1.50 mM, at T=298 K, in solution water/TFE-d<sub>3</sub> 20%.

AA	$\delta_{\text{NH}}$	$\delta_{\alpha}$	$\delta_{\beta}$	$\delta$	
1	Aib	-	-	1.700	-
2	Val	7.923	4.026	2.142	$\gamma_{\text{CH}_3} = 1.019$
3	Aib	8.444	-	1.472	-
4	Glu	8.053	4.154	2.081	$\gamma_{\text{CH}_2} = 2.502, 2.397$
5	Ile	7.883	4.034	1.977	$\gamma_{\text{CH}_2} = 1.596, 1.245$ $\gamma_{\text{CH}_3} = 0.940$ $\delta_{\text{CH}_3} = 0.890$
6	Gln	8.108	4.275	2.127, 2.049	$\gamma_{\text{CH}_2} = 2.406, 2.352$ $\delta_{\text{NH}_2} = 7.319, 6.737$
7	Leu	8.049	4.257	1.705, 1.608	$\gamma_{\text{CH}} = 1.608$ $\delta_{\text{CH}_3} = 0.922$
8	D-Nle	8.164	4.088	1.764	$\gamma_{\text{CH}_2} = 1.258, 1.168$ $\delta_{\text{CH}_2}, \epsilon_{\text{CH}_3} = 0.868$
9	His	8.409	4.696	3.388, 3.217	$\text{H}^2 = 8.635$ $\text{H}^4 = 7.324$
10	Gln	8.351	4.336	2.173, 2.111	$\gamma_{\text{CH}_2} = 2.440$ $\delta_{\text{NH}_2} = 7.501, 6.776$
11	Har	8.209	4.297	1.884, 1.778	$\gamma_{\text{CH}_2} = 1.633$ $\delta_{\text{CH}_2} = 1.491, 1.442$ $\epsilon_{\text{CH}_2} = 3.196$ $\delta_{\text{N}} = 7.158$ $\omega_{\text{NH-term}} = 7.477, 7.031$

### D-His<sup>9</sup>-HarPTH

Chemical Shift for [Aib<sup>1,3</sup>, D-His<sup>9</sup>, Gln<sup>10</sup>, Har<sup>11</sup>]-PTH(1-11)NH<sub>2</sub>, in conc: 1.50 mM, at T=298 K, in solution water/TFE-d<sub>3</sub> 20%.

AA	$\delta_{\text{NH}}$	$\delta_{\alpha}$	$\delta_{\beta}$	$\delta$	
1	Aib	-	-	1.704	-
2	Val	7.934	4.022	2.158	$\gamma_{\text{CH}_3} = 1.025$
3	Aib	8.471	-	1.472	-
4	Glu	8.088	4.093	2.092	$\gamma_{\text{CH}_2} = 2.534, 2.410$

5	Ile	7.814	3.917	2.002	$\gamma_{\text{CH}_2}= 1.620, 1.275$ $\gamma_{\text{CH}_3}= 0.960$ $\delta_{\text{CH}_3}= 0.902$
6	Gln	8.038	4.222	2.162, 2.106	$\gamma_{\text{CH}_2}= 2.438, 2.372$ $\delta_{\text{NH}_2}= 7.294, 6.748$
7	Leu	7.965	4.254	1.767, 1.680	$\gamma_{\text{CH}}= 1.630$ $\delta_{\text{CH}_3}= 0.905$
8	Nle	7.898	4.059	1.752	$\gamma_{\text{CH}_2}= 1.314, 1.170$ , $\delta_{\text{CH}_2}$ , $\epsilon_{\text{CH}_3}= 0.856$
9	D-His	8.332	4.568	3.321, 3.401	$\text{H}^2= 7.344$ $\text{H}^4= 8.627$
10	Gln	8.271	4.307	2.180, 2.090	$\gamma_{\text{CH}_2}= 2.390$ $\delta_{\text{NH}_2}= 7.469, 6.770$
11	Har	8.136	4.269	1.906, 1.827	$\gamma_{\text{CH}_2}= 1.632$ $\delta_{\text{CH}_2}= 1.520, 1.456$ $\epsilon_{\text{CH}_2}= 3.191$ $\delta_{\text{N}}= 7.156$ $\omega_{\text{NH-term}}= 7.427, 7.015$

### D-Gln<sup>10</sup>-HarPTH

Chemical Shift for [Aib<sup>1,3</sup>, Nle<sup>8</sup>, D-Gln<sup>10</sup>, Har<sup>11</sup>]-PTH(1-11)NH<sub>2</sub>, in conc:  
1.66 mM, at T=298 K, in solution water/TFE-d<sub>3</sub> 20%.

AA	$\delta_{\text{NH}}$	$\delta\alpha$	$\delta\beta$	$\delta$	
1	Aib	-	-	1.724, 1.686	-
2	Val	7.946	3.992	2.159	$\gamma_{\text{CH}_3}= 1.030$
3	Aib	8.470	-	1.470	-
4	Glu	8.082	4.079	2.111	$\gamma_{\text{CH}_2}= 2.563, 2.417$
5	Ile	7.805	3.909	2.02	$\gamma_{\text{CH}_2}= 1.647, 1.274$ $\gamma_{\text{CH}_3}= 0.957$ $\delta_{\text{CH}_3}= 0.898$
6	Gln	8.048	4.193	2.158	$\gamma_{\text{CH}_2}= 2.462, 2.366$ $\delta_{\text{NH}_2}= 7.246, 6.736$
7	Leu	8.016	4.268	1.806, 1.704	$\gamma_{\text{CH}}= 1.386, 1.296$ $\delta_{\text{CH}_3}= 0.868$
8	Nle	7.929	4.139	1.807	$\gamma_{\text{CH}_2}= 1.386, 1.296$ $\delta_{\text{CH}_2}$ , $\epsilon_{\text{CH}_3}= 0.868$
9	His	7.993	4.662	3.435, 3.240	$\text{H}^2= 8.603$ $\text{H}^4= 7.392$
10	D-Gln	8.160	4.321	2.189, 2.101	$\gamma_{\text{CH}_2}= 2.382$ $\delta_{\text{NH}_2}= 7.520, 6.795$
11	Har	8.291	4.334	1.905, 1.764	$\gamma_{\text{CH}_2}= 1.623$ $\delta_{\text{CH}_2}= 1.472, 1.406$ $\epsilon_{\text{CH}_2}= 3.201$ $\delta_{\text{N}}= 7.152$ $\omega_{\text{NH-term}}= 7.489, 6.972$

### D-Har<sup>11</sup>-HarPTH

Chemical Shift for [Aib<sup>1,3</sup>, Nle<sup>8</sup>, Gln<sup>10</sup>, D-Har<sup>11</sup>]-PTH(1-11)NH<sub>2</sub>, in conc:  
1.53 mM, at T=298K, in solution water/ TFE-d<sub>3</sub> 20%.

AA	$\delta_{\text{NH}}$	$\delta\alpha$	$\delta\beta$	$\delta$	
1	Aib	-	-	1.733, 1.682	-
2	Val	7.945	3.976	2.13	$\gamma_{\text{CH}_3}= 1,030$



3	Aib	8.478	-	1.469	-
4	Glu	8.140	4.052	2.128, 2.065	$\gamma_{\text{CH}_2}$ = 2.559, 2.398
5	Ile	7.777	3.874	2.016	$\gamma_{\text{CH}_2}$ = 1.651, 1.268 $\gamma_{\text{CH}_3}$ = 0.941 $\delta_{\text{CH}_3}$ = 0.889
6	Gln	8.019	4.183	2.175, 2.137	$\gamma_{\text{CH}_2}$ = 2.438, 2.359 $\delta_{\text{NH}_2}$ = 7.248, 6.740
7	Leu	8.021	4.197	1.796, 1.684	$\gamma_{\text{CH}}$ = 1.684 $\delta_{\text{CH}_3}$ = 0.910
8	Nle	8.026	4.094	1.839, 1.811	$\gamma_{\text{CH}_2}$ = 1.420, 1.301 $\delta_{\text{CH}_2}$ , $\epsilon_{\text{CH}_3}$ = 0.863
9	His	7.997	4.588	3.415, 3.289	$\text{H}^2$ = 8.584 $\text{H}^4$ = 7.374
10	Gln	8.104	4.366	2.209, 2.125	$\gamma_{\text{CH}_2}$ = 2.467 $\delta_{\text{NH}_2}$ = 7.439, 6.769
11	D-Har	8.060	4.269	1.907, 1.831	$\gamma_{\text{CH}_2}$ = 1.637 $\delta_{\text{CH}_2}$ = 1.500, 1.433 $\epsilon_{\text{CH}_2}$ = 3.209 $\delta_{\text{N}}$ = 7.154 $\omega_{\text{NH-term}}$ = 7.625, 6.975

### § Synthesis of Retro-inverse Series

All retroinverse analogues of PTH(1–11)NH<sub>2</sub> were synthesized on automated peptide synthesizer (model 348  $\Omega$  Advanced ChemTect, Louisville, KY) using Fmoc (*N*-(9-fluorenyl)methoxycarbonyl) main chain protecting group chemistry, HBTU/HOBt/DIPEA (4:4:8 molar ratio) for coupling reactions and HATU/HOAt/Collidine for the coupling of Fmoc-Aib-OH and Fmoc-D-Val-OH, and trifluoroacetic acid-mediated cleavage/side chain deprotection. The solid support is Rink Amide MHBA Resin (Novabiochem) (0.73 mmol/g loading). (Table 2)

TABLE 2

Name	Peptide sequence	MW	Yields	p.c.(%)	Purity
<b>RI</b>	Har-Gln-His-Nle-Leu-Gln-Ile-Glu-Aib-Val-Aib-NH <sub>2</sub>	1316	23,7%	69	>97%
<b>RII</b>	Abu-Gln-His-Nle-Leu-Gln-Ile-Glu-Aib-Val-Aib-NH <sub>2</sub>	1231	46,9%	45	>97%
<b>RIII</b>	Amc-Gln-His-Nle-Leu-Gln-Ile-Glu-Aib-Val-Aib-NH <sub>2</sub>	1259	50,4%	64	>97%

**Note:** All Amino Acids in the retroinverse analogues of PTH(1-11) are D; “D” label is not present for simplicity reasons.

The peptides were analyzed by reverse phase high-performance liquid chromatography using a Vydac C18 218TP510 column with linear gradient (20-45% in 10 min) of 90% CH<sub>3</sub>CN and water containing 0.1% trifluoroacetic acid, and flow 1ml/min. The peptides were purified by reverse phase high-performance liquid chromatography using Water Delta Pak C18 100Å with linear gradient (30-40% in 10 min) of 90% CH<sub>3</sub>CN and water containing 0.1% trifluoroacetic acid, and flow 17 ml/min. The molecular weights were determined on a Perseptive Biosystems MARINER™ Atmospheric Pressure Ionization-Time of Flight (API-TOF) spectrometer, and purity was determined by analytical HPLC with linear gradient (10-90% in 30 min). Peptide content was determined by UV methodology.

Analytic analysis on HPLC gives these retention times:

- RI:  $t_R = 14,8$  min 40,5% B;
- RII:  $t_R = 15,8$  min 37,9% B;
- RIII:  $t_R = 15,0$  min 40% B.

HPLC conditions are from 10% to 90% B.

### Retro-HarPTH

Chemical Shift for **RI**, in conc: 2,15 mM, at T=298K, in solution water/ TFE-d<sub>3</sub> 20%.

AA		$\delta_{NH}$	$\delta_{H_\alpha}$	$\delta_{H_\beta}$	$\delta$
1	Har	-	4,10	1,90	$\gamma(CH_2) = 1,64$ ; $\delta(CH_2) = 1,45$ ; $\varepsilon(CH_2) = 3,20$ ; $\eta(NH) = 7,18$
2	Gln	8,82	4,35	2,00	$\gamma(CH_2) = 2,38$ ; $\delta(NH_2) = 7,52$
3	His	8,75	4,70	3,22; 3,30	$H^2 = 8,62$ ; $H^4 = 7,33$
4	Nle	8,32	4,25	1,75	$\gamma(CH_2) = 1,30$ ; $\delta(CH_2) = 1,26$ ; $\varepsilon(CH_3) = 0,88$
5	Leu	8,20	4,32	1,68	$\gamma(CH) = 1,62$ ; $\delta(CH_3) = 0,95$ ; 0,90
6	Gln	8,26	4,30	2,00	$\gamma(CH_2) = 2,36$ ; $\varepsilon(NH_2) = 7,50$
7	Ile	7,95	4,11	1,90	$\gamma(CH) = 1,48$ ; $\delta(CH_2) = 1,18$ ; $\gamma(CH_3) = 0,92$ ; $\varepsilon(CH_3) = 0,86$
8	Glu	8,21	4,22	2,02; 2,10	$\gamma(CH_2) = 2,48$
9	Aib	8,12	-	1,46; 2,02	-
10	Val	7,41	4,06	2,14	$\gamma(CH_3) = 0,96$
11	Aib	8,10	-	1,48; 2,15	-
	Amide	6,78	-	-	-

### Retro-AbuPTH

Chemical Shift for **RII**, in conc: 2,98 mM, at T=298K, in solution water/ TFE-d<sub>3</sub> 20%.

AA		$\delta_{NH}$	$\delta_{H_\alpha}$	$\delta_{H_\beta}$	$\delta$
1	Abu	-	3,05 (CH <sub>2</sub> )	1,98 (CH <sub>2</sub> )	$\gamma(CH_2) = 2,45$
2	Gln	8,33	4,28	1,98	$\gamma(CH_2) = 2,38$ ; $\delta(NH_2) = 7,50$
3	His	8,65	4,73	3,22; 3,30	$H^2 = 7,32$ ; $H^4 = 6,75$

4	Nle	8,18	4,22	1,78	$\gamma(\text{CH}_2) = 1,35; \delta(\text{CH}_2) = 1,32;$ $\varepsilon(\text{CH}_2) = 0,90$
5	Leu	8,12	4,30	1,70	$\gamma(\text{CH}) = 1,60; \delta(\text{CH}_3) = 0,97; 0,90$
6	Gln	8,18	4,28	2,10	$\gamma(\text{CH}_2) = 2,40 \delta(\text{NH}_2) = 7,48$
7	Ile	7,81	4,07	1,92	$\gamma(\text{CH}) = 1,50; \delta(\text{CH}_2) = 1,20;$ $\gamma(\text{CH}_3) = 0,94; \varepsilon(\text{CH}_3) = 0,87$
8	Glu	8,19	4,20	2,12	$\gamma(\text{CH}_2) = 2,48; 2,54$
9	Aib	8,02	-	1,52; 2,12	-
10	Val	7,36	4,11	2,31	$\gamma(\text{CH}_3) = 0,95$
11	Aib	8,00	-	1,50; 2,20	-
	Amide	6,75	-	-	-

### Retro-AmcPTH

Chemical Shift for **RIII**, in conc: 2,38 mM, at T=298K, in solution water/  
TFE-d<sub>3</sub> 20%.

AA		$\delta\text{NH}$	$\delta\text{H}_\alpha$	$\delta\text{H}_\beta$	$\delta$
1	Amc	-	3,00 (CH <sub>2</sub> )	1,70 (CH <sub>2</sub> )	$\gamma(\text{CH}_2) = 1,44 ; \delta(\text{CH}_2) = 1,65;$ $\varepsilon(\text{CH}_2) = 2,35$
2	Gln	8,26	4,20	1,98	$\gamma(\text{CH}_2) = 2,35; \delta(\text{NH}_2) = 7,48$
3	His	8,63	4,70	3,22; 3,31	$\text{H}^2 = 7,31; \text{H}^4 = 6,72$
4	Nle	8,03	4,17	1,80	$\gamma(\text{CH}_2) = 1,35; \delta(\text{CH}_2) = 1,32;$ $\varepsilon(\text{CH}_2) = 0,90$
5	Leu	8,10	4,24	1,74	$\gamma(\text{CH}) = 1,61; \delta(\text{CH}_3) = 0,98; 0,90$
6	Gln	8,11	4,22	2,12	$\gamma(\text{CH}_2) = 2,41 \delta(\text{NH}_2) = 7,48$
7	Ile	7,75	4,03	1,94	$\gamma(\text{CH}) = 1,51; \delta(\text{CH}_2) = 1,18;$ $\gamma(\text{CH}_3) = 0,91; \varepsilon(\text{CH}_3) = 0,85$
8	Glu	8,20	4,12	2,10	$\gamma(\text{CH}_2) = 2,47; 2,53$
9	Aib	8,00	-	1,52; 2,12	-
10	Val	7,38	4,10	2,28	$\gamma(\text{CH}_3) = 0,97$
11	Aib	7,98	-	1,50; 2,23	-
	Amide	6,72	-	-	-

### § Synthesis of PTH(1-11) analogues containing $\alpha\text{MeVal}$

*Preparation of Fmoc  $\alpha\text{-Me-Val-OH}$ :* 100 mg of  $\alpha\text{-Me-Val}$  (0.76 mmol) were suspended in 4 ml of DCM under nitrogen atmosphere. 190  $\mu\text{l}$  of TMS-Cl (1.52 mmol, 2 eq.) were

added and the mixture on reflux for 2h. Then a second eq. of TMS-Cl was added and refluxed. After one hour, the mixture was cooled at 0°C and 260 µl of DIEA (2.27 mmol, 3 eq.) and last 196.6 mg Fmoc-Cl (0.76 mmol, 1 eq.) were added. The reaction progress was controlled by TLC (Chloroform: Methanol 9:1). At the end of the reaction, the solvent was evaporated and the crude material was dissolved in 20 ml of NaHCO<sub>3</sub> 10% and extracted with ethylic ether (three times). Then a retro-extraction of organic layers was carried out with NaHCO<sub>3</sub> 10%. Water layers were acidified to pH=2 by HCl conc., and extracted with ethyl acetate (five times). Then the organic layers were anhydrified on Na<sub>2</sub>SO<sub>4</sub>. The solvent was evaporated to obtain a yellow oil which became solid. The yield was 88% and the M.W. was 354.2 determined by Mass Spectroscopy.

<sup>1</sup>H NMR (200MHz; CDCl<sub>3</sub>): 7.8-7.3 (8H Fmoc); 6.4 (mb, 1H NH(amide)); 4.4 (d, 2H CH<sub>2</sub>(Fmoc)); 4.25-4.20 (mb, 1H H-(Fmoc)); 2.20 (m, 2H), 1.40 (s, 3H), 1.1-0.9 (m, 6H).

*Preparation of Fmoc-α-Me-Val-F:* To 150 mg of Fmoc-αMeVal-OH (0.42 mmol) in 2 ml of DCM 34 µl of pyridine (0.42 mmol, 1 eq.) and 72 µl of cyanuric fluoride (0.85 mmol, 2 eq.) were added at 0°C. The mixture was left reach at room temperature and after 3 hours the mixture was extracted with water and ice (three times). The organic layer was then washed with cold water. Before evaporating under vacuum the solvent, the organic layer was anhydrified on Na<sub>2</sub>SO<sub>4</sub>. The purity of the product was confirmed by IR analysis (1836 cm<sup>-1</sup> (s C-F)).

*Preparation of Fmoc-Aib-F:* To 130 mg of Fmoc-Aib-OH (0.4 mmol, 1 eq) in 2 ml of DCM 32 µl of pyridine ( 0.4 mmol, 1 eq.) and 67 µl of cyanuric fluoride (0.8 mmol, 2 eq.) were added at 0°C. The mixture was left reach at room temperature and after 3 hours the mixture was extracted with water and ice (three times). The organic layer was then washed with cold water. Before evaporating under vacuum the solvent, the organic layer was anhydrified on Na<sub>2</sub>SO<sub>4</sub>. The purity of the product was confirmed by IR analysis (1841 cm<sup>-1</sup> (s C-F)).

*Preparation of Fmoc-Ser(tBu)-F:* To 160 mg of Fmoc-Ser(tBu)-OH (0.41 mmol, 1 eq) in 2 ml of DCM 33.6  $\mu$ l of pyridine (0.41 mmol, 1 eq.) and 70.5  $\mu$ l of cyanuric fluoride (0.83 mmol, 2 eq.) were added at 0°C. The mixture left reach at room temperature and after 3 hours the mixture was extracted with water and ice (three times). The organic layer was then washed with cold water. Before evaporating under vacuum the solvent, the organic layer was anhydrified on Na<sub>2</sub>SO<sub>4</sub>. The purity of the product was confirmed by IR analysis (1852 cm<sup>-1</sup> (s C-F)).

*Preparation of Fmoc-Ala-F:* To 160 mg of Fmoc-Ala-OH (0.51 mmol, 1 eq) in 2 ml of DCM 41.0  $\mu$ l of pyridine (0.48 mmol, 1 eq.) and 86  $\mu$ l of cyanuric fluoride (1.02 mmol, 2 eq.) were added at 0°C. The mixture left reach at room temperature and after 3 hours the mixture was extracted with water and ice (three times). The organic layer was then washed with cold water. Before evaporating under vacuum the solvent, the organic layer was anhydrified on Na<sub>2</sub>SO<sub>4</sub>. The purity of the product was confirmed by IR analysis (1842 cm<sup>-1</sup> (s C-F)).

*Preparation of Fmoc-Ac5c-F:* To 750 mg of Fmoc-Ac5c-OH (2.14 mmol, 1 eq.) in 2 ml of DCM 170  $\mu$ l of pyridine (2.14 mmol, 1 eq.) and 363  $\mu$ l of cyanuric fluoride (4.3 mmol, 2 eq.) were added at 0°C. The mixture left reach at room temperature and after 3 hours the mixture was extracted with water and ice (three times). The organic layer was then washed with cold water. Before evaporating under vacuum the solvent, the organic layer was anhydrified on Na<sub>2</sub>SO<sub>4</sub>. The purity of the product was confirmed by IR analysis (1836 cm<sup>-1</sup> (s C-F)).

### **Synthesis on SPPS**

The solid-phase synthesis of PTH(1-11) analogue containing  $\alpha$ MeVal is outlined in Scheme 1. The synthetic protocol for the other analogues is similar. The analogues were prepared using Fmoc methodology with Rink Amide MHBA Resin (Novabiochem) (0.73 mmol/g loading) as a solid support. The side-chain protecting groups were compatible with the Fmoc methodology. The  $\alpha$ MeVal was prepared as Fmoc- $\alpha$ MeVal-OF. The first amino acid was linked to the resin using the HBTU/HOBt/DIPEA

protocol; the most common peptide coupling additive is HOBt, used either as a carbocation with another coupling agent or incorporated into a stand-alone reagent such as an uronium salt. Deprotection of amino groups was achieved under standard conditions, with 20% piperidine solution in NMP. The next amino acids in the sequence were coupled in the same way. The Fmoc- $\alpha$ -Me-Val-OF was used with 3 eq. in excess, with 1 eq. of DIEA. The coupling time was 2h and repeated two times. The next amino acid in the sequence was introduced on resin with the same protocol.

Peptide Cleavage and Purification: the resin was treated with a cleavage solution of TFA/TIS/water (95:2.5:2.5 v/v/v) at room temperature for 2h. After filtration, the filtrate was concentrated under nitrogen and precipitated with methyl tert-butyl ether. Peptide purification was performed by reversed-phase HPLC on Vydac C<sub>18</sub> (218TP510) column. The peptide homogeneity (>95%) was determined by analytical HPLC using the same solvents with a gradient of 10-35 % (v/v) acetonitrile over 15 min. Peptide content is determined by UV methodology.

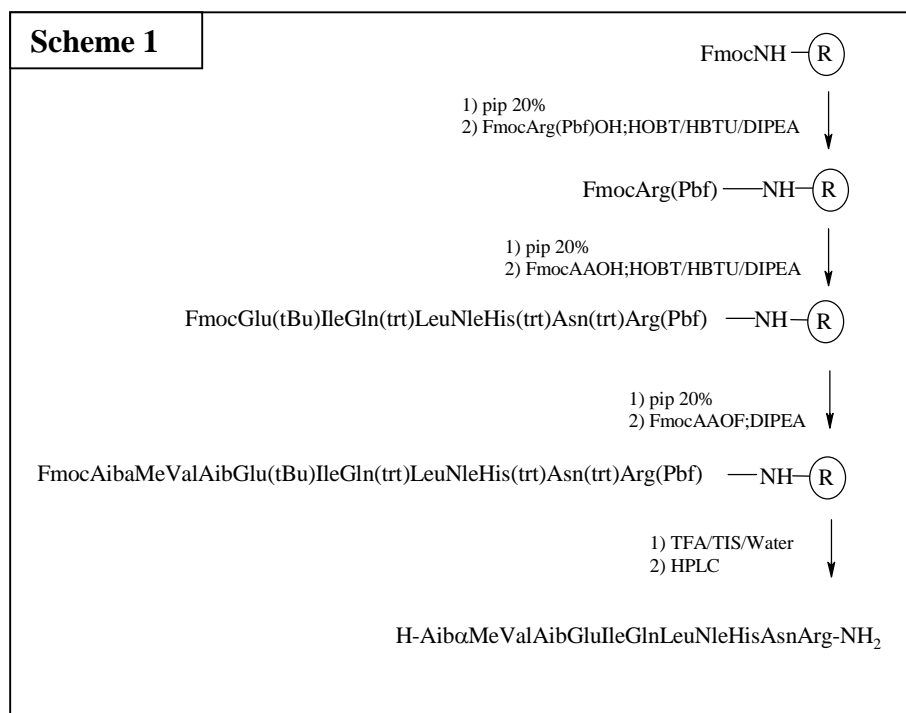


**Table 3**

Name	Peptide sequence	MW	Yield	p.c.%	Purity
AMEVAL1	Aib- $\alpha$ MeVal -Aib-Glu-Ile-Gln-Leu-Nle-His-Gln-Har-NH <sub>2</sub>	1332.6	15%	81	>97%
AMEVAL2	Ac5c - $\alpha$ MeVal -Aib-Glu-Ile-Gln-Leu-Nle-His-Gln-Har-NH <sub>2</sub>	1358.6	14%	87	>97%
9	Aib- $\alpha$ MeVal -Ser-Glu-Ile-Gln-Leu-Nle-His-Gln-Arg-NH <sub>2</sub>	1305	32%	40.5	>97%
11	Ala- $\alpha$ MeVal-Ser-Aib-Ile-Gln-Leu-Nle-His-Gln-Arg-NH <sub>2</sub>	1246	24%	56	>97%
12	Ala- $\alpha$ MeVal -Aib-Glu-Ile-Gln-Leu-Nle-His-Gln-Arg-NH <sub>2</sub>	1289	24%	56	>97%
13	Aib- $\alpha$ MeVal -Aib-Glu-Ile-Gln-Leu-Nle-His-Gln-Arg-NH <sub>2</sub>	1303	19%	53.5	>97%

**9**

Chemical Shift for [Aib<sup>1</sup>, ( $\alpha$ Me)Val<sup>2</sup>, Nle<sup>8</sup>, Arg<sup>11</sup>]-rPTH(1-11)NH<sub>2</sub>, in conc: 1.43 mM, at T=298K, in solution water/ TFE-d<sub>3</sub> 20%.

AA	$\delta$ NH	$\delta\alpha$	$\delta\beta$	$\delta$
1 Aib	-	-	1.648, 1.750	-
2 ( $\alpha$ Me)Val	7.723	1.446 (*)	2.164	$\gamma_{\text{CH}_3}$ = 1.029, 0.937
3 Ser	7.971	4.335	3.979, 3.931	-
4 Glu	8.244	4.187	2.167	$\gamma_{\text{CH}_2}$ = 2.507, 2.422
5 Ile	7.697	3.943	1.999	$\gamma_{\text{CH}_2}$ = 1.589, 1.294 $\gamma_{\text{CH}_3}$ = 0.917 $\delta$ = 0.917
6 Gln	8.043	4.138	2.133	$\gamma_{\text{CH}_2}$ = 2.444, 2.377 $\delta_{\text{NH}_2}$ = 7.369, 6.781
7 Leu	7.932	4.227	1.792, 1.673	$\gamma_{\text{CH}}$ = 1.673 $\delta_{\text{CH}_3}$ = 0.921
8 Nle	7.858	4.091	1.804	$\gamma_{\text{CH}_2}$ = 1.406, 1.288 $\delta_{\text{CH}_3} + \epsilon_{\text{CH}_3}$ = 0.867
9 His	8.168	4.596	3.371, 3.241	H <sup>2</sup> = 7.347 H <sup>4</sup> = 8.611
10 Asn	8.238	4.687	2.914, 2.851	$\delta_{\text{NH}_2}$ = 7.582, 6.885
11 Arg	8.122	4.305	1.950, 1.832	$\gamma_{\text{CH}_2}$ = 1.734, 1.687 $\delta_{\text{CH}_2}$ = 3.220 $\epsilon_{\text{NH}}$ = 7.227 NH <sub>2 term</sub> = 7.465, 7.084

## 11

Chemical Shift for  $[(\alpha\text{Me})\text{Val}^2, \text{Aib}^4, \text{Nle}^8, \text{Arg}^{11}]$ -rPTH(1-11)NH<sub>2</sub>, in conc: 1.53 mM, at T=298K, in solution water/ TFE-d<sub>3</sub> 20%.

AA	$\delta\text{NH}$	$\delta\alpha$	$\delta\beta$	$\delta\text{altri}$
1 Ala	-	4.142	1.616	-
2 ( $\alpha\text{Me}$ )Val	8.305	1.531( $\alpha\text{Me}$ )	2.088	$\gamma_{\text{CH}_3}=1.036, 0.941$
3 Ser	7.570	4.384	4.021, 3.982	-
4 Aib	8.346	-	1.547	-
5 Ile	7.627	3.864	1.962	$\gamma_{\text{CH}_2}=1.565, 1.362$ $\gamma_{\text{CH}_3}=0.953$ $\delta=0.912$
6 Gln	7.842	4.100	2.226, 2.185	$\gamma_{\text{CH}_2}=2.445, 2.421$ $\delta_{\text{NH}_2}=7.385, 6.795$
7 Leu	7.755	4.288	1.826, 1.762	$\gamma_{\text{CH}}=1.708$ $\delta_{\text{CH}_3}=0.918$
8 Nle	7.955	4.055	1.816	$\gamma_{\text{CH}_2}=1.490, 1.305$ $\delta_{\text{CH}_3} + \epsilon_{\text{CH}_3} = 0.868$
9 His	8.165	4.580	3.403, 3.283	$\text{H}^2=7.357$ $\text{H}^4=8.611$
10 Asn	8.108	4.703	2.943, 2.885	$\delta_{\text{NH}_2}=6.888, 7.573$
11 Arg	8.095	4.320	1.984, 1.867	$\gamma_{\text{CH}_2}=1.759, 1.722$ $\delta_{\text{CH}_2}=3.237$ $\epsilon_{\text{NH}}=7.241$ $\text{NH}_2 \text{ term}=7.446, 7.062$

## 12

Chemical Shift for  $[(\alpha\text{Me})\text{Val}^2, \text{Aib}^3, \text{Nle}^8, \text{Arg}^{11}]$ -rPTH(1-11)NH<sub>2</sub>, in conc: 2.0 mM, at T=298K, in solution water/ TFE-d<sub>3</sub> 20%.

AA	$\delta\text{NH}$	$\delta\alpha$	$\delta\beta$	$\delta$
1 Ala	-	4.172	1.645	--
2 ( $\alpha\text{Me}$ )Val	8.442	1.407	2.127	$\gamma_{\text{CH}_3}=1.54, 0.919$
3 Aib	8.012	-	1.52, 1.424	-
4 Glu	7.814	4.011	2.257, 2.187	$\gamma_{\text{CH}_2}=2.461, 2.566$
5 Ile	7.941	3.904	2.084	$\gamma_{\text{CH}_2}=1.619, 1.369$ $\gamma_{\text{CH}_3}=0.946$ $\delta=0.879$
6 Gln	7.675	4.157	2.199, 2.126	$\gamma_{\text{CH}_2}=2.435, 2.364$ $\delta_{\text{NH}_2}=7.233, 6.751$
7 Leu	7.907	4.212	1.819, 1.662	$\gamma_{\text{CH}}=1.710$ $\delta_{\text{CH}_3}=0.919$
8 Nle	7.880	4.085	1.820	$\gamma_{\text{CH}_2}=1.414, 1.301$ $\delta_{\text{CH}_3} + \epsilon_{\text{CH}_3} = 0.869$
9 His	8.054	4.583	3.394, 3.267	$\text{H}^2=7.366$ $\text{H}^4=8.611$
10 Asn	8.217	4.687	2.929, 2.864	$\delta_{\text{NH}_2}=7.574, 6.887$
11 Arg	8.090	4.305	1.958, 1.844	$\gamma_{\text{CH}_2}=1.748, 1.696$ $\delta_{\text{CH}_2}=3.223$ $\epsilon_{\text{NH}}=7.231$ $\text{NH}_2 \text{ term}=7.452, 7.082$



Chemical Shift for [Aib<sup>1</sup>, (αMe)Val<sup>2</sup>, Aib<sup>3</sup>, Nle<sup>8</sup>, Arg<sup>11</sup>]-rPTH(1-11)NH<sub>2</sub>,  
in conc: 2.0 mM, at T=298K, in solution water/ TFE-d<sub>3</sub> 20%.

AA	δNH	δα	δβ	δ	
1	Aib	-	-	1.774, 1.660	-
2	(αMe)Val	7.626	1.382(αMe)	2.147	γ <sub>CH3</sub> =1.051, 0.935
3	Aib	8.055	-	1.494, 1.429	
4	Glu	7.813	4.008	2.242, 2.158	γ <sub>CH2</sub> = 2.614, 2.453
5	Ile	7.895	3.888	2.091	γ <sub>CH2</sub> = 1.642, 1.355 γ <sub>CH3</sub> = 0.937 δ <sub>CH3</sub> =0.884, 0.865
6	Gln	7.813	4.138	2.201, 2.140	γ <sub>CH2</sub> = 2.450, 2.362 δ <sub>NH2</sub> = 7.183, 6.745
7	Leu	7.969	4.207	1.831, 1.721	γ <sub>CH</sub> = 1.676 δ <sub>CH3</sub> = 0.921
8	Nle	7.889	4.079	1.836	γ <sub>CH2</sub> = 1.430, 1.307 δ <sub>CH3</sub> =0.872
9	His	8.072	4.577	3.404, 3.273	H <sup>2</sup> = 7.375 H <sup>4</sup> = 8.610
10	Asn	8.219	4.689	2.933, 2.869	δ <sub>NH2</sub> = 7.574, 6.892
11	Arg	8.219	4.307	1.963, 1.849	γ <sub>CH2</sub> = 1.753, 1.700 δ <sub>CH2</sub> = 4.310 ω <sub>NH-term</sub> = 7.184, 6.744

## § Synthesis of PTH(1-11) analogues containing αMeNle

### Synthesis of alpha methyl Norleucine

*First Step* – Solutions of ammonia (150 ml) and NaCN (12 g dissolved in 28 ml of water) were poured in reaction vessel kept at 25°C. Acetic Acid (14.3 ml) was slowly added with a dropping funnel to avoid a raising temperature over 35°C. To the clear solution 2-Hexanone was finally added under vigorous stirring. The emulsion was stirred overnight at 35°C. The temperature was lowered to 25°C and three dichloromethane extractions were performed. The organic solvent was removed under reduced pressure yielding yellow oil.

*Second Step* – The aminonitrile, formed in the first step, was dissolved in formic acid (100 ml) at 0°C. Gaseous HCl bubbled for 3 h into the solution under stirring. The reaction mixture was then stirred overnight at room temperature. To the dark solution water (4.5 ml) was added. After stirring for additional 10 min. the solution was

evaporated to dryness, the residue was taken up in toluene (x3) and again evaporated and to remove completely HCl and water the residue was taken again up in diethyl ether. The solid residue was triturated with diethyl ether and isolated by filtration and washed with ether. Yield's 71.6%.

*Third Step* – The HCl·NH<sub>2</sub>NleNH<sub>2</sub> (17.36 g, 0,036 mol), was dissolved in HCl 6N (105 ml) and refluxed for 4 h. The volume was reduced and the formed precipitate was collected by filtration. The process was repeated for a second time. The solid product was triturated in toluene to remove HCl. Yield's 81.4%.

<sup>1</sup>H NMR (200MHz; CDCl<sub>3</sub>): 2.20-2.00 (2 m, 2H), 1.60-1.40 (mb, 4H), 1.40 (s, 3H), 1.1-0.9 (m, 3H).

*Preparation of Fmoc α-Me-Nle-OH*: 100 mg of HCl α-Me-Nle (0.14 mmol, 1 eq.) were suspended in 4 ml of dry DCM under nitrogen atmosphere and 210 μl of TMS-Cl (0.28 mmol, 2 eq.) were added and the mixture was refluxed for 2h. Then a third eq. of TMS-Cl was added and refluxed. After one hour, the mixture was cooled at 0°C and 280 μl of DIEA (0.42 mmol, 3 eq.) and last 157 mg Fmoc-Cl (0.15 mmol, 1.1 eq.) were added. The reaction was followed by TLC (Light Petroleum Ether: Ethyl Acetate 7:3). The solvent was evaporated and the crude material was dissolved in 20 ml of water containing NaHCO<sub>3</sub> 10% and extracted with ethylic ether (three times). Then a retro-extraction of organic layers was made with a solution of NaHCO<sub>3</sub> (10%). Water layers were acidified using HCl conc. to pH=2, and extracted with ethyl acetate (five times). Then the organic layers were anhydriified on Na<sub>2</sub>SO<sub>4</sub>. The solvent was evaporated to obtain yellow oil which became solid. The yield was 60.0% and M.W. was determined by Mass Spectroscopy: calcd 367.4 found 367.2 [M+H<sup>+</sup>].

<sup>1</sup>H NMR (200MHz; CDCl<sub>3</sub>): 7.8-7.3 (8H Fmoc); 6.4 (mb, 1H NH(amide)); 4.4 (d, 2H CH<sub>2</sub>(Fmoc)); 4.25-4.20 (mb, 1H H-(Fmoc)); 2.20-2.00 (2 m, 2H), 1.60-1.40 (mb, 4H), 1.40 (s, 3H), 1.1-0.9 (m, 3H).

*Preparation of Fmoc-α-Me-Nle-F*: To 550 mg of Fmoc-αMeNle-OH (1.5 mmol, 1 eq) in 10 ml of DCM 121 μl of pyridine (1.5 mmol, 1 eq.) and 253 μl of cyanuric fluoride

(3.0 mmol, 2 eq.) were added at 0°C. The mixture was left reach at room temperature and after 3 hours the mixture was extracted with water and ice (three times). The organic layer was then washed with cold water. Before evaporating under vacuum the solvent the organic layer was anhydriified on Na<sub>2</sub>SO<sub>4</sub>. The purity of the product was confirmed by IR analysis (1837 cm<sup>-1</sup> (s C-F)).

*Preparation of Fmoc-Leu-F:* To 700 mg of Fmoc-Leu-OH (1.9 mmol, 1 eq.) in 10 ml of DCM 154. µl of pyridine ( 1.9 mmol, 1 eq.) and 325 µl of cyanuric fluoride (3.8 mmol, 2 eq.) were added at 0°C. The mixture was left reach at room temperature and after 3 hours the mixture was extracted with water and ice (three times). The organic layer was then washed with cold water. Before evaporate under vacuum the solvent the organic layer was anhydriified on Na<sub>2</sub>SO<sub>4</sub>. The purity of the product was confirmed by IR analysis (1839 cm<sup>-1</sup> (s C-F)).

### **Synthesis on SPPS**

The solid-phase synthesis of PTH(1-11) analogue containing αMeNle is outlined in Scheme 1. The synthetic protocol for the other analogues is similar. The analogues were prepared using Fmoc methology with Rink Amide MHBA Resin (Novabiochem) (0.73 mmol/g loading) as a solid support. The side-chain protecting groups were compatible with the Fmoc methodology. The αMeNle was prepared as Fmoc-αMeNle-OF. The first amino acid was anchored to the resin using the HBTU/HOBt/DIPEA protocol; the most common peptide coupling additive is HOBt, used either as a carbocation with another coupling agent or incorporated into a stand-alone reagent such as an uronium salt. Cleavage of amino groups was achieved under standard conditions, with 20% piperidine solution in NMP. The next amino acids in the sequence were coupled in the same way. The Fmoc-α-Me-Nle-OF was used with an excess of 3 eq., with an eq. of DIEA. The coupling time was 2h and repeated two times. The following amino acid was introduced on resin with the same protocol.

Peptide Cleavage and Purification: the resin was treated with a cleavage solution of TFA/TIS/water (95:2.5:2.5 v/v/v) at room temperature for 2h. After filtration, the filtrate was concentrated under nitrogen and precipitated with methyl tert-butyl ether.

Peptide purification was performed by reversed-phase HPLC on Vydac C<sub>18</sub> (218TP510) column. The two diastereoisomeric peptides were resolved during purification in HPLC. The correct configuration of αMeNle was determined using NMR technique. The peptide homogeneity (>95%) was determined by analytical HPLC using the same solvents with a gradient of 10-35 % (v/v) acetonitrile over 15 min. Yield after purification and lyophilization, the peptide content was determined by UV methodology.

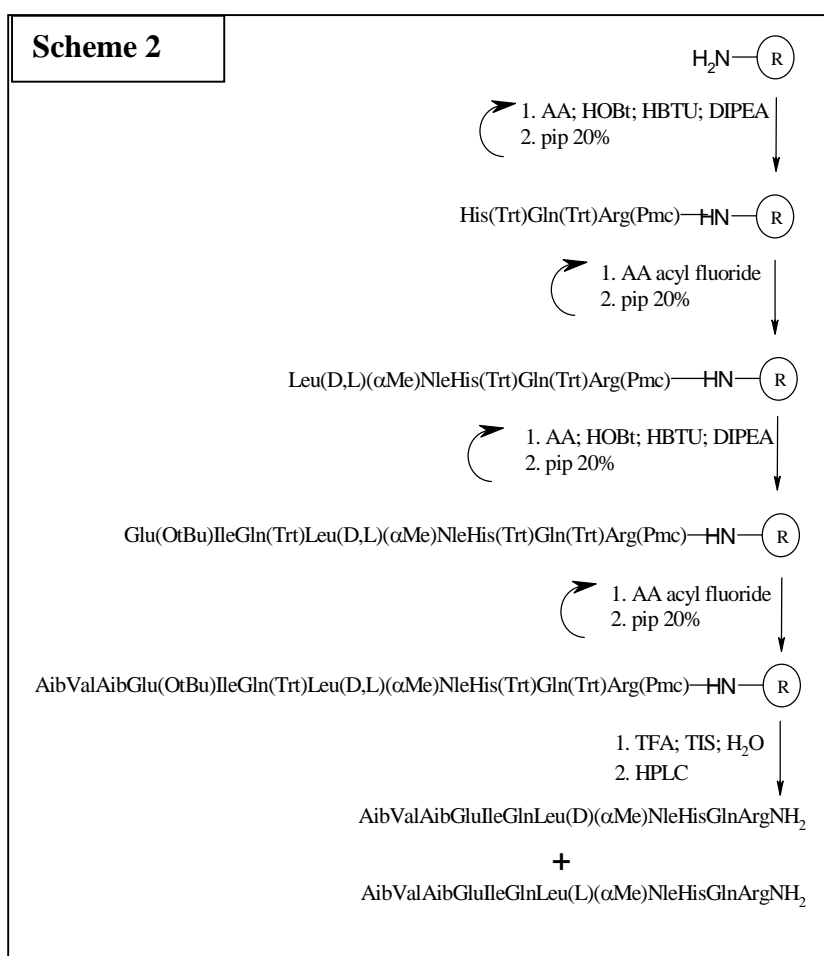


**Table 4**

Name	Peptide sequence	MW	Yield	p.c.%	purity
<b>AMeLAla3</b>	Aib-Val-Ala-Glu-Ile-Gln-Leu-L( $\alpha$ Me)Nle-His-Gln-Arg-NH <sub>2</sub>	1304	17%	79	>97%
<b>AMeDAla3</b>	Aib-Val-Ala-Glu-Ile-Gln-Leu-D( $\alpha$ Me)Nle-His-Gln-Arg-NH <sub>2</sub>	1304	15%	51	>97%
<b>AMeLAla1</b>	Ala-Val-Aib-Glu-Ile-Gln-Leu-L( $\alpha$ Me)Nle-His-Gln-Arg-NH <sub>2</sub>	1304	20%	75	>97%
<b>AMeDAla1</b>	Ala-Val-Aib-Glu-Ile-Gln-Leu-D( $\alpha$ Me)Nle-His-Gln-Arg-NH <sub>2</sub>	1304	19%	48	>97%
<b>AMeLAib1,3</b>	Aib-Val-Aib-Glu-Ile-Gln-Leu-L( $\alpha$ Me)Nle-His-Gln-Arg-NH <sub>2</sub>	1318	21%	23	>97%
<b>AMeDAib1,3</b>	Aib-Val-Aib-Glu-Ile-Gln-Leu-D( $\alpha$ Me)Nle-His-Gln-Arg-NH <sub>2</sub>	1318	19%	81	>97%

**AMeLAla3**

Chemical Shift for [Aib<sup>1</sup>, Ala<sup>3</sup>, R( $\alpha$ Me)Nle<sup>8</sup>, Gln<sup>10</sup>, Arg<sup>11</sup>]-rPTH(1-11)NH<sub>2</sub>,  
in conc: 1mM, T=298 K, in solution water/TFE-d<sub>3</sub> 20%.

AA	$\delta$ NH	$\delta\alpha$	$\delta\beta$	$\delta$	
1	Aib	-	-	-	
2	Val	7.929	4.099	2.128	$\gamma_{\text{CH}_3}$ = 1.004
3	Ala	8.529	4.329	1.464	-
4	Glu	8.427	4.143	2.119	$\gamma_{\text{CH}_2}$ = 2.452, 2.510
5	Ile	7.908	3.971	1.933	$\gamma_{\text{CH}_2}$ = 1.582, 1.249 $\gamma_{\text{CH}_3}$ = 0.945 $\delta_{\text{CH}_3}$ = 0.945
6	Gln	8.065	4.192	2.18	$\gamma_{\text{CH}_2}$ = 2.440, 2.389 NH <sub>2</sub> = 7.415, 6.756
7	Leu	7.923	4.142	1.724	$\gamma_{\text{CH}_2}$ = 1.624, $\delta_{\text{CH}_2}$ = 0.926
8	( $\alpha$ Me)Nle	8.113	(CH <sub>3</sub> )1.429	2.091, 1.705	$\gamma_{\text{CH}_2}$ = 1.313, 1.248 $\delta_{\text{CH}_2}$ = 1.105, $\epsilon_{\text{CH}_2}$ = 0.877
9	His	7.947	4.559	3.439, 3.293	H <sup>2</sup> = 8.603 H <sup>4</sup> = 7.400
10	Gln	8.202	4.289	2.22	$\gamma_{\text{CH}_2}$ = 2.229, 2.479, NH <sub>2</sub> = 7.415, 6.756
11	Arg	8.025	4.329	1.985, 1.836	$\gamma_{\text{CH}_2}$ = 1.727 $\delta_{\text{CH}_2}$ = 3.223 $\epsilon_{\text{NH}}$ = 7.258 NH <sub>2</sub> -term= 7.365, 7.088

**AMeDAla3**

Chemical Shift for [Aib<sup>1</sup>, Ala<sup>3</sup>, S(αMe)Nle<sup>8</sup>, Gln<sup>10</sup>, Arg<sup>11</sup>]-rPTH(1-11)NH<sub>2</sub>,  
in conc: 1mM, T=298 K, in solution water/TFE-d<sub>3</sub> 20%.

AA	δNH	δα	δβ	δ	
1	Aib	-	-	-	
2	Val	7.933	4.075	2.142	γ <sub>CH3</sub> = 1.017
3	Ala	8.555	4.304	1.468	-
4	Glu	8.404	4.119	2.143	γ <sub>CH2</sub> = 2.544, 2.446
5	Ile	7.840	3.932	1.969	γ <sub>CH2</sub> = 1.616, 1.275 γ <sub>CH3</sub> = 0.951 δ <sub>CH3</sub> = 0.920, 0.902
6	Gln	8.075	4.158	2.220, 2.158	γ <sub>CH2</sub> = 2.457, 2.399 NH <sub>2</sub> = 7.386, 6.730
7	Leu	7.835	4.128	1.752, 1.691	γ <sub>CH2</sub> = 1.691 δ <sub>CH2</sub> = 0.927
8	S(αMe)Nle	8.070	(αMe):1.438		γ <sub>CH2</sub> = 1.269 δ <sub>CH2</sub> = 0.902 ε <sub>CH2</sub> = 0.845
9	His	7.934	4.502	3.431, 3.303	H <sup>2</sup> = 8.603 H <sup>4</sup> = 7.424
10	Gln	8.215	4.270	2.259	γ <sub>CH2</sub> = 2.495, 2.564 NH <sub>2</sub> = 7.317, 6.760
11	Arg	8.003	4.312	2.001, 1.862	γ <sub>CH2</sub> = 1.783 δ <sub>CH2</sub> = 3.211 ε <sub>NH</sub> = 7.244 NH <sub>2</sub> -term= 7.317, 7.072

**AMeLAla1**

Chemical Shift for [Ala<sup>1</sup>, Aib<sup>3</sup>, R(αMe)Nle<sup>8</sup>, Gln<sup>10</sup>, Arg<sup>11</sup>]-rPTH(1-11)NH<sub>2</sub>,  
in conc: 1mM, T=298 K, in solution water/TFE-d<sub>3</sub> 20%.

AA	δNH	δα	δβ	δ	
1	Ala		4.198	1.608	-
2	Val	8.464	4.044	2.170	γ <sub>CH3</sub> = 1.053
3	Aib	8.479		1.477	-
4	Glu	8.210	4.030	2.128	γ <sub>CH2</sub> = 2.441
5	Ile	7.703	3.889	2.028	γ <sub>CH2</sub> =1.618 γ' <sub>CH2</sub> =1.282 γ <sub>CH3</sub> =0.956 δ <sub>CH3</sub> =0.917
6	Gln	7.789	4.172	2.144	γ <sub>CH2</sub> =2.430 γ' <sub>CH2</sub> =2.358 NH <sub>2</sub> =7.268 / 6.478
7	Leu	8.037	4.104	1.723	γ <sub>CH2</sub> =1.649 δ <sub>CH2</sub> =0.919
8	R(αMe)Nle	8.114	αMe:1.445	β=2.138 β'=1.700	γ <sub>CH2</sub> =1.296 γ' <sub>CH2</sub> =1.121 δ <sub>CH2</sub> ,ε <sub>CH2</sub> =0.883
9	His	7.885	4.525	β=3.444 β'=3.311	H <sup>2</sup> =8.596 H <sup>4</sup> = 7.424
10	Gln	8.221	4.278	2.232	γ <sub>CH2</sub> =2.543 γ' <sub>CH2</sub> =2.484 NH <sub>2</sub> =7.405 / 6.748

11	Arg	8.005	4.323	$\beta=1.993$ $\beta'=1.843$	$\gamma_{\text{CH}_2}=1.730$ $\delta_{\text{CH}_2}= 3.215$ $\epsilon_{\text{NH}}=7.261$ $\text{NH}_2\text{-term}= 7.095 / 7.305$
----	-----	-------	-------	---------------------------------	---

### AMeDAla1

Chemical Shift for [Ala<sup>1</sup>, Aib<sup>3</sup>, S( $\alpha$ Me)Nle<sup>8</sup>, Gln<sup>10</sup>, Arg<sup>11</sup>]-rPTH(1-11)NH<sub>2</sub>,  
in conc: 1mM, T=298 K, in solution water/TFE-d<sub>3</sub> 20%.

AA	$\delta_{\text{NH}}$	$\delta_{\alpha}$	$\delta_{\beta}$	$\delta$	
1	Ala		4.194	1.604	-
2	Val	8.464	4.039	2.170	$\gamma_{\text{CH}_3}= 1.056$
3	Aib	8.529		$\beta= 1.606$ $\beta'=1.476$	-
4	Glu	8.301	4.019	2.134	$\gamma_{\text{CH}_2}=2.548$ $\gamma'_{\text{CH}_2}=2.423$
5	Ile	7.691	3.890	2.051	$\gamma_{\text{CH}_2}=1.613$ $\gamma_{\text{CH}_3}=1.306$ $\delta_{\text{CH}_3}=0.948$
6	Gln	7.795	4.167	2.149	$\gamma_{\text{CH}_2}=2.436$ $\gamma'_{\text{CH}_2}= 2.357$ $\text{NH}_2= 7.288 / 6.751$
7	Leu	7.936	4.098	1.742	$\gamma_{\text{CH}_2}=1.672$ $\delta_{\text{CH}_2}= 0.914$
8	S( $\alpha$ Me)Nle	8.041	$\alpha\text{Me}:1.431$	$\beta= 1.947$ $\beta'=1.814$	$\gamma_{\text{CH}_2}= 1.276$ $\delta_{\text{CH}_2}= 1.217$ $\epsilon_{\text{CH}_2}= 0.843$
9	His	7.858	4.508	$\beta= 3.433$ $\beta'=3.308$	$\text{H}^2=8.609$ $\text{H}^4= 7.434$
10	Gln	8.237	4.270	2.253	$\gamma_{\text{CH}_2}=2.493$ $\gamma'_{\text{CH}_2}=2.571$ $\text{NH}_2= 7.396 / 6.739$
11	Arg	7.999	4.303	$\beta= 1.997$ $\beta'=1.856$	$\gamma_{\text{CH}_2}= 1.705$ $\gamma'_{\text{CH}_2}= 1.781$ $\delta_{\text{CH}_2}=3.206$ $\epsilon_{\text{NH}}=7.242$ $\text{NH}_2\text{-term}= 7.305 / 7.092$

### AMeLAib1,3

Chemical Shift for [Aib<sup>1,3</sup>, R( $\alpha$ Me)Nle<sup>8</sup>, Gln<sup>10</sup>, Arg<sup>11</sup>]-rPTH(1-11)NH<sub>2</sub>, in  
conc: 1.0 mM, T=298 K, in solution water/TFE-d<sub>3</sub> 20%.

AA	$\delta_{\text{NH}}$	$\delta_{\alpha}$	$\delta_{\beta}$	$\delta$	
1	Aib	-	-	1.671, 1.728	-
2	Val	7.970	3.952	2.153	$\gamma_{\text{CH}_3}= 1.041, 1.024$
3	Aib	8.514	-	1.735, 1.465	-
4	Glu	8.203	4.024	2.139, 2.086	$\gamma_{\text{CH}_2}= 2.569, 2.390$
5	Ile	7.758	3.863	2.005	$\gamma_{\text{CH}_2}= 1.667, 1.247$ $\gamma_{\text{CH}_3}= 0.944$ $\delta_{\text{CH}_3}= 0.892$
6	Gln	7.985	4.159	2.150	$\gamma_{\text{CH}_2}= 2.451, 2.354$ $\text{NH}_2= 7.226, 6.743$
7	Leu	8.034	4.107	1.731	$\gamma_{\text{CH}_2}= 1.646$ $\delta_{\text{CH}_2}= 0.919$
8	R( $\alpha$ Me)Nle	8.106	$\alpha\text{Me}: 1.445$	2.126, 1.698	$\gamma_{\text{CH}_2}= 1.275$ $\delta_{\text{CH}_2}= 1.110$ $\epsilon_{\text{CH}_2}= 0.879$
9	His	7.902	4.527	3.441, 3.306	$\text{H}^2= 8.591$ $\text{H}^4= 7.412$

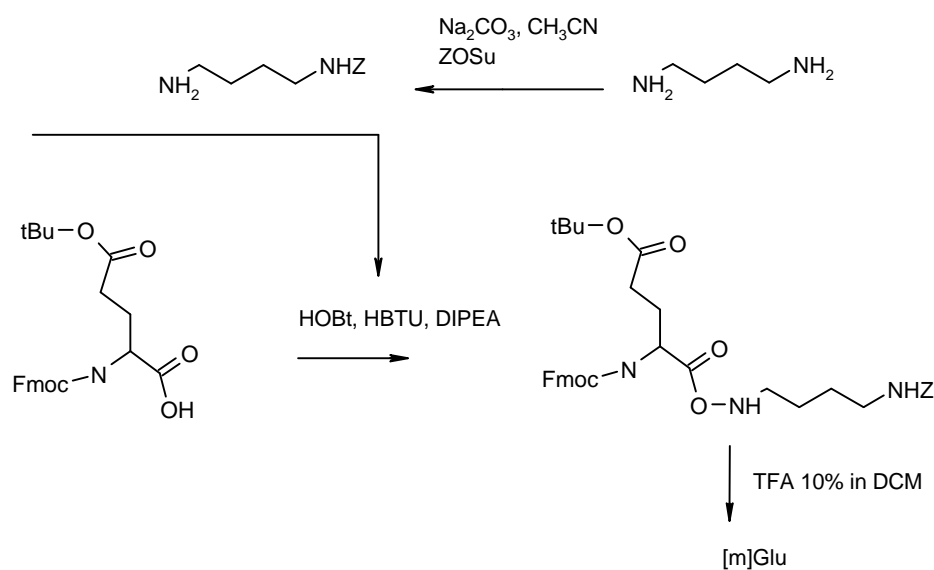
10	Gln	8.222	4.272	2.227	$\gamma_{\text{CH}_2}$ = 2.544, 2.475 $\text{NH}_2$ = 7.411, 6.752
11	Arg	8.012	4.320	1.985, 1.836	$\gamma_{\text{CH}_2}$ = 1.726 $\delta_{\text{CH}_2}$ = 3.208 $\epsilon_{\text{NH}}$ = 7.258 $\text{NH}_2$ -term= 7.335, 7.097

### AMeDAib1,3

Chemical Shift for [Aib<sup>1, 3</sup>, S( $\alpha$ Me)Nle<sup>8</sup>, Gln<sup>10</sup>, Arg<sup>11</sup>]-rPTH(1-11)NH<sub>2</sub>, in conc: 1.0 mM, T=298 K, in solution water/TFE-d<sub>3</sub> 20%.

AA	$\delta_{\text{NH}}$	$\delta_{\alpha}$	$\delta_{\beta}$	$\delta_{\text{altri}}$	
1	Aib	-	-	1.727, 1.668	-
2	Val	7.980	3.943	2.159	$\gamma_{\text{CH}_3}$ = 1.038
3	Aib	8.544	-	1.454	-
4	Glu	8.215	4.006	2.153, 2.083	$\gamma_{\text{CH}_2}$ = 2.590, 2.398
5	Ile	7.736	3.854	2.029	$\gamma_{\text{CH}_2}$ = 1.664, 1.274 $\gamma_{\text{CH}_3}$ = 0.943 $\delta_{\text{CH}_3}$ = 0.881
6	Gln	7.965	4.149	2.164	$\gamma_{\text{CH}_2}$ = 2.451, 2.350 $\text{NH}_2$ = 7.217, 6.740
7	Leu	7.916	4.092	1.743, 1.684	$\gamma_{\text{CH}_2}$ = 1.684 $\delta_{\text{CH}_2}$ = 0.912
8	S( $\alpha$ Me)Nle	8.078	$\alpha$ Me:1.424	1.972, 1.803	$\gamma_{\text{CH}_2}$ = 1.282 $\delta_{\text{CH}_2}$ = 1.212 $\epsilon_{\text{CH}_2}$ = 0.832
9	His	7.867	4.491	3.432, 3.307	$\text{H}^2$ = 8.601 $\text{H}^4$ = 7.434
10	Gln	8.248	4.260	2.250	$\gamma_{\text{CH}_2}$ = 2.571, 2.486 $\text{NH}_2$ = 7.388, 6.734
11	Arg	8.003	4.297	1.994, 1.851	$\gamma_{\text{CH}_2}$ = 1.774, 1.705 $\delta_{\text{CH}_2}$ = 3.200 $\epsilon_{\text{NH}}$ = 7.240 $\text{NH}_2$ -term= 7.298, 7.092

### § Synthesis of Series of Analogues containing diamine peptidomimetics of PTH(1-11)





## General Procedure:

First step: diamine (11 mmol, 5 eq) was dissolved in 100ml of mixture of NaHCO<sub>3</sub> 10% and acetonitrile (50/50). Z succinimide (2.2 mmol, 1 eq) was added and was stirred overnight. The reaction was controlled on TLC (1<sup>st</sup> run in CH<sub>2</sub>Cl<sub>2</sub>/MeOH 9/1 and 2<sup>nd</sup> run in CHCl<sub>3</sub>/MeOH/NH<sub>4</sub>OH 17% 6/2/2). Solvent was evaporated and the crude material was dissolved in water and filtrated. Aqueous solution was extracted with DCM. The organic layers were dried on Na<sub>2</sub>SO<sub>4</sub>. The yield was 45%.

Second Step: Protected diamine (0.7 mmol, 1 eq) was dissolved in 20 ml of DCM and was added Fmoc-Glu(OtBu)OPfp (1.0 mmol, 1.5 eq) with HOBt (1.0 mmol, 1.5 eq) and DIPEA (2.0 mmol, 3 eq) to the solution. It was stirred overnight. The solution was dried and the solid was dissolved again in ethyl acetate, and the organic layers were extracted with water, NaHCO<sub>3</sub> 5% and brine. The crude material was purified via flash chromatography (ethyl acetate/light petroleum ether 1/1). The yield was 70%.

FmocGlu(OtBu)NH(CH<sub>2</sub>)<sub>4</sub>NHZ: NMR 400 MHz, CDCl<sub>3</sub>: ppm 7.77-7.3 (13H Fmoc + Z); 6.4 (mb, 1H NH(amide)); 5.75 (mb, 1H NH(Fmoc)); 5.08 (s, 2H CH<sub>2</sub>(Z)); 4.8 (mb, 1H NH(Z)); 4.4 (d, 2H CH<sub>2</sub>(Fmoc)); 4.22-4.18 (t; mb, 2H H $\alpha$ -Glu; H-(Fmoc)); 3.3-3.1 (2qb, 4H NCH<sub>2</sub>); 2.3 (2mb, 2H  $\gamma$ CH<sub>2</sub>-Glu) ; 2.0 (2mb, 2H  $\beta$ CH<sub>2</sub>-Glu); 1.6-1.4 (m; s, 13H NCH<sub>2</sub>CH<sub>2</sub>; tBu); Calculated mass : 630; Found mass: 631.12 [M+1].

FmocGlu(OtBu)NH(CH<sub>2</sub>)<sub>5</sub>NHZ: NMR 400 MHz, CDCl<sub>3</sub>: ppm 7.77-7.3 (13H Fmoc + Z); 6.4 (mb, 1H NH(amide)); 5.75 (mb, 1H NH(Fmoc)); 5.08 (s, 2H CH<sub>2</sub>(Z)); 4.8 (mb, 1H NH(Z)); 4.4 (d, 2H CH<sub>2</sub>(Fmoc)); 4.22-4.18 (t; mb, 2H H $\alpha$ -Glu; H-(Fmoc)); 3.3-3.1 (2qb, 4H NCH<sub>2</sub>); 2.3 (2mb, 2H  $\gamma$ CH<sub>2</sub>-Glu) ; 2.0 (2mb, 2H  $\beta$ CH<sub>2</sub>-Glu); 1.6-1.4 (m; s, 15H NCH<sub>2</sub>CH<sub>2</sub>; tBu); Calculated mass: 644; Found mass 645.2 [M+1].

FmocGlu(OtBu)NH(CH<sub>2</sub>)<sub>6</sub>NHZ: NMR 400 MHz, CDCl<sub>3</sub>: ppm 7.77-7.3 (13H Fmoc + Z); 6.4 (mb, 1H NH(amide)); 5.75 (mb, 1H NH(Fmoc)); 5.08 (s, 2H CH<sub>2</sub>(Z)); 4.8 (mb, 1H NH(Z)); 4.4 (d, 2H CH<sub>2</sub>(Fmoc)); 4.22-4.18 (t; mb, 2H H $\alpha$ -Glu; H-(Fmoc)); 3.3-3.1

(2qb, 4H NCH<sub>2</sub>); 2.3 (2mb, 2H  $\gamma$ CH<sub>2</sub>-Glu) ; 2.0 (2mb, 2H  $\beta$ CH<sub>2</sub>-Glu); 1.6-1.4 (m; s, 17H NCH<sub>2</sub>CH<sub>2</sub>; tBu); Calculated mass: 658; Found mass: 659.15 [M+1].

Name	Peptide sequence	MW	Yield	p.c. (%)	Purity
K	Aib Val Aib Glu Ile Gln Leu Nle His Gln Lys-NH <sub>2</sub>	1276.4	10%	70	>97%
n=4	Aib Val Aib Glu Ile Gln Leu Nle His Gln NH(CH <sub>2</sub> ) <sub>4</sub> NH <sub>2</sub>	1219.4	7%	66	>97%
n=5	Aib Val Aib Glu Ile Gln Leu Nle His Gln NH(CH <sub>2</sub> ) <sub>5</sub> NH <sub>2</sub>	1233.4	11%	79	>97%
n=6	Aib Val Aib Glu Ile Gln Leu Nle His Gln NH(CH <sub>2</sub> ) <sub>6</sub> NH <sub>2</sub>	1247.4	12%	90	>97%

### § Synthesis of Series of PTH(1-11) Analogues containing hybrid peptoid-peptides

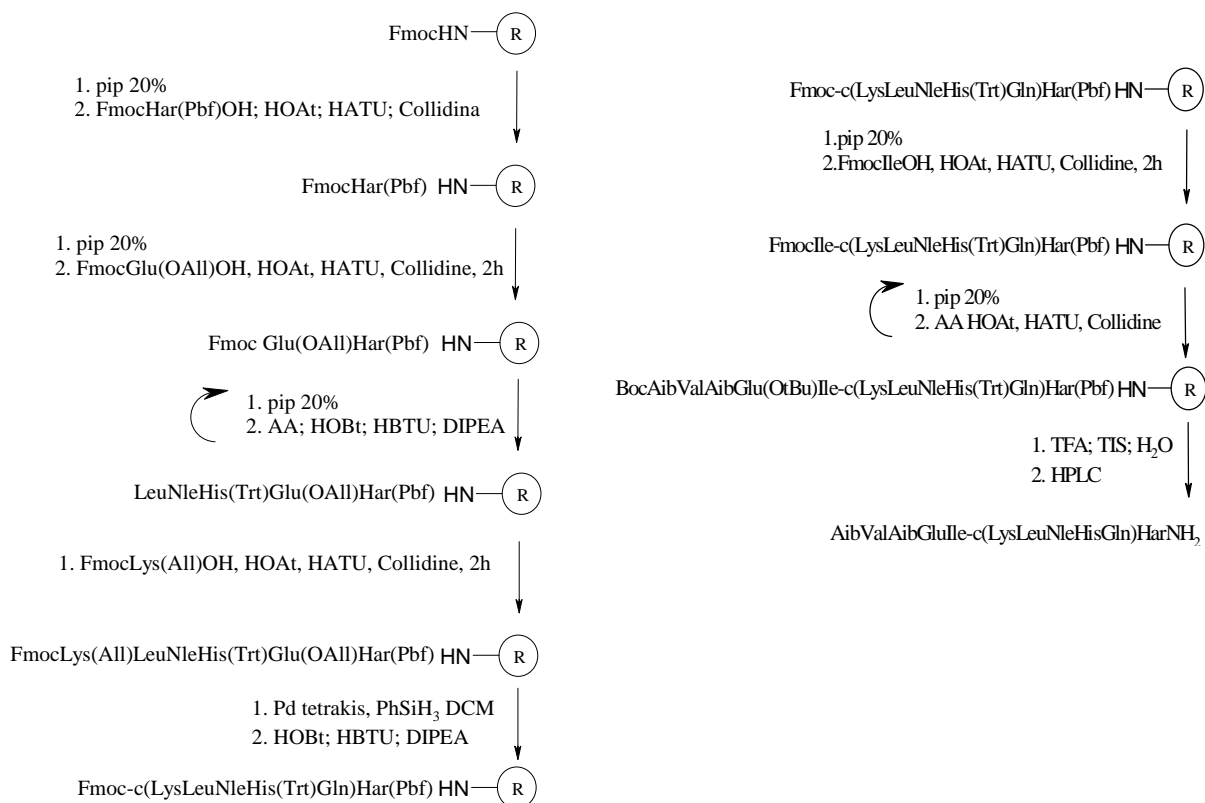
Peptide-peptoid hybrids were synthesized using a suitable combination of standard Fmoc solid-phase peptide synthesis for amino acid residues<sup>7</sup> and of the submonomer approach for NSG residues. The required NSG residues, NVal, NNle and NArg, were synthesized according to the procedure reported in references 8 and 9. The side chain protecting groups were removed under acidic conditions at the time of cleavage of the oligomers from the Rink-amide-MBHA resin. Traditionally, in solid-phase peptoid synthesis an acid labile solid support such as Rink-amide-MBHA resin is used, which allows cleavage from the resin using acidic conditions such as 95% trifluoroacetic acid (TFA). For the insertion of Aib and Val, we used the HOAt/HATU/collidine system<sup>4</sup>.

All peptides had the correct molecular weight as verified by ESI-TOF mass spectrometry. For all amino acids, the coupling reagents were HOBt; HBTU and 1,3-diisopropylcarbodiimide; HOAt; HATU; Collidine and all solvents were purchased from commercial sources and used without further purification. For peptide 1 with NVal in position 2, we replaced Aib in position 1 with Ala due to steric hindrance caused by N-alkylglycine. All crude peptide-peptoid hybrid analogues were purified using reversed-phase HPLC and analytically characterized in co-solvent system (solvent A: water + 0.1% TFA and solvent B: 90% acetonitrile + 0.1% TFA).

**Table 5**

Name	Peptide	MW	Yield	P.C. (%)	Purity
NVal	H-Ala NVal Aib Glu Ile Gln Leu Nle His Gln HarNH <sub>2</sub>	1304	7%	68	>97%
NNle	H-Aib Val Aib Glu Ile Gln Leu NNle His Gln HarNH <sub>2</sub>	1316	11%	81	>97%
NArg	H-Aib Val Aib Glu Ile Gln Leu Nle His Gln NArgNH <sub>2</sub>	1304	12%	67	>97%

**§ Synthesis of Series of Cyclo Analogues of PTH(1-11)**



Cyclopeptides are synthesized directly on resin using a suitable system of reagents and conditions.

Traditionally, in solid-phase peptide synthesis an acid labile solid support such as Rink-amide-MBHA resin is used, which allows cleavage from the resin using acidic conditions such as 95% trifluoroacetic acid (TFA). The introduction of first residue is

used a HOAt/HATU/Collidine system. Then, the elongation of peptide follows the normal procedure used in conventional SPPS. For the insertion of Aib and Val, we used the HOAt/HATU/collidine system.

First cyclic peptide : *H Aib Val Aib Glu Ile c(Lys Leu Nle His Glu) Har-NH<sub>2</sub>*

The resins is swelled with two 30 min cycles in DMF and then the first amino acid is coupled to resin following this workplane.

	[g/mL]	MW[g/mol]	mmol	eq.	Amount
<b>Resina Rink Amide MBHA</b>			<b>0,073</b>	1	<b>105 mg</b>
<b><i>Cleavage PIP 20% in DMF (45 minutes)</i></b>					<b>3 mL</b>
<b>Fmoc-Har(Pbf)-OH</b>		<b>648,8</b>	<b>0,304</b>	4	<b>192,7 mg</b>
<b>HOAt</b>		<b>136,2</b>	<b>0,304</b>	4	<b>41,4 mg</b>
<b>HATU</b>		<b>380,0</b>	<b>0,304</b>	4	<b>115,5 mg</b>
<b>Collidine</b>	<b>0,92</b>	<b>121,2</b>	<b>0,608</b>	8	<b>80 µL</b>
<b>DMF</b>					<b>2 mL</b>
<b><i>Time = 2 hours</i></b>					
<b><i>Cleavage PIP 20% in DMF (45 minutes)</i></b>					<b>3 mL</b>
<b>Fmoc-Glu(Allyl)-OH</b>		<b>409,4</b>	<b>0,304</b>	4	<b>123,0 mg</b>
<b>HOAt</b>		<b>136,2</b>	<b>0,304</b>	4	<b>41,4 mg</b>
<b>HATU</b>		<b>380,0</b>	<b>0,304</b>	4	<b>115,5 mg</b>
<b>Collidine</b>	<b>0,92</b>	<b>121,2</b>	<b>0,608</b>	8	<b>80 µL</b>
<b>DMF</b>					<b>2 mL</b>
<b><i>Time = 2 hours</i></b>					
<b><i>Cleavage PIP 20% in DMF (45 minutes)</i></b>					<b>3 mL</b>
<b>Fmoc-His(Trt)-OH</b>		<b>619,7</b>	<b>0,304</b>	4	<b>188,4 mg</b>
<b>HOBt</b>		<b>135,3</b>	<b>0,304</b>	4	<b>41,1 mg</b>
<b>HBTU</b>		<b>379,1</b>	<b>0,304</b>	4	<b>115,2 mg</b>
<b>DIPEA</b>	<b>0,72</b>	<b>129,4</b>	<b>0,608</b>	8	<b>109 µL</b>
<b>DMF</b>					<b>2 mL</b>
<b><i>Time = double coupling</i></b>					
<b><i>Cleavage PIP 20% in DMF (45 minutes)</i></b>					<b>3 mL</b>
<b>Fmoc-Nle-OH</b>		<b>353,4</b>	<b>0,304</b>	4	<b>107,4 mg</b>
<b>HOBt</b>		<b>135,3</b>	<b>0,304</b>	4	<b>41,1 mg</b>
<b>HBTU</b>		<b>379,1</b>	<b>0,304</b>	4	<b>115,2 mg</b>
<b>DIPEA</b>	<b>0,72</b>	<b>129,4</b>	<b>0,608</b>	8	<b>109 µL</b>
<b>DMF</b>					<b>2 mL</b>
<b><i>Time = 1 hours</i></b>					
<b><i>Cleavage PIP 20% in DMF (45 minutes)</i></b>					<b>3 mL</b>

	[g/mL]	MW[g/mol]	mmol	eq	Amount
<b>Fmoc-Leu-OH</b>		<b>353,4</b>	<b>0,304</b>	4	<b>107,4 mg</b>
<b>HOBt</b>		<b>135,3</b>	<b>0,304</b>	4	<b>41,1 mg</b>
<b>HBTU</b>		<b>379,1</b>	<b>0,304</b>	4	<b>115,2 mg</b>
<b>DIPEA</b>	<b>0,72</b>	<b>129,4</b>	<b>0,608</b>	8	<b>109 µL</b>
<b>DMF</b>					<b>2 mL</b>
<i>Time = double coupling of 1 h</i>					
<i>Cleavage PIP 20% in DMF (45 minutes)</i>					<b>3 mL</b>
<b>Fmoc-Lys(Alloc)-OH</b>			<b>0,304</b>	4	
<b>HOAt</b>		<b>136,2</b>	<b>0,304</b>	4	<b>41,4 mg</b>
<b>HATU</b>		<b>380,0</b>	<b>0,304</b>	4	<b>115,5 mg</b>
<b>Collidine</b>	<b>0,92</b>	<b>121,2</b>	<b>0,608</b>	8	<b>80 µL</b>
<b>DMF</b>					<b>2 mL</b>
<i>Time = double coupling of 1 h</i>					

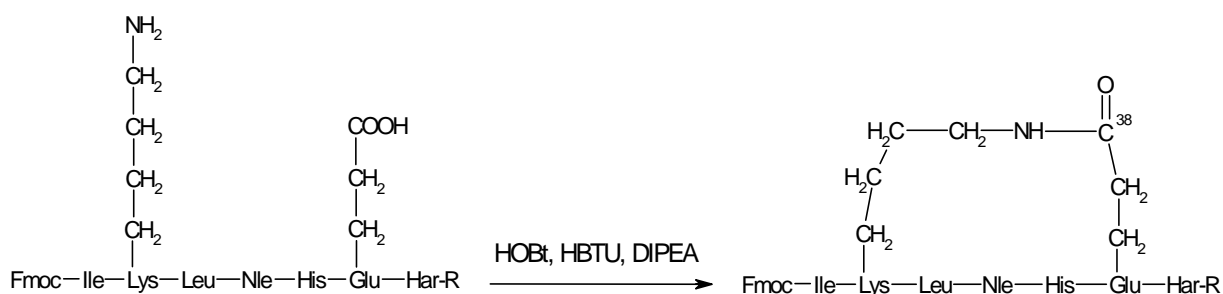
### Cleavage of Allyl and Alloc

#### Reagents:

	[g/mL]	MW [g/mol]	mmol	eq.	amount
<b>Resin</b>			<b>0,073</b>	<b>1</b>	
<b>PhSiH<sub>3</sub></b>	<b>0,878</b>	<b>108,22</b>	<b>1,75</b>	<b>24</b>	<b>216 µL</b>
<b>Pd(Ph<sub>3</sub>)<sub>4</sub></b>		<b>1155,5</b>	<b>0,02</b>	<b>0,25</b>	<b>21 mg</b>
<b>DCM dry</b>					<b>2 mL</b>

Protective groups Alloc and Allyl on Lys<sup>6</sup> and Glu<sup>10</sup> are removed in neutral condition: the peptide-resin washed with CH<sub>2</sub>Cl<sub>2</sub> under Nitrogen and a solution of Pd(PPh<sub>3</sub>)<sub>4</sub> (21 mg, 0.020, 0.25 equiv.) and PhSiH<sub>3</sub> (216 µl, 1.75 mmol, 24 equiv.) in CH<sub>2</sub>Cl<sub>2</sub> (2 mL) was added and the resin was shaken for 30 min. Then, the peptide resin was washed with CH<sub>2</sub>Cl<sub>2</sub> (3x3 ml, 2 min), DMF (3x3 ml, 1 min) and again with CH<sub>2</sub>Cl<sub>2</sub> (3x3 mL, 2 min) and the process was repeated 3 times.

#### Cyclization:



The peptide-resin was suspended in 4ml of NMP/DMF 50/50, followed by cyclization of the peptide via the free carboxylic acid side-chain of Glu and the free amino group side-chain of Lys by addition of HBTU (166 mg, 0.44 mmol, 6 equiv.), HOBt (59 mg, 0.44 mmol, 6 equiv.), and DIEA (150 ml, 0.88 mmol, 12 equiv.) for 2 and 1/2 h. This process was repeated until a negative Kaiser test resulted. The acylation step was accomplished using Ac<sub>2</sub>O (20 equiv.) and DIEA (1 equiv.) in CH<sub>2</sub>Cl<sub>2</sub>.

	[g/mL]	MW[g/mol]	Mmol	eq.	amount
<b>HOBt</b>		<b>135</b>	<b>0,438</b>	<b>6</b>	<b>59 mg</b>
<b>HBTU</b>		<b>379</b>	<b>0,438</b>	<b>6</b>	<b>166 mg</b>
<b>DIPEA</b>	<b>0.72</b>	<b>129</b>	<b>0,876</b>	<b>12</b>	<b>150 µL</b>
<b>DMF dry</b>					<b>4 mL</b>

A small cleavage is runned in order to test reaction in mass spectroscopy. The resin was swelled again in DMF and the synthesis is concluded following normal SPPS protocol.

	[g/mL]	MW[g/mol]	mmol	eq.	amount
<i>Cleavage PIP 20% in DMF (45 minuti)</i>					<b>3 mL</b>
<b>Fmoc-Ile-OH</b>		<b>353,4</b>	<b>0,304</b>	4	<b>107,4 mg</b>
<b>HOAt</b>		<b>135,3</b>	<b>0,304</b>	4	<b>41 mg</b>
<b>HATU</b>		<b>379,1</b>	<b>0,304</b>	4	<b>115 mg</b>
<b>Collidine</b>	<b>0,92</b>	<b>121,2</b>	<b>0,608</b>	8	<b>80 µL</b>
<b>DMF</b>					<b>2 mL</b>
<i>Time = double coupling</i>					
<i>Cleavage PIP 20% in DMF (45 minuti)</i>					<b>3 mL</b>
<b>Fmoc-Glu(OtBu)-OPfp</b>		<b>591,5</b>	<b>0,304</b>	4	<b>179,8 mg</b>
<b>HOBt</b>		<b>135,3</b>	<b>0,304</b>	4	<b>41,1 mg</b>
<b>DIPEA</b>	<b>0,72</b>	<b>129,4</b>	<b>0,608</b>	8	<b>109 µL</b>
<b>DMF</b>					<b>2 mL</b>
<i>Time = 1 h</i>					
<i>Cleavage PIP 20% in DMF (45 minuti)</i>					<b>3 mL</b>
<b>Fmoc-Aib-OH</b>		<b>325,4</b>	<b>0,304</b>	4	<b>98,9 mg</b>
<b>HOAt</b>		<b>136,2</b>	<b>0,304</b>	4	<b>41,1 mg</b>
<b>HATU</b>		<b>380,0</b>	<b>0,304</b>	4	<b>115,5 mg</b>
<b>Collidine</b>	<b>0,92</b>	<b>121,2</b>	<b>0,608</b>	8	<b>80 µL</b>
<b>DMF</b>					<b>2 mL</b>
<i>Time = double coupling</i>					
<i>Cleavage PIP 20% in DMF (45 minuti)</i>					<b>3 mL</b>

	[g/mL]	MW[g/mol]	mmol	eq.	quantità
<b>Fmoc-Val-OH</b>		<b>619,7</b>	<b>0,304</b>	4	<b>188,4 mg</b>
<b>HOAt</b>		<b>136,2</b>	<b>0,304</b>	4	<b>41,1 mg</b>
<b>HATU</b>		<b>380,0</b>	<b>0,304</b>	4	<b>115,5 mg</b>
<b>Collidine</b>	<b>0,92</b>	<b>121,2</b>	<b>0,608</b>	8	<b>80 µL</b>
<b>DMF</b>					<b>2 mL</b>
<i>Time = double coupling (overnight + 2 h)</i>					
<i>Cleavage PIP 20% in DMF (45 minuti)</i>					<b>3 mL</b>
<b>Boc-Aib-OH</b>		<b>203,2</b>	<b>0,304</b>	4	<b>61,8 mg</b>
<b>HOAt</b>		<b>136,2</b>	<b>0,304</b>	4	<b>41,1 mg</b>
<b>HATU</b>		<b>380,0</b>	<b>0,304</b>	4	<b>115,5 mg</b>
<b>Collidine</b>	<b>0,92</b>	<b>121,2</b>	<b>0,608</b>	8	<b>80 µL</b>
<b>DMF</b>					<b>2 mL</b>
<i>Time = double coupling (overnight + 2 h)</i>					
<b>Acetylation: Ac<sub>2</sub>O (20 equiv.) and DIEA (1 equiv.) in DMF</b>					

Peptide Cleavage and Purification. The resin was treated with a cleavage solution of TFA/TIS/water (95:2.5:2.5 v/v/v) at room temperature for 2h. After filtration, the filtrate was concentrated under nitrogen and precipitated with methyl tert-butyl ether. Peptide purification was performed by reversed-phase HPLC on Vydac C<sub>18</sub> (218TP510) column. The peptide homogeneity (>95%) was determined by analytical HPLC using the same solvents with a gradient of 10-35 % (v/v) acetonitrile over 15 min. Analogue: RT=18.5 min; yield after purification and lyophilization : 4.2%

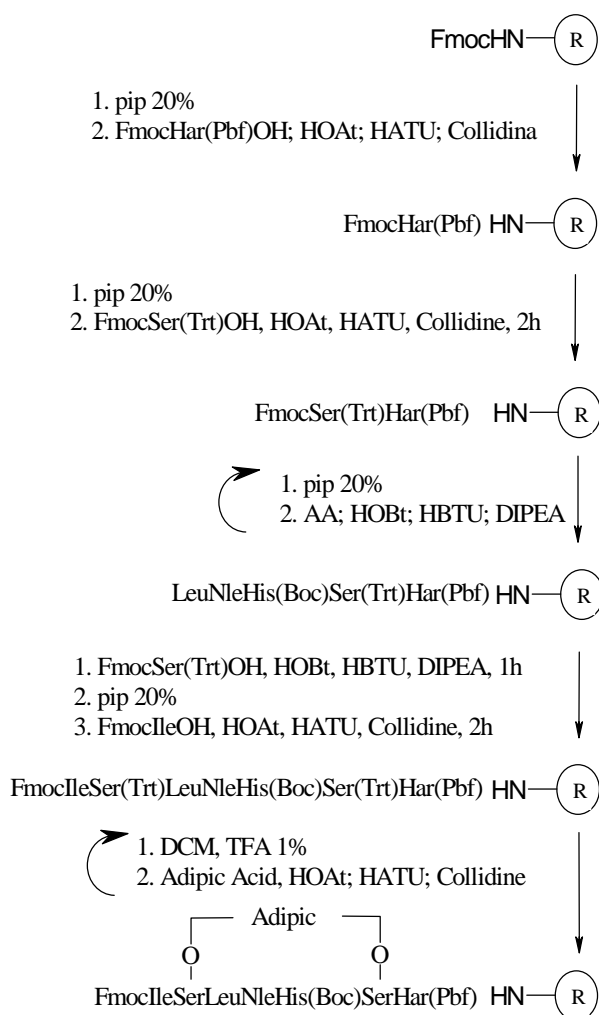
Peptide content was determined by UV methodology : 88%.

Chemical Shift for first cyclic peptide of PTH: conc: 2.40 mM, T=298 K, in solution water/TFE-d<sub>3</sub> 20%.

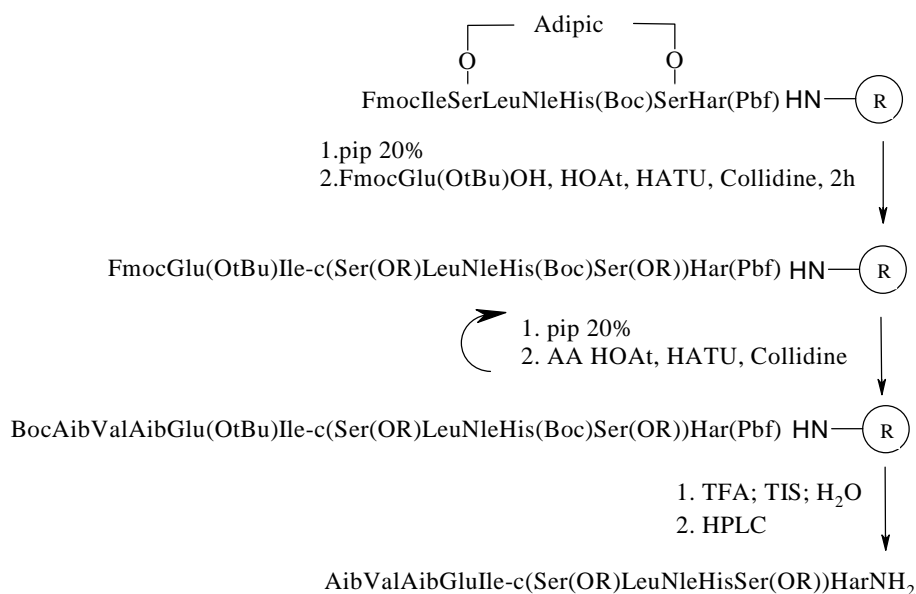
AA	δNH	δH <sub>α</sub>	δH <sub>β</sub>	δ
1   Aib	-	-	1,60; 1,70	-
2   Val	7,87	3,84	2,08	γ(CH <sub>3</sub> ) = 0,97
3   Aib	8,35	-	0,95; 2,38	-
4   Glu	8,20	3,91	1,97; 2,11	γ(CH <sub>2</sub> ) = 2,28; 2,53
5   Ile	7,66	3,77	1,97	γ(CH) = 1,67 ; δ(CH <sub>2</sub> ) = 1,18; γ(CH <sub>3</sub> ) = 0,91 ; ε(CH <sub>3</sub> ) = 0,82
6   Lys	7,89	4,07	1,85; 1,97	γ(CH <sub>2</sub> ) = 1,42; 1,55; δ(CH <sub>2</sub> ) = 1,28; ε(CH <sub>2</sub> ) = 2,89; 3,24; η(NHCO) = 7,37
7   Leu	8,15	4,02	1,55; 1,81	γ(CH) = 1,74; δ(CH <sub>3</sub> ) = 0,86

8	Nle	8,12	3,97	1,74; 1,82	$\gamma(\text{CH}_2) = 1,42; \delta(\text{CH}_2) = 1,24;$ $\epsilon(\text{CH}_2) = 0,79$
9	His	7,92	4,50	3,28; 3,47	$\text{H}^2 = 8,52; \text{H}^4 = 7,42$
10	Glu	7,92	4,29	2,10; 2,18	$\gamma(\text{CH}_2) = 2,34; 2,49$
11	Har	8,01	4,23	1,79; 1,87	$\gamma(\text{CH}_2) = 1,45; \delta(\text{CH}_2) = 1,57;$ $\epsilon(\text{CH}_2) = 3,14; \eta(\text{NH}) = 7,09$
	Amide	6,97; 7,26	-	-	-

### Second cyclic peptide :







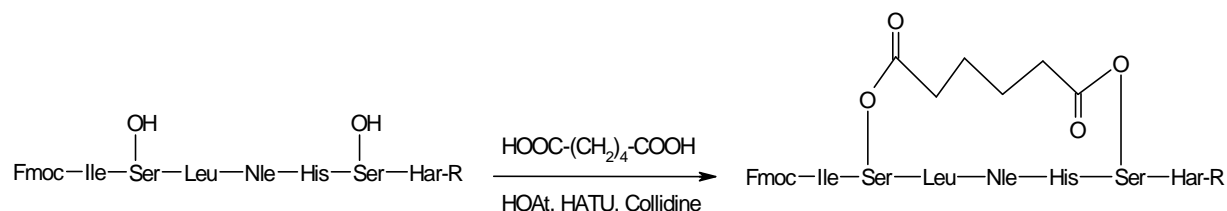
The resin was swelled with two 30 min cycles in DMF and then the first amino acid was coupled to resin following this workplane.

	[g/mL]	PM [g/mol]	mmol	eq.	Amount
<b>Resin Rink Amide MBHA</b>			<b>0,076</b>	1	<b>105 mg</b>
<b>Cleavage PIP 20% in DMF (45 minutes)</b>					<b>3 mL</b>
<b>Fmoc-Har(Pbf)-OH</b>		<b>648,8</b>	<b>0,304</b>	4	<b>192,7 mg</b>
<b>HOAt</b>		<b>136,2</b>	<b>0,304</b>	4	<b>41,4 mg</b>
<b>HATU</b>		<b>380,0</b>	<b>0,304</b>	4	<b>115,5 mg</b>
<b>Collidine</b>	<b>0,92</b>	<b>121,2</b>	<b>0,608</b>	8	<b>80 µL</b>
<b>DMF</b>					<b>2 mL</b>
<b>Time = 2 hours</b>					
<b>Cleavage PIP 20% in DMF (45 minutes)</b>					<b>3 mL</b>
<b>Fmoc-Ser(OTrt)-OH</b>		<b>569,7</b>	<b>0,304</b>	4	<b>173,2 mg</b>
<b>HOBt</b>		<b>135,3</b>	<b>0,304</b>	4	<b>41,1 mg</b>
<b>HBTU</b>		<b>379,1</b>	<b>0,304</b>	4	<b>115,2 mg</b>
<b>DIPEA</b>	<b>0,72</b>	<b>129,4</b>	<b>0,608</b>	8	<b>109 µL</b>
<b>DMF</b>					<b>2 mL</b>
<b>Time = 2 hours</b>					
<b>Cleavage PIP 20% in DMF (45 minutes)</b>					<b>3 mL</b>

	[g/mL]	PM [g/mol]	mmol	eq.	Amount
<b>Fmoc-His(Boc)-OPfp</b>		<b>643,5</b>	<b>0,304</b>	4	<b>195,6 mg</b>
<b>HOBt</b>		<b>135,3</b>	<b>0,304</b>	4	<b>41,1 mg</b>
<b>DIPEA</b>	<b>0,72</b>	<b>129,4</b>	<b>0,608</b>	8	<b>109 µL</b>
<b>DMF</b>					<b>2 mL</b>
<i>Time = 2 hours</i>					
<i>Cleavage PIP 20% in DMF (45 minutes)</i>					<b>3 mL</b>
<b>Fmoc-Nle-OH</b>		<b>353,4</b>	<b>0,304</b>	4	<b>107,4 mg</b>
<b>HOBt</b>		<b>135,3</b>	<b>0,304</b>	4	<b>41,1 mg</b>
<b>HBTU</b>		<b>379,1</b>	<b>0,304</b>	4	<b>115,2 mg</b>
<b>DIPEA</b>	<b>0,72</b>	<b>129,4</b>	<b>0,608</b>	8	<b>109 µL</b>
<b>DMF</b>					<b>2 mL</b>
<i>Time = 2 hours</i>					
<i>Cleavage PIP 20% in DMF (45 minutes)</i>					<b>3 mL</b>
<b>Fmoc-Leu-OPfp</b>		<b>353,4</b>	<b>0,304</b>	4	<b>107,4 mg</b>
<b>HOBt</b>		<b>135,3</b>	<b>0,304</b>	4	<b>41,1 mg</b>
<b>DIPEA</b>	<b>0,72</b>	<b>129,4</b>	<b>0,608</b>	8	<b>109 µL</b>
<b>DMF</b>					<b>2 mL</b>
<i>Time = 2 hours</i>					
<i>Cleavage PIP 20% in DMF (45 minutes)</i>					<b>3 mL</b>
<b>Fmoc-Ser(OTrt)-OH</b>		<b>569,7</b>	<b>0,304</b>	4	<b>173,2 mg</b>
<b>HOBt</b>		<b>135,3</b>	<b>0,304</b>	4	<b>41,1 mg</b>
<b>HBTU</b>		<b>379,1</b>	<b>0,304</b>	4	<b>115,2 mg</b>
<b>DIPEA</b>	<b>0,72</b>	<b>129,4</b>	<b>0,608</b>	8	<b>109 µL</b>
<b>DMF</b>					<b>2 mL</b>
<i>Time = 2 hours</i>					
<i>Cleavage PIP 20% in DMF (45 minutes)</i>					<b>3 mL</b>
<b>Fmoc-Ile-OH</b>		<b>353,4</b>	<b>0,304</b>	4	<b>107,4 mg</b>
<b>HOBt</b>		<b>135,3</b>	<b>0,304</b>	4	<b>41,1 mg</b>
<b>HBTU</b>		<b>379,1</b>	<b>0,304</b>	4	<b>115,2 mg</b>
<b>DIPEA</b>	<b>0,72</b>	<b>129,4</b>	<b>0,608</b>	8	<b>109 µL</b>
<b>DMF</b>					<b>2 mL</b>
<i>Time = 2 hours</i>					
<i>TNBS test</i>					

After coupling Ile, a TNBS test was made to evaluate total acylation of free amine. Before finishing the solid phase synthesis, a small cleavage (5 mg of resin), in TFA : TIS : H<sub>2</sub>O 95 : 2,5 : 2,5 (v/v/v), was made to observe the purity of linear peptide to mass spectroscopy. Mass spectroscopy confirmed the correct linear peptide *Fmoc-Ile-Ser-Leu-Nle-His-Ser-Har-NH<sub>2</sub>*. A control in HPLC confirmed a good purity and allowed to control next cyclization. Before ciclyzation, protecting groups Trt of side chains of Ser were removed. The resin was pre-swelled in DCM and then, after filtration, an acid

labile cleavage mixture DCM :TFA:TIS (95:1: 5) was added and the resin was shaken for 2 min. The filtrated solvent was controlled on UV spot test to follow reaction. This step was repeated 20 times controlling the disappearing of UV adsorbance. Then, the dry resin was swelled in DMF/NMP 50/50 and the reaction of cyclization was made.



As reported in following table, a double coupling with adipic acid and reagents was made:

	[g/mL]	MW [g/mol]	mmol	eq	amount
<b>Resin-peptide</b>			<b>0,076</b>	<b>1</b>	
<b>adipic acid</b>		<b>146,2</b>	<b>0,053</b>	<b>0,7</b>	<b>7,7 mg</b>
<b>HOAt</b>		<b>136,1</b>	<b>0,426</b>	<b>5,6</b>	<b>58,0 mg</b>
<b>HATU</b>		<b>380</b>	<b>0,426</b>	<b>5,6</b>	<b>161,7 mg</b>
<b>Collidine</b>	<b>0,92</b>	<b>121,2</b>	<b>0,775</b>	<b>10,2</b>	<b>102 µL</b>
<b>DMF/DMP 50/50 v/v</b>					<b>1 mL</b>
<b>Time for a single coupling = 2 hours</b>					

A small cleavage was runned in order to test reaction in mass spectroscopy and in HPLC ( $t_R = 26$  min). The resin was swelled again in DMF and the synthesis was concluded following normal SPPS protocol.

	[g/mL]	PM [g/mol]	mmol	eq.	Amount
<b>cleavage PIP 20% in DMF (45 minutes)</b>					<b>3 mL</b>
<b>Fmoc-Glu(OtBu)-OPfp</b>		<b>591,5</b>	<b>0,304</b>	<b>4</b>	<b>179,8 mg</b>
<b>HOBt</b>		<b>135,3</b>	<b>0,304</b>	<b>4</b>	<b>41,1 mg</b>
<b>DIPEA</b>	<b>0,72</b>	<b>129,4</b>	<b>0,608</b>	<b>8</b>	<b>109 µL</b>
<b>DMF</b>					<b>2 mL</b>
<b>Time = 2 ore</b>					
<b>cleavage PIP 20% in DMF (45 minutes)</b>					<b>3 mL</b>
<b>Fmoc-Aib-OH</b>		<b>325,4</b>	<b>0,304</b>	<b>4</b>	<b>98,9 mg</b>
<b>HOAt</b>		<b>136,2</b>	<b>0,304</b>	<b>4</b>	<b>41,1 mg</b>
<b>HATU</b>		<b>380,0</b>	<b>0,304</b>	<b>4</b>	<b>115,5 mg</b>
<b>Collidine</b>	<b>0,92</b>	<b>121,2</b>	<b>0,608</b>	<b>8</b>	<b>80 µL</b>
<b>DMF</b>					<b>2 mL</b>
<b>Time = double coupling</b>					

	[g/mL]	PM [g/mol]	mmol	eq.	Amount
<i>cleavage PIP 20% in DMF (45 minutes)</i>					<b>3 mL</b>
<b>Fmoc-Val-OH</b>		<b>619,7</b>	<b>0,304</b>	4	<b>188,4 mg</b>
<b>HOAt</b>		<b>136,2</b>	<b>0,304</b>	4	<b>41,1 mg</b>
<b>HATU</b>		<b>380,0</b>	<b>0,304</b>	4	<b>115,5 mg</b>
<b>Collidine</b>	<b>0,92</b>	<b>121,2</b>	<b>0,608</b>	8	<b>80 <math>\mu</math>L</b>
<b>DMF</b>					<b>2 mL</b>
<i>Time = double coupling</i>					
<i>cleavage PIP 20% in DMF (45 minutes)</i>					<b>3 mL</b>
<b>Boc-Aib-OH</b>		<b>203,2</b>	<b>0,304</b>	4	<b>61,8 mg</b>
<b>HOAt</b>		<b>136,2</b>	<b>0,304</b>	4	<b>41,1 mg</b>
<b>HATU</b>		<b>380,0</b>	<b>0,304</b>	4	<b>115,5 mg</b>
<b>Collidine</b>	<b>0,92</b>	<b>121,2</b>	<b>0,608</b>	8	<b>80 <math>\mu</math>L</b>
<b>DMF</b>					<b>2 mL</b>
<i>Time = double coupling</i>					

Peptide Cleavage and Purification. The resin was treated with a solution of TFA/EDT/TIS/water (94:2.5:1:2.5 v/v/v/v) at room temperature for 2h. After filtration, the filtrate was concentrated under nitrogen and precipitated with methyl tert-butyl ether. Peptide purification was performed by reversed-phase HPLC on Vydac C<sub>18</sub> (218TP510) column. The peptide homogeneity (>95%) was determined by analytical HPLC using the same solvents with a gradient of 10-35 % (v/v) acetonitrile over 15 min. Analogue: RT=18.8 min; yield after purification and lyophilization was 6.9%.

Peptide content determined by UV methodology was 63%.

Chemical Shift for second cyclic peptide of PTH: conc: 2.43 mM, T=298 K, in solution water/TFE-d<sub>3</sub> 20%.

AA	$\delta$ NH	$\delta$ H <sub><math>\alpha</math></sub>	$\delta$ H <sub><math>\beta</math></sub>	$\delta$
1   Aib	-	-	1,53; 1,48	-
2   Val	7,93	3,93	2,16	$\gamma$ (CH <sub>3</sub> ) = 1,06
3   Aib	8,48	-	1,53; 1,48	-
4   Glu	7,89	3,98	2,20; 2,06	$\gamma$ (CH <sub>2</sub> ) = 2,62; 2,45
5   Ile	7,66	3,82	2,02	$\gamma$ (CH) = 1,70; $\delta$ (CH <sub>2</sub> ) = 1,29; $\gamma$ (CH <sub>3</sub> ) = 0,97; $\epsilon$ (CH <sub>3</sub> ) = 0,90
6   Ser	7,95	4,66	4,35	-
Adipic Bridge	-	2,60; 2,30	1,75	$\gamma$ = 1,42; 0,95; $\delta$ = 2,30
7   Leu	8,07	4,02		$\gamma$ (CH) = ; $\delta$ (CH <sub>3</sub> ) =

8	Nle	8,38	3,99	1,94; 1,85	$\gamma(\text{CH}_2) = 1,51$ ; $\delta(\text{CH}_2) = 1,33$ ; $\epsilon(\text{CH}_2) = 0,87$
9	His	8,13	4,48	3,53; 3,47	$\text{H}^2 = 8,57$ ; $\text{H}^4 = 7,41$
10	Ser	7,98	4,85	4,40	-
11	Har	7,85	4,22	1,98; 1,88	$\gamma(\text{CH}_2) = 1,63$ ; $\delta(\text{CH}_2) = 1,50$ ; $\epsilon(\text{CH}_2) = 3,20$ ; $\eta(\text{NH}) = 7,13$
	Amide	7,03; 7,28	-	-	-

### Synthesis of Cyclopeptides in backbone.

**Synthesis of oNsHN-Ile-OMe<sup>10</sup>:** Methyl protected amino acid HCl·H<sub>2</sub>N-Ile-OMe (1g, 0.0055 mol, 1 eq.) was reacted with ortho-nitrobenzenesulfonyl chloride (1.34g, 0.00605 mol, 1.1 eq.) and pyridine (0.97 ml, 0.012 mol, 2.2 eq.) in dichloromethane (20 ml) to provide the corresponding sulfonamides. The reaction mixture was controlled by TLC (7:3 light petroleum ether: ethyl acetate). The reaction was stirred overnight. The solvent was evaporated and the crude material was dissolved in ethyl acetate. The organic layer was washed with KHSO<sub>4</sub> 10% (x3), then with water, NaHCO<sub>3</sub> 10% (x3) and finally with water (x3). Then the crude product was purified on gravimetric column. The yield was 88.5%.

<sup>1</sup>H-NMR (300 MHz, CDCl<sub>3</sub>): ppm 8.1-7.6 (m, 4H, CHoNs), 6.8 (mb, 1H NH); 4.6 (mb, 1H H $\alpha$ ); 3.5 (s, 3H, CH<sub>3</sub>); 2.0-1.9 (mb, 1H); 1.8-1.6 (mb, 1H); 1.1-1.0 (mb, 1H); 1.0-0.8 (m; 6H).

**Synthesis of H<sub>2</sub>N-Nle-OMe:** SOCl<sub>2</sub> (2 ml) was added to 5 ml of MeOH at -10°C and then 2 g of H<sub>2</sub>N-Nle-OH were added. The mixture was warmed up to 50°C for 2h and then 1 ml was added at -10°C. The mixture was stirred overnight. The solvent was evaporated under vacuum and the residue was dissolved in water and NaHCO<sub>3</sub> was added to obtain a basic pH. Then the aqueous layer was extracted with ethyl ether (9x30ml) and then dried (MgSO<sub>4</sub>), filtered, and concentrated in vacuum obtaining an oil 79.2%.

<sup>1</sup>H-NMR (300 MHz, CDCl<sub>3</sub>): ppm 4.6 (mb, 1H H $\alpha$ ); 3.5 (s, 3H, CH<sub>3</sub>); 2.0-1.9 (mb, 1H); 1.8-1.6 (mb, 1H); 1.4-1.2 (mb, 4H); 1.0-0.8 (t; 3H).

**Synthesis of oNsHN-Nle-OMe:** Methyl protected amino acid H<sub>2</sub>N-Nle-OMe (1.75g, 0.012 mol, 1 eq.) was reacted with ortho-nitrobenzenesulfonyl chloride (2.67g, 0.012 mol, 1 eq.) and pyridine (0.97 ml, 0.012 mol, 1 eq.) in dichloromethane (60 ml) to provide the corresponding sulfonamides. The reaction was controlled by TLC (7:3 light petroleum ether: ethyl acetate). The reaction mixture was stirred overnight. The solvent was evaporated and the crude material was dissolved in ethyl acetate. The organic layer was washed with KHSO<sub>4</sub> 10% (x3), then with water, NaHCO<sub>3</sub> 10% (x3) and finally with water (x3). Then the crude product was purified on gravimetric column. The yield was 81.4%.

<sup>1</sup>H-NMR (300 MHz, CDCl<sub>3</sub>): ppm 8.1-7.6 (m, 4H, CHoNs), 6.8 (mb, 1H NH); 4.6 (mb, 1H H $\alpha$ ); 3.5 (s, 3H, CH<sub>3</sub>); 2.0-1.9 (mb, 1H); 1.8-1.6 (mb, 1H); 1.4-1.2 (mb, 4H); 1.0-0.8 (t; 3H).

**Synthesis of oNs-N(Allyl)-Ile-OMe:** Allyl bromide (0.39 ml, 4.60 mmol, 1.85 eq.) was added to a solution of oNs-Ile-OMe (0.83 g, 2.5 mmol, 1 eq.) and K<sub>2</sub>CO<sub>3</sub> (0.69 g, 5.01 mmol, 2 eq.) in dry DMF (15 ml). The mixture was stirred overnight, and then poured into water (15 mL). The aqueous layer was extracted with ether (3 x 30 mL) and the combined organic layers were dried (MgSO<sub>4</sub>), filtered, and concentrated in vacuum obtaining a pale yellow solid. MALDI Mass: 370 Da calcd, 393.2 Da [M+Na<sup>+</sup>] and 409.1 [M+K<sup>+</sup>]. The yield was 90%.

<sup>1</sup>H NMR (300 MHz, CDCl<sub>3</sub>): ppm 8.0 (m, 1H), 7.8-7.4(m, 3H); 5.85 (ddt, 1H); 5.2-5.0 (dd, 2H), 4.30 (dd, 1H); 4.2-3.9 (dd, AB pattern, 2H); 3.5 (s, 3H); 2.0-1.8 (mb, 1H); 1.7-1.4 (mb, 1H); 1.2-1.0 (mb, 1H); 0.9-0.8 (mb, 6H).

**Synthesis of oNs-N(Allyl)-Nle-OMe:** Allyl bromide (0.39 ml, 4.60 mmol, 1.85 eq.) was added to a solution of oNs-Nle-OMe (0.83 g, 2.5 mmol, 1 eq.) and K<sub>2</sub>CO<sub>3</sub> (0.69 g, 5.01 mmol, 2 eq.) in dry DMF (15 ml). The mixture was stirred overnight, and then poured into water (15 mL). The aqueous layer was extracted with ether (3 x 30 mL) and the combined organic layers were dried (MgSO<sub>4</sub>), filtered, and concentrated in vacuum obtaining a pale yellow solid. MALDI Mass: 370 Da calcd, 393.2 Da [M+Na<sup>+</sup>] and 409.1 [M+K<sup>+</sup>]. The yield was 90%.

<sup>1</sup>H NMR (300 MHz, CDCl<sub>3</sub>): ppm 8.0 (m, 1H), 7.8-7.4(m, 3H); 5.85 (ddt, 1H); 5.2-5.0 (dd, 2H), 4.60 (dd, 1H); 4.2-4.1 (dd, AB pattern, 1H); 3.9-3.8 (dd, AB pattern, 1H); 3.5 (s, 3H); 2.0-1.9 (mb, 1H); 1.8-1.5 (mb, 1H); 1.4-1.2 (mb, 4H); 0.9-0.8 (mb, 3H).

**Synthesis of oNs-N(Allyl)-Ile-OH:** 1.33 ml of a solution 2M of LiOH were added to oNs-N(Allyl)-Ile-OMe (900 mg, 2.43 mmol, 1 eq) in 1 ml MeOH. The mixture was stirred overnight. The reaction was controlled by TLC (light petroleum ether/ethyl acetate 5/5). 1.1 eq (1.33 ml) of LiOH were added. After a week, MeOH was evaporated under vacuum and the residue was acidified. The aqueous layer was extracted with ethyl acetate and the organic layers collected were washed with water and brine, dried (MgSO<sub>4</sub>), filtered, and concentrated in vacuum obtaining yellow oil. MALDI Mass: 356 Da calcd, 379.2 Da [M+Na<sup>+</sup>] and 395.1 [M+K<sup>+</sup>]. The yield was 75%.

<sup>1</sup>H NMR (300 MHz, CDCl<sub>3</sub>): ppm 8.0 (m, 1H), 7.8-7.4(m, 3H); 5.85 (ddt, 1H); 5.2-5.0 (dd dd, 2H), 4.30 (dd dd, 1H); 4.2-3.9 (dd dd, AB pattern, 2H); 2.0-1.8 (mb, 1H); 1.7-1.4 (mb md, 1H); 1.2-1.0 (mb, 1H); 0.9-0.8 (md mb, 6H).

**Synthesis of oNs-N(Allyl)-Nle-OH:** 1.33 ml of a solution 2M of NaOH were added to oNs-N(Allyl)-Nle-OMe (900 mg, 2.43 mmol, 1 eq) in 1 ml MeOH. The mixture was stirred overnight. The reaction was controlled by TLC (light petroleum ether/ethyl acetate 5/5). After 3 days, MeOH was evaporated under vacuum and the residue was acidified. The aqueous layer was extracted with ethyl acetate and the organic layers collected were washed with water and brine, dried (MgSO<sub>4</sub>), filtered, and concentrated in vacuum obtaining yellow oil. MALDI Mass: 356 Da calcd, 379.2 Da [M+Na<sup>+</sup>] and 395.1 [M+K<sup>+</sup>]. The yield was 75%.

<sup>1</sup>H NMR (300 MHz, CDCl<sub>3</sub>): ppm 8.0 (m, 1H), 7.8-7.4(m, 3H); 5.85 (ddt, 1H); 5.2-5.0 (dd, 2H), 4.30 (q, 1H); 4.2-3.9 (dd, AB pattern, 2H); 2.0-1.8 (mb, 1H); 1.7-1.4 (mb, 1H); 1.2-1.0 (mb, 1H); 0.9-0.8 (mb, 6H).

**Synthesis of oNs-N(Allyl)-Ile-OH (I):** oNs-N(Allyl)-Ile-OMe (200 mg, 0.54 mmol, 1 eq.) was dissolved in acetone and phosphate buffer 0.1 M at pH 7.2. 1 mg of Esterase BS3 was added to the mixture. To keep in solution the amino acid, acetone was added

to up to a 30% content. After 3 days, 1 mg of Esterase BS3 was added. The reaction was controlled by TLC TLC (light petroleum ether/ethyl acetate 5/5) no product was obtained. Aceton was evaporated and solution was acidified with some drops of HCl. The aqueous layers were extracted with ethyl acetate, dried (MgSO<sub>4</sub>), filtered, and concentrated in vacuum to obtain starting material.

**Synthesis of oNs-N(Allyl)-Ile-OH (II):** oNs-N(Allyl)-Ile-OMe (200 mg, 0.54 mmol, 1 eq.) was dissolved in MeOH and phosphate buffer 0.1 M at pH 7.2. 10 mg of Esterase BS3 were added to the mixture. To keep in solution the amino acid, to the mixture MeOH was added up to 90%. The reaction was stirred at 37°C for a week. The reaction was controlled by TLC (light petroleum ether/ethyl acetate 5/5). No traduct was obtained. MeOH was evaporated and solution was acidified with some drops of HCl. The aqueous layers were extracted with ethyl acetate, dried (MgSO<sub>4</sub>), filtered, and concentrated in vacuum to obtain starting material.

**Synthesis of oNs-NH-Ile-OtBu:** Methyl protected amino acid HCl·H<sub>2</sub>N-Ile-OtBu (1 g, 0.0045 mol, 1 eq.) was treated with ortho-nitrobenzenesulfonyl chloride (0.95g, 0.00425 mol, 0.95 eq.) and pyridine (0.72 ml, 0.0089 mol, 2.0 eq.) in dichloromethane (25 ml) to form the corresponding sulfonamides. The reaction mixture was controlled by TLC (8:2 light petrolium ether: ethyl acetate). The mixture was stirred overnight. The reaction was diluited with DCM and extracted with HCl 10% and then washed with water and brine. The organic layer was dried (MgSO<sub>4</sub>), filtered, and concentrated in vacuum obtaining a crude product which was purified on gravimetric column. The yield was 27.5%.

<sup>1</sup>H-NMR (300 MHz, CDCl<sub>3</sub>): ppm 8.1-7.6 (m, 4H, CHoNs), 6.8 (mb, 1H NH); 4.6 (mb, 1H H $\alpha$ ); 2.0-1.9 (mb, 1H); 1.8-1.6 (mb, 1H); 1.1-1.0 (mb, 1H); 1.0-0.8 (m; 15H).

**Synthesis of oNs-N(Allyl)-Ile-OtBu:** Allyl bromide (0.25 ml, 2.88 mmol, 2.40 eq.) was added to a solution of oNsNH-Ile-OtBu (0.44 g, 1.2 mmol, 1 eq.) and K<sub>2</sub>CO<sub>3</sub> (0.33 g, 2.4 mmol, 2 eq.) in dry DMF (5 ml). The mixture was stirred overnight, and then poured into water (5 mL). The aqueous layer was extracted with ether (5 x 30 mL) and the



combined organic layers were dried (MgSO<sub>4</sub>), filtered, and concentrated in vacuum obtaining pale yellow oil. The yield was 75%.

<sup>1</sup>H NMR (300 MHz, CDCl<sub>3</sub>): ppm 8.0 (m, 1H), 7.8-7.4(m, 3H); 5.85 (ddt, 1H); 5.2-5.0 (dd, 2H), 4.30 (dd, 1H); 4.2-3.9 (dd, AB pattern, 2H); 2.0-1.8 (mb, 1H); 1.7-1.4 (mb, 1H); 1.2-1.0 (mb, 1H); 0.9-0.8 (mb, 15H).

**Synthesis of oNs-N(Allyl)-Ile-OH:** oNs-N(Allyl)-Ile-OtBu (410g, 1.0mol, 1 eq) was dissolved in 6 ml TFA/DCM 1/5. The mixture was stirred and controlled on TLC (light petroleum ether/ethyl acetate 8/2). After 3 h, the reaction was complete. A yellow oil was obtained. The yield was quantitative.

	[g/mL]	MW[g/mol]	mmol	eq.	Amount
<b>Resin Rink Amide MBHA</b>			<b>0,076</b>	1	<b>105 mg</b>
<i>Cleavage PIP 20% in DMF (45 minutes)</i>					<b>3 mL</b>
<b>Fmoc-Har(Pbf)-OH</b>		<b>648,8</b>	<b>0,304</b>	4	<b>192,7 mg</b>
<b>HOAt</b>		<b>136,2</b>	<b>0,304</b>	4	<b>41,4 mg</b>
<b>HATU</b>		<b>380,0</b>	<b>0,304</b>	4	<b>115,5 mg</b>
<b>Collidine</b>	<b>0,92</b>	<b>121,2</b>	<b>0,608</b>	8	<b>80 µL</b>
<b>DMF</b>					<b>2 mL</b>
<i>Time = 2 hours</i>					
<i>Cleavage PIP 20% in DMF (45 minutes)</i>					<b>3 mL</b>
<b>Fmoc-Gln(Trt)-OH</b>		<b>610,7</b>	<b>0,304</b>	4	<b>152,7 mg</b>
<b>HOBt</b>		<b>135,3</b>	<b>0,304</b>	4	<b>41,1 mg</b>
<b>HBTU</b>		<b>379,1</b>	<b>0,304</b>	4	<b>115,2 mg</b>
<b>DIPEA</b>	<b>0,72</b>	<b>129,4</b>	<b>0,608</b>	8	<b>109 µL</b>
<b>DMF</b>					<b>2 mL</b>
<i>Time = 2 hours</i>					
<i>Cleavage PIP 20% in DMF (45 minutes)</i>					<b>3 mL</b>
<b>Fmoc-His(Trt)-OH</b>		<b>619,7</b>	<b>0,304</b>	4	<b>155.0 mg</b>
<b>HOBt</b>		<b>135,3</b>	<b>0,304</b>	4	<b>41,1 mg</b>
<b>HBTU</b>		<b>379,8</b>	<b>0,304</b>	4	<b>115.2 mg</b>
<b>DIPEA</b>	<b>0,72</b>	<b>129,4</b>	<b>0,608</b>	8	<b>109 µL</b>
<b>DMF</b>					<b>2 mL</b>
<i>Time = 2 hours</i>					
<i>Cleavage PIP 20% in DMF (45 minutes)</i>					<b>3 mL</b>

	[g/mL]	MW[g/mol]	mmol	eq.	Amount
oNsN(AlI)NleOH		356,3	0,304	4	108,3 mg
HOBt		135,1	0,304	4	41.1 mg
HBTU		379,8	0,304	4	115.2 mg
DIPEA (d=0,76 g/ml)	0.72	129,2	0,608	8	109µl
DMF					2 ml
<i>Cleavage</i>					
Sodium thiophenolate		132	1,46	20	1.52 mg
4-Methylthiophenol		124	0,380	5	47.0 mg
DMF					2 ml
Fmoc-Leu-OH		353,4	0,304	4	107,4 mg
HOBt		135,3	0,304	4	41,1 mg
HBTU		379,8	0,304	4	115.2 mg
DIPEA	0,72	129,4	0,608	8	109 µL
DMF					2 mL
<i>Time = 1 hours</i>					
<i>Cleavage PIP 20% in DMF (45 minutes)</i>					3 mL
Fmoc-Gln(Trt)-OH		610.7	0,304	4	152,7 mg
HOBt		135,3	0,304	4	41,1 mg
HBTU		379,1	0,304	4	115,2 mg
DIPEA	0,72	129,4	0,608	8	109 µL
DMF					2 mL
<i>Time = 1 hours</i>					
<i>Cleavage PIP 20% in DMF (45 minues)</i>					3 mL
oNsN(Allyl)-Ile-OH		356,3	0,304	4	108,3 mg
HOBt		135,1	0,304	4	41.1 mg
HBTU		379,8	0,304	4	115.2 mg
DIPEA	0,72	129,2	0,608	8	109µl
DMF					2 ml
<i>Time = 2 hours</i>					
<i>Kaiser test</i>					

**Cyclization in backbone through ring closing metathesis using Hoveyda-Grubbs catalyst.**

**First method:** 30 mg (0.022 mmol) of resin-peptide was dried under vacuum overnight and then swelled in 1.0 ml of anhydrous 1, 2-dichloroethane (DCE) under a nitrogen atmosphere for 30 min. The Hoveyda-Grubbs catalyst (7 mg, 0.011mmol) in 0.5 mL of DCE were added, and the mixture was stirred at 60°C. After 24 h, the resin was washed with DCM, 10% 1, 3-bis(diphenylphosphino)propane in DCM, DCM and MeOH. After drying overnight, the resin was cleaved and the crude peptide was collected and analysed by MALDI mass. The correct peptide was not found.

**Second method:** 30 mg (0.022 mmol) of resin-peptide was dried under vacuum overnight and then swelled in 1.0 ml of anhydrous 1, 2-dichloroethane (DCE) in the presence of Hoveyda-Grubbs catalyst (0.5 equiv) in a glass microwave reaction vessel<sup>11</sup>. The vessel was sealed and put in a microwave reactor (CEM Discover) and radiated (first time: 300 W maximum power, 200°C, ramp 5 min, hold 10 min; second time: 300 W maximum power, 150°C, ramp 5 min, hold 10 min ). Then the resin was washed with DCM, 10% 1, 3-bis(diphenylphosphino)propane in DCM, DCM and MeOH. After drying overnight, the resin was cleaved and the crude peptide was collected and analysed by MALDI mass. The correct peptide was not found.

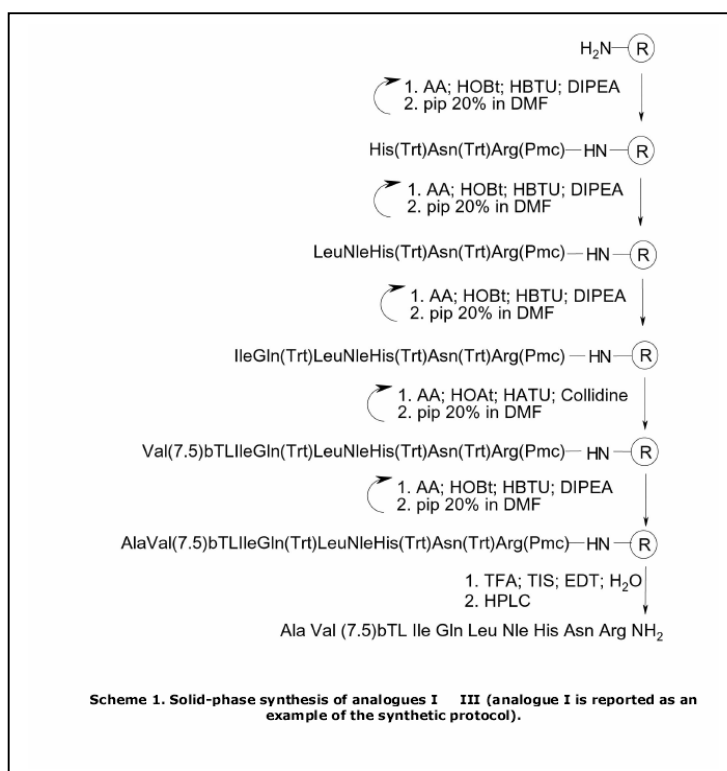
### **Example of Peptidomimetic of PTH (1-11)**

The solid-phase synthesis of the PTH(1-11) analogues is outlined in Scheme 1. Only analogue I is reported because the synthetic protocol is the same for other ones. The protecting groups of the side-chains were compatible with the Fmoc Strategy. This choice allowed the use of Rink Amide MBHA Resin as solid support.

The bicyclic lactams 7,5 bTL were prepared<sup>12</sup> and protected at the free amino acid as fluorenyl carbamate, to be compatible with Fmoc Strategy. The first amino acid was anchored to the resin by protocol HBTU/HOBt/DIPEA. Deprotection of amino groups was achieved under standard conditions, with 20% piperidine solution in NMP. The next amino acids were coupled in the same way. For the coupling of 7,5 bTL the more potent L. Carpino's condensation system HATU/HOAt/2,4,6 Collidine<sup>13</sup> was used. Because of 7,5 bTL's high synthetic value, the lactam was used in a stoichiometric amount with respect to the resin<sup>14</sup> and to improve the yield a longer reaction time was used. After end-capping with Ac<sub>2</sub>O, the next amino acid was introduced on the sterically hindered free amino group of the lactam using the same system and a large excess of reagents.

**Peptide Deprotection, Cleavage from the Resin and Purification.** The resin-bound peptide was treated with a deprotection and cleavage solution of TFA/EDT/TIS/water (94:2.5:1:2.5 v/v/v/v) at room temperature for 2h. After filtration, the filtrate was concentrated under nitrogen and precipitated with methyl tert-butyl ether. Peptide purification was performed by reverse phase HPLC on a Vydac C18 (218TP510)

column. The peptide homogeneity (>95%) was determined by analytical HPLC using the same solvents with a linear gradient of 10-35 % (v/v) acetonitrile over 15 min. Analogue I: RT=13.27 min; yield after purification and lyophilization : 10%; Mass (ESI-MS) (M+H) 1321.7 m/z. Analogue II: RT=13.70 min; yield after purification and lyophilization : 11%; Mass (ESI-MS) (M+H) 1298 m/z. Analogue III: RT=13.61 min; yield after purification and lyophilization : 5%; Mass (ESI-MS) (M+H) 1286.7 m/z.



### Analogue I

Chemical Shift for [(5,7)bTL<sup>3,4</sup> Nle<sup>8</sup>, Arg<sup>11</sup>]-rPTH(1-11)NH<sub>2</sub>, in conc: 1.9 mM, T=298 K, in solution water/TFE-d<sub>3</sub> 20%.

		δNH	δα	δβ	δ
1	Ala	-	4.155	1.548	-
2	Val	8.343	4.389	2.069	γ <sub>CH3</sub> = 0.969
3	(5,7)bTL	8.870	5.352	H <sup>7</sup> = 4.132, H <sup>8</sup> = 4.140, H <sup>9</sup> = 4.086 H <sup>9a</sup> = 5.819	
4	(5,7)bTL	-	4.614	3.556, 3.417	-
5	Ile	9.369	3.845	1.768	γ <sub>CH2</sub> = 1.466, 1.288 γ <sub>CH3</sub> & δ <sub>CH3</sub> = 0.907
6	Gln	7.431	4.078	2.357, ~2.08	γ <sub>CH2</sub> = 2.436 δ <sub>NH2</sub> = 7.560, 6.909
7	Leu	8.005	4.108	1.805, 1.671	γ <sub>CH</sub> = 1.671 δ <sub>CH3</sub> = 0.890, 0.900

8	Nle	7.865	4.011	1.785	$\gamma_{\text{CH}_2} = 1.419, 1.272$ $\gamma_{\text{CH}_3} = 0.842$
9	His	7.990	4.548	3.395, 3.260	$H^2 = 8.616$ $H^4 = 7.365$
10	Asn	8.157	4.673	2.916, 2.879	$\delta_{\text{NH}_2} = 7.570, 6.885$
11	Arg	8.042	4.292	1.958, 1.843	$\gamma_{\text{CH}_2} = 1.749$ $\delta_{\text{CH}_2} = 3.214$ $\epsilon_{\text{NH}} = 7.224$ NH-term = 7.413, 7.081

### Analogue II

Chemical Shift for [(5,7)bTL<sup>6,7</sup> Nle<sup>8</sup>, Arg<sup>11</sup>]-rPTH(1-11)NH<sub>2</sub>, in conc: 1.9 mM, T=298 K, in solution water/TFE-d<sub>3</sub> 20%.

AA	$\delta_{\text{NH}}$	$\delta_{\alpha}$	$\delta_{\beta}$	$\delta$
1 Ala	-	4.171	1.566	-
2 Val	8.494	4.221	2.118	$\gamma_{\text{CH}_3} = 0.987$
3 Ser	8.375	4.502	3.886, 3.844	-
4 Glu	8.430	4.414	2.119, 1.990	$\gamma_{\text{CH}_2} = 2.420$
5 Ile	8.103	4.435	1.870	$\gamma_{\text{CH}_2} = 1.529, 1.198$ $\gamma_{\text{CH}_3} = 0.932$ $\delta_{\text{CH}_3} = 0.855$
6 (5,7)bTL	8.423	5.373	$H^7 = 4.107, H^8 = 4.172, H^9 = 4.062$ $H^{9a} = 5.687$	
7 (5,7)bTL	-	4.699	3.426, 3.477	-
8 Nle	8.839	4.132	1.687, 1.545	$\gamma_{\text{CH}_2} = 1.273$ $\gamma_{\text{CH}_3} = 0.884$
9 His	7.780	4.776	3.377, 3.151	$H^2 = 7.359$ $H^4 = 8.621$
10 Asn	8.294	4.790	2.929	$\delta_{\text{NH}_2} = 7.519, 6.791$
11 Arg	8.174	4.349	1.941, 1.791	$\gamma_{\text{CH}_2} = 1.678$ $\delta_{\text{CH}_2} = 3.228$ $\epsilon_{\text{NH}} = 7.224$ NH-term = 7.579, 7.062

### Analogue III

Chemical Shift for [Nle<sup>8</sup>, (5,7)bTL<sup>9,10</sup> Arg<sup>11</sup>]-rPTH(1-11)NH<sub>2</sub>, in conc: 1.9 mM, T=298 K, in solution water/TFE-d<sub>3</sub> 20%.

AA	$\delta_{\text{NH}}$	$\delta_{\alpha}$	$\delta_{\beta}$	$\delta$
1 Ala	-	4.164	1.558	-
2 Val	8.470	4.234	2.111	$\gamma_{\text{CH}_3} = 0.983$
3 Ser	8.367	4.526	3.941, 3.872	-
4 Glu	8.499	4.344	2.133, 2.032	$\gamma_{\text{CH}_2} = 2.454$
5 Ile	8.010	4.079	1.867	$\gamma_{\text{CH}_2} = 1.497, 1.236$ $\gamma_{\text{CH}_3} = 0.920$ $\delta_{\text{CH}_3} = 0.890$

6	Gln	8.216	4.308	2.083	$\gamma_{\text{CH}_2} = 2.380$ $\delta_{\text{NH}_2} = 7.516, 6.807$
7	Leu	8.034	4.373	1.722, 1.653	$\gamma_{\text{CH}_2} = 0.939$ $\delta_{\text{CH}_3} = 0.881$
8	Nle	7.956	4.381	1.869, 1.759	$\gamma_{\text{CH}_2} = 1.399, 1.335$ $\delta_{\text{CH}_2} = 0.890$
9	(5,7)bTL	8.037	5.329	$\text{H}^7 = 4.093, \text{H}^8 = 4.175, \text{H}^9 = 4.034$ $\text{H}^{9a} = 5.715$	
10	(5,7)bTL	-	4.65	3.755, 3.658	-
11	Arg	8.734	4.246	1.943	$\gamma_{\text{CH}_2} = 1.672$ $\delta_{\text{CH}_2} = 3.218$ $\text{NH}_2\text{-term} = 7.232/7.081$

## REFERENCES

- <sup>1</sup> Yang, J. T.; Wu, C. S.; Martinez, H. M. *Methods in Enzymology* 1986, 130, 208-269
- <sup>2</sup> Rance, M.; Sorensen, O.W.; Bodenhausen, G.; Wagner, G.; Ernest, R.R.; Wuthrich, K. *Biochem. Biophys. Res. Comm.*, **1983**, 117, 479-485.
- <sup>3</sup> Bax, A.; Davis, D.G. *J. Magn. Reson.*, **1985**, 65, 355-360.
- <sup>4</sup> Griesinger, C.; Otting, G.; Wuthrich, K.; Ernst, R.R. *J. Am. Chem. Soc.* **1988**, 110, 7870-7872
- <sup>5</sup> Feichtinger K., Sings H. L., Baker T. J., Matthews K., Goodman M., *J. Org. Chem.* 1998, 63, 8432-8439
- <sup>6</sup> Gers T., Kunc D., Markowski P., Izdebski J., *Synthesis* 2004, 1, 37-42
- <sup>7</sup> Carpino L. A., El-Faham A., Albericio F. *J. Org. Chem.* 1995,60, 3561-3564; Carpino L. A., El-Faham A., *J. Org. Chem.*, Vol. 59, No. 4, 1994; Carpino L. A , *J. Am. Chem. Soc.*, 1993, 115, 4397-4398; Konig, W.; Geiger, R. *Ber. Dtsch. Chem. Ges.* 1970, 103,788.
- <sup>8</sup> Kruijtzter, J. A. W.; Hofmeyer, L. J. F.; Heerma, W.; Versluis, C.; Liskamp, R. M. *J. Chem. Eur. J.* 1998, 4, 1570
- <sup>9</sup> Uno T., Beausoleil E., Goldsmith R. A., Levine B. H., Zuckermann R. N., *Teth. Lett.* 1999, 40, 1475-1478
- <sup>10</sup> Chapman R. N.; Dimartino G., Arora P. S., 2004. *J. Am. Chem. Soc.*, 126, 12252
- <sup>11</sup> Dimartino, G., Wang, D., Chapman, R. N., Arora, P. S. *Org. Lett.* 2005, 7, 2389-2392.
- <sup>12</sup> Geyer A., Moser, F. *Eur. J. Org. Chem.*, 2000, 1113-1120
- <sup>13</sup> Carpino, L. A. *JACS*, 1993, 115, 4397, *JOC*, 1995, 60, 3561, *JOC*, 1994, 59, 695
- <sup>14</sup> L. Belvisi, A. Bernardi, A. Checchia, L. Manzoni, D. Potenza, C. Scolastico, M. Castorina, A. Cupelli, G. Giannini, P. Carminati, C. Pisano, *Org. Lett.* 2001, 7, 1001

## *APPENDIX A*

The following article is the result of these years of PhD course. We had the possibility to participate to the most important international meeting and symposia of peptides sciences. In these occasions we brought our contributions to find new peptidomimetics and possibility of solutions to conformational analysis. Our contributions are collected in the Proceeding Book of:

- 3<sup>rd</sup> International and 28<sup>th</sup> European Peptide Symposium – Bridge between Disciplines – Prague, Czech Republic, September 5 – 10, 2004
- 19<sup>th</sup> American Peptide Symposium – Understanding Biology using Peptides – S. Diego, California, U.S.A., June 18 – 23, 2005
- 1<sup>st</sup> European Conference on Chemistry for Life Sciences – Understanding the Chemical Mechanisms of Life – Rimini, Italy, October 4 – 8, 2005
- 29<sup>th</sup> European Peptide Symposium – Gdańsk – Poland – September 3 – 8, 2006
- 20<sup>th</sup> American Peptide Society Symposium – Peptide for Youth – Montréal, Quebec, Canada – June 26 – 30, 2007





# Structure–function relationship studies of PTH(1–11) analogues containing sterically hindered dipeptide mimetics

NEREO FIORI,<sup>a</sup> ANDREA CAPORALE,<sup>a</sup> ELISABETTA SCHIEVANO,<sup>a</sup> STEFANO MAMMI,<sup>a</sup> ARMIN GEYER,<sup>b</sup> PETER TREMMEL,<sup>b</sup> ANGELA WITTELSBERGER,<sup>c</sup> IWONA WOZNICA,<sup>c</sup> MICHAEL CHOREV<sup>d</sup> and EVARISTO PEGGION<sup>a\*</sup>

<sup>a</sup> University of Padova, Department of Chemical Sciences, Institute of Biomolecular Chemistry, CNR, Italy

<sup>b</sup> Philipps Universität, Marburg Fachbereich Chemie, Germany

<sup>c</sup> Tufts University School of Medicine, Department of Physiology, USA

<sup>d</sup> Harvard Medical School, Laboratory for Translational Research, USA

Received 2 March 2007; Revised 29 March 2007; Accepted 10 April 2007

**Abstract:** The *N*-terminal 1–34 fragment of parathyroid hormone (PTH) is fully active *in vitro* and *in vivo* and reproduces all biological responses characteristic of the native intact PTH. In order to develop safer and non-parenteral PTH-like bone anabolic agents, we have studied the effect of introducing conformationally constrained dipeptide mimetics into the *N*-terminal portion of PTH in an effort to generate miniaturized PTH-mimetics. To this end, we have synthesized and conformationally and biologically characterized PTH(1–11) analogues containing 3*R*-carboxy-6*S*-amino-7,5-bicyclic thiazolidinlactam (7,5-bTL), a rigidified dipeptide mimetic unit. The wild type sequence of PTH(1–11) is H-Ser-Val-Ser-Glu-Ile-Gln-Leu-Met-His-Asn-Leu-NH<sub>2</sub>. The following pseudo-undecapeptides were prepared: [Ala<sup>1</sup>, 7,5-bTL<sup>3,4</sup>, Nle<sup>8</sup>, Arg<sup>11</sup>]hPTH(1–11)NH<sub>2</sub> (**I**); [Ala<sup>1</sup>, 7,5-bTL<sup>6,7</sup>, Nle<sup>8</sup>, Arg<sup>11</sup>]hPTH(1–11)NH<sub>2</sub> (**II**); [Ala<sup>1</sup>, Nle<sup>8</sup>, 7,5-bTL<sup>9,10</sup>, Arg<sup>11</sup>]hPTH(1–11)NH<sub>2</sub> (**III**). In aqueous solution containing 20% TFE, only analogue **I** exhibited the typical CD pattern of the  $\alpha$ -helical conformation. NMR experiments and molecular dynamics calculations located the  $\alpha$ -helical stretch in the sequence Ile<sup>5</sup>-His<sup>9</sup>. The dipeptide mimetic unit 7,5-bTL induces a type III  $\beta$ -turn, occupying the positions *i* – 1 and *i* of the turn. Analogue **II** exhibited an equilibrium between a type I  $\beta$ -turn and an  $\alpha$ -helix, and analogue **III** did not show any ordered structure. Biological tests revealed poor activity for all analogues (EC<sub>50</sub> > 0.1 mM). Apparently, the relative side-chain orientation of Val<sup>2</sup>, Ile<sup>5</sup> and Met<sup>8</sup> can be critical for effective analogue-receptor interaction. Considering helicity as an essential property to obtain active PTH agonists, one must decorate the correctly positioned dipeptide mimetic azabicycloalkane scaffold with substitutions corresponding to the displaced amino acids. Copyright © 2007 European Peptide Society and John Wiley & Sons, Ltd.

Supplementary electronic material for this paper is available in Wiley InterScience at <http://www.interscience.wiley.com/jpages/1075-2617/suppmat/>

**Keywords:** PTH; NMR; peptide mimetics; molecular modeling

## INTRODUCTION

Parathyroid hormone (PTH) is an 84-amino-acid peptide responsible for the regulation of calcium homeostasis in the body extracellular fluids. These activities are mediated through interaction with its cognate receptor, PTH1R, a G-protein-coupled seven transmembrane domain-containing receptor (GPCR) of class B. The *N*-terminal (1–34) fragment of PTH is fully active *in vivo*, and reproduces all biological responses characteristic of the native intact PTH [1]. Clinical

studies have demonstrated that PTH(1–34) is a powerful bone anabolic agent capable of restoring bone mineral density. Recombinant human PTH(1–34) has been approved by FDA with the name of FORTEO (Teriparatide) to treat osteoporosis in postmenopausal women who are at high risk for fractures.

The prevailing view of the biologically relevant conformation of PTH(1–34) includes a flexible molecule with no tertiary structure. NMR analyses of PTH(1–34) analogues in a variety of polar and non-polar solvents suggest that the *N*-terminal portion of PTH, known to be responsible for receptor activation, contains a short  $\alpha$ -helical segment from Ser<sup>3</sup> to Lys<sup>13</sup>. This *N*-terminal helix is followed by a more stable C-terminal  $\alpha$ -helical segment (from Arg<sup>20</sup> to Val<sup>31</sup>), in which the principal receptor binding domain is located. These two helices are separated by two hinge-like motifs located around positions 12 and 19 [2]. Previous studies demonstrated that enhancement of the  $\alpha$ -helicity in the PTH(1–11) sequence (H-Ser-Val-Ser-Glu-Ile-Gln-Leu-Met-His-Asn-Leu-NH<sub>2</sub>) yielded potent PTH(1–11)NH<sub>2</sub> analogues [3–5]. On the basis of mutagenesis studies

Abbreviations: Aib,  $\alpha$ -amino butyric acid; Ac5c, amino-pentacyclo carboxylic acid; HBTU, 2-(1*H*-benzotriazole-1-yl)-1,1,3,3-tetramethyluronium hexafluorophosphate; HOBt, 1-hydroxybenzotriazole; DIPEA, diisopropylethyl amine; DMF, Dimethyl formamide; NMP, *N*-methyl pyrrolidone; HATU, 2-(1*H*-7-azabenzotriazole-1-yl)-1,1,3,3-tetramethyluronium hexafluorophosphate; HOAt, 1-hydroxy-7-azabenzotriazole; Ac<sub>2</sub>O, acetic anhydride; TFA, trifluoroacetic acid; TIS, triisopropylsilane; EDT, ethanedithiol; PBS, phosphate buffered saline; BSA, bovine serum albumin.

\* Correspondence to: E. Peggion, University of Padova, Department of Chemical Sciences, Institute of Biomolecular Chemistry, CNR, Italy; e-mail: evaristo.peggion@unipd.it

and on the position and shape of the binding sites for residues in position 2, 5 and 8, high helicity has been suggested to be essential for receptor activation [6,7]. Furthermore, location of residue 8 on the same face of the helix as Ile<sup>5</sup>, as well as the position of Val<sup>2</sup> projecting towards the third extracellular loop (EC3), has been hypothesized to be fundamental requirements for the activation of PTH1R [6].

This work provides useful new information on the requirements for PTH ligand bioactivity and on general aspects of peptide mimetic design work. We synthesized and biologically and conformationally characterized three PTH-mimetic molecules, all containing 3*R*-carboxy-6*S*-amino-7,5-bicyclic thiazolidinlactam (7,5-bTL) (Figure 1), a polyol dipeptide mimetic derived from a carbohydrate precursor [8] which can mimic hydroxyl amino acids: [Ala<sup>1</sup>, 7,5-bTL<sup>3,4</sup>, Nle<sup>8</sup>, Arg<sup>11</sup>] hPTH(1-11) NH<sub>2</sub> (**I**); [Ala<sup>1</sup>, 7,5-bTL<sup>6,7</sup>, Nle<sup>8</sup>, Arg<sup>11</sup>] hPTH(1-11) NH<sub>2</sub> (**II**); [Ala<sup>1</sup>, Nle<sup>8</sup>, 7,5-bTL<sup>9,10</sup>, Arg<sup>11</sup>] hPTH(1-11) NH<sub>2</sub> (**III**). Introduction of conformational constraints into peptides can improve their activity and receptor binding selectivity [9-11]. This approach, applied to PTH(1-11) has already been shown to yield compounds with enhanced activity [12].

The dipeptide mimetic was inserted in strategic positions, in order to leave the side chain of the essential residues 2, 5 and 8 unmodified. The replacement of Met<sup>8</sup> with Nle<sup>8</sup> is known to be well tolerated, producing no loss of binding affinity [13,] and prevents methionine oxidation, which would result in a decrease in the biological response [14]. The replacement of Leu<sup>11</sup> with Arg<sup>11</sup> is known to enhance autoactivation [15] in the PTH1R/[Arg<sup>11</sup>]PTH(1-11) tethered system, which lacks most of the extracellular *N*-terminal domain (N-ECD) of PTH(1-34) is essential for bioactivity. Moreover, the presence of Arg<sup>11</sup>/Har<sup>11</sup> turned some analogues of PTH(1-11) into potential agonists [12,16], while analogues of PTH truncated at position 10 displayed poor binding and low activity [17].

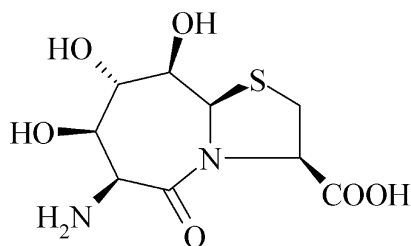


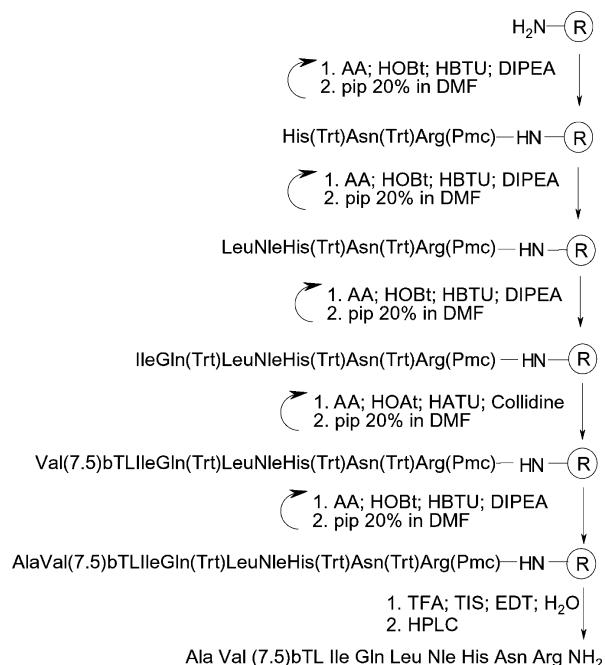
**Figure 1** Structure of the rigidified dipeptide mimetic unit derived from 3*R*-carboxy-6*S*-amino-7,5-bicyclic thiazolidinlactam (7,5-bTL).

## MATERIALS AND METHODS

### Synthesis

The solid-phase synthesis of [Ala<sup>1</sup>, 7,5-bTL<sup>3,4</sup>, Nle<sup>8</sup>, Arg<sup>11</sup>] hPTH(1-11)NH<sub>2</sub> (analogue **I**) is outlined in Scheme 1. The synthetic protocol for the other analogues is similar. The analogues were prepared using Fmoc methodology with Rink Amide MHBA resin (Novabiochem) (0.73 mmol/g loading) as a solid support [18]. The bicyclic lactam 7,5-bTL was prepared [8] and protected at the free amino group as fluorenyl carbamate. The first amino acid was anchored to the resin using the HBTU/HOBt/DIPEA protocol; the most common peptide coupling additive is HOBt, used either as a carbocation with another coupling agent or incorporated into a stand-alone reagent such as a uronium salt [19]. Such additions generally inhibit side reactions and reduce epimerization. In this case, we used HOBt as an auxiliary nucleophile. Deprotection of Fmoc from the  $\alpha$ -amino groups was achieved under standard conditions, with 20% piperidine solution in DMF. The following amino acids were coupled in the same way. The coupling of 7,5-bTL was accomplished with the more potent condensation reagent HATU/HOAt/2,4,6-collidine [20-22]. For reasons yet unclear, 2,4,6-collidine as a base appears to be particularly suitable for systems derived from HOAt [20-22]. Because of the high synthetic value of 7,5-bTL, it was used in a stoichiometric amount with respect to the resin [23], and a longer reaction time was used to improve the yield of incorporation. After end-capping with Ac<sub>2</sub>O, the next amino acid was introduced on the sterically hindered free amino group of the lactam using the same method and a large excess of reagents.

**Peptide deprotection, cleavage from the resin and purification.** The resin-bound peptide was treated with a deprotection and cleavage solution of TFA/EDT/TIS/water (94 : 2.5 : 1 : 2.5



**Scheme 1** Solid-phase synthesis of analogues **I-III** (analogue **I** is reported as an example of the synthetic protocol).

v/v/v/v) at room temperature for 2 h. After filtration, the filtrate was concentrated under nitrogen and precipitated with methyl tert-butyl ether. Peptide purification was performed by reverse-phase HPLC on a Vydac C<sub>18</sub> (218TP510) column. The peptide homogeneity (>95%) was determined by analytical HPLC using the same solvents with a linear gradient of 10–35% (v/v) acetonitrile over 25 min. Analogue **I**: Retention time (RT) = 13.27 min; yield after purification and lyophilization: 10%; Mass (ESI-MS) (M + H) *m/z* 1321.7. Analogue **II**: RT = 13.70 min; yield after purification and lyophilization: 11%; Mass (ESI-MS) (M + H) *m/z* 1298. Analogue **III**: RT = 13.61 min; yield after purification and lyophilization: 5%; Mass (ESI-MS) (M + H) *m/z* 1286.7.

### Circular Dichroism

CD measurements were carried out on a JASCO J-715 spectropolarimeter interfaced with a PC. The CD spectra were acquired and processed using the J-700 program for Windows. All experiments were carried out at room temperature using HELMA quartz cells with Suprasil windows and optical path lengths of 0.01 and 0.1 cm. All spectra were recorded using a bandwidth of 2 nm and a time constant of 8 s at a scan speed of 20 nm/min. The signal-to-noise ratio was improved by accumulating eight scans. Measurements were performed in the wavelength range 190–250 nm and the concentration of the peptides was in the range 0.07–1.07 mM. The peptides were analysed in aqueous solution containing 2,2,2-trifluoroethanol (TFE) 20% (v/v). The spectra are reported in terms of mean residue molar ellipticity (deg cm<sup>2</sup> dmol<sup>-1</sup>). The helical content for each peptide was estimated according to the literature [24].

### NMR Measurements and Molecular Modelling Calculations

NMR spectra were recorded at 298 K on a BRUKER AVANCE DMX-600 spectrometer. The experiments were carried out in H<sub>2</sub>O/TFE-*d*<sub>3</sub> (4:1 v/v). The sample concentration was approximately 1 mM in 600 μl of solution. The water signal was suppressed by pre-saturation during the relaxation delay. The spin systems of all amino acid residues were identified using standard DQF-COSY [25] and CLEAN-TOCSY [26,27] spectra. In the latter case, the spin-lock pulse sequence was 70 ms long. The sequence-specific assignment was accomplished using the rotating-frame Overhauser enhancement spectroscopy (ROESY), using a mixing time of 150 ms. In all homonuclear experiments, the spectra were acquired by collecting 400–512 experiments, each one consisting of 32–256 scans and 4 K data points.

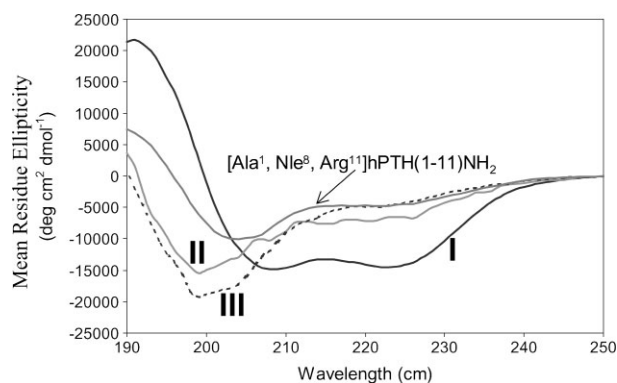
Spectral processing was carried out using XWINNMR. Spectra were calibrated against the TMS signal. Inter-proton distances were obtained by integration of the ROESY spectra using the AURELIA software package. The calibration was generally based on the geminal γ protons of Ile<sup>5</sup>, set to a distance of 1.78 Å. This was not possible for analogue **II** because the cross-peak was partially overlapped with the diagonal. The calibration was then performed on the αH–βH distance of Ala<sup>1</sup>, set to 2.73 Å. The offset correction was performed setting the B1-field value (2500 Hz) and the B1-frequency (ca 4.80 ppm), according to the formulas published by Bull [28].

Distance geometry (DG) and molecular dynamics (MD) calculations were carried out using the simulated annealing (SA) protocol of the X-PLOR 3.0 program. For distances involving equivalent or non-stereo-assigned protons, *r*<sup>-6</sup> averaging was used. The MD calculations involved a minimization stage of 100 cycles, followed by SA and a refinement stage. The SA consisted of 30 ps of dynamics at 1500 K (10 000 cycles, in 3 fs steps) and of 30 ps of cooling from 1500 to 100 K in 50 K decrements (15 000 cycles, in 2 fs steps). The SA procedure, in which the weights of ROE and non-bonded terms were gradually increased, was followed by 200 cycles of energy minimization. In the SA refinement stage, the system was cooled from 1000 to 100 K in 50 K decrements (20 000 cycles, in 1 fs steps). Finally, the calculations were completed with 200 cycles of energy minimization using an ROE force constant of 50 cal/(mole Å). One hundred and fifty structures were generated for each analogue, and the 20 minimum energy structures containing no distance constraint violation (<0.5 Å from the integration value) were chosen for conformational study, using the INSIGHT II and MOLMOL (version 2.6) programs with a SILICON GRAPHICS O2 R 10 000 workstation. The secondary structure was determined using H-bond analysis, dihedral angle calculations and the Kabsch and Sander algorithm [29].

### Activity Assays

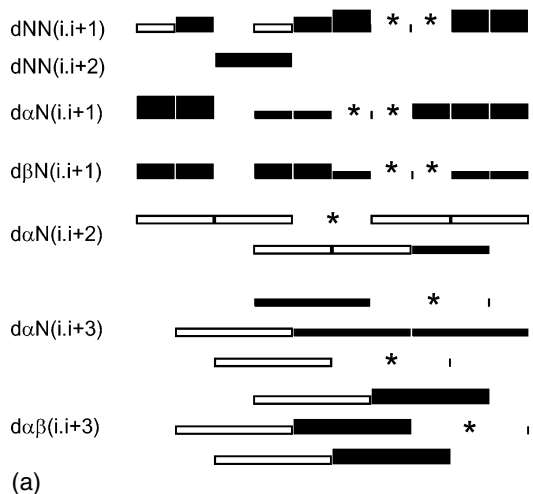
C20 HEK293 cells stably expressing the PTH1R were seeded at 10<sup>5</sup> cells/well in collagen-coated 24-well plates. Twenty-four hours later, the cells were treated with FuGENE 6 Transfection Reagent (1 μl/well) and CRE-luc plasmid (0.2 μg/well) in 0.5 ml/well serum-free Opti-Mem 1, according to the manufacturer's procedure.

Eighteen hours after transfection, the medium was replaced with 225 μl/well of Dulbecco's Modified Eagle Medium. To this, 25 μl/well of a solution of peptide in PBS/0.1% BSA was added, and the cells were incubated for 4 h at 37 °C, yielding maximal response to luciferase. Each peptide concentration was used in triplicate. The medium was aspirated and the cells were washed once with PBS pH 7.4 (250 μl/well). The cells were lysed by addition of 200 μl of Passive Lysis Buffer per well and gentle shaking for 5 min. The suspension was then transferred to labelled low-binding eppendorf tubes and centrifuged for 2 min, and 80 μl of the supernatant was transferred into labelled glass tubes.

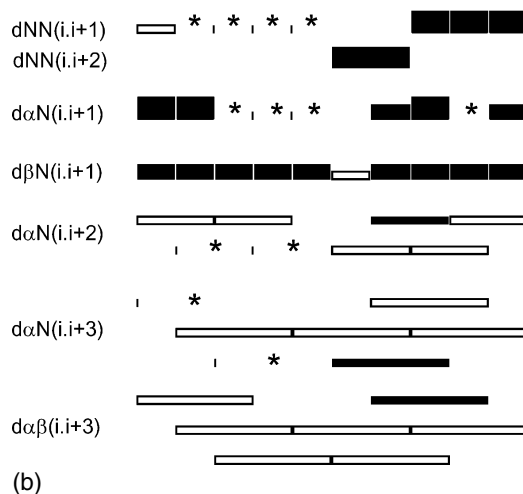


**Figure 2** CD spectra in aqueous solution containing 20% TFE(v/v). Concentrations: 1.074 mM (**I**); 0.428 mM (**II**); 0.066 mM (**III**). [Ala<sup>1</sup>, Nle<sup>8</sup>, Arg<sup>11</sup>]hPTH(1–11)NH<sub>2</sub> is included as a reference (1.240 mM).

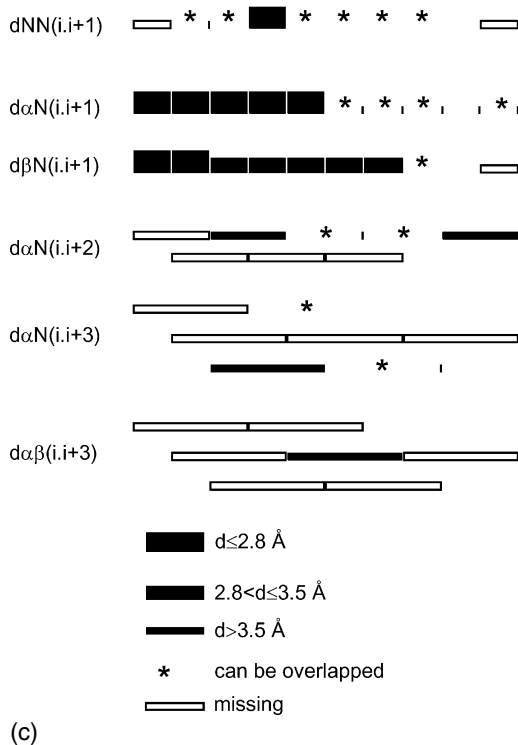
## Analogue I

A<sup>1</sup> V<sup>2</sup> (7,5-bTL)<sup>3,4</sup> I<sup>5</sup> Q<sup>6</sup> L<sup>7</sup> M<sup>8</sup> H<sup>9</sup> Q<sup>10</sup> R<sup>11</sup>

## Analogue II

A<sup>1</sup> V<sup>2</sup> S<sup>3</sup> E<sup>4</sup> I<sup>5</sup> (7,5-bTL)<sup>6,7</sup> M<sup>8</sup> H<sup>9</sup> Q<sup>10</sup> R<sup>11</sup>

## Analogue III

A<sup>1</sup> V<sup>2</sup> S<sup>3</sup> E<sup>4</sup> I<sup>5</sup> Q<sup>6</sup> L<sup>7</sup> M<sup>8</sup> (7,5-bTL)<sup>9,10</sup> R<sup>11</sup>

**Figure 3** Summary of ROESY connectivities of analogues I–III. Peaks are grouped into three classes, based upon their integrated volumes.

Luciferase activity was measured on a Lumat LB 9507 luminometer (EG&G Berthold). This instrument automatically injects pre-defined volumes of two solutions, A and B, with the compositions described below. Initially, a Solution 0 was prepared, containing glycylglycine 25 mM, MgSO<sub>4</sub> 15 mM and ethyleneglycol-bis(β-aminoethyl ether)-N, N', N'-tetraacetic acid (EGTA) 4 mM in deionized water. Solution A was 0.2 mM

D-luciferin in Solution 0. Solution B was K<sub>3</sub>PO<sub>4</sub> 0.02 M, ATP 2.5 mM and dithiothreitol 1 mM in Solution 0. The instrument was calibrated to add 100 μl of Solution A and 300 μl of Solution B to a sample tube, and the measurement was performed for 20 s. The mean read out from three wells with identical peptide concentrations was used to present the data.

## RESULTS AND DISCUSSION

### CD Results

The conformational properties of the three peptide mimetics were initially investigated by CD in TFE/water 20%, as in our previous experiments on potentially bioactive PTH-derived peptides [5]. The spectra in the far-UV region were collected at room temperature and are shown in Figure 2. The spectrum of analogue **I** exhibits the typical shape usually associated with the  $\alpha$ -helical conformation, showing two negative bands of comparable magnitude near 222 and 208 nm and a stronger positive band near 190 nm. For analogue **I**, the  $\alpha$ -helix content is estimated at 66% [24]. The presence of  $\beta$ -turns is not excluded, since their CD patterns qualitatively resembles that of an  $\alpha$ -helix [30]. Analogues **II** and **III** are characterized by negative bands at  $\sim 200$  nm, showing a lower content of ordered structure with respect to analogue **I**. However, the shape of these curves does not exclude the presence of some contribution of  $\alpha$ -helix or  $\beta$ -turn for these analogues, as well as the co-presence of two or more conformations. No concentration dependence of the CD profiles was observed for any of these analogues (data not shown).

### Resonance Assignment and NMR Solution Structures

Complete proton resonance assignment was possible using the standard procedure [31]. Tables S1–S3 in the Supporting Information contain the full chemical shift information. Figure 3 summarizes the sequential and medium range ROE connectivities observed for analogues **I–III** in 20% v/v TFE- $d_3$ . For analogue **I**, the observation of continuous  $d_{NN}(i, i+1)$  contacts together with characteristic  $d_{\alpha N}(i, i+3)$  and  $d_{\alpha\beta}(i, i+3)$

ROEs indicates the presence of an  $\alpha$ -helix spanning the sequence Ile<sup>5</sup>-Arg<sup>11</sup>. Analogue **II** contains a smaller number of these ROE interactions, and only in the C-terminal portion, starting from Nle<sup>8</sup>. Analogue **III** shows only one  $d_{NN}(i, i+1)$  interaction because of a large number of overlapped peaks. The small number of  $d_{\alpha N}(i, i+3)$  and  $d_{\alpha\beta}(i, i+3)$  connectivities indicates the absence of significant secondary structure.

Figure 4 shows the chemical shift differences of the  $\alpha$ H protons with respect to the values of the random coil conformation [32] and identifies a short helical segment in the sequence Ile<sup>5</sup>-Nle<sup>8</sup> for analogue **I** (negative values  $\geq 0.1$  ppm), while analogues **II** and **III** exhibit no helical structure. The inactive reference peptide [Ala<sup>1</sup>, Nle<sup>8</sup>, Arg<sup>11</sup>]hPTH(1–11)NH<sub>2</sub> has a reduced preference for the  $\alpha$ -helical conformation with respect to analogue **I**, as found in the CD spectra (Figure 2), indicating that the insertion of 7,5-bTL stabilizes the secondary structure, at least under the conditions used here.

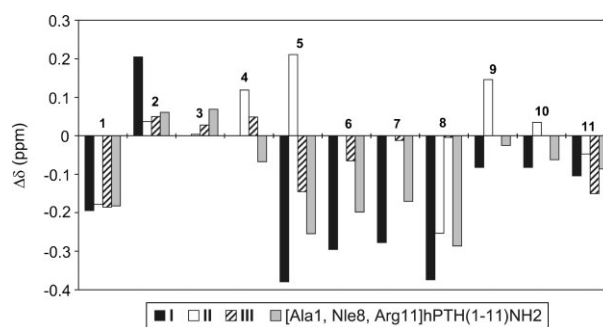


**Figure 4** Chemical shift differences of the  $\alpha$ H protons of analogues **I–III**. The data relative to [Ala<sup>1</sup>, Nle<sup>8</sup>, Arg<sup>11</sup>]hPTH(1–11)NH<sub>2</sub> are also included as a reference.

**Table 1** Structural statistics for analogues **I–III**

	Analogue <b>I</b>	Analogue <b>II</b>	Analogue <b>III</b>
<i>Experimental NMR constraints</i>			
Intra-residue ( $i - j = 0$ )	45	46	34
Sequential ( $ i - j  = 1$ )	32	20	22
Medium range ( $2 \leq  i - j  \leq 4$ )	16	11	3
Total	95	77	59
<i>(RMSD) from experimental constraints (Å)</i>			
Distance	0.088 ± 0.010	0.116 ± 0.002	0.116 ± 0.004
<i>Atomic (RMSD) (Å)</i>			
Backbone (1–11)	0.7 ± 0.3	2.0 ± 1.1	2.2 ± 1.0
Heavy atoms (1–11)	1.4 ± 0.4	3.2 ± 1.2	3.3 ± 1.1
<i>Mean energy (kcal/mol)</i>			
$E_{\text{tot}}$	72 ± 10	95 ± 3	83 ± 3
$E_{\text{bonds}}$	3.3 ± 0.4	6.0 ± 0.3	4.3 ± 0.4
$E_{\text{angles}}$	25.5 ± 1.1	27.9 ± 1.3	28 ± 2
$E_{\text{NOE}}$	37 ± 8	51.3 ± 1.7	43 ± 3

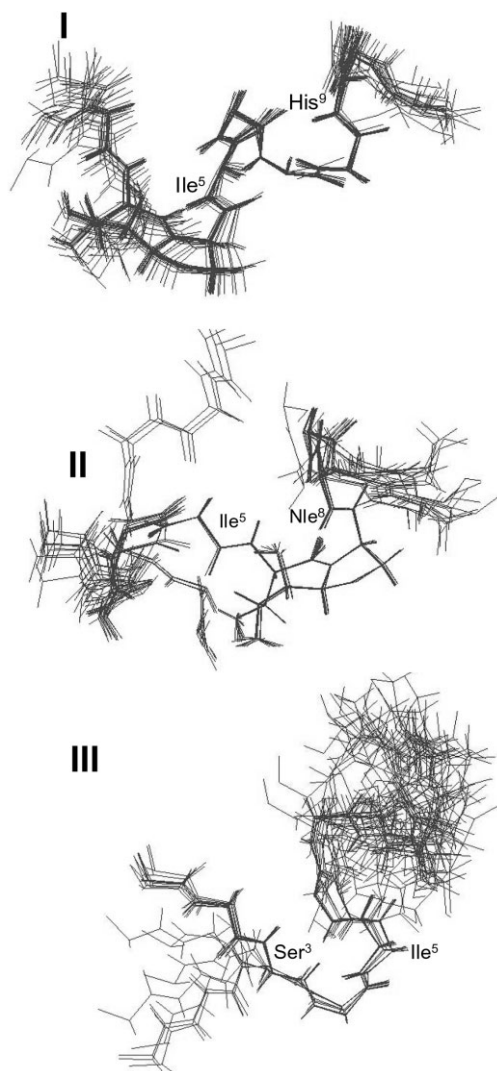


**Figure 5** Superimposition of the ensembles of calculated structures of analogues **I–III**. Heavy backbone atoms of the sequences indicated were superimposed.

## Structure Calculations

The experimental NMR constraints used in the structure calculations are reported in Table 1. The root mean-square deviation (RMSD) values from experimental constraints and the atomic RMSD<sup>33</sup> among the various structures are lower for analogue **I**, thus confirming a better defined secondary structure with respect to analogues **II** and **III**.

The mean values of the  $\varphi$  and  $\psi$  dihedral angle for all residues of analogue **I** were distributed in energetically acceptable regions, with angular order parameter (OP) values  $>0.95$  [33], except for Ala<sup>1</sup>, Val<sup>2</sup> and Arg<sup>11</sup> (see Figures S1–S3 in the Supporting Information). OPs for analogues **II** and **III** show that the dihedral angles  $\varphi$  and  $\psi$  are not very well defined for residues preceding the peptide mimetic moiety, indicating that the dipeptide-mimetic unit 7,5-bTL disrupts the tendency to form an ordered structure in the immediately preceding sequence. In fact, analogue **III** appears to be completely random (see Figure S3 in the Supporting Information). The superimposition of the ensemble of the low-energy structures of the three peptides is shown in Figure 5. A schematic representation of one of the lowest energy structures of analogues **I–III** is presented in Figure S4 in the Supporting Information.

It has been shown that 7,5-bTL can occupy the  $i$  to  $i + 1$  positions of type I and type II  $\beta$ -turns in cyclic hexapeptides [34]. In analogue **I**, we found a type III  $\beta$ -turn involving residues 4–7 (Table 2), immediately following the 7,5-bTL<sup>3,4</sup> residue. The  $\beta$ -turn can therefore be favoured by the dipeptide mimetic unit. The location of the  $\beta$ -turn is further supported by the H-bond analysis, which indicated that a (CO<sup>4</sup>–NH<sup>7</sup>) H-bond involving the backbone atoms occurs in 11 out of 20 structures (Table 3). Furthermore, there are significant occurrences of ( $i, i + 4$ ) H-bonds with  $i = 4$ ,

**Table 2** Average values of torsion angles  $\phi$  and  $\psi$  and relative standard deviations resulting from the 20 lowest energy structures calculated for analogues **I–III**

		Analogue I		Analogue II		Analogue III			
Residue		$\phi_m$ (°)	$\psi_m$ (°)	Residue	$\phi_m$ (°)	$\psi_m$ (°)	Residue	$\phi_m$ (°)	$\psi_m$ (°)
1	Ala	—	140 ± 30	Ala	—	149 ± 4	Ala	—	161 ± 9
2	Val	-70 ± 90	85 ± 6	Val	-111 ± 8	-30 ± 4	Val	-117 ± 2	164.3 ± 1.1
3	7,5-bTL	-154 ± 3	-100.8 ± 0.3	Ser	0 ± 40	-70 ± 40	Ser	-100 ± 40	173 ± 16
4	7,5-bTL	-77.9 ± 0.5	-42.3 ± 1.1	Glu	-80 ± 20	-40 ± 100	Glu	-70 ± 30	-37 ± 3
5	Ile	-47 ± 2	-39 ± 4	Ile	-90 ± 20	172 ± 3	Ile	-129 ± 10	-16 ± 4
6	Gln	-85 ± 6	-19 ± 12	7,5-bTL	155 ± 8	-105.0 ± 0.4	Gln	-50 ± 30	170 ± 70
7	Leu	-83 ± 13	-10 ± 8	7,5-bTL	-78.1 ± 0.4	-45.0 ± 0.9	Leu	40 ± 70	-68 ± 18
8	Nle	-109 ± 12	-27 ± 12	Nle	-41.4 ± 1.4	-25.3 ± 1.8	Nle	-50 ± 50	75 ± 10
9	His	-93 ± 12	-13 ± 6	His	-137 ± 8	-40 ± 40	7,5-bTL	-159.7 ± 0.9	-100.7 ± 0.9
10	Asn	-107 ± 10	0 ± 9	Asn	-80 ± 50	-30 ± 14	7,5-bTL	-76.7 ± 0.5	2.3 ± 0.9
11	Arg	-120 ± 40	0 ± 120	Arg	-10 ± 70	—	Arg	50 ± 110	—

5 and 6. This means that in analogue **I** 7,5-bTL is able to induce a  $3_{10}$  helix loop which develops into an  $\alpha$ -helical structure. This hypothesis agrees with the calculation of a secondary structure with the Kabsch and Sander algorithm [29], which indicates for analogue **I** an  $\alpha$ -helical segment in the region Ile<sup>5</sup>–His<sup>9</sup>. The same calculations for analogues **II** and **III** show no preference for secondary structure.

(*i, i + 4*) H-bonds with *i* = 6, 7 are present with a 50% frequency in analogue **II** (Table 3), and suggest a certain degree of structural order in the 7,5-bTL<sup>6,7</sup>-Asn<sup>10</sup> region, despite the CD analysis which indicates a non-helical preference. This apparent discrepancy can be explained by the presence of a (CO<sup>7</sup>-NH<sup>10</sup>) H-bond in 5 out of 20 structures, which leads to the hypothesis of a  $\beta$ -turn. The mean values for dihedral angles  $\varphi$  and  $\psi$  at position 8 and 9 (Table 2) are reasonable for a type I  $\beta$ -turn, and are even better if calculated only for the five (CO<sup>7</sup>-NH<sup>10</sup>) H-bond-containing structures:  $\varphi^8$ ,  $\psi^8$  and  $\varphi^9$  have a smaller relative error and the value for  $\psi^9$  is better ( $\psi^9 = +26 \pm 2^\circ$ ).

Comparing these data with the secondary chemical shift values and the CD analysis, we found that analogue **II** presents an equilibrium between  $\alpha$ -helical conformation and  $\beta$ -turn structure. There are no H-bonds involving the backbone atoms in analogue **III** and the same behaviour can be seen also in analogues **I** and **II** for residues preceding 7,5-bTL. Our hypothesis is that 7,5-bTL, because of its sterically hindered structure, prevents the formation of an ordered conformation in the segment preceding its position. Therefore, its closer proximity to the amino terminus in analogue **I** relative to analogues

**Table 3** Backbone H-bond analysis carried out on the 20 minimum energy structures of each analogue, fixing 2.4 Å as the maximum distance between the donor (H) and the acceptor (O) and 45° as the maximum deviation from the planar angle (180°) between N–H and C=O

Analogue I		
<i>i</i>	H-bond ( <i>i, i + 3</i> ) occurrence (%)	H-bond ( <i>i, i + 4</i> ) occurrence (%)
<i>Analogue I</i>		
4	55	25
5	0	25
6	0	35
8	5	0
<i>Analogue II</i>		
2	45	0
6	0	45
7	25	50
<i>Analogue III</i>		
5	10	0
6	5	0

**II** and **III** allows the presence of a stable helical conformation in the first but not in the last two analogues.

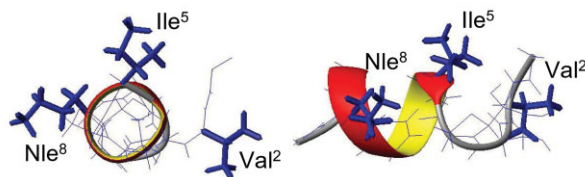
The bioactivity assays on C20 HEK293 cells (Table 4) indicate that analogues **I–III** are poorly active in comparison with the fully active PTH(1–34). Considering that [Ala<sup>1</sup>, Nle<sup>8</sup>, Arg<sup>11</sup>]hPTH(1–11)NH<sub>2</sub> is also inactive, the 7,5-bTL substitution does not necessarily imply a reduction in activity.

However, there are substitutions in PTH(1–11) analogues that generate potent agonists of PTH(1–34), with EC<sub>50</sub> values in the nanomolar range [4,5]. Apparently,

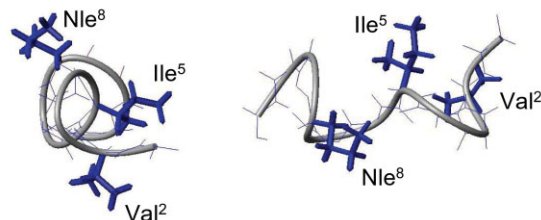
**Table 4** Biological activity of PTH(1–11) analogues **I–III** (cAMP stimulation responses in C20 cells, Luciferase reporter assays). Data relating to [Ala<sup>1</sup>, Nle<sup>8</sup>, Arg<sup>11</sup>]hPTH(1–11)NH<sub>2</sub> and PTH(1–34)NH<sub>2</sub> are included as reference

Analogue	EC <sub>50</sub> (nM)
[Ala <sup>1</sup> , 7,5-bTL <sup>3,4</sup> , Nle <sup>8</sup> , Arg <sup>11</sup> ]h PTH(1–11)NH <sub>2</sub>	>10 <sup>5</sup>
[Ala <sup>1</sup> , 7,5-bTL <sup>6,7</sup> , Nle <sup>8</sup> , Arg <sup>11</sup> ]hPTH(1–11)NH <sub>2</sub>	>10 <sup>5</sup>
[Ala <sup>1</sup> , Nle <sup>8</sup> , 7,5-bTL <sup>9,10</sup> , Arg <sup>11</sup> ]hPTH(1–11)NH <sub>2</sub>	>10 <sup>5</sup>
[Ala <sup>1</sup> , Nle <sup>8</sup> , Arg <sup>11</sup> ]hPTH(1–11)NH <sub>2</sub>	>10 <sup>5</sup>
PTH(1–34)NH <sub>2</sub>	1.03 ± 0.12

Analogue I



Analogue II



Analogue III

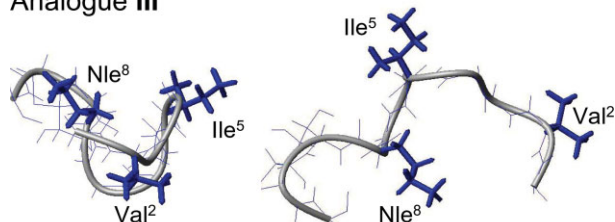


**Figure 6** Comparison of top (left) and side (right) views of the relative orientation of Val<sup>2</sup>, Ile<sup>5</sup> and Nle<sup>8</sup> side chains in representative structures of analogues **I–III**.

our efforts to minimize the PTH pharmacophore by introducing conformational constraint into the backbone of PTH(1–11) as a general strategy to optimize the bioactive conformation leaving unmodified the clearly critical residues, i.e. Val<sup>2</sup>, Ile<sup>5</sup> and Met<sup>8</sup>/Nle<sup>8</sup>, were not sufficient to generate potent PTH-like analogues. In fact, analogue **I** is not active although 7,5-bTL in position (3,4) can putatively mimic the Ser<sup>3</sup> and to some extent the Glu<sup>4</sup> side chains, and permits the presence of helical structural elements from position 4 on. These results underline that stabilization of a helical segment at the *N*-terminus of PTH(1–11) analogues, as observed in analogue **I**, may be necessary but not sufficient to generate a bioactive PTH-like compound. It is possible that the side chain of Glu<sup>4</sup> is not well mimicked by 7,5-bTL, or that substitution with the peptide mimetic between the residues Val<sup>2</sup> and Ile<sup>5</sup> constrains the side chains in an unfavourable interaction with the receptor. To investigate the relative side-chain orientation of the critical residues 2, 5 and 8, we used the ligand-tethered PTH1R model [6]. Previous studies had suggested that PTH1R could adopt at least several different conformations, and that neither the (12–34) portion of PTH(1–34) nor the *N*-terminal extracellular domain of the receptor was required for high ligand–receptor affinity. Analogues such as [Ac5c<sup>1</sup>, Aib<sup>3</sup>, Gln<sup>10</sup>, Arg<sup>11</sup>]PTH(1–11)NH<sub>2</sub> are in a well-defined  $\alpha$ -helical structure and show high activity in the luciferase reporter assay on HEK 293 cells [5], and PTH1R lacking the *N*-terminus is constitutively active if PTH(1–11) is tethered to it through a four glycine linker [15]. We hypothesized that analogues **I–III** interact with PTH1R through the same conformation assumed by the receptor in the tethered model.

An effective ligand-PTH1R interaction occurs if the so-called bioactive conformation can display the side chains in the correct topology. Figure 6 pictorially explains the different side-chain orientations of the three analogues with respect to the conformation and side-chain topology of PTH(1–11) in the ligand-tethered PTH1R model. In the latter case, the side chain of Nle<sup>8</sup> (replacing Met<sup>8</sup>) is on the same face of the *N*-terminal helix as Ile<sup>5</sup> and therefore can share the same deep hydrophobic pocket in PTH1R [6]. For analogue **III**, in which no secondary structure was detected, the PTH-like bioactive topology cannot be achieved. In analogue **II**, the type I  $\beta$ -turn –  $\alpha$ -helix conformation equilibrium probably does not favour the interaction with the receptor. Analogue **I** presents a spatial orientation of the Val<sup>2</sup>, Ile<sup>5</sup> and Nle<sup>8</sup> side chains significantly different with respect to PTH(1–11). Taken together, these results suggest that a very stable helix encompassing these residues appears to be fundamental, although not sufficient, for PTH-like ligand-PTH1R interaction.

In conclusion, in this work we introduced a dipeptide mimetic unit to generate PTH analogues based on the *N*-terminal miniaturized sequence, which was previously

demonstrated to effectively activate the PTH1R. The procedure to insert a dipeptide mimetic unit into the PTH-derived sequence is fully described. In particular, we demonstrated that 7,5-bTL can occupy the *i* – 1 and *i* positions of a type III  $\beta$ -turn, inducing a 3<sub>10</sub> helix loop which can develop into a  $\alpha$ -helix. Considering helicity as fundamental for PTH active agonists, further use of these sugar-based mimetics can be strategic, because the azabicycloalkane backbone can be functionalized to mimic specific side chains, preserving the helical secondary structure and reproducing the topology essential for productive ligand-PTH1R interaction.

## Supplementary Material

Supplementary electronic material for this paper is available in Wiley InterScience at: <http://www.interscience.wiley.com/jpages/1075-2617/suppmat/>

For analogues **I–III**: proton resonance frequency tables; angular order parameter graphics; schematic representation of one of the lowest energy structures.

## Acknowledgements

The authors thank MIUR, Ministry of Education and University of Italy, CNR, the National Research Council of Italy and Abiogen S.p.A. for financial support and Dr. Barbara Biondi for assistance in mass spectroscopy.

## REFERENCES

- Chorev M, Rosenblatt M. *The Parathyroids*. Raven Press: New York, 1994; 139–156.
- Scian M, Marin M, Bellanda M, Tou L, Alexander JM, Rosenblatt M, Chorev M, Peggion E, Mammi S. Backbone dynamics of human parathyroid hormone (1–34): flexibility of the central region under different environmental conditions. *Biopolymers* 2006; **84**: 147–160.
- Shimizu M, Petroni BD, Khatri A, Gardella TJ. Functional evidence for an intramolecular side chain interaction between residues 6 and 10 of receptor-bound parathyroid hormone analogues. *Biochemistry* 2003; **42**: 2282–2290.
- Tsomaia N, Pellegrini M, Hyde K, Gardella TJ, Mierke DF. Toward parathyroid hormone minimization: conformational studies of cyclic PTH(1–14) analogues. *Biochemistry* 2004; **43**: 690–699.
- Barazza A, Wittelsberger A, Fiori N, Schievano E, Mammi S, Toniolo C, Alexander JM, Rosenblatt M, Peggion E, Chorev M. Bioactive *N*-terminal undecapeptides derived from parathyroid hormone: the role of alpha-helicity. *J. Pept. Res.* 2005; **65**: 23–35.
- Monticelli L, Mammi S, Mierke DF. Molecular characterization of a ligand-tethered parathyroid hormone receptor. *Biophys. Chem.* 2002; **95**: 165–172.
- Shimizu M, Potts JT Jr., Gardella TJ. Toward parathyroid hormone minimization: conformational studies of cyclic PTH(1–14) analogues. *J. Biol. Chem.* 2000; **275**: 21836–21843.
- Geyer A, Moser E. Polyol peptidomimetics. *Eur. J. Org. Chem.* 2000; **7**: 1113–1120.
- Hirschmann R. Medicinal chemistry in the golden age of biology: lessons from steroid and peptide research. *Angew. Chem. Int. Ed.* 1991; **30**: 1278–1301.
- Gante J. Peptidomimetics – tailored enzyme inhibitors. *Angew. Chem. Int. Ed.* 1994; **33**: 1699–1720.



11. Kessler H, Diefenbach B, Finsinger D, Geyer A, Gurrath M, Goodman SL, Hölzemann G, Haubner R, Jonczyk A, Müller G, Graf v. Roedern E, Wermuth J. Design of superactive and selective integrin receptor antagonists containing the RGD sequence. *Let. Pept. Sci.* 1995; **2**: 155–160.
12. Shimizu M, Guo J, Gardella TJ. Parathyroid hormone (PTH)-(1-14) and -(1-11) analogs conformationally constrained by alpha-aminoisobutyric acid mediate full agonist responses via the juxtamembrane region of the PTH-1 receptor. *J. Biol. Chem.* 2001; **276**: 49003–49012.
13. Rosenblatt M, Goltzmann D, Keutmann HT, Tregear GW, Potts JT Jr. Chemical and biological properties of synthetic, sulfur-free analogues of parathyroid hormone. *J. Biol. Chem.* 1976; **251**: 159–164.
14. Frelinger AL, Zull JE. Oxidized forms of parathyroid hormone with biological activity. Separation and characterization of hormone forms oxidized at methionine 8 and methionine 18. *J. Biol. Chem.* 1984; **259**: 5507–5513.
15. Shimizu M, Carter PH, Gardella TJ. Autoactivation of type-1 parathyroid hormone receptors containing a tethered ligand. *J. Biol. Chem.* 2000; **275**: 19456–19460.
16. Shimizu M, Carter PH, Khatri A, Potts JT Jr., Gardella TJ. Enhanced activity in parathyroid hormone-(1-14) and -(1-11): novel peptides for probing ligand-receptor interactions. *Endocrinology* 2001; **142**: 3068–3074.
17. Shimizu M, Dean T, Khatri A, Gardella TJ. Amino-terminal parathyroid hormone fragment analogs containing alpha, alpha-di-alkyl amino acids at positions 1 and 3. *J. Bone Miner. Res.* 2004; **19**: 2078–2086.
18. Carpino LA, El-Faham A, Minor CA, Albericio F. Advantageous applications of azabenzotriazole (triazolopyridine)-based coupling reagents to solid-phase peptide synthesis. *J. Chem. Soc., Chem. Commun.* 1994; 201–203.
19. Knorr R, Trzeciak A, Bannwarth W, Gillessen D. New coupling reagents in peptide chemistry. *Tetrahedron Lett.* 1989; **30**: 1927–1930.
20. Carpino LA. 1-Hydroxy-7-azabenzotriazole. An efficient peptide coupling additive. *J. Am. Chem. Soc.* 1993; **115**: 4397–4398.
21. Carpino LA, El-Faham A, Albericio F. Efficiency in peptide coupling: 1-hydroxy-7-azabenzotriazole vs 3,4-dihydro-3-hydroxy-4-oxo-1,2,3-benzotriazine. *J. Org. Chem.* 1995; **60**: 3561–3564.
22. Carpino LA, El-Faham A. Effect of tertiary bases on O-benzotriazolyluronium salt-induced peptide segment coupling. *J. Org. Chem.* 1994; **59**: 695–698.
23. Belvisi L, Bernardi A, Checchia A, Manzoni L, Potenza D, Scolastico C, Castorina M, Cupelli A, Giannini G, Carminati P, Pisano C. Potent integrin antagonists from a small library of RGD-including cyclic pseudopeptides. *Org. Lett.* 2001; **3**: 1001–1004.
24. Yang JT, Wu CS, Martinez HM. Calculation of protein conformation from circular dichroism. *Meth. Enzymol.* 1986; **130**: 208–269.
25. Rance M, Sørensen OW, Bodenhausen G, Wagner G, Ernst RR, Wüthrich K. Improved spectral resolution in COSY <sup>1</sup>H NMR spectra of proteins via double quantum filtering. *Biochem. Biophys. Res. Commun.* 1983; **117**: 479–485.
26. Bax A, Davis DG. MLEV-17-based two-dimensional homonuclear magnetization transfer spectroscopy. *J. Magn. Reson.* 1985; **65**: 355–360.
27. Griesinger C, Otting G, Wüthrich K, Ernst RR. Clean TOCSY for proton spin system identification in macromolecules. *J. Am. Chem. Soc.* 1988; **110**: 7870–7872.
28. Bull TE. ROESY relaxation theory. *J. Magn. Reson.* 1988; **80**: 470–481.
29. Kabsch W, Sander C. Dictionary of protein secondary structure: pattern recognition of hydrogen-bonded and geometrical features. *Biopolymers* 1983; **22**: 2577–2637.
30. Rose GD, Gierasch LM, Smith JA. Turns in peptides and proteins. *Adv. Protein Chem.* 1985; **37**: 1–109.
31. Wüthrich K. *NMR of Proteins and Nucleic Acids*. John Wiley & Sons: New York, 1986; 117–175.
32. Pastore A, Saudek V. The relationship between chemical shift and secondary structure in proteins. *J. Magn. Reson.* 1990; **90**: 165–176.
33. Hyberts SG, Goldberg MS, Havel TF, Wagner G. The solution structure of eglin c based on measurements of many NOEs and coupling constants and its comparison with X-ray structures. *Protein Sci.* 1992; **1**: 736–751.
34. Tremmel P, Geyer A. Coupled hydrogen-bonding networks in polyhydroxylated peptides. *Angew. Chem. Int. Ed.* 2004; **43**: 5789–5791.



## APPENDIX B

Peptides are important in a number of physiological processes. The potential benefits to understand the actions of peptides include: improved knowledge of biomolecular rules; improved capability to predict natural biomolecular assemblies or to use them to diagnostic or medical purposes; and increased capability in engineering and de novo designing of natural and bioinspired materials.

During these years, we collaborated with many researchers and research groups with specific competences. The following papers are an example of how peptides can solve simple problems of biocompatibility and help to understand the biological mechanism or to diagnostic complexes or materials.

Peptides, as neurotransmitters, neuromodulators and hormones, influence a number of physiological processes by signal transduction mediated through receptors. In addition, during the last 20 years their role in the appearance or maintenance of various diseases could be unequivocally proven. Agents that can imitate or block the biological functions of bioactive peptides (agonists or antagonists, respectively) can be considered as aids for the investigation of peptidergic systems and also as therapeutic agents. The suitability of bioactive peptides as therapeutic agents was examined after preliminary pharmacological experiments. Alpha-Synuclein is a protein abundant in presynaptic terminals in the brain; the sequence is an imperfect 11-residue repeat in the N-terminal region. To understand the physiological role of the protein we investigated the ability of three fragments of the protein, which include one, two, and all repeats, respectively, to bind to vesicles of different phospholipid composition.

During the past decade, radiolabeled receptor-binding peptides were shown to form an important class of radiopharmaceuticals for tumor diagnosis and therapy. The specific receptor binding property of the ligand can be exploited by labeling the ligand with a radionuclide and using the radiolabeled ligand as a vehicle to address the radioactivity to the tissues with a particular receptor. The concept of using radio-labelled receptor binding peptides to target receptor-expressing tissues in vivo stimulated a large body of research in nuclear medicine. Receptor binding peptides labelled with gamma emitters ( $^{123}\text{I}$ ,  $^{111}\text{In}$ ,  $^{99\text{m}}\text{Tc}$ ) can visualize receptor-expressing tissues, a technique referred to as peptide-receptor radionuclide imaging. The first and

most successful imaging agent to date is the somatostatin analogue octreotide. It is used for somatostatin receptor scintigraphy and peptide-receptor radionuclide therapy of neuroendocrine cancers. Other peptides such as Minigastrin, GLP-1, CCK, bombesin, substance P, neurotensin, and RGD peptides are currently under development or undergoing clinical trials<sup>1</sup>. To investigate the effective applicability of  $[\text{Tc}(\text{N})(\text{PNP})]^{2+}$  technology, which has recently been studied<sup>2</sup>, avidin–biotin system was selected as a model to preparing of target-specific molecule. A small library of [O–,S–]-N functionalized cysteine–biotin derivatives was synthesized by coupling the amino group of the cysteine, through a group spacer, to the carboxyl group of the vitamin. To study the steric and the electronic influence of the Tc-carrying complex on the biotin–avidin receptor interaction, the effect of the length and flexibility of the spacer was evaluated. Although significant progresses have been made in medical techniques that reconstitute damaged organs or tissues as a result of an accident, trauma or cancer, transplantation of organs or tissues is still a widely accepted therapy to treat patients. The surgical procedure that takes tissues from a patient and transplants them back to the defect site in the patient's body has often been successful. However, autologous transplantation is limited because of donor site morbidity and infection or pain to patients because of secondary surgery. Alternative tissue sources originated from other humans or animals are problematic mainly due to immunogenic responses by the patients upon implantation and a shortage of donor organs. Tissue engineering paradigm, which applies methods from engineering and life sciences to create artificial constructs to direct tissue regeneration<sup>3</sup>, is to isolate specific cells through a small biopsy from a patient, to grow them on a three-dimensional biomimetic scaffold under precisely controlled culture conditions, to deliver the construct to the desired site in the patient's body, and to direct new tissue formation into the scaffold that can be degraded over time<sup>4</sup>. In order to achieve successful regeneration of damaged organs or tissues based on the tissue engineering concept, several critical elements should be considered including biomaterial scaffolds that serve as a mechanical support for cell growth, progenitor cells

---

<sup>1</sup> Dijkgraaf I.; Boerman O. C.; Oyen W. J.G.; Corstens F. H. M.; Gotthardt M. *Current Medicinal Chemistry* 7, 2007, pp. 543-551.

<sup>2</sup> Bolzati C, Mahmood A, Malagò E, Uccelli L, Boschi A, Jones AJ, Refosco F., Duatti A. *Tisato F. Bioconjug. Chem* 2003;14:1231–42.

<sup>3</sup> Vacanti JP, Langer R. *Lancet* 1999;354(suppl I):32–4.

<sup>4</sup> Lee KY, Mooney DJ. *Chem. Rev* 2001;101:1869–79.

that can be differentiated into specific cell types, and inductive growth factors that can modulate cellular activities<sup>5, 6</sup>. The biomaterials play an important role in most tissue engineering strategies<sup>7</sup>. The development of biomaterials for tissue engineering applications has recently focused on the design of biomimetic materials that are able to interact with surrounding tissues by biomolecular recognition<sup>8, 9, 10</sup>. When biomaterials are exposed to biological environments, extracellular matrix (ECM) proteins are non-specifically adsorbed on the surface of nearly all the biomaterials, then cells indirectly interact with the biomaterial surface through the adsorbed ECM proteins. The design of biomimetic materials is an attempt to make the materials capable of eliciting specific cellular responses and to direct new tissue formation mediated by specific interactions, which can be manipulated by altering design parameters instead of non-specifically adsorbed ECM proteins.

One possible design strategy for new biomaterials involves incorporation of cell-binding peptides into biomaterials via chemical or physical modification. The cell-binding peptides include a native long chain of ECM proteins as well as short peptide sequences derived from intact ECM proteins that can incur specific interactions with cell receptors. The biomimetic materials potentially mimic many roles of ECM in tissues. For example, the immobilization of signaling peptides makes the surface of biomaterials cell adhesive that inherently are non-adhesive to cells<sup>11</sup>. The incorporation of peptide sequences into materials can also make the material degradable by specific protease enzymes<sup>12</sup> or induce cellular responses that may be not present in a local native tissue<sup>13</sup>. The development of biomaterials for tissue engineering applications has focused on the design of ideal biomaterials that can elicit specific cellular responses<sup>14</sup>. The most widely recognised and characterised ligand peptide motif is the RGD sequence, found in a variety of ECM proteins. Functionalisation of biocompatible polyurethanes (PU) with cell adhesive peptides to promote cell-matrix specific

---

<sup>5</sup> Putnam AJ, Mooney DJ. *Nature Med* 1996;2:824–6.

<sup>6</sup> Heath CA. *TIBTECH* 2000;18:17–9.

<sup>7</sup> Hubbell JA. *Bio/technology* 1995;13:565–76.

<sup>8</sup> Hubbell JA. *Curr Opin Biotechnol* 1999;10:123–9

<sup>9</sup> Healy KE. *Curr Opin Solid State Mater Sci* 1999;4:381–7.

<sup>10</sup> Sakiyama-Elbert SE, Hubbell JA. *Annu Rev Mater Res*. 2001;31:183–201

<sup>11</sup> Shin H, Jo S, Mikos AG. *J Biomed Mater Res* 2002;61:169–79.

<sup>12</sup> West JL, Hubbell JA. *Macromolecules* 1999;32:241–4

<sup>13</sup> Suzuki Y, Tanihara M, Suzuki K, Saitou A, Sufan W, Nishimura Y. *J Biomed Mater Res* 2000;50:405–9.

<sup>14</sup> Temenoff J.S., Steinbis E.S., Mikos A.G., *J Biomater Sci Polym Ed*. 2003;14(9), 989-1004

interactions is still a strategy with limited diffusion. A few approaches are known<sup>15</sup> that can be applied for the introduction of peptide sequences into the chain back-bone; moreover these synthetic procedures reduce conformational mobility of the peptide which becomes less effective for the interaction with the cell receptors. In the following work, a strategy for functionalisation of PU was proposed by a novel approach based on the insertion of the RGDS cell binding peptide as a side chain. The presence of a spacer was provided to allow the peptide to stand out from the artificial surface and to reach the binding site of the cell receptors.

---

<sup>15</sup> Jun H.W., West J., J Biomater Sci Polym Ed. 2004, 15(1), 73-94

**Marco Bisaglia**  
**Elisabetta Schievano**  
**Andrea Caporale**  
**Evaristo Peggion**  
**Stefano Mammi**  
*Institute for Biomolecular  
Chemistry, CNR, Department  
of Chemical Sciences,  
University of Padova, Via F.  
Marzolo 1, 35131, Padova, Italy*

*Received 22 August 2005;  
revised 13 December 2005;  
accepted 20 December 2005*

*Published online 12 January 2006 in Wiley InterScience (www.interscience.wiley.com). DOI 10.1002/bip.20440*

# The 11-mer Repeats of Human $\alpha$ -Synuclein in Vesicle Interactions and Lipid Composition Discrimination: A Cooperative Role

**Abstract:**  $\alpha$ -Synuclein is a protein abundant in presynaptic terminals in the brain. The N-terminal region of the sequence contains an imperfect 11-residue periodicity also found in A-class apolipoproteins and able to fold into an amphipathic helix. Here, the ability of three fragments of the protein, which include one, two, and all repeats, respectively, to bind to vesicles of different phospholipid composition is described. The results suggest a cooperative action of the repeats in selecting target membranes for interaction based on their lipid composition. This deduction is possibly related to the physiological role of the protein, which is still poorly understood. © 2006 Wiley Periodicals, Inc. *Biopolymers (Pept Sci)* 84: 310–316, 2006

*This article was originally published online as an accepted preprint. The “Published Online” date corresponds to the preprint version. You can request a copy of the preprint by emailing the Biopolymers editorial office at [biopolymers@wiley.com](mailto:biopolymers@wiley.com)*

**Keywords:**  $\alpha$ -synuclein; amphipathic helix;  $\alpha$ 11/3-helix; phospholipid vesicles; circular dichroism

## INTRODUCTION

Synucleins are small, highly conserved proteins whose physiological function is still poorly understood. The family includes  $\alpha$ -,  $\beta$ -, and  $\gamma$ -synuclein, which share 55–62% sequence identity. Within this family,  $\alpha$ -synuclein is the most studied because of its involvement in Parkinson's disease.<sup>1</sup> Human  $\alpha$ -synuclein is a 140-residue, soluble protein that is abundantly expressed in neurons, where it is localized at

presynaptic terminals, particularly in the neocortex, hippocampus, striatum, thalamus, and cerebellum.<sup>2,3</sup> Several functions are ascribed to  $\alpha$ -synuclein. It might play a role in synaptic plasticity, by helping to maintain the size of the presynaptic vesicular pool,<sup>4</sup> and in regulation of dopamine neurotransmission via effects on vesicular dopamine storage.<sup>5,6</sup> An important neuronal function of  $\alpha$ -synuclein could be to regulate the formation of synaptic vesicles from early endosome through interaction with phospholipase

*Correspondence to:* Stefano Mammi; e-mail: [stefano.mammi@unipd.it](mailto:stefano.mammi@unipd.it)

Contract grant sponsor: Ministero dell'Istruzione, Università e Ricerca (MIUR) and Università degli Studi di Padova (USP)  
Contract grant number: PRIN 2004032851 (MIUR) and CPDA027314 (USP)

*Biopolymers (Peptide Science)*, Vol. 84, 310–316 (2006)

© 2006 Wiley Periodicals, Inc.

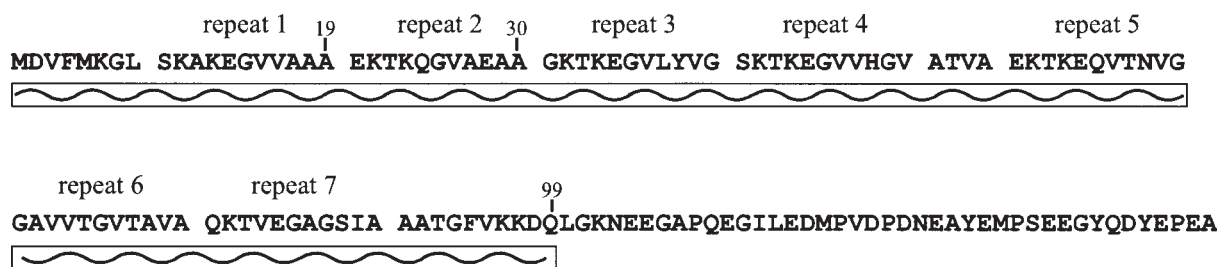


**FIGURE 1** Amino acid sequence of  $\alpha$ -synuclein. The imperfect 11-mer repeats and the lipid-interacting region are emphasized.

D2, an enzyme that hydrolyzes phosphatidylcholine to phosphatidic acid and may be involved in vesicle trafficking in the secretory pathway.<sup>7,8</sup> It has been demonstrated that, *in vitro*,  $\alpha$ -synuclein can inhibit phospholipase D2.<sup>9</sup>

$\alpha$ -Synuclein adopts a random conformation in water under physiological conditions.<sup>10</sup> On the other hand, the first  $\sim$ 100 residues interact with sodium dodecyl sulfate micelles or acidic small unilamellar vesicles (SUV), undergoing a conformational transition to a helical state.<sup>11–13</sup> Recently, we proposed a topological model in which the helix is mainly positioned on the surface of the membrane with approximately the last 10 residues partially embedded in the membrane.<sup>12</sup> A key feature of  $\alpha$ -synuclein is the presence of an imperfect 11-residue periodicity in the first 89 residues (Figure 1). Such a periodicity, which is also present in the other proteins of the synuclein family, is similar to that of the amphipathic helices of the lipid-binding domains of A-class apolipoproteins.<sup>14</sup> This class of proteins is characterized by a clustering of basic residues at the polar/nonpolar interface and acidic residues at the center of the polar face.<sup>15</sup> According to the so-called “snorkel” hypothesis,<sup>15</sup> the location of these charged residues is important in determining the free energy of association with the bilayer and the depth of the helix in the bilayer. An important difference between apolipoproteins and  $\alpha$ -synuclein exists, possibly related to their different physiological function: apolipoproteins are able to interact with neutral phospholipids,<sup>15</sup> whereas  $\alpha$ -synuclein only binds to acidic vesicles.<sup>14,16</sup>

To better understand the role of the 11-mer repeats of  $\alpha$ -synuclein in vesicle interaction, in this work we analyzed the conformational changes of three fragments derived from wild-type human  $\alpha$ -synuclein upon addition of SUV of different compositions. The two N-terminal fragments,  $\alpha$ syn1–19 and  $\alpha$ syn1–30, contain one and two 11-residue repeats, respectively. The third fragment,  $\alpha$ syn1–99, contains the whole region of human  $\alpha$ -synuclein involved in the interaction of the protein with the membranes.<sup>11</sup>

## MATERIALS AND METHODS

Protected amino acids and reagents for peptide synthesis were purchased from Fluka BioChemika; 1,2-dimyristoyl-*sn*-glycero-3-phosphocholine (DMPC), 1,2-dimyristoyl-*sn*-glycero-3-[phospho-*rac*-(1-glycerol)] (DMPG), sodium phosphate salts, and cobalt-agarose resin were purchased from Sigma-Aldrich; thrombin protease was purchased from Amersham Pharmacia.

### Peptide Synthesis

$\alpha$ syn1–19 and  $\alpha$ syn1–30 were synthesized as free amino, free carboxy peptides by solid-phase methodology on an Advanced ChemTech 348 $\Omega$  Peptide Synthesizer using 9-fluorenylmethyloxycarbonyl (Fmoc) chemistry.<sup>17</sup> The peptides were purified by reverse phase high-performance liquid chromatography using a Vydac C<sub>18</sub> 218TP510 column with linear gradient (30–40% in 10 min) of 90% CH<sub>3</sub>CN and water containing 0.1% trifluoroacetic acid. The molecular masses were determined on a Perceptive Biosystems MARINER<sup>TM</sup> Atmospheric Pressure Ionization-Time of Flight (API-TOF) spectrometer. ( $\alpha$ Syn1–19, calculated: 1952.03 Da, found: 1951.15 Da;  $\alpha$ syn1–30, calculated: 3063.61 Da, found: 3063.61 Da).

### Overexpression of $\alpha$ Syn1–99

Histidine-tagged  $\alpha$ syn1–99 was obtained as described elsewhere.<sup>12</sup> In brief, overexpression of the protein was achieved by growing the cells in Luria Bertani broth at 37°C to an OD<sub>600</sub> (OD: optical density) of about 0.6, followed by induction with 0.5 mM isopropyl- $\beta$ -thiogalactopyranoside for 4 h. The protein was purified on a cobalt-agarose resin using the manufacturer’s recommended protocol. To eliminate the His tag, the purified protein was digested with thrombin using the manufacturer’s protocol. Finally,  $\alpha$ syn1–99 was dialyzed, lyophilized, and stored at  $-20^{\circ}\text{C}$ .

### Preparation of SUV

SUV composed of DMPC:DMPG in 75:25, 50:50, or 0:100 molar ratios were prepared by extrusion. The lipids were dissolved in 1 mL chloroform/methanol 4:1, and the solutions were evaporated using a dry nitrogen stream in a round-bottomed flask. The lipid film was thoroughly dried



on a vacuum pump to remove residual organic solvent. The dry lipid film was suspended in 40 mM Na-phosphate buffer (pH 7.4) to give a final concentration of 30 mM and mixed for 1 h above the melting temperature. The hydration product was filtered through a large pore size (0.45  $\mu\text{m}$ ) filter and subsequently extruded through a 50-nm pore filter utilizing an Avanti<sup>®</sup> miniextruder.

### Circular Dichroism (CD) Experiments

CD measurements were carried out on a JASCO J-715 spectropolarimeter interfaced with a personal computer. The CD spectra were acquired and processed using the J-700 program for Windows. The experiments were carried out at room temperature using HELLMA quartz cells with Suprasil<sup>®</sup> windows and an optical path length of 0.01–0.02 cm. All spectra were recorded in the 190–260-nm wavelength range, using a bandwidth of 2 nm and a time constant of 4 s at a scan speed of 50 nm/min. The signal-to-noise ratio was improved by accumulating 4 scans. The spectra are reported in terms of mean residue ellipticity  $[\Theta]_R$  (deg cm<sup>2</sup> dmol<sup>-1</sup>). Peptide concentrations were determined by measuring the absorbance at 205 nm.<sup>18</sup>  $\alpha\text{Syn1-99}$  concentration was evaluated using the Coomassie Blue Protein Assay.<sup>19</sup>

### RESULTS

$\alpha$ -Synuclein has been reported to bind to acidic synthetic membranes such as PC/PA, PC/PG, PC/PS, PE/PA, PE/PG, and PE/PS (PA, phosphatidic acid; PC, phosphatidylcholine; PS, phosphatidylserine; PE, phosphatidylethanolamine; PG, phosphatidylglycerol).<sup>12,14,20</sup> The effects of acidic SUV containing PC and PG at different molar ratios on the conformation of  $\alpha$ -synuclein fragments were studied by far-ultraviolet (UV) CD spectroscopy. It has been suggested that the dimensions of the vesicles are a critical factor for the lipid/ $\alpha$ -synuclein interactions and that the protein interacts only with small vesicles.<sup>14,16</sup> Therefore, 50 nm SUV were obtained by extrusion and were always kept above their melting temperature (23°C in all cases). The strong curvature of SUV would cause their spontaneous fusion to form larger vesicles when stored below their phase-transition temperature.

Lipid-free  $\alpha\text{syn1-19}$  and  $\alpha\text{syn1-30}$  are unstructured in water under physiological conditions. This is in agreement with the results obtained with wild-type  $\alpha$ -synuclein.<sup>10,11</sup> The two fragments interact with vesicles in a very different way. The conformation of  $\alpha\text{syn1-19}$  remains unchanged even after the addition of DMPC:DMPG = 75:25 and DMPC:DMPG = 50:50 SUV in a molar lipid : peptide ratio of 130:1 (Figure 2A,B), suggesting that the peptide does not interact with these vesicles. Upon addition of 100% DMPG SUV,  $\alpha\text{syn1-19}$  undergoes a conformational transition to a helical state

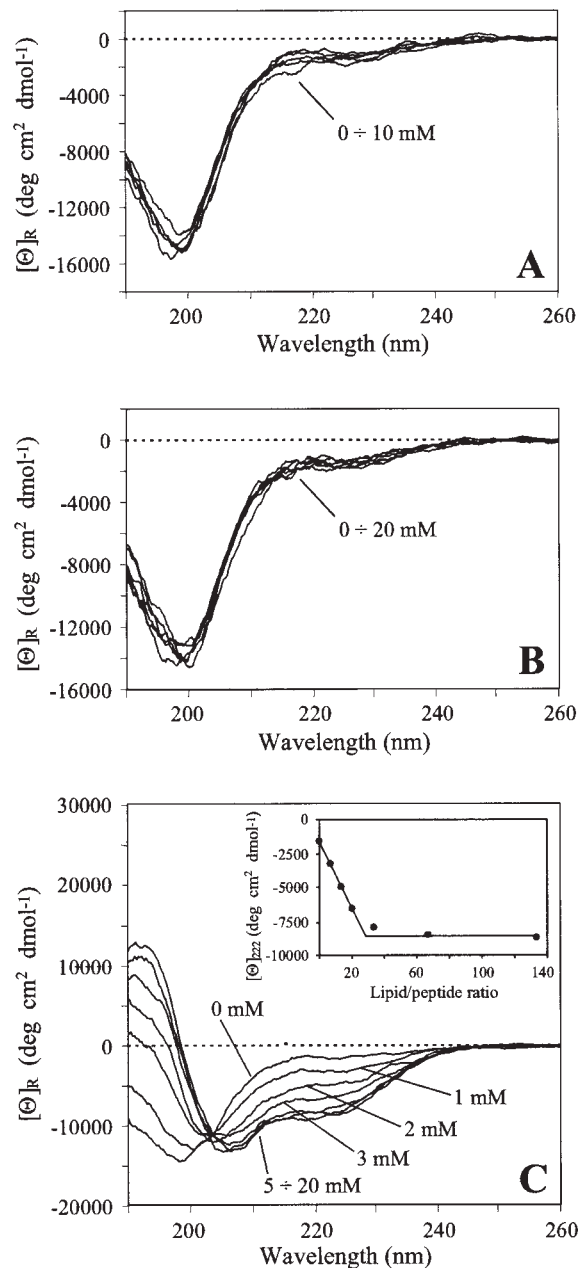


**FIGURE 2** Far-UV CD spectra of  $\alpha\text{syn1-19}$  (150  $\mu\text{M}$ ) in the presence of 20 mM phosphate buffer (pH 7.4) and after the addition of increasing amounts of SUV. (A) DMPC:DMPG = 75:25, (B) DMPC:DMPG = 50:50, and (C) 100% DMPG. Lipid concentrations are indicated. Inset in panel (C): molar residue ellipticity at 222 nm vs. molar lipid/peptide ratio.

in a dose-dependent manner (Figure 2C). The saturation value is reached at a molar lipid/peptide ratio of about 25 (Figure 2C, inset), and the estimated helical content is about 30%. The presence of a well-defined isodichroic point indicates that the equilibrium is between only two conformational states, i.e., a random coil and a helical structure.

Also in the case of  $\alpha$ syn1–30, the addition of DMPC:DMPG = 75:25 SUV does not induce any conformational change (Figure 3A). However, in contrast with  $\alpha$ syn1–19, the peptide adopts a helical conformation in the presence of DMPC:DMPG = 50:50 SUV (Figure 3B). The saturation value is reached at a molar lipid/peptide ratio of about 35 (Figure 3B, inset), and the estimated helical content is about 30%.  $\alpha$ Syn1–30 interacts more strongly with 100% DMPG SUV (Figure 3C): the helical content is higher (70%), and maximum folding is achieved at a lower lipid/peptide molar ratio.<sup>20</sup> As in the case of  $\alpha$ syn1–19, the presence of a well-defined isodichroic point in the spectra indicates an equilibrium between only a random coil and a helical structure.

These results confirm the importance of the negative charges located on the vesicle surface for interaction with  $\alpha$ -synuclein but, in addition, underline a possible cooperative effect of the different 11-mer repeats of the protein. In other words, the number of repeats seems relevant to determine the lipid composition of vesicles with which  $\alpha$ -synuclein is able to interact. To confirm this hypothesis, we compared these results with the ability of the 1–99 N-terminal deletion fragment of  $\alpha$ -synuclein to interact with acidic vesicles. This fragment encompasses all the 11-mer repeats present in the  $\alpha$ -synuclein sequence and contains the whole region of the protein involved in the interaction with the membranes.<sup>11</sup> Our results show that the protein binds to SUV already at a composition DMPC:DMPG = 70:30. A progressive folding was observed upon addition of increasing amounts of vesicles (Figure 4). Also in this case, an isodichroic point is present in the spectrum. The helical content can be estimated to be about 80%, and the saturation value is reached at a molar lipid/protein ratio of about 70. This value is higher than those obtained for the two small peptides interacting with 100% DMPG SUV (the lipid composition that maximizes the helical content). A possible explanation resides in the different dimensions of the  $\alpha$ -synuclein fragments considered here; this view is in agreement with the value estimated by Ramakrishnan et al.<sup>21</sup> for the wild-type protein (ratio of about 100) using 100% DMPG vesicles.

## DISCUSSION

Amphipathic  $\alpha$ -helices have been described in many lipid-associating proteins and peptides.<sup>22–25</sup> Like exchangeable apolipoproteins, the synuclein sequences are characterized by the presence of a set of imperfect 11-residue repeats. On the basis of this 11-mer periodicity, Segrest et al. have suggested the possibility that apolipoprotein A-I forms an  $\alpha$ 11/3 helix with a

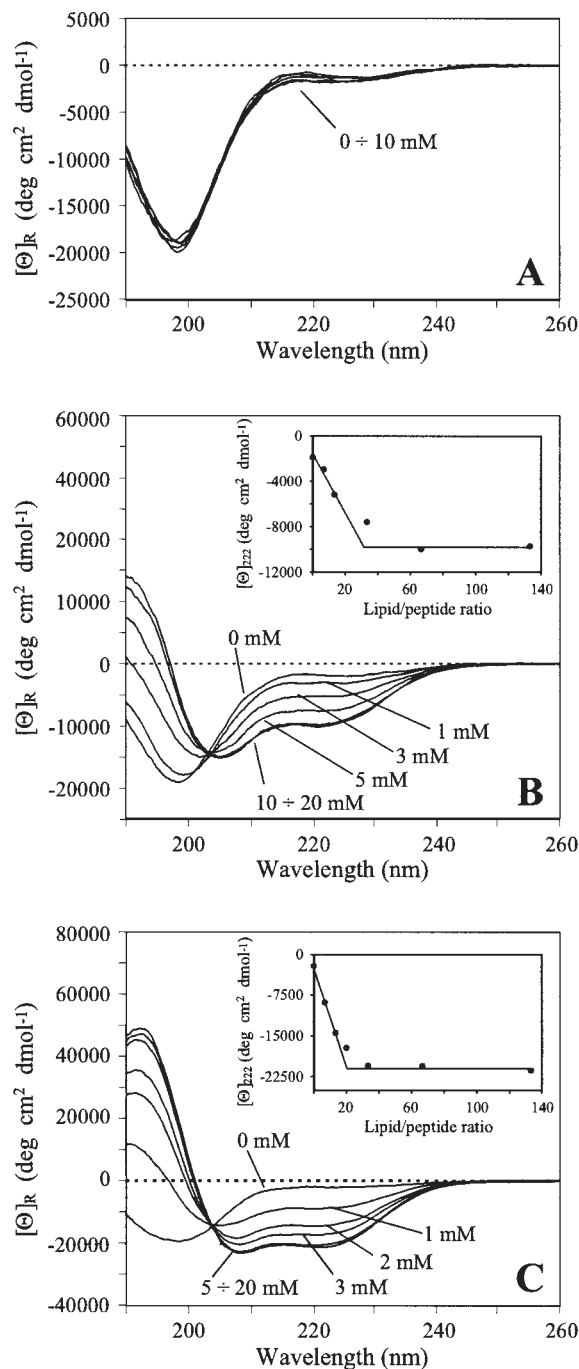


**FIGURE 3** Far-UV CD spectra of  $\alpha$ syn1–30 (150  $\mu$ M) in the presence of 20 mM phosphate buffer (pH 7.4) and after the addition of increasing amounts of SUV. (A) DMPC:DMPG = 75:25, (B) DMPC:DMPG = 50:50, and (C) 100% DMPG. Lipid concentrations are indicated. Inset in panels (B) and (C): molar residue ellipticity at 222 nm vs. molar lipid/peptide ratio.

pitch of 3 turns per 11 residues.<sup>26,27</sup> This model was recently proposed also for  $\alpha$ -synuclein.<sup>28,29</sup> However, this structure is essentially indistinguishable from an

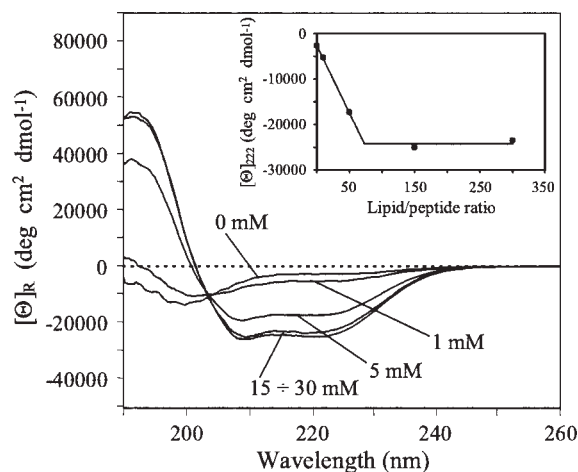


**FIGURE 4** Far-UV CD spectra of  $\alpha$ syn1–99 (100  $\mu$ M) in the presence of 20 mM phosphate buffer (pH 7.4) and after the addition of increasing amounts of DMPC:DMPG = 70:30 SUV. Lipid concentrations are indicated. Inset: molar residue ellipticity at 222 nm vs. molar lipid/peptide ratio.

idealized  $\alpha$ -helix<sup>26</sup> and in our hands the two conformations are equally plausible.

For each peptide, we calculated the mean hydrophobic moment  $\langle\mu_H\rangle$  in the  $\alpha$ 11/3- and  $\alpha$ -helical conformation using the following equation<sup>30</sup>:

$$\mu_H = \left\{ \left[ \sum_{n=1}^N H_n \sin(\delta n) \right]^2 + \left[ \sum_{n=1}^N H_n \cos(\delta n) \right]^2 \right\}^{1/2}$$

in which  $N$  is the number of residues,  $H_n$  is the hydrophobicity of the  $n$ th residue according to the normalized scale proposed by Eisenberg,<sup>30</sup> and  $\delta$  is the regular interval at which the side chains protrude perpendicular to the helix axis ( $100^\circ$  for the  $\alpha$ -helix and  $98.18^\circ$  for the  $\alpha$ 11/3-helix). The  $\langle\mu_H\rangle$  values obtained for  $\alpha$ syn1–19 and  $\alpha$ syn1–30 in an  $\alpha$ 11/3 helical conformation are 0.387 and 0.381, respectively. These values are very similar, because they reflect a similar distribution of hydrophobic and charged residues in a helical wheel representation (Figure 5A,B). They are also very similar to the mean hydrophobic moment calculated for the same peptides in the classical  $\alpha$ -helical conformation shown in Figure 5C,D ( $\langle\mu_H\rangle_{1-19} = 0.388$ ;  $\langle\mu_H\rangle_{1-30} = 0.374$ ).

Considering the mean hydrophobic moment and the isoelectric points of  $\alpha$ syn1–19 and  $\alpha$ syn1–30, calculated through the ExPaSy web page (8.25 and 8.14, respectively), we expected to obtain very similar results in the study of lipid/peptide interactions. Interestingly, the ability of  $\alpha$ syn1–19,  $\alpha$ syn1–30, and  $\alpha$ syn1–99 to interact with the vesicles we tested is

very different, suggesting a cooperative role of the 11-mer repeats in the lipid composition discrimination. At least two hypotheses can explain these results. One explanation is reduction of dimensionality: if two motifs with intrinsic weak avidity for lipid membranes are separated by a flexible link, they can lead to strong membrane adsorption. As soon as one motif binds, the second one is confined to a small volume with a high lipid concentration and therefore tends to bind better. This could account for the increase of binding affinity when going from  $\alpha$ syn1–30 to  $\alpha$ syn1–99, in which the various repeats are not all contiguous. A second explanation is that helix nucleation is less favorable than helix propagation.<sup>31</sup> So, if two motifs are adjacent and one of them folds upon membrane adsorption as a helix, the other helix does not need to fold independently, but elongates the first one. Considering that binding to 100% DMPG results in different helical contents for  $\alpha$ syn1–19 and  $\alpha$ syn1–30 (30 and 70%, respectively), it is likely that helix propagation effects apply for these two fragments of  $\alpha$ -synuclein. The analysis of the sequence of the two peptides in a helical conformation (Figure 5) suggests that the lysine residues (positions 10, 12, 21, and 23) exert an essential role in promoting the interactions with the negatively charged membrane surface. From this point of view, the 11/3 periodicity fits better with the peptide sequence.

This cooperativity, which was confirmed by the analysis of the  $\alpha$ syn1–99 fragment, could be crucial in selecting the lipid composition of the membrane with which  $\alpha$ -synuclein interacts. In that way, the specific interactions between  $\alpha$ -synuclein and its target membranes could be a direct consequence of the specific number of 11-mer repeats. If we consider that the main difference between  $\alpha$ - and  $\beta$ -, or  $\gamma$ -synuclein is the absence or the presence of one additional repeat, this aspect may be relevant.

The lipid composition of synaptic vesicles has been estimated to be 40–48% PC, 24–36% PE, 7–12% PS, 4–12% sphingomyelin, 3–4% PI, and 0–2% PA, with a cholesterol:phospholipid ratio of  $\sim 0.5$ – $0.6$ .<sup>14</sup> The proportion of acidic phospholipids is approximately 10–18% even if it is difficult to relate these values directly to the local composition, because of the asymmetric distribution of phospholipid species between the two leaflets of the synaptic vesicles.<sup>14</sup>

The preference for acidic phospholipids suggests that ionic interactions may occur between the protein and the lipid surface. The effect of NaCl on the binding of  $\alpha$ syn to mixed PA/PC liposomes has been studied.<sup>14,20,21</sup> It was demonstrated that increasing NaCl concentrations affect affinity, but binding is not abolished even at 1.5M NaCl, indicating that additional

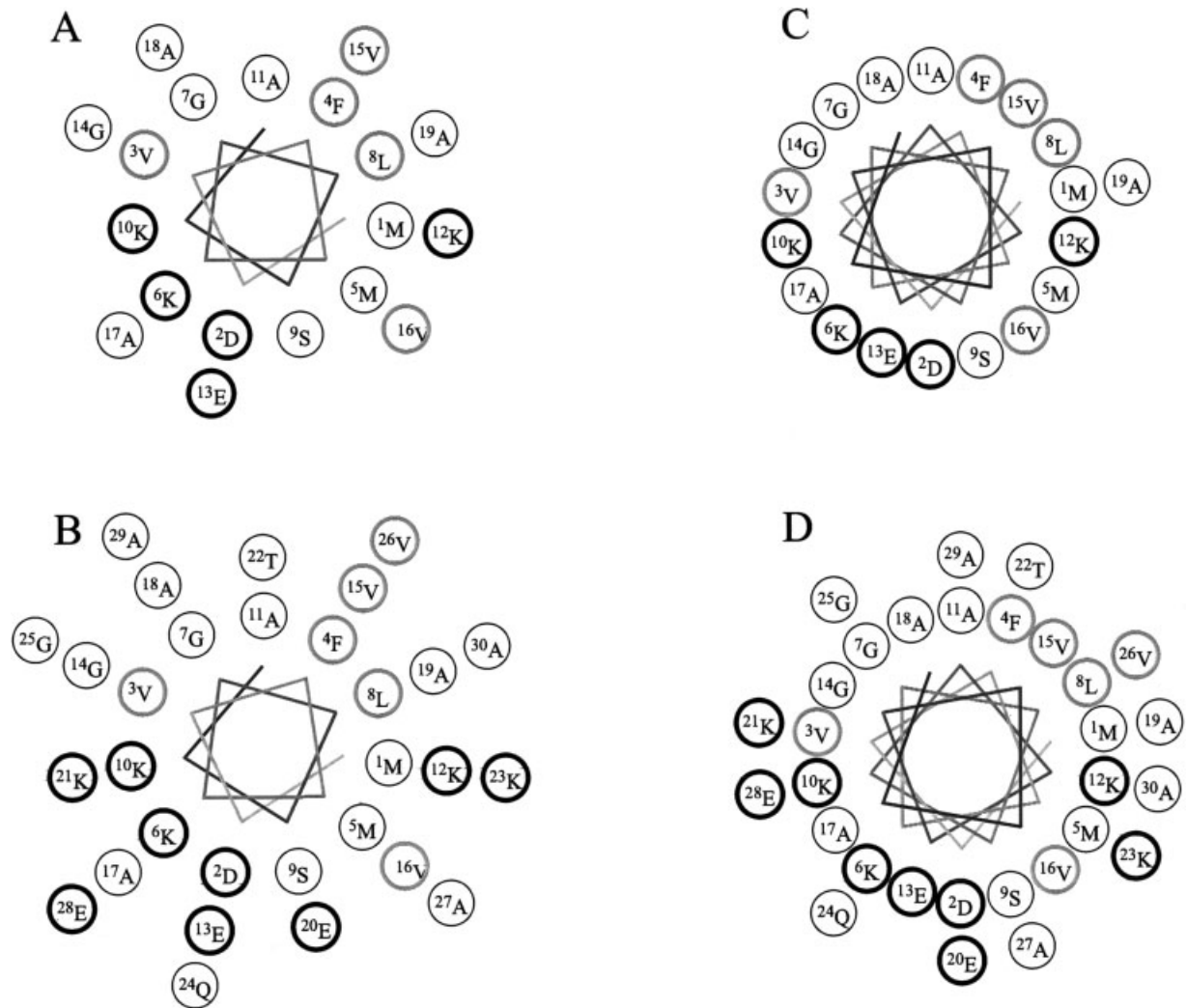


**FIGURE 5** Helical pinwheel plot of  $\alpha$ -synuclein fragments. (A)  $\alpha$ syn1–19,  $\alpha$ 11/3-helix; (B)  $\alpha$ syn1–30,  $\alpha$ 11/3-helix; (C)  $\alpha$ syn1–19,  $\alpha$ -helix, (D)  $\alpha$ syn1–30,  $\alpha$ -helix. Hydrophobic residues are in gray and charged residues are in black.

forces are implicated in stabilizing the protein–lipid interaction. To maximize the conformational changes induced by the membranes, we decided to carry out our experiments in the absence of salt.

Our results on model peptides in model lipid systems confirm the importance of the presence of negative charges on the vesicle surface for lipid/protein binding. Moreover, they demonstrate the cooperativity among the different repeats as an additional determinant of lipid affinity and selectivity. In neurons,  $\alpha$ -synuclein is highly localized in presynaptic terminals.<sup>16</sup> On the basis of our results and the results of others,<sup>16,32</sup> this localization seems to be regulated by lipid composition. The direct consequence of this specific distribution and of the interaction with phospholipase D2 could be the involvement of  $\alpha$ -synuclein in synaptic plasticity and maintenance that is

necessary for a correct storage and release of dopamine.

This work was partially supported by Ministero dell’Istruzione, Università e Ricerca (MIUR) (Grant: PRIN Project No. 2004032851) and Università degli Studi di Padova (Project No. CPDA027314). We are grateful to B. Biondi for performing and analyzing molecular mass determinations. The help of F. Dal Cero and A. Famengo in obtaining the CD spectra is also gratefully acknowledged.

## REFERENCES

1. Lansbury, P. T., Jr. *Neuron* 1997, 19, 1151–1154.
2. Iwai, A.; Masliah, E.; Yoshimoto, M.; Ge, N.; Flanagan, L.; de Silva, H. A.; Kittel, A.; Saitoh, T. *Neuron* 1995, 14, 467–475.

3. Nakajo, S.; Shioda, S.; Nakai, Y.; Nakaya, K. *Brain Res Mol Brain Res* 1994, 27, 81–86.
4. Murphy, D. D.; Rueter, S. M.; Trojanowski, J. Q.; Lee, V. M. *J Neurosci* 2000, 20, 3214–3220.
5. Lotharius, J.; Barg, S.; Wiekop, P.; Lundberg, C.; Raymond, H. K.; Brundin, P. *J Biol Chem* 2002, 277, 38884–38894.
6. Lotharius, J.; Brundin, P. *Nat Rev Neurosci* 2002, 3, 932–942.
7. Exton, J. H. *Physiol Rev* 1997, 77, 303–320.
8. Chen, Y. G.; Siddhanta, A.; Austin, C. D.; Hammond, S. M.; Sung, T. C.; Frohman, M. A.; Morris, A. J.; Shields, D. *J Cell Biol* 1997, 138, 495–504.
9. Jenco, J. M.; Rawlingson, A.; Daniels, B.; Morris, A. J. *Biochemistry* 1998, 37, 4901–4909.
10. Weinreb, P. H.; Zhen, W.; Poon, A. W.; Conway, K. A.; Lansbury, P. T., Jr. *Biochemistry* 1996, 35, 13709–13715.
11. Eliezer, D.; Kutluay, E.; Bussell, R., Jr.; Browne, G. *J Mol Biol* 2001, 307, 1061–1073.
12. Bisaglia, M.; Tessari, I.; Pinato, L.; Bellanda, M.; Giraud, S.; Fasano, M.; Bergantino, E.; Bubacco, L.; Mammi, S. *Biochemistry* 2005, 44, 329–339.
13. Ulmer, T. S.; Bax, A.; Cole, N. B.; Nussbaum, R. L. *J Biol Chem* 2005, 280, 9595–9603.
14. Davidson, W. S.; Jonas, A.; Clayton, D. F.; George, J. M. *J Biol Chem* 1998, 273, 9443–9449.
15. Segrest, J. P.; Jones, M. K.; De Loof, H.; Brouillette, C. G.; Venkatachalapathi, Y. V.; Anantharamaiah, G. M. *J Lipid Res* 1992, 33, 141–166.
16. Perrin, R. J.; Woods, W. S.; Clayton, D. F.; George, J. M. *J Biol Chem* 2000, 275, 34393–34398.
17. Fields, C. G.; Lloyd, D. H.; McDonald, R. L.; Otteson, K. M.; Noble, R. L. *Peptide Res* 1991, 4, 95–101.
18. Scopes, R. K. *Anal Biochem* 1974, 59, 277–282.
19. Bradford, M. M. *Anal Biochem* 1976, 72, 248–254.
20. Zhu, M.; Li, J.; Fink, A. L. *J Biol Chem* 2003, 278, 40186–40197.
21. Ramakrishnan, M.; Jensen, P. H.; Marsh, D. *Biochemistry* 2003, 42, 12919–12926.
22. Hong, E.; Jeong, P. Y.; Jung, J. W.; Kim, Y.; Cheong, C.; Paik, Y. K.; Lee, W. *Biochem Biophys Res Commun* 2000, 276, 1278–1285.
23. Cross, T. A.; Opella, S. J. *Curr Opin Struct Biol* 1994, 4, 574–581.
24. Monticelli, L.; Pedini, D.; Schievano, E.; Mammi, S.; Peggion, E. *Biophys Chem* 2002, 101–102, 577–591.
25. Schievano, E.; Calisti, T.; Menegazzo, I.; Battistutta, R.; Peggion, E.; Mammi, S.; Palù, G.; Loregian, A. *Biochemistry* 2004, 43, 9343–9351.
26. Segrest, J. P.; Jones, M. K.; Klön, A. E.; Sheldahl, C. J.; Hellinger, M.; De Loof, H.; Harvey, S. C. *J Biol Chem* 1999, 274, 31755–31758.
27. Li, L.; Chen, J.; Mishra, V. K.; Kurtz, J. A.; Cao, D.; Klön, A. E.; Harvey, S. C.; Anantharamaiah, G. M.; Segrest, J. P. *J Mol Biol* 2004, 343, 1293–1311.
28. Bussell, R., Jr.; Eliezer, D. *J Mol Biol* 2003, 329, 763–778.
29. Bussell, R., Jr.; Ramlall, T. F.; Eliezer, D. *Protein Sci* 2005, 14, 862–872.
30. Eisenberg, D.; Schwarz, E.; Komaromy, M.; Wall, R. *J Mol Biol* 1984, 179, 125–142.
31. Creighton, T. E. *Protein Folding*; Freeman: New York, 1992.
32. Bussell, R., Jr.; Eliezer, D. *Biochemistry* 2004, 43, 4810–4818.





# Avidin–biotin system: a small library of cysteine biotinylated derivatives designed for the $[\text{}^{99\text{m}}\text{Tc}(\text{N})(\text{PNP})]^{2+}$ metal fragment

Cristina Bolzati<sup>a,\*</sup>, Andrea Caporale<sup>c</sup>, Stefania Agostini<sup>b</sup>, Davide Carta<sup>b</sup>,  
Mario Cavazza-Ceccato<sup>b</sup>, Fiorenzo Refosco<sup>a</sup>, Francesco Tisato<sup>a</sup>,  
Elisabetta Schievano<sup>c</sup>, Giuliano Bandoli<sup>b</sup>

<sup>a</sup>ICIS-CNR, Corso Stati Uniti, 4, 35127 Padova, Italy

<sup>b</sup>Department of Pharmaceutical Sciences, University of Padua, 35131 Padova, Italy

<sup>c</sup>Department of Chemical Sciences, University of Padua, 35131 Padova, Italy

Received 2 October 2006; received in revised form 5 April 2007; accepted 6 April 2007

## Abstract

Using the avidin–biotin system as model, we investigate here the effective application of  $[\text{Tc}(\text{N})\text{L}(\text{PNP})]^{+0}$  technology (L=N-functionalized cysteine  $[\text{O}^-, \text{S}^-]$ ; PNP=aminodiphosphine) to the preparation of target-specific radiopharmaceuticals.

A series of  $^{99\text{m}}\text{Tc}$ -nitrido complexes containing functionalized biotin ligands was prepared and their biological profile was determined. To minimize the steric and the electronic influences of the Tc-carrying complex on the biotin–avidin receptor interaction, the following N-functionalized cysteine–biotin derivatives were synthesized: (1) Biot-CysOSH; (2) Biot-Abu-CysOSH; (3) Biot-Abz-CysOSH; (4) Biot-L-(Ac)Lys-CysOSH; (5) Biot-D-(Ac)Lys-CysOSH; (6) Biot-Glu-CysOSH.

The asymmetrical nitrido-Tc(V)  $^{99\text{m}}\text{Tc}(\text{N})(\text{Biot-X-CysOS})(\text{PNP3})$  (X=spacer) complexes, where PNP3 was *N,N*-bis-[(dimethoxypropyl)phosphinoethyl] methoxy-ethylamine, were obtained by simultaneous addition of PNP3 and the relevant biotinylated ligand to a solution containing a  $^{99\text{m}}\text{Tc}$ -nitrido precursor (yields >95%). In all cases, a mixture of syn- and anti isomers was observed. In vitro challenge experiments with glutathione and cysteine indicated that no transchelation reactions occurred. Assessment of the in vitro binding to avidin of the complexes revealed that only the complexes containing Biot-Abu-CysOS and Biot-Glu-CysOS ligand maintained a good affinity for the concentrator. Stability studies carried out in human and mouse plasma as well as in rat and mouse liver homogenate evidenced a rapid enzymatic degradation for the  $^{99\text{m}}\text{Tc}(\text{N})(\text{Biot-Abu-CysOS})(\text{PNP3})$  complex, whereas the  $^{99\text{m}}\text{Tc}(\text{N})(\text{Biot-Glu-CysOS})(\text{PNP3})$  one was stable in all conditions. Tissue biodistribution in normal Balb/C mice of the most stable candidate showed a rapid clearance both from the blood and the other tissues. The activity was eliminated both through the hepatobiliary system and the urinary tract.

© 2006 Published by Elsevier Inc.

**Keywords:** Avidin–biotin system; Cysteine biotinylated derivative; Technetium

## 1. Introduction

Recently, we have described the synthesis of a new class of asymmetrical nitrido complexes, based on the chemical properties of the substitution labile  $[\text{Tc}(\text{N})\text{X}_2(\text{PNP})]$  complex (PNP=amino-diphosphine), which represent an interesting opportunity in design receptor-specific Tc-99m agents [1,2]. According to this strategy, the strong electrophilic  $[\text{Tc}(\text{N})$

$(\text{PNP})]^{2+}$  moiety efficiently reacts with bifunctional ligands (L) carrying  $\pi$ -donors as coordinating atoms to afford asymmetrical nitrido heterocomplexes of the type  $[\text{Tc}(\text{N})(\text{L})(\text{PNP})]^{0/+}$ . In particular, it was found that N-functionalized cysteine  $[\text{O}^-, \text{S}^-]$  ligands react with  $[\text{}^{99\text{m}}\text{Tc}(\text{N})(\text{PNP})]^{2+}$  to yield the final mixed complex in very high specific activity (180 GBq/ $\mu\text{mol}$ ) [3]. This demonstrates that cysteine can be used as an efficient bifunctional chelating system (BFCS) to include a bioactive molecule in a Tc(N) complex.

Attempts to develop Tc-99m target-specific agents for the central nervous system using the  $[\text{Tc}(\text{N})(\text{PNP})]^{2+}$  synthon have recently been investigated [4,5]. Receptor-specific

\* Corresponding author. Tel.: +39 049 8275352; fax: +39 049 8275366.  
E-mail address: [bolzati@icis.cnr.it](mailto:bolzati@icis.cnr.it) (C. Bolzati).

compounds for imaging 5HT<sub>1A</sub> and benzodiazepine receptors were prepared, coupling the bioactive molecules to the cysteine amino group to obtain N-functionalized O,S-cysteine ligands. These ligands were reacted with the [Tc(N)(PNP)]<sup>2+</sup> fragment to yield asymmetrical complexes of the type Tc(~CysOS)(PNP). In these mixed compounds, the pharmacophore group was conjugated to the chelating system through two or three unit spacers, thus leaving the bioactive molecule close to the [Tc(N)(PNP)]<sup>2+</sup> building block. In vitro binding experiments with the corresponding <sup>99g</sup>Tc-analogs on isolated membranes showed a partial loss of receptor affinity, which was tentatively attributed to an interaction between the bioactive molecule and the pendant group associated to the tertiary amino nitrogen of the PNP ligand. This contact could be responsible for the increased steric hindrance of the pharmacophore group which proved unable to fit closely the receptor site [4]. This hypothesis suggested that the affinity for the receptor site could be improved by manipulating the structure of the complex, in particular, by increasing the length of the spacer between the bioactive moiety and the cysteine fragment.

Consequently, to further investigate the effective applicability of [Tc(N)(PNP)]<sup>2+</sup> technology to the preparation of

target-specific molecule, avidin–biotin system was selected as a model. The attractiveness of this system lies in the very high affinity of the avidin for the biotin ( $K_d=10^{-15}$ ) used in a number of applications [6,7].

The design of new radiolabeled biotin conjugates has recently been facilitated by the considerable amount of information concerning the structural elements of biotin which are involved in binding to avidin as well as processing by biotinidase. Biotin derivatives are, in general, prepared by direct amidation of the carboxyl group of the vitamin, thus leaving the urea moiety and nonoxidized thioether for the binding to avidin or streptavidin [8–12]. Biotinidase is present in the serum and tissues of both animals and humans in nanomolar concentrations. Its primary function is to cleave the amide bond linking biotin and lysine in biocytin in such a way that the essential vitamin H can be recycled [13]. Avoiding biotinidase degradation has been obtained by generating steric hindrance at the amido bond level or reversing the amido bond between biotin and the labeled prosthetic group [11,14].

Considering these criteria, a small library of [O<sup>-</sup>,S<sup>-</sup>]-N-functionalized cysteine–biotin derivatives was synthesized by coupling the amino group of the cysteine, via an

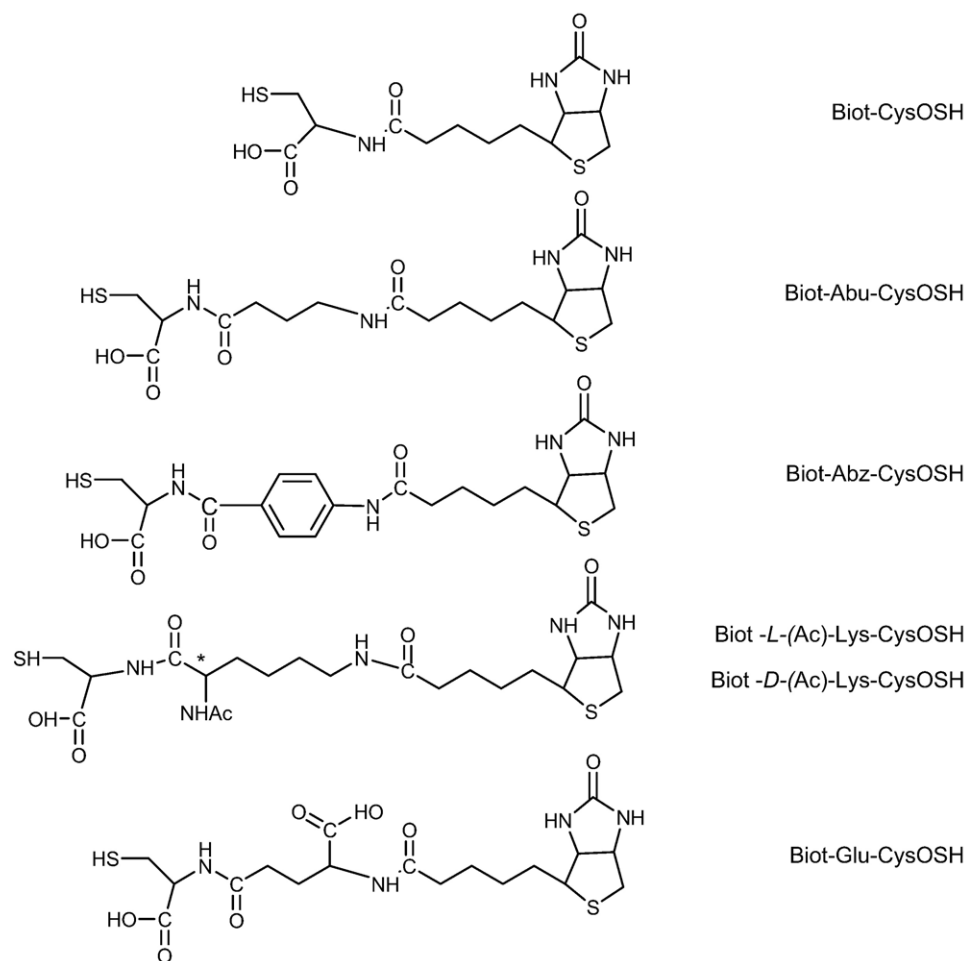


Fig. 1. [O<sup>-</sup>,S<sup>-</sup>]-N-functionalized cysteine–biotin ligands.



opportune group spacer (X), to the carboxyl group of the vitamin. To study the steric and the electronic influence of the Tc-carrying complex on the biotin–avidin receptor interaction, the effect of the length and flexibility of the spacer was evaluated. The biotin derivative ligands used in our experiments are reported in Fig. 1.

As illustrated, alkyl chain or aromatic group spacers have been used to bridge the vitamin and metal chelating system. A sterical hindrance group has been introduced on the carbon adjacent to the amido NH-CO group in Biot-L- or D-(Ac)Lys-CysOSH and Biot-Glu-CysOSH derivatives to obtain enzymatically resistant ligands.

The bulky aminodiphosphine ligand *N,N*-bis[(dimethoxypropyl)phosphinoethyl]methoxyethylamine [PNP3=(CH<sub>3</sub>-OC<sub>3</sub>H<sub>6</sub>)<sub>2</sub>P(CH<sub>2</sub>)<sub>2</sub>N(C<sub>2</sub>H<sub>4</sub>OCH<sub>3</sub>)(CH<sub>2</sub>)<sub>2</sub>P(C<sub>3</sub>H<sub>6</sub>OCH<sub>3</sub>)<sub>2</sub>] was used as co-ligand, for its recognised ability in stabilization of the [Tc<sup>99m</sup>N]<sup>2+</sup> core.

The resulting <sup>99m</sup>Tc(N) mixed compounds have been evaluated with regard to the following criteria: (a) ease of radiosynthesis, (b) retention of binding to avidin, (c) stability toward transchelation with Cys and GSH and degradation by biotinidase.

Clearance of the best radiolabeled compound from normal tissues and its in vivo stability was evaluated in healthy male Balb/C mice.

## 2. Materials and methods

### 2.1. Caution!

<sup>99g</sup>Tc is a weak β-emitter ( $E_{\beta^-}=0.292$  MeV,  $t_{1/2}=2.13\times 10^5$  years). All manipulations were carried out in laboratories approved for low-level radioactivity using monitored hoods and glove boxes. When handled in milligram amounts, <sup>99g</sup>Tc does not present a serious health hazard since common

laboratory glassware provides adequate shielding. Bremsstrahlung is not a significant problem due to the low energy of the β<sup>-</sup> particles. However, normal radiation safety procedure must be used at all times, especially with solid samples, to prevent contamination and inhalation.

### 2.2. General

All chemicals and reagents were purchased from Aldrich Chemicals. All solvents were reagent grade and were used without further purification. PNP3 was purchased from Argus Chemicals (Prato, Italy). To avoid oxidation, all the solvents used in reactions with PNP3 were previously degassed. N-Functionalized cysteine–biotin (Biot-X-Cys-OS) derivatives were synthesized according to standardized peptide methods, and their characterization was reported elsewhere [9,15–17]. Commercially available NH<sub>4</sub>[<sup>99g</sup>TcO<sub>4</sub>] (Oak Ridge National Lab) was purified from a black contaminant (<sup>99g</sup>TcO<sub>2</sub>·*n*H<sub>2</sub>O) by addition of H<sub>2</sub>O<sub>2</sub> and NH<sub>4</sub>OH solutions. [<sup>99g</sup>Tc(N)Cl<sub>2</sub>(PPh<sub>3</sub>)<sub>2</sub>] was prepared according to the literature [18]. <sup>99m</sup>Tc as Na[<sup>99m</sup>TcO<sub>4</sub>] was eluted from a <sup>99</sup>Mo/<sup>99m</sup>Tc generator provided by Nycomed Amersham-Sorin (Saluggia, Italy).

### 2.3. Analysis

Elemental analyses (C, H, N, S) were performed on a Carlo Erba 1106 elemental analyzer. <sup>1</sup>H, <sup>13</sup>C and <sup>31</sup>P NMR spectra were collected on a Bruker 300 instrument, using SiMe<sub>4</sub> as internal reference (<sup>1</sup>H and <sup>13</sup>C) and 85% aqueous H<sub>3</sub>PO<sub>4</sub> as external reference (<sup>31</sup>P).

Thin-layer chromatography (TLC) (SiO<sub>2</sub> F<sub>254S</sub> and C18 F<sub>254S</sub>, Merck) and high-performance liquid chromatography (HPLC) analysis were used to evaluate the radiochemical purity (RCP) and stability of the compounds. Radioactivity on TLC plates was detected and measured using a Cyclone

Table 1  
Chromatographic data for <sup>99g/99m</sup>Tc-complexes

Complex	TLC		Retention time (min)		% yield	
	SiO <sub>2</sub>	C18	<sup>99g</sup> Tc	<sup>99m</sup> Tc	<sup>99g</sup> Tc	<sup>99m</sup> Tc
Tc(N)X <sub>2</sub> (PNP3)	0.0	0.0,		6.38 <sup>b</sup>		90.27
Syn-Tc(N)(Biot-CysOS)(PNP3)	0.28		21.07 <sup>a</sup>	21.37 <sup>a</sup>	37.89	17.28
Anti-Tc(N)(Biot-CysOS)(PNP3)	0.23		22.22 <sup>a</sup>	22.52 <sup>a</sup>	45.09	72.95
Syn-Tc(N)(Biot-Abz-CysOS)(PNP3)	0.29		12.67 <sup>b</sup>	12.95 <sup>b</sup>		12.42
Anti-Tc(N)(Biot-Abz-CysOS)(PNP3)	0.37		14.02 <sup>b</sup>	14.28 <sup>b</sup>		80.23
Syn-Tc(N)(Biot-Abu-CysOS)(PNP3)	0.34	0.36,		14.32 <sup>c</sup>	34.00	20.75
Anti-Tc(N)(Biot-Abu-CysOS)(PNP3)	0.28	0.47,		19.38 <sup>c</sup>	42.90	74.16
Syn-Tc(N)(Biot-L-(Ac)-Lys-CysOS)(PNP3)				13.20 <sup>b</sup> ; 14.19 <sup>d</sup>		19.21
Anti-Tc(N)(Biot-L-(Ac)-Lys-CysOS)(PNP3)				14.73 <sup>b</sup> ; 16.99 <sup>d</sup>		77.07
Syn-Tc(N)(Biot-D-(Ac)-Lys-CysOS)(PNP3)	0.13			14.08 <sup>d</sup>		16.91
Anti-Tc(N)(Biot-D-(Ac)-Lys-CysOS)(PNP3)	0.21	0.5		16.70 <sup>d</sup>		75.98
Syn-Tc(N)(Biot-Glu-CysOS)(PNP3)		0.61 <sup>ii</sup>		13.55 <sup>d</sup>		14.08
Anti-Tc(N)(Biot-Glu-CysOS)(PNP3)		0.71 <sup>ii</sup>		16.45 <sup>d</sup>		58.80

TLC: SiO<sub>2</sub> MeOH/CHCl<sub>3</sub> (10/90). C18: <sup>i</sup>CH<sub>3</sub>CN/NH<sub>4</sub>Ac 0.05 M pH 7 (70/30); <sup>ii</sup>CH<sub>3</sub>CN/Et<sub>3</sub>N 0.01 M pH 3 (70/30). HPLC: reverse phase C<sub>18</sub> column; <sup>a</sup>A=NH<sub>4</sub>Ac 0.05 M pH 6=6=5, B=CH<sub>3</sub>CN. <sup>a</sup>Gradient: 0–3 min, B=25%; 3–23 min, B=35%; 23–25 min, B=35%; 25–27 min, B=80%; 27–33 min, B=80%; 33–35 min, B=25%. <sup>c</sup>Gradient: 0–2 min, B=30%; 2–12 min, B=35%; 12–17 min, B=35%; 17–19 min, B=80%; 19–28 min, B=80%; 28–30 min, B=30%. <sup>b,d</sup>A=Et<sub>3</sub>N 0.01 M pH 3, B=CH<sub>3</sub>CN. Gradient: <sup>b</sup>0–3 min, B=25%; 3–23 min, B=50%; 23–25 min, B=80%; 25–33 min, B=80%; 33–35 min, B=25%. <sup>d</sup>Gradient: 0–3 min, B=25%; 3–23 min, B=35%; 23–25 min, B=80%; 25–33 min, B=80%; 33–35 min, B=25%.

instrument equipped with a phosphorus imaging screen and OptiQuant image analysis software (Packard, Meridian, CT, USA). HPLC was performed on a Beckman System Gold instrument equipped with a programmable solvent Model 126, a sample injection valve 210A, a scanning detector Module 166 ( $\lambda=215 \mu\text{m}$ ) and a radioisotope detector Model 3200 Bioscan. HPLC analysis was carried out on a reversed-phase C18 precolumn Backman (45 $\times$ 4.1 mm) and a reversed-phase SymmetryShield RP<sub>18</sub> column (250 $\times$ 4.6 mm) using the chromatographic condition reported in Table 1; flow rate: 1 ml/min.

Instant thin layer chromatography (ITLC) (ITLC-SG, Pall Life Science) was used to assess the in vitro binding of the radiolabeled biotin derivatives to avidin.

#### 2.4. Synthesis of representative <sup>99g</sup>Tc complexes

##### 2.4.1. <sup>99g</sup>Tc(N)(Biot-CysOS)(PNP3)

To [Tc(N)Cl<sub>2</sub>(PPh<sub>3</sub>)<sub>2</sub>] (42.51 mg, 0.06 mmol) suspended in CH<sub>2</sub>Cl<sub>2</sub> (10 ml) was added PNP3 (29.0 mg, 0.06 mmol) dissolved in EtOH (5 ml) under a di-nitrogen atmosphere. The solution was stirred at reflux for 30 min during which time the initial orange-pink solution changed color to yellow. Then, an equimolar amount of Biot-CysOS (20.0 mg, 0.06 mmol) dissolved in EtOH (5 ml) containing an excess of Et<sub>3</sub>N (three drops) was added. The reaction mixture was refluxed for an additional 30 min without observing a significant change in color. After cooling, the solvent was removed under a gentle di-nitrogen stream and the oily residue was treated with a 1:1 Et<sub>2</sub>O/*n*-hexane mixture (10 ml) to afford a pale yellow solid. The crude product was dissolved in CH<sub>2</sub>Cl<sub>2</sub> (1 ml), loaded on a silica column and eluted with CHCl<sub>3</sub>/MeOH 9:1; two yellow bands were separated and isolated. The first was identified as the anti isomer (vide infra) and fully characterized by means of multinuclear NMR spectroscopy. Anti-<sup>99g</sup>Tc(N)(Biot-CysOS)(PNP3) was soluble in chlorinated solvents and alcohols, and insoluble in diethyl ether and *n*-hexane. <sup>1</sup>H NMR (CDCl<sub>3</sub>):  $\delta$  (ppm)=7.10 (d, 1H, NH $^{\alpha}$ ); 6.15 (s, 1H, NHC(O)NH); 5.35 (s, 1H, NHC(O)NH); 4.80 (m, 1H, CH $^{\alpha}$ ); 4.50 (m, 1H, NHCHCH<sub>2</sub>); 4.30 (m, 1H, NHCHCH); 3.45 (m, 8H, P(CH<sub>2</sub>CH<sub>2</sub>CH<sub>2</sub>OCH<sub>3</sub>)<sub>2</sub>); 3.35 (m, 12H, P(CH<sub>2</sub>CH<sub>2</sub>CH<sub>2</sub>OCH<sub>3</sub>)<sub>2</sub>); 3.35 (m, 2H, NCH<sub>2</sub>CH<sub>2</sub>OCH<sub>3</sub>); 3.25 and 2.40 (m, 2H, CH<sub>2</sub>S); 3.20 (s, 3H, NCH<sub>2</sub>CH<sub>2</sub>OCH<sub>3</sub>); 3.15 (m, 1H, NHCHCH); 2.95 and 2.75 (m, 2H, NHCHCH<sub>2</sub>); 2.90 and 2.50 (m, 2H, NCH<sub>2</sub>CH<sub>2</sub>OCH<sub>3</sub>); 2.80–2.40 (m, 2H, PCH<sub>2</sub>CH<sub>2</sub>N); 2.30 (t, 2H, CH<sub>2</sub>C(O)NH); 2.30–1.70 (m, 16H, P(CH<sub>2</sub>CH<sub>2</sub>CH<sub>2</sub>OCH<sub>3</sub>)<sub>2</sub>); 2.25 (t, 2H, PCH<sub>2</sub>CH<sub>2</sub>N); 2.05 (t, 2H, PCH<sub>2</sub>CH<sub>2</sub>N); 1.80 and 1.60 (m, 4H, (CH<sub>2</sub>)<sub>2</sub>); 1.45 (m, 2H, SCHCH<sub>2</sub>CH<sub>2</sub>).

<sup>13</sup>C NMR (CDCl<sub>3</sub>):  $\delta$  (ppm)=178.0, 172.0, 163.5, 73.0, 68.5, 62.0, 60.5, 59.0, 56.5, 55.5, 52.0, 47.0, 46.5, 41.0, 36.5, 30.0, 28.5, 27.0, 22.0, 18.5, 16.5. <sup>31</sup>P (CDCl<sub>3</sub>):  $\delta$  (ppm)=33, 1 (bs); 25, 4 (bs). Anal. Calcd for C<sub>36</sub>H<sub>72</sub>N<sub>5</sub>O<sub>8</sub>P<sub>2</sub>S<sub>2</sub>Tc: C, 43.60; H, 8.26; N, 8.00; S, 7.26; found: C, 43.51; H, 8.19; N, 7.98; S, 7.10.

The second eluted yellow band corresponded to the syn-<sup>99g</sup>Tc(N)(Biot-CysOS)(PNP3) as assessed by characteristic NH<sub>amide</sub> signals appearing in the NMR spectra in CDCl<sub>3</sub> at  $\delta=7.70$  ppm (doublet, cysteine-NH $^{\alpha}$ ), and 6.15 and 5.95 ppm (two singlets, biotin-NHC(O)NH), which were different from those collected for the anti isomer [4]. However, full NMR characterization in the solution state of the syn isomer was precluded by its fast rearrangement into the thermodynamically more stable anti-species. Syn-<sup>99g</sup>Tc(N)(Biot-CysOS)(PNP3) was soluble in chlorinated solvents and alcohols, and insoluble in diethyl ether and *n*-hexane.

Anal. Calcd for C<sub>36</sub>H<sub>72</sub>N<sub>5</sub>O<sub>8</sub>P<sub>2</sub>S<sub>2</sub>Tc: C, 43.60; H, 8.26; N, 8.00; S, 7.26; found: C, 43.55; H, 8.24; N, 7.91; S, 7.15.

##### 2.4.2. <sup>99g</sup>Tc(N)(Biot-Abu-CysOS)(PNP3)

The complex was prepared as reported above for <sup>99g</sup>Tc(N)(Biot-CysOS)(PNP3), using equimolar amounts of [<sup>99g</sup>Tc(N)Cl<sub>2</sub>(PPh<sub>3</sub>)<sub>2</sub>] (30.15 mg, 0.0425 mmol), PNP3 (20.5 mg, 0.0425 mmol) and Biot-Abu-CysOS (18.4 mg, 0.0425 mmol). Anti-<sup>99g</sup>Tc(N)(Biot-Abu-CysOS)(PNP3) was soluble in chlorinated solvents and alcohols, and insoluble in diethyl ether and *n*-hexane. <sup>1</sup>H NMR (CDCl<sub>3</sub>):  $\delta$  (ppm)=7.15 (d, 1H, NH $^{\alpha}$ ); 7.10 (t, 1H, NH); 6.55 (s, 1H, NHC(O)NH); 5.75 (s, 1H, NHC(O)NH); 4.80 (dd, 1H, CH $^{\alpha}$ ); 4.50 (m, 1H, NHCHCH<sub>2</sub>); 4.35 (m, 1H, NHCHCH); 3.45 (m, 8H, P(CH<sub>2</sub>CH<sub>2</sub>CH<sub>2</sub>OCH<sub>3</sub>)<sub>2</sub>); 3.35 (m, 12H, P(CH<sub>2</sub>CH<sub>2</sub>CH<sub>2</sub>OCH<sub>3</sub>)<sub>2</sub>); 3.35 (m, 2H, NCH<sub>2</sub>CH<sub>2</sub>OCH<sub>3</sub>); 3.20 (s, 3H, NCH<sub>2</sub>CH<sub>2</sub>OCH<sub>3</sub>); 3.25 (dd, 2H, NHCH<sub>2</sub>); 3.25 and 2.40 (m, 2H, CH<sub>2</sub>S); 3.15 (m, 1H, NHCHCH); 2.95 and 2.80 (m, 2H, NHCHCH<sub>2</sub>); 2.85 and 2.45 (dd, 2H, NCH<sub>2</sub>CH<sub>2</sub>OCH<sub>3</sub>); 2.80–2.40 (m, 2H, PCH<sub>2</sub>CH<sub>2</sub>N); 2.30 (t, 2H, CH<sub>2</sub>CO); 2.25 (t, 2H, PCH<sub>2</sub>CH<sub>2</sub>N); 2.20 (t, 2H, CH<sub>2</sub>C(O)NH); 2.10–1.70 (m, 16H, P(CH<sub>2</sub>CH<sub>2</sub>CH<sub>2</sub>OCH<sub>3</sub>)<sub>2</sub>); 2.05 (t, 2H, PCH<sub>2</sub>CH<sub>2</sub>N); 1.60, 1.50 and 1.30 (m, 6H, (CH<sub>2</sub>)<sub>2</sub>); 1.40 (m, 2H, NHCH<sub>2</sub>CH<sub>2</sub>).

<sup>13</sup>C NMR (CDCl<sub>3</sub>):  $\delta$  (ppm)=178.0, 174.0, 172.0, 164.0, 73.0, 68.5, 62.0, 60.5, 59.0, 56.5, 55.5, 52.0, 47.0, 46.5, 41.0, 39.5, 36.5, 34.5, 30.0, 28.5, 27.0, 22.0, 18.5, 16.5. <sup>31</sup>P (CDCl<sub>3</sub>):  $\delta$  (ppm)=32, 8 (bs); 25, 3 (bs). Anal. Calcd for C<sub>40</sub>H<sub>77</sub>N<sub>6</sub>O<sub>10</sub>P<sub>2</sub>S<sub>2</sub>Tc: C, 46.77; H, 7.55; N, 8.22; S, 6.21; found: C, 46.56; H, 7.60; N, 8.20; S, 6.09.

The second yellow band eluted from silica corresponded to the syn-<sup>99g</sup>Tc(N)(Biot-Abu-CysOS)(PNP3) as assessed by characteristic NH<sub>amide</sub> signals appearing in the NMR spectra in CDCl<sub>3</sub> at  $\delta=7.85$  (doublet, cysteine-NH $^{\alpha}$ ) and 7.40 ppm (triplet, abu-NH), and 6.35 and 4.85 ppm (two singlets, biotin-NHC(O)NH), which were different from those collected for the anti isomer. As above, full NMR characterization in the solution state of the syn isomer was precluded by its fast rearrangement into the thermodynamically more stable anti-species.

Syn-<sup>99g</sup>Tc(N)(Biot-Abu-CysOS)(PNP3) was soluble in chlorinated solvents and alcohols, and insoluble in diethyl ether and *n*-hexane.

Anal. Calcd for C<sub>40</sub>H<sub>77</sub>N<sub>6</sub>O<sub>10</sub>P<sub>2</sub>S<sub>2</sub>Tc: C, 46.77; H, 7.55; N, 8.22; S, 6.21; found: C, 46.71; H, 7.62; N, 8.20; S, 6.13.

### 2.5. Synthesis of $^{99m}\text{Tc}(\text{N})(\text{Biot-X-CysOS})(\text{PNP3})$ complexes

$\text{Na}[^{99m}\text{TcO}_4]$  (0.250 ml, 50.0 MBq–3.0 GBq) was added to a vial containing succinic dihydrazide (SDH) (5.0 mg),  $\text{SnCl}_2$  (0.1 mg) suspended in saline (0.1 ml) and ethanol (1.0 ml). The vial was kept at room temperature for 30 min giving a mixture of  $^{99m}\text{Tc}$ -nitrido precursors  $[^{99m}\text{TcN}]^{2+}_{\text{int}}$ . The PNP3 ligand (1.0 mg) dissolved in EtOH (0.1 ml) and the selected Biot-X-CysOS ligand (0.25 mg) dissolved in EtOH (0.2 ml) were simultaneously added, and the reaction mixture was heated at 80°C for 20 min. The pH measured at the end of the reaction was 7.5.

In all cases, TLC and HPLC characterization showed the presence of two separate radioactive spots which resulted from the formation of two distinct isomeric forms, syn and anti, of the complexes  $^{99m}\text{Tc}(\text{N})(\text{Biot-X-CysOS})(\text{PNP3})$ . Total RCP determined by TLC and HPLC chromatography for the heterocomplexes is reported in Table 1.

In all cases, the syn- and anti isomers, isolated by HPLC, were concentrated on a Sep pack C18 column rinsed with  $\text{H}_2\text{O}$  (10 ml) and eluted using EtOH 70% (1×0.4 ml; 1×0.6 ml). The second fraction containing all the activity was utilized for in vitro and in vivo studies. After purification, the RCP of both isomeric forms evaluated by TLC and HPLC chromatography was >95%.

### 2.6. Radiolabeling efficiency of Biot-Glu-CysOS ligand

As example, the radiolabeling efficiency of the Biot-Glu-CysOS ligand was determined following the standardized labeling condition reported above. The amount of PNP3 and Biot-Glu-CysOS ligands used in these experiments is reported in Table 2.

### 2.7. Syn- vs. anti isomerization of $^{99m}\text{Tc}(\text{N})(\text{Biot-Abz-CysOS})(\text{PNP3})$

An alcoholic solution of the selected  $^{99m}\text{Tc}$ -isomer (0.1 ml) was added to a propylene test tube containing phosphate buffer ( $\text{H}_2\text{PO}_4^-/\text{HPO}_4^{2-}$ , 0.50 ml, 0.2 M pH 7.4)

and  $\text{H}_2\text{O}$  (0.3 ml). The mixture was vortexed and kept at 37°C or 80°C. Aliquots of the reaction mixtures were withdrawn at the appropriate time (0, 15 min, 1, 2, 3 and 24 h) and analyzed immediately by TLC and HPLC chromatography. A similar experiment was carried out using  $^{99m}\text{Tc}(\text{N})(\text{Biot-L-(Ac)Lys-CysOS})(\text{PNP3})$ .

### 2.8. In vitro studies

The experiments were performed in duplicate.

#### 2.8.1. In vitro binding to avidin

Preliminary evaluation of the binding characteristics of the radiolabeled biotin derivatives to avidin was assessed according to literature methods [11]. A constant activity (10–15  $\mu\text{Ci}/10 \mu\text{l}$ ) of syn- or anti complex was mixed with an increased amount of avidin (0, 1, 10, 50  $\mu\text{g}/10.0 \mu\text{l}$  of distillate water) in a propylene test tube containing phosphate buffer (80.0  $\mu\text{l}$ , 0.1 M; pH 7.4). The mixture was vortexed and incubated at 37°C for 24 h.

A specific binding to avidin was evaluated as follows: a biotin solution (10.0  $\mu\text{l}$ , 10 mM) in phosphate buffer (0.1 M, pH 7.4) was added to a propylene test tube containing phosphate buffer (70.0  $\mu\text{l}$ , 0.1 M, pH 7.4) and an aliquot of a water solution of avidin (0, 1, 10, 50  $\mu\text{g}/10.0 \mu\text{l}$ ). The mixture was vortexed and incubated at 37°C for 1 h. Then, a constant activity (10–15  $\mu\text{Ci}/10.0 \mu\text{l}$ ) of syn- or anti compounds was mixed and the resulting solution was incubated at 37°C for 24 h.

A control was performed incubating a constant activity (10–15  $\mu\text{Ci}/10.0 \mu\text{l}$ ) of syn- or anti compounds in phosphate buffer (80.0  $\mu\text{l}$ , 0.1 M; pH 7.4) at 37°C for 24 h.

At 1 and 24 h, aliquots (3.0  $\mu\text{l}$ ) of the reaction mixture were withdrawn and analyzed by silica gel ITLC. The plates were eluted with a mixture of saline and isopropyl alcohol 1:1. The radiolabeled biotin–avidin complex stayed at the origin, whereas the free biotinylated compounds moved with the solvent front. Each plate was cut horizontally, 2 cm above the origin, and the activity levels in the two parts were quantified using a gamma counter. The percentage of activity associated to the avidin was calculated using the following formula: [activity at the baseline/the total activity (activity at the baseline+activity at the front)]×100.

For the best compound,  $^{99m}\text{Tc}(\text{N})(\text{Biot-Glu-CysOS})(\text{PNP3})$ , the binding to avidin was evaluated after exposure to biological fluids (human serum and homogenate of rat and mouse liver). Before the assay, the complex was treated with an OASIS HLB extraction cartridge (see below) and purified by HPLC to eliminate eventual competitions toward the concentrator exercised by the biotin endogenous present in the biological fluids.

#### 2.8.2. Biotin competitive binding assay

A fixed amount of an aqueous solution of avidin (50  $\mu\text{g}/10.0 \mu\text{l}$ ;  $7.3 \times 10^{-5}$  M) was added to a propylene test tube containing a constant activity (10–15  $\mu\text{Ci}/10 \mu\text{l}$ ) of the HPLC-isolated syn- or anti- $^{99m}\text{Tc}(\text{N})(\text{Biot-Glu-CysOS})$

Table 2

Effect of the ligand amount on % RCY formation of the complex  $^{99m}\text{Tc}(\text{N})(\text{Biot-Glu-CysOS})(\text{PNP3})$

PNP3		Biot-Glu-CysOS		PNP3/Biot-Glu-CysOS	%RCY
mg	mmol	mg	mmol		
1	$2.06 \times 10^{-3}$	0.250	$0.54 \times 10^{-3}$	3.74	94.0±0.91
0.5	$1.03 \times 10^{-3}$	0.250	$0.54 \times 10^{-3}$	1.91	94.8±0.64
1	$2.06 \times 10^{-3}$	0.125	$0.27 \times 10^{-3}$	7.63	83.0±2.01
1	$2.06 \times 10^{-3}$	0.065	$0.14 \times 10^{-3}$	14.71	76.4±1.09
1	$2.06 \times 10^{-3}$	0.035	$0.70 \times 10^{-4}$	29.43	70.3±0.98
1	$2.06 \times 10^{-3}$	0.015	$0.35 \times 10^{-4}$	58.85	54.8±2.89
1	$2.06 \times 10^{-3}$	0.005	$0.17 \times 10^{-4}$	121.17	23.0±1.99
0.5	$1.03 \times 10^{-3}$	0.250	$0.54 \times 10^{-3}$	1.91	94.8±0.78
0.250	$0.52 \times 10^{-3}$	0.125	$0.27 \times 10^{-3}$	1.91	88.7±1.65
0.125	$0.26 \times 10^{-3}$	0.065	$0.14 \times 10^{-3}$	1.91	80.5±2.22
0.065	$0.13 \times 10^{-3}$	0.035	$0.70 \times 10^{-4}$	1.91	75.7±1.88

Experiments were performed in triplicate.



(PNP3) complex mixed with a different quantity of D-biotin dissolved in phosphate buffer (80.0  $\mu$ l, 0.1 M, pH 7.4). This allowed for a range in stoichiometry from 0:1 to 32:1 D-biotin/avidin ratio. The solutions were incubated at 37°C for 24 h. At 1 and 24 h, aliquots (3.0  $\mu$ l) of the reaction mixture were withdrawn and analyzed by silica gel ITLC as reported above.

### 2.8.3. Cysteine and glutathione challenge

Challenge experiments were carried out on the single isomeric form isolated by HPLC of the complexes:  $^{99m}\text{Tc}(\text{N})(\text{Biot-Abu-CysOS})(\text{PNP3})$ ,  $^{99m}\text{Tc}(\text{N})(\text{Biot-L-,D-(Ac)Lys-CysOS})(\text{PNP3})$  and  $^{99m}\text{Tc}(\text{N})(\text{Biot-Glu-CysOS})(\text{PNP3})$ . An aliquot (50.0  $\mu$ l) of an aqueous stock solution of cysteine hydrochloride (10.0 or 1 mM) was added to a propylene test tube containing phosphate buffer (250.0  $\mu$ l, 0.2 M; pH 7.4), water (100.0  $\mu$ l) and the syn- or anti isomer of the selected compound (100.0  $\mu$ l). The mixture was vortexed and incubated at 37°C for 24 h. A control reaction containing an equal volume of water, instead of cysteine hydrochloride, was studied in parallel. At 30 min, 1, 2, 3 and 24 h, aliquots of the reaction mixture were withdrawn and analyzed by TLC and HPLC chromatography.

A similar procedure was applied using GSH (50  $\mu$ l, 10.0 mM) as challenge ligand.

### 2.8.4. In vitro stability studies

The in vitro stability of the complexes (syn/anti)  $^{99m}\text{Tc}(\text{N})(\text{Biot-Abu-CysOS})(\text{PNP3})$ ,  $^{99m}\text{Tc}(\text{N})(\text{Biot-L- or D-(Ac)Lys-CysOS})(\text{PNP3})$  and  $^{99m}\text{Tc}(\text{N})(\text{Biot-Glu-CysOS})(\text{PNP3})$  was evaluated by monitoring the RCP at different time points using the following procedures. In a propylene test tube, HPLC-purified Tc-99m complexes (50.0  $\mu$ l) were added to (a) 950.0  $\mu$ l of saline, (b) 450.0  $\mu$ l of rat serum, (c) 450.0  $\mu$ l of human serum, (d) 450.0  $\mu$ l of homogenate of rat liver and (e) 450.0  $\mu$ l of homogenate of mouse liver. The resulting mixtures were incubated at 37°C for 2 h. At 15 min, 1 and 2 h, aliquots (200.0  $\mu$ l) of each solution were withdrawn, diluted with phosphate buffer (800.0  $\mu$ l, 0.2 M; pH 7.4) and treated using an OASIS HLB extraction cartridge before HPLC injection. The sample was loaded on a cartridge, previously conditioned with MeOH (1 ml) and equilibrated with water (1 ml), washed with MeOH 5% (3 ml) and the activity was eluted with MeOH (1 ml). In all investigated conditions, 90–95% of the initial activity was collected. One hundred microliters of this part was analyzed by HPLC.

### 2.9. Animal studies

Animal experiments were carried out in compliance with the relevant national laws relating to the conduct of animal experimentation.

After purification, the activity recovered was diluted with a saline solution to obtain a final solution 5% in ethanol content. A biodistribution study was carried out in normal male Balb/C mice (weight 25 g) anesthetized with an intraperitoneal injection of a mixture of Zoletil (40 mg/kg)

and xylazine (2 mg/kg). One hundred microliters (10  $\mu$ Ci) of the (syn/anti)- $^{99m}\text{Tc}(\text{N})(\text{Biot-Glu-CysOS})(\text{PNP3})$  complex was injected through the tail vein. The animals ( $n=3$ ) were sacrificed by cardiac puncture at different times postinjection. The blood was withdrawn from the heart with a syringe immediately after sacrifice and was counted. Organs were excised, washed, weighed and counted in a NaI well counter. Results were expressed as percentage of injected dose per gram (%ID/g).

### 2.9.1. Metabolites in the intestine

The intestinal lumen was rinsed with water (2 ml). Ninety percent of the total activity was found in the endo-luminal content. The liquid fraction was separated from the intestinal content by centrifugation at 3000 rpm for 10 min and counted. Fifty percent of the activity was found in this first fraction. Exhaustive extraction of the activity was performed by using MeCN (2 ml). An aliquot of each fraction (1 ml) was eluted through an OASIS HPL extraction cartridge, following the procedure reported above and analyzed by TLC and HPLC.

## 3. Results

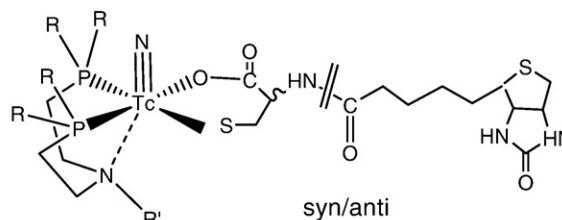
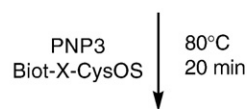
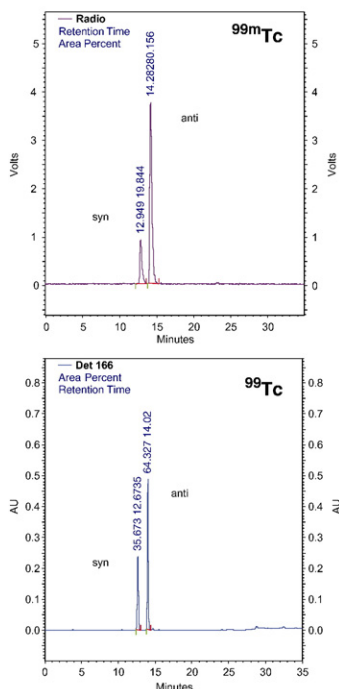
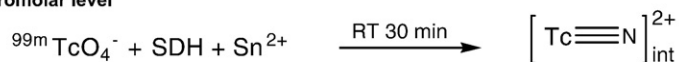
### 3.1. Preparation of $^{99m}\text{Tc}$ -labeled compounds

The method employed for preparing neutral asymmetric  $^{99m}\text{Tc}$ -nitrido complexes of the type  $^{99m}\text{Tc}(\text{N})(\text{Biot-X-CysOS})(\text{PNP3})$  is reported in Scheme 1. The labeling procedure has been carried out using a two-step approach.

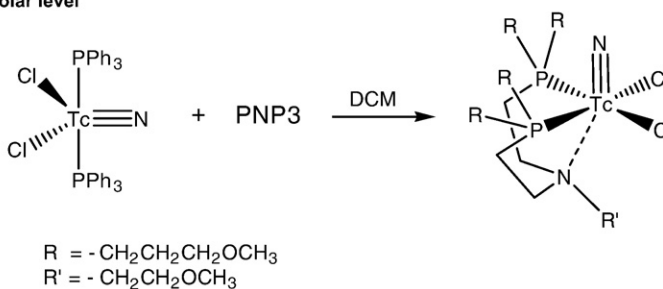
As normal, the first step was required to generate a mixture of  $^{99m}\text{Tc}$ -nitrido precursors, all containing the  $[\text{Tc}g\text{N}]^{2+}$  core, through the reduction of pertechnetate with tin (II) chloride in the presence of SDH as donor of the nitrido nitrogen atom. After production of the  $[\text{Tc}g\text{N}]^{2+}$  intermediates, PNP3 and the relevant bidentate Biot-X-CysOS ligand were simultaneously added to the reaction vial to produce the final product in high yield, after 20 min at 80°C.

In all cases, both TLC and HPLC techniques (Table 1) revealed the existence of two different compounds approximately in 15:85 ratios. These two species were recognized, as the syn/anti isomeric forms of the mixed complexes, depending on the orientation of the N-substituted cysteine pendant group with respect to the central Tc<sub>g</sub>N terminal core. The chemical identity of two representative compounds, syn/anti- $^{99m}\text{Tc}(\text{N})(\text{Biot-CysOS})(\text{PNP3})$  and syn/anti- $^{99m}\text{Tc}(\text{N})(\text{Biot-Abu-CysOS})(\text{PNP3})$ , was established by comparing their HPLC profile with those of the corresponding  $^{99g}\text{Tc}$ -complexes prepared via ligand-exchange reactions of the labile precursor  $^{99g}\text{Tc}(\text{N})\text{Cl}_2(\text{PPh}_3)_2$  (Scheme 1). Anti- $^{99g}\text{Tc}$  compounds were fully characterized by multinuclear ( $^1\text{H}$ ,  $^{13}\text{C}$  and  $^{31}\text{P}$ ) NMR spectroscopy. According to the magnetic inequivalence of the two aminodiphosphine Ps (see Scheme 1; each P faces different trans coordinated donor atoms, O or S, in the equatorial plane), two broad singlets appeared in the  $^{31}\text{P}$  spectrum. Such a signal

## Synthesis at micromolar level



## Synthesis at millimolar level



Scheme 1. Synthesis at the micromolar level.

broadening is typical of diamagnetic  $d^2$  nitrido Tc-complexes and is attributed to the quadrupole relaxation induced by the  ${}^{99}\text{Tc}$  nucleus ( $I=9/2$ ) on the neighboring P atoms [4].  ${}^1\text{H}$  and  ${}^{13}\text{C}$  signals were in agreement with the proposed formulation. The pseudo-octahedral molecular structure exhibited by  ${}^{99g}\text{Tc}(\text{N})(\text{Biot-CysOS})(\text{PNP3})$  and  ${}^{99g}\text{Tc}(\text{N})(\text{Biot-Abu-CysOS})(\text{PNP3})$  compared well with those reported previously for similar nitrido technetium and rhenium mixed heterocomplexes [2,4].

## 3.2. Radiolabeling efficiency of Biot-Glu-CysOS ligand

The dependence of the radiochemical yield (RCY) of  ${}^{99m}\text{Tc}(\text{N})(\text{Biot-Glu-CysOS})(\text{PNP3})$  formation as a function of the aminodiphosphine and biotinylated derivative concentration is reported in Table 2. Data showed that the highest RCY was achieved using a PNP3/Biot-Glu-CysOSH molar

ratio in the range of 4–2:1. Moreover, by fixing the molar ratio at 2:1, and progressively reducing the ligand amount, in terms of milligrams, the final compound was quantitatively obtained after 30 min at  $80^\circ\text{C}$ , using 0.5–0.250 mg of PNP3 and 0.250–0.125 mg of Biot-Glu-CysOSH.

3.3. Syn- vs. anti isomerization of the  ${}^{99m}\text{Tc}$ -complexes

The syn→anti and anti→syn isomerization of  ${}^{99m}\text{Tc}(\text{N})(\text{Biot-Abz-CysOS})(\text{PNP3})$  and  ${}^{99m}\text{Tc}(\text{N})(\text{Biot-L-(Ac)Lys-CysOS})(\text{PNP3})$  was found to occur as a reversible temperature-dependent process. In fact, no variation of syn→anti or anti→syn was observed by incubating the complexes at room temperature or at  $37^\circ\text{C}$  for 24 h. Reversible syn→anti and vice versa conversion was evidenced at  $80^\circ\text{C}$ . In this case, a faster syn→anti change was observed for both complexes. In fact, monitoring the conversion by TLC or

Table 3

Temperature dependence of syn→anti and anti→syn isomerization for the complex  $^{99m}\text{Tc}(\text{N})(\text{Biot-Abz-CysOS})(\text{PNP3})$  evaluated in phosphate buffer (0.2 M pH 7.4) as a function of time

% RCP of the complex	T (°C)	Time					
		0	15 min	1 h	2 h	3 h	24 h
Syn- $^{99m}\text{Tc}(\text{N})(\text{Biot-Abz-CysOS})(\text{PNP3})$	RT	95.48	92.10	91.30	88.01	86.09	75.98
Anti- $^{99m}\text{Tc}(\text{N})(\text{Biot-Abz-CysOS})(\text{PNP3})$	RT	–	–	–	–	–	–
Syn- $^{99m}\text{Tc}(\text{N})(\text{Biot-Abz-CysOS})(\text{PNP3})$	37	96.98	92.04	90.30	87.70	84.06	75.98
Anti- $^{99m}\text{Tc}(\text{N})(\text{Biot-Abz-CysOS})(\text{PNP3})$	37	–	–	–	–	–	–
Syn- $^{99m}\text{Tc}(\text{N})(\text{Biot-Abz-CysOS})(\text{PNP3})$	80	96.98	72.60	42.41	29.35	–	–
Anti- $^{99m}\text{Tc}(\text{N})(\text{Biot-Abz-CysOS})(\text{PNP3})$	80	–	23.22	52.56	50.28	–	–
Anti- $^{99m}\text{Tc}(\text{N})(\text{Biot-Abz-CysOS})(\text{PNP3})$	RT	96.02	95.61	93.59	91.76	88.90	85.21
Syn- $^{99m}\text{Tc}(\text{N})(\text{Biot-Abz-CysOS})(\text{PNP3})$	RT	–	–	–	–	–	–
Anti- $^{99m}\text{Tc}(\text{N})(\text{Biot-Abz-CysOS})(\text{PNP3})$	37	96.72	94.60	92.56	90.36	88.03	80.20
Syn- $^{99m}\text{Tc}(\text{N})(\text{Biot-Abz-CysOS})(\text{PNP3})$	37	–	–	–	–	–	–
Anti- $^{99m}\text{Tc}(\text{N})(\text{Biot-Abz-CysOS})(\text{PNP3})$	80	96.72	83.96	64.40	51.20	–	–
Syn- $^{99m}\text{Tc}(\text{N})(\text{Biot-Abz-CysOS})(\text{PNP3})$	80	–	14.58	30.53	28.29	–	–

HPLC (see Table 3), we observed that after 1 h of heating the syn/anti ratio was 45:55. At the same time, the anti→syn gave a syn/anti ratio of 30:70. The isomerization reached the final 15:85 syn/anti ratio after 2 h at 80°C.

### 3.4. In vitro studies

#### 3.4.1. Studies of binding to avidin

Preliminary affinity of syn- and anti- $^{99m}\text{Tc}(\text{N})(\text{Biot-X-OS})(\text{PNP3})$  complexes to avidin was evaluated in vitro according to the procedure reported in the experimental section. ITLC was used to separate bound and unbound radio-compound, and in all cases both of the isomeric forms were tested under identical conditions as the control group. The average percentage of activity not specifically retained by the concentrator (ca. 5%) was subtracted from the count. The percent of radiolabeled biotin bound, evaluated after 1 h of incubation, is reported in Fig. 2.

In general, a different affinity was evidenced for the two isomeric forms. A lower affinity toward avidin was observed for the syn isomers, with the exception of syn- $^{99m}\text{Tc}(\text{N})(\text{Biot-Abu-OS})(\text{PNP3})$  and syn- $^{99m}\text{Tc}(\text{N})(\text{Biot-Glu-CysOS})(\text{PNP3})$  complexes which maintained an acceptable affinity for the concentrator: in the presence of 1 µg of avidin the percentage of radioligand bound was 67.87% for syn- $^{99m}\text{Tc}(\text{N})(\text{Biot-Abu-OS})(\text{PNP3})$  and 72.12% for syn- $^{99m}\text{Tc}(\text{N})(\text{Biot-Glu-CysOS})(\text{PNP3})$ ; increasing the amount of avidin to 50 µg the percent of activity bound was 79.94% and 90.45%, respectively.

Binding saturation curves of anti isomers revealed a good affinity toward the concentrator depending on the nature of the spacer interposed between the biotin moiety and the cysteine fragment.

The best affinity was observed for the complexes anti- $^{99m}\text{Tc}(\text{N})(\text{Biot-Abu-OS})(\text{PNP3})$  and anti- $^{99m}\text{Tc}(\text{N})(\text{Biot-Glu-CysOS})(\text{PNP3})$ . The percentage of activity bound was, respectively, 79.3% and 75.15% in the presence of 1 µg of avidin; 88.10% and 90.32% with 10 µg and 90.37% and 93.06% in the presence of 50 µg.

Partial loss of the affinity was observed for anti- $^{99m}\text{Tc}(\text{N})(\text{Biot-CysOS})(\text{PNP3})$  and anti- $^{99m}\text{Tc}(\text{N})(\text{Biot-Abz-CysOS})(\text{PNP3})$ . For these two complexes, the percentage of radiolabeled compound bound to the concentrator was almost the same (26.67% and 30.59% in the presence of 1 µg of avidin), irrespective of the presence or absence of the spacer.

For the four agents retaining the affinity for the concentrator at 1 h, the stability of the interaction was evaluated by incubation at 37°C for 24 h. In the case of anti- $^{99m}\text{Tc}(\text{N})(\text{Biot-Abu-CysOS})(\text{PNP3})$  and anti- $^{99m}\text{Tc}(\text{N})(\text{Biot-Glu-CysOS})(\text{PNP3})$ , such interaction was almost irreversible (loss <5%), while syn- $^{99m}\text{Tc}(\text{N})(\text{Biot-Glu-CysOS})(\text{PNP3})$  showed 20% release. Instead, data established that approximately 40–50% of bound activity of

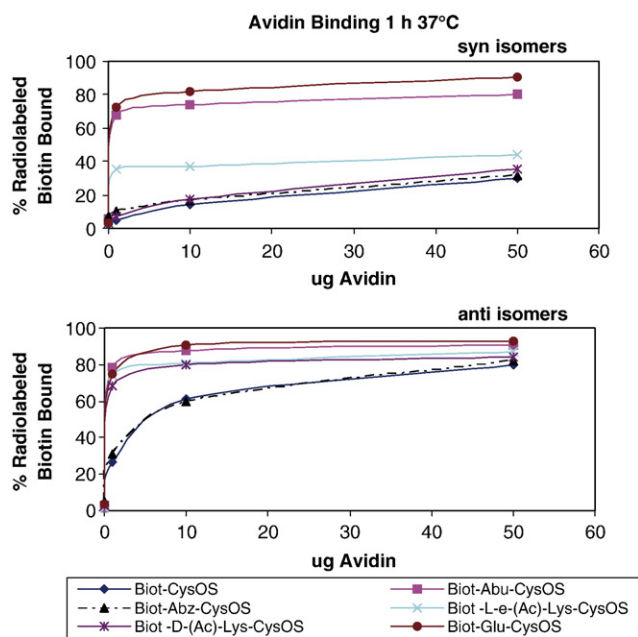


Fig. 2. In vitro binding of syn- and anti-complexes to avidin, as a function of avidin concentration evaluated after 1 h at 37°C.

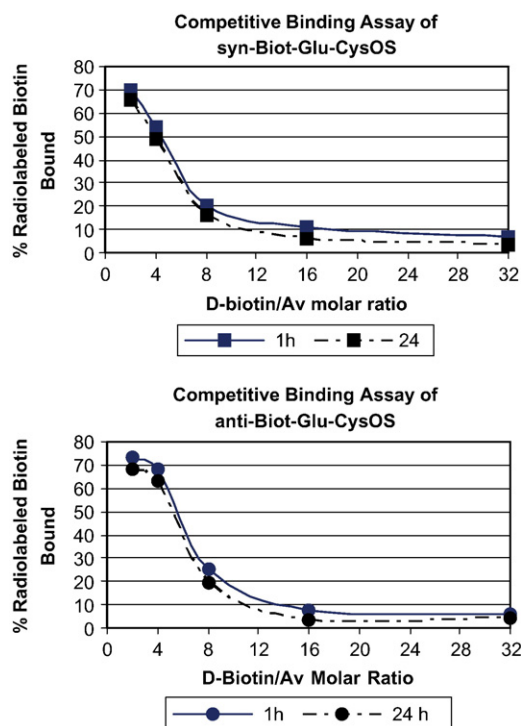


Fig. 3. Saturation curves of syn-<sup>99m</sup>Tc(N)(Biot-Glu-CysOS)(PNP3) and anti-<sup>99m</sup>Tc(N)(Biot-Glu-CysOS)(PNP3) expressed as % of bound radiolabeled biotin as a function of the D-biotin/avidin molar ratio evaluated at 1 and 24 h.

syn-<sup>99m</sup>Tc(N)(Biot-Abu-CysOS)(PNP3) and anti-<sup>99m</sup>Tc(N)(Biot-L- or D-(Ac)Lys-CysOS)(PNP3) derivatives was released from the avidin complex, indicating the presence of an aspecific interaction.

### 3.4.2. Competitive binding assay

Since D-biotin is present in the human body naturally, the competitive binding to avidin in the presence of increasing concentration of D-biotin was measured for syn- and anti-<sup>99m</sup>Tc(N)(Biot-Glu-CysOS)(PNP3), which showed the better biological properties of the series. Equivalent affinities of radiolabeled biotin and D-biotin for avidin would result in 50% molar activity bound to avidin at the saturation point of avidin, which is 4 Meq, since avidin is capable of binding four biotin molecules. The saturation curves of the syn- and anti-<sup>99m</sup>Tc(N)(Biot-Glu-CysOS)(PNP3) compounds are shown in Fig. 3.

The results were comparable with those obtained in the preliminary binding experiments. Both the isomeric forms maintained a good affinity toward the concentrator.

For the anti compound, data collected at 1 and 24 h were almost superimposable, indicating that the binding occurred rapidly and irreversibly.

### 3.4.3. Cysteine and glutathione challenge

All complexes were found to be inert toward transchelation with an excess of free glutathione and 1 mM cysteine. On the contrary, syn isomers were found to be weakly unstable in the presence of 10 mM cysteine. For the latter

complexes, HPLC profiles evaluated after 1, 3 and 24 h of incubation at 37°C revealed the presence of a more hydrophilic compound, indicating that a transchelation reaction had occurred. These behaviors suggested that the anti isomer was the kinetically and thermodynamically favored configuration of the mixed complex.

### 3.4.4. Stability studies

The in vitro stability of the best four compounds was compared following incubation at 37°C for 2 h with (i) human serum, (ii) rat serum, (iii) homogenate of rat liver, (iv) homogenate of mouse liver and (v) phosphate buffer. At 15 min, 1 and 2 h, an aliquot of each sample was eluted through an OASIS HPL extraction cartridge and analyzed by TLC and HPLC. All complexes, with the exception of [<sup>99m</sup>Tc(N)(Biot-Abu-OS)(PNP3)], were found to be stable in all conditions. For <sup>99m</sup>Tc(N)(Biot-L- or D-(Ac)Lys-CysOS)(PNP3) and <sup>99m</sup>Tc(N)(Biot-Glu-CysOS)(PNP3), the main activity remained associated to the intact conjugated complexes. On the contrary, <sup>99m</sup>Tc(N)(Biot-Abu-CysOS)(PNP3) was rapidly degraded and, with time, an increasing fraction of a more hydrophilic compound was found after HPLC injection of aliquots of rat serum, homogenate of rat liver and homogenate of mouse liver. The complex was found to be stable after incubation with human serum, and the percentage of activity remaining as <sup>99m</sup>Tc(N)(Biot-Abu-CysOS)(PNP3) at 2 h was 87%.

### 3.5. Animal studies

The tissue distribution in normal Balb/c mice of the selected compound (syn/anti)-<sup>99m</sup>Tc(N)(Biot-Glu-CysOS)(PNP3) was investigated, and the results, expressed as percentage of dose per gram (% ID/g), are reported in Table 4.

The complex was rapidly cleared from the blood (0.69 % ID/g at 1 h postinjection) and from normal tissues such as heart, lungs, stomach, liver, spleen, kidneys and muscle. High and persistent level of activity was observed in the intestine at 3 h postinjection. Measurement of the radioactivity in the small intestine revealed that the main activity was present in the endoluminal content as possible metabolic products, while only a small amount was found associated to the intestinal tissue. Thus, at 3 h postinjection, the activity

Table 4  
Biodistribution in Balb/C mice ( $n=3$ ) of the (syn/anti)-<sup>99m</sup>Tc(N)(Biot-Glu-CysOS)(PNP3) complex (% dose/g±S.D.)

Organs	30 min	1 h	2 h	3 h
Blood	0.96±0.08	0.69±0.12	0.15±0.06	0.06±0.02
Heart	0.42±0.15	0.67±0.20	0.05±0.00	0.07±0.03
Lung	0.59±0.01	0.44±0.06	0.20±0.07	0.17±0.13
Liver	3.66±0.57	3.76±1.24	1.96±0.94	0.94±0.47
Stomach	0.13±0.04	0.13±0.01	0.07±0.04	0.04±0.01
Spleen	8.06±2.14	3.55±0.63	1.32±0.28	1.97±0.06
Kidney	0.65±0.37	12.88±3.75	12.26±0.26	7.15±0.91
Small intestine	41.34±16.20	36.50±11.11	43.62±11.05	35.57±4.81
Large intestine	1.34±0.20	2.53±0.11	3.65±1.01	3.56±0.81
Muscle	0.35±0.13	0.30±0.09	0.07±0.03	0.10±0.08



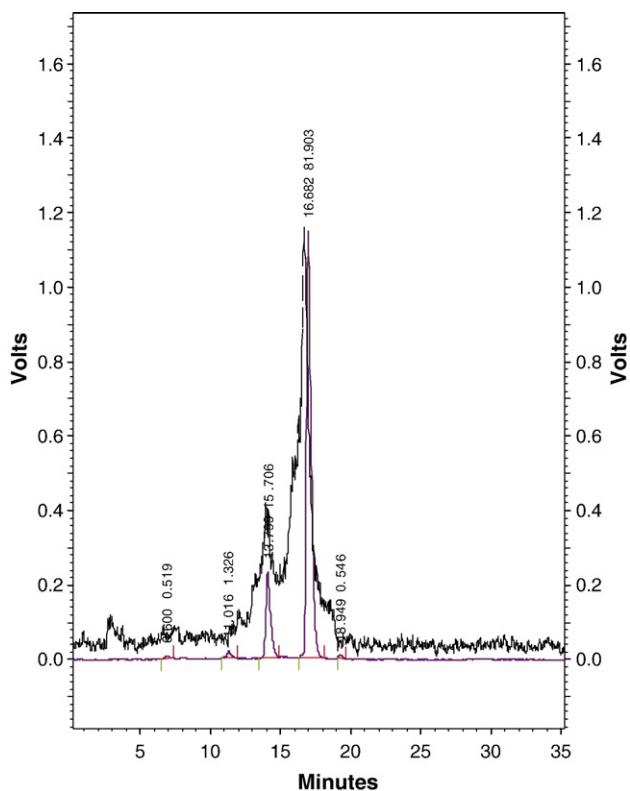


Fig. 4. (—)  $^{99m}\text{Tc}(\text{N})(\text{Biot-Glu-CysOS})(\text{PNP3})$ ; (---)  $^{99m}\text{Tc}(\text{N})(\text{Biot-Glu-CysOS})(\text{PNP3})$  extract from the endoluminal content.

was extracted and analyzed by HPLC to assess the molecular integrity of the complex. The results showed that the complex was stable *in vivo*. In fact, the chromatographic profile of the extracted activity was found to be exactly coincident with the control peak, suggesting that no metabolization process of the complex had occurred (Fig. 4).

#### 4. Discussion

Technetium mixed-ligand complexes displaying characteristic substitution-inert metal fragments ( $[\text{Tc}(\text{CO})_3]^+$  and  $[\text{Tc}(\text{N})(\text{PNP})]^{2+}$ ) have emerged as alternative platforms in the design of potential  $^{99m}\text{Tc}$  ‘target-specific’ radiopharmaceuticals [19,20]. In this context, attempts to develop  $\text{Tc-}^{99m}$  target-specific agents using the  $[\text{Tc}(\text{N})(\text{PNP})]^{2+}$  synthon have recently been undertaken [4,5]. However, *in vitro* studies showed that the labeling procedure determined the complete loss of the receptor affinity of the conjugate complexes, presumably due to the strong perturbation determined by the proximity of the metal-containing block to the bioactive group.

In order to overcome this drawback and to evaluate the possible application of  $[\text{Tc}(\text{N})(\text{PNP})]^{2+}$  technology to the production of target-specific radiopharmaceuticals, a series of  $^{99m}\text{Tc}$ -labeled biotin conjugate was prepared. In these compounds, biotin was conjugated to the amino group of cysteine (BFCS) through different group spacers aiming at the evaluation of the influence of the linker on the affinity of

biotin for the concentrator. Moreover, a bulky group in  $\alpha$  position to the amido bonds between biotin and the labeled prosthetic group was introduced on Biot-L- or D-(Ac)Lys-CysOSH and Biot-Glu-CysOSH ligands to reduce recognition by hydrolytic enzymes (e.g., biotinidase).

Nitrido- $\text{Tc}(\text{V})$   $^{99m}\text{Tc}(\text{N})(\text{Biot-X-CysOS})(\text{PNP3})$  complexes were prepared through a two-step procedure which required the simultaneous addition of PNP3 and the biotinylated ligand (Biot-X-CysOSH) to a mixture of  $^{99m}\text{Tc}$ -nitrido precursors (see Scheme 1). In these reactions, the quantitative formation of the final mixed complexes (yields >95%) was obtained using <0.250 mg of biotinylated ligand. The use of a relatively high amount of Biot-Glu-CysOSH was determined by its poor aqueous solubility. However, it was previously demonstrated that higher radiolabeling efficiency had been achieved using cysteine-derived  $[\text{Tc}(\text{N})(\text{PNP})]$  agents [3].

TLC and HPLC analysis revealed the presence of a mixture of two forms in 15:85 ratios, which were identified by comparison with the chromatographic profiles of the corresponding characterized  $^{99g}\text{Tc}$ -compounds, as syn- and anti isomers. In particular, the syn configuration was attributed to the more hydrophilic compound, and the anti configuration to the lipophilic one. The difference observed in the syn/anti ratio in  $^{99m}\text{Tc}$  and  $^{99g}\text{Tc}$  preparations was attributed to the higher temperature employed in  $^{99m}\text{Tc}$  synthesis which accelerated the syn to anti conversion [4]. Both isomers were isolated by HPLC and utilized in *in vitro* studies.

Generally, binding saturation curves revealed a superior affinity toward the concentrator for anti isomers, and, among these, the affinity was found to depend on the nature of the spacer. On the contrary, syn isomers exhibited lower affinity, the only exceptions being syn- $^{99m}\text{Tc}(\text{N})(\text{Biot-Abu-CysOS})(\text{PNP3})$  and syn- $^{99m}\text{Tc}(\text{N})(\text{Biot-Glu-CysOS})(\text{PNP3})$ .

Among tested complexes, those containing a BFCS with an aliphatic spacer having five or seven atoms sequence retained high affinity for avidin (Biot-Abu-CysOS, Biot-L-(Ac)Lys-CysOS, Biot-D-(Ac)Lys-CysOS and Biot-Glu-CysOS). Presumably, in these conjugate complexes the length of the spacer allowed the bioactive residue to remain sufficiently distant from the  $[\text{Tc}(\text{N})(\text{PNP})]^{2+}$  moiety, thus minimizing reciprocal interactions. On the contrary, partial loss of the receptor affinity was observed for anti- $^{99m}\text{Tc}(\text{N})(\text{Biot-CysOS})(\text{PNP3})$  and anti- $^{99m}\text{Tc}(\text{N})(\text{Biot-Abz-CysOS})(\text{PNP3})$  complexes containing no spacer or a rigid six-member spacer in the BFCS framework, respectively. Biotinylated complexes containing a seven-term spacer revealed an unstable interaction for the concentrator at 24 h. Finally, biotinylated agents containing a flexible five-term spacer showed that, despite the linkage with the sterically demanding  $[\text{Tc}(\text{N})(\text{PNP})]^{2+}$  molecular fragment, the binding occurred rapidly and irreversibly at 1 and 24 h.

Stability studies toward biotinidase hydrolysis, carried out in human and mouse serum as well as in mouse liver homogenate, evidenced a rapid enzymatic degradation for



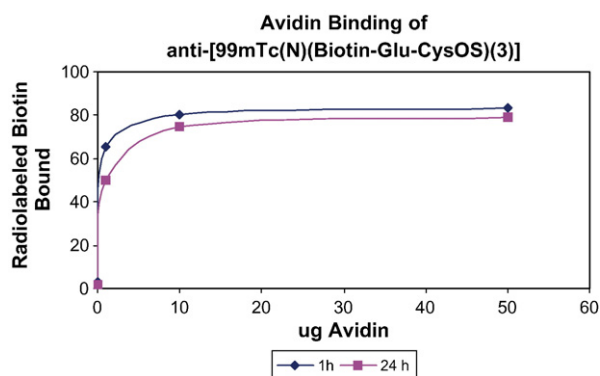


Fig. 5. In vitro binding of anti- $^{99m}\text{Tc}(\text{N})(\text{Biot-Glu-CysOS})(\text{PNP3})$  to avidin, as a function of avidin concentration, evaluated at 1 and 24 h at 37°C after exposure to biological fluids.

$^{99m}\text{Tc}(\text{N})(\text{Biot-Abu-CysOS})(\text{PNP3})$ . Conversely, the presence of an acetyl or a carboxyl function close to the  $-\text{CO}-\text{NH}-$  bonds, as protecting group, in  $^{99m}\text{Tc}(\text{N})(\text{Biot-L}(\text{Ac})\text{Lys-CysOS})(\text{PNP3})$  and  $^{99m}\text{Tc}(\text{N})(\text{Biot-Glu-CysOS})(\text{PNP3})$  compounds markedly increased their stability, minimizing recognition of these conjugates by biotinidase without affecting the affinity of biotin toward avidin. This achievement was supported by the fact that the  $^{99m}\text{Tc}(\text{N})(\text{Biot-Glu-CysOS})(\text{PNP3})$  complex, isolated by HPLC after in vitro exposure to biological fluids, maintained its affinity for the interaction site (Fig. 5).

The tissue distribution of (syn/anti)- $^{99m}\text{Tc}(\text{N})(\text{Biot-Glu-CysOS})(\text{PNP3})$  was evaluated in normal Balb/c mice. The complex was rapidly cleared from the blood and from the other tissues with the exception of the intestine, where a high percentage of the injected dose was observed at 3 h postinjection as unmetabolized product evidencing the remarkable stability of this compound.

Only limited information concerning the intestinal uptake of other radiolabeled biotin conjugates is available from the literature, and a number of these studies do not include data for intestines [21,22]. However, similar high levels of intestinal accumulation were previously observed for some iodinated compounds and  $^{99m}\text{Tc}$ -MAG3-biotin derivatives [9,11]. Despite a high level of intestinal uptake (5–12 %ID/g at 2 h postinjection) being previously observed for a series of different compounds all containing the  $[\text{}^{99m}\text{Tc}(\text{N})(\text{PNP3})]^{2+}$  building block [23–25], in this case the intestinal accumulation of the  $^{99m}\text{Tc}(\text{N})(\text{Biot-Glu-CysOS})(\text{PNP3})$  complex (43 %ID/g at 2 h postinjection) appeared to be dominated by the biotin moiety. This possibility is in agreement with the known biosynthetic pathways of vitamins [26] and the assessment of biotin uptake and biotinidase activity in the intestines [27,28].

Therefore, in view of the application of  $[\text{}^{99m}\text{Tc}(\text{N})(\text{PNP3})]^{2+}$  technology in nuclear imaging, modification of the hydrophilic/lipophilic properties of the system to increase its renal clearance will be necessary. This goal could be achieved by enhancing the hydrophilic properties

of the  $[\text{}^{99m}\text{Tc}(\text{N})(\text{PNP3})]^{2+}$  moiety through the introductions of more hydrophilic or more easily metabolizable groups on the phosphorus atoms or, alternatively, through a change of the net charge of the final mixed complex. Monopositive compounds of the type  $[\text{}^{99m}\text{Tc}(\text{N})(\sim\text{CysNH}_2\text{S})(\text{PNP3})]^+$ , in which cysteine is joined to the bioactive molecule through the carboxyl group thus leaving the  $[\text{NH}_2, \text{S}^-]$  pair for the coordination to the metal fragment, can be prepared with high specific activity as well [3].

## 5. Conclusion

A new class of technetium biotinylated complexes of the type  $^{99m}\text{Tc}(\text{N})(\text{Biot-X-CysOS})(\text{PNP3})$  has been successfully obtained in high yield through the application of the labeling procedure based on  $[\text{}^{99m}\text{Tc}(\text{N})(\text{PNP3})]^{2+}$  technology.

The complex binding affinity for avidin was found to be dependent on the nature of the spacer interposed between the BFCS and the bioactive molecule. For the best compound  $^{99m}\text{Tc}(\text{N})(\text{Biot-Glu-CysOS})(\text{PNP3})$ , the two isomeric forms almost retained the same binding affinity. Determination of the competitive binding of syn/anti- $^{99m}\text{Tc}(\text{N})(\text{Biot-Glu-CysOS})(\text{PNP3})$  revealed equivalent affinities of the complexes and D-biotin to avidin. The presence of appropriate sterically hindered groups adjacent to the amido  $\text{NH}-\text{CO}$  group of biotin made these conjugate complexes resistant to enzymatic degradation. Moreover, syn/anti- $^{99m}\text{Tc}(\text{N})(\text{Biot-Glu-CysOS})(\text{PNP3})$  showed a remarkable in vivo stability.

These findings suggested that a careful selection of the spacer may prevent perturbation of the pharmacophore group operated by the inorganic moiety, thus leaving the biomolecule free to interact with the receptor.

This study actually established, for the first time, the effective applicability of  $[\text{}^{99m}\text{Tc}(\text{N})(\text{PNP3})]^{2+}$  technology to the preparation of target-specific radiopharmaceuticals.

## Acknowledgments

The authors are grateful to Dr. Dario Casara for his collaboration, Mariano Schiavon for his assistance in the biological studies and Anna Rosa Moresco for her work on the elemental analysis.

## References

- [1] Bolzati C, Boschi A, Duatti A, Prakash S, Uccelli L, Refosco F, et al. Geometrically controlled selective formation of nitrido technetium(V) asymmetrical heterocomplexes with bidentate ligands. *J Am Chem Soc* 2000;122:4510–1.
- [2] Bolzati C, Boschi A, Uccelli L, Tisato F, Refosco F, Cagnolini A, et al. Chemistry of the strong electrophilic metal fragment  $[\text{}^{99}\text{Tc}(\text{N})(\text{PXP})]^{2+}$  (PXP=diphosphine ligand). A novel tool for the selective labeling of small molecules. *J Am Chem Soc* 2002;124:11468–79.
- [3] Boschi A, Bolzati C, Benini E, Malagò E, Uccelli L, Duatti A, et al. A novel approach to the high-specific-activity labeling of small peptides with the technetium-99m fragment  $[\text{}^{99m}\text{Tc}(\text{N})(\text{PXP})]^{2+}$  (PXP=diphosphine ligand). *Bioconjug Chem* 2001;12:1035–42.

- [4] Bolzati C, Mahmood A, Malagò E, Uccelli L, Boschi A, Jones AJ, et al. The  $[\text{}^{99\text{m}}\text{Tc}(\text{N})(\text{PNP})]^{2+}$  metal fragment: a technetium-nitrido synthon for use with biologically active molecules the *n*-(2-methoxyphenyl)piperazyl-cysteine analogues as examples. *Bioconjug Chem* 2003;14:1231–42.
- [5] Boschi A, Uccelli L, Duatti A, Bolzati C, Refosco F, Tisato F, et al. Asymmetrical nitrido Tc-99m heterocomplexes as potential imaging agents for benzodiazepine receptors. *Bioconjug Chem* 2003;14:1279–88.
- [6] Sakahara H, Saga T. Avidin–biotin system for delivery of diagnostic agents. *Adv Drug Deliv Rev* 1999;37:89–101.
- [7] James S, Maresca KP, Babich JW, Valliant JF, Doering L, et al. Isostructural Re and  $^{99\text{m}}\text{Tc}$  complexes of biotin derivatives for fluorescence and radioimaging studies. *Bioconjug Chem* 2006;17:590–6.
- [8] Nock B, Koch P, Evard F, Paganelli G, Mäcke H.  $^{99\text{m}}\text{TcN}_4$ -lys-biotin, a new biotin derivate useful for pretargeted avidin–biotin immunoscintigraphy: synthesis, evaluation and comparison with other  $^{99\text{m}}\text{Tc}$ -biotin conjugates. In: Nicolini M, Bandoli G, Mazzi U, editors. *Technetium and rhenium in chemistry and nuclear medicine V*. Padova (Italy): SG Editoriali; 1995. p. 429–32.
- [9] Van Gog FB, Visser GWM, Gowrising RWA, Snow GB, van Dongen GAMS. Synthesis and evaluation of  $^{99\text{m}}\text{Tc}/^{99}\text{Tc}$ -Mag3-biotin conjugates for antibody pretargeting strategies. *Nucl Med Biol* 1998;25:611–8.
- [10] Sabatino G, Chinol M, Paganelli G, Papi S, Chelli M, Leone G, et al. A new biotin derivate-DOTA conjugate as a candidate for pretargeted diagnosis and therapy of tumors. *J Med Chem* 2003;46:3170–3.
- [11] Foulon CF, Alston KL, Zalutsky MR. Synthesis and preliminary biological evaluation of (3-iodobenzoyl)nor-biotinamide and ((5-iodo-3-pyridinyl)carbonyl)nor-biotinamide: two radioiodinated biotin conjugates with improved stability. *Bioconjug Chem* 1997;8:179–86.
- [12] James S, Maresca KP, Allis DG, Valliant JF, Eckelman W, Babich JW, et al. Extension of the single amino acid chelate concept (SAAC) to bifunctional biotin analogues for complexation of the  $\text{M}(\text{CO})_3^{+1}$  core (M=Tc and Re): synthesis, characterization, biotinidase stability, and avidin binding. *Bioconjug Chem* 2006;17:579–89.
- [13] Hymes J, Wolf B. Biotinidase and its roles in biotin metabolism. *Clin Chim Acta* 1996;255:1–11.
- [14] Wilbur DS, Hamlin DK, Chyan M-K, Kegley BB, Pathare PM. Biotin reagents for antibody pretargeting: 5. Additional studies of biotin conjugate design to provide biotinidase stability. *Bioconjug Chem* 2001;12:616–23.
- [15] Knorr R, Trzeciak A, Bannwarth W, Gillessen D. New coupling reagents in peptide chemistry. *Tetrahedron Lett* 1989;30:1927–30.
- [16] Carpino LA, El-Faham A. Efficiency in peptide coupling: 1-hydroxy-7-azabenzotriazole vs 3,4-dihydro-3-hydroxy-4-oxo-1,2,3-benzotriazine. *J Org Chem* 1995;60:3561–4.
- [17] Bolzati C, Caporale A, Carta D, Cofano L, Schievano E, Tisato F, et al. A library of cysteine–biotin derivatives useful for pretargeting avidin–biotin radioimmunoscintigraphy. In: Blondelle SE, editor. *19th American Peptide Symposium Proceedings, Understanding Biology Using Peptides*. American Peptide Society; 2005. p. 349.
- [18] Abram U, Lorenz B, Kaden L, Scheller D. Nitrido complexes of technetium with tertiary phosphines and arsines. *Polyhedron* 1988;7:285–9.
- [19] Alberto R, Schibli R, Waibel R, Abram U, Schubiger AP. Basic aqueous chemistry of  $[\text{M}(\text{OH})_2(\text{CO})_3]^+$  (M=Re, Tc) directed towards radiopharmaceutical application. *Coord Chem Rev* 1999;190–192:901–19.
- [20] Boschi A, Duatti A, Uccelli L. Development of technetium-99m and rhenium-188 radiopharmaceuticals containing a terminal metal-nitrido multiple bond for diagnosis and therapy. *Top Curr Chem* 2005;252:85–115.
- [21] Shoup TM, Fischman AJ, Jaywood S, Babich JW, Strauss HW, Elmaleh DR. Synthesis of fluorine-18-labeled biotin derivatives: biodistribution and infection localization. *J Nucl Med* 1994;35:1685–90.
- [22] Virzi F, Fritz B, Rusckowski M, Gionet M, Misra H, Hnatowich DJ. New indium-111 labeled biotin derivatives for improved immunotargeting. *Nucl Med Biol* 1991;18:719–26.
- [23] Boschi A, Uccelli L, Bolzati C, Duatti A, Sabba N, Moretti E, et al. Biological evaluation of monocationic asymmetrical nitride Tc-99m heterocomplexes showing high heart uptake and improved imaging properties. *J Nucl Med* 2003;44:806–14.
- [24] Bolzati C, Benini E, Cazzola E, Jung C, Tisato F, Refosco F, et al. Synthesis, characterization, and biological evaluation of neutral nitrido technetium(V) mixed ligand complexes containing dithiolates and aminodiphosphines. A novel system for linking technetium to biomolecules. *Bioconjug Chem* 2004;15:628–37.
- [25] Agostini S, Bolzati C, Didonè E, Cavazza-Ceccato M, Aloj L, Arra C, et al. The  $[\text{Tc}(\text{N})\text{PNP}]^{2+}$  metal fragment labeled cholecystokinin-8 (CCK8) peptide for CCK receptors imaging: in vitro and in vivo studies. In: Mazzi U, editor. *Technetium, rhenium and other metals in chemistry and nuclear medicine 7*. Padova (Italy): SGE Editoriali; 2006. p. 341–2.
- [26] Suormala T, Wick H, Bonjour J-P, Baumgartner ER. Intestinal absorption and renal excretion of biotin in patients with biotinidase deficiency. *Eur J Pediatr* 1985;144:21–6.
- [27] Leon-del-Rio A, Velasquez A, Vizcaino G, Robles-Diaz G, Gonzalez-Noriega A. Association of pancreatic biotinidase activity and intestinal uptake of biotin and biocytin in hamster and rat. *Ann Nutr Metab* 1990;34:266–72.
- [28] Dakshinamurti K, Chauhan J, Ebrahim H. Intestinal absorption of biotin and biocytin in the rat. *Biosci Rep* 1987;7:667–73.

# Bioactive polyurethanes in clinical applications<sup>†</sup>

G. Ciardelli<sup>1,2\*</sup>, A. Rechichi<sup>2,3</sup>, S. Sartori<sup>2</sup>, M. D'Acunto<sup>2</sup>, A. Caporale<sup>4</sup>, E. Peggion<sup>4</sup>, G. Vozzi<sup>3</sup> and P. Giusti<sup>2,3</sup>

<sup>1</sup>Department of Mechanics, Politecnico in Turin, Corso Duca degli Abruzzi, 24, Torino, Italy

<sup>2</sup>Department of Chemical Engineering, University of Pisa, via Diotisalvi 2, 56126 Pisa, Italy

<sup>3</sup>CNR-IMCB, via Diotisalvi 2, 56126 Pisa, Italy

<sup>4</sup>Department of Chemical Sciences, University of Padua, Via Marzolo, 1-35131 Padova, Italy

Received 21 March 2006; Revised 5 April 2006; Accepted 7 April 2006

**Biomaterials play an important role in most tissue engineering strategies. They can serve as substrates on which cell populations can attach and migrate, can be used as cell delivery vehicles and as bioactive factor carriers to activate specific cellular functions. A series of biodegradable polyurethanes (PUs) with tunable chemical, physical and degradation properties, showing an adequate response to *in vitro* tests was proposed for applications in soft tissue engineering. Three-dimensional scaffolds of superimposed square meshed grids were prepared by using a rapid prototyping technique (pressure activated microsyringe, PAM) and tested *in vivo*. Functionalization of PU systems was performed in order to control the chemistry of the materials for the promotion of highly specific binding interactions between materials and biological environments. Two different approaches were used for the coupling of bioactive molecules such as gelatin. The first involved the modification of the polymer chain through a novel monomer and the second one consisted in a surface modification by plasma-induced graft copolymerization of acrylic acid. Copyright © 2006 John Wiley & Sons, Ltd.**

**KEYWORDS:** polyurethanes; bioactivity; surfaces; functionalization of polymers; biodegradable

## INTRODUCTION

Polyurethanes (PUs) represent a main class of synthetic elastomers applied for long-term medical implants.<sup>1</sup> They present tunable chemical properties, excellent mechanical properties, good biocompatibility and can be designed to degrade in biological environments.<sup>2</sup> The main problem in their use as biodegradable materials in the biomedical field, due to the release of toxic diamines from conventional isocyanates, can be overcome using an L-lysine derived diisocyanate (LDI) or 1,4-diisocyanatobutane.<sup>3</sup>

Much research has been devoted to the bulk or surface modification of polymers using signaling proteins or peptides to prepare bioactive materials that are able to interact with surrounding tissues by biomolecular recognition.<sup>4</sup> Covalent functionalization of PUs with bioactive molecules (e.g. Arg-Gly-Asp containing peptides), giving the synthetic systems several characteristics of biological ones, is still a strategy of limited diffusion. Optimal results have been otherwise obtained in the field of surface functionalization, using plasma technology, which induces the formation of

reactive radicals initiating graft polymerization of monomers containing functional groups for the subsequent coupling.<sup>5</sup>

In recent work<sup>6</sup> the synthesis, characterization and degradation of novel linear PUs was proposed. The polymers were obtained using LDI as diisocyanate, a cyclic diol and a L-phenylalanine based diamine (Phe diester) as chain extender, and tri-block copolymers based on polyethylene-glycol (PEG) and poly(epsilon-caprolactone) diol as macrodiols. In this work similar PUs at higher molecular weight were prepared and characterized. Their response to *in vitro* (citotoxicity, fibroblast adhesion and proliferation) and *in vivo* tests showing their biocompatibility and capability of integration with the biological environment is examined. Two different strategies were also proposed for the functionalization of the PU systems: the first involved a surface modification by plasma activation and the second one consisted in a covalent modification of the polymeric chain through an Arg-Gly-Asp (RGD) containing peptide.

## EXPERIMENTAL

### Polymer synthesis and characterization

Biodegradable PUs were prepared as previously described<sup>6</sup> by using polycaprolactone (PCL) diol or low molecular

\*Correspondence to: G. Ciardelli, Department of Mechanics, Politecnico in Turin, Corso Duca degli Abruzzi, 24, Torino, Italy. E-mail: gianluca.ciardelli@polito.it

<sup>†</sup>8th International Symposium on Polymers for Advanced Technologies 2005 (PAT 2005), Budapest, 13–16 September, 2005, Part 1

weight tri-block PCL-PEG-PCL copolymers as soft segments in combination with an LDI and 1,4-cyclohexane dimethanol (CDM) or a (L-phenylalamine) diester (Phediester) as chain extender.

Polymer characterization was performed by differential scanning calorimetry (DSC) (Perkin–Elmer Pyris Diamond, scan rates of  $10^{\circ}\text{C min}^{-1}$ , temperature range from  $-80$  to  $+100^{\circ}\text{C min}^{-1}$ ), dynamic mechanical analysis (DMA) (Triton 2000 DMA, powder samples in Material Pockets, isochronal conditions, temperature range from  $-100$  and  $+60^{\circ}\text{C}$ , heating rate of  $5^{\circ}\text{C min}^{-1}$ ), attenuated total reflectance Fourier transform infrared (ATR-FT-IR) (Perkin–Elmer Spectrum One spectrometer, film samples), atomic force microscopy (AFM) (Autoprobe CP system Park Scientific Instruments PSI, contact mode, microlevers<sup>TM</sup> microfabricated from low-stress silicon nitride with a spring constant of  $0.01\text{ N m}^{-1}$ , and nominal radius of  $20\text{ nm}$ ). The adhesive forces between the phospholipid-coated  $\text{Si}_3\text{N}_4$  tip (radius values between  $40$  and  $70\text{ nm}$ ) and polymer samples were measured with the standard technique of force-distance curves in aqueous solution.

### *In vitro* and *in vivo* assays

The cytotoxicity experiments were performed culturing NIH-3T3 with culture medium (supplemented DMEM) obtained leaving a fixed quantity of PUs in contact with it for 4 hr, 24 hr, 48 hr, 7 days and 15 days respectively. The cells were fixed and stained at different times (4, 24 and 48 hr) in order to evaluate their vitality. Cytocompatibility tests were carried out using NIH-3T3 mouse fibroblasts. Film samples were seeded with a cell density of  $500,000\text{ cells ml}^{-1}$ , fixed with paraformaldehyde solution 4% in PBS and stained with Coomassie solution.

Three-dimensional scaffolds for tissue engineering were realized by the pressure activated microsyringe (PAM) technique developed at the University of Pisa. Line width of  $100\text{--}150\ \mu\text{m}$  was obtained with deposition pressure of 30 cbar and deposition speed of  $2500\ \mu\text{m sec}^{-1}$ . Selected structures and control films were implanted subcutaneously in Wistar rats. Constructs with surrounding soft tissue were removed and examined after 1, 3 and 6 months.

### Surface functionalization

PCL based PU films were modified by plasma induced graft polymerization of acrylic acid (AA). Polymer samples were first treated with Argon RF Plasma reactor (Plasma System Junior SN 001/072, Europlasma, 200 W, 60 sec), then exposed to the atmosphere to allow the formation of peroxides necessary for the subsequent copolymerization. Two different procedures were used for graft copolymerization: deposition of liquid monomer on activated films or exposition *in situ* to the monomer vapors. Albumin fluorescein isothiocyanate conjugate bovine, gelatin (type A) and poly-L-lysine were finally immobilized on polymer surfaces by carbodiimide coupling in aqueous solution (*N*-hydroxysuccinimide as activating agent). Functionalized surfaces were characterized by ATR-FT-IR, polarized optical microscopy (POM), scanning electron microscopy (SEM) and water contact angle (WCA) measurements. Topographic and

mechanical characterization images were collected using an AFM operating in contact mode.

### Bulk functionalization

The functionalization of PU with biologically active peptides was performed using the sequence of interest (for instance KGRGDG). The amino groups of Phe residue were used for the coupling to the polymer backbone; guanidino and acid functions were protected with Pbf and  $\text{O}^t\text{Bu}$  respectively. A peptide containing a spacer group consisting of a methylene sequence, was also prepared (KHexGRGDG).

Prepolymer synthesis was performed using PCL and LDI as previously indicated in this section. A solution of the peptide in anhydrous solvent was added dropwise to the prepolymer solution and the reaction was continued at room temperature for 18 hr. Polymer deprotection was performed using trifluoroacetic acid solution (25% in dichloromethane).

## RESULTS AND DISCUSSION

The experimental data concerning molecular weights and calorimetric analysis of the PUs are collected in Table 1. PU nomenclature is based on the nature of the constituent segments (C corresponds to CDM, Phe corresponds to Phe diester, L corresponds to LDI, C-1250 corresponds to PCL,  $M_n = 1250$ ). Tri-block copolymer nomenclature is based on the composition of the constituent blocks (CE650 indicates a copolymer containing a PEG segment with molecular weight 600 and a molar percentage of oxyethylene unit of 50%). PU average molecular weights decrease with increasing PEG content. It can be expected that hydrophilicity of PEG lead to the presence of traces of water in the reaction medium. Isocyanate moieties readily react with water, reducing the length of the polymer chain. The isocyanate reactivity with water respect to amines is much smaller than with primary hydroxyl groups, so Phe diester containing PU-ureas showed higher molecular weight than the analogous PUs.

The DSC data showed the changes occurring in thermal properties due to the connection of macrodiols with the hard segments (diisocyanate plus chain extender) to form PUs. The PU glass transition temperature ( $T_g$ ) values are higher than the  $T_g$  values of the starting macrodiols in all cases, indicating the presence of some mixing of hard segment in the soft segment phase.<sup>7</sup> No remarkable differences in chain

**Table 1.** Experimental data concerning PUs

Polymer	$[\eta]$ ( $\text{dl g}^{-1}$ )	$T_g$ ( $^{\circ}\text{C}$ )	$T_m$ ( $^{\circ}\text{C}$ )	$\Delta H$ ( $\text{J g}^{-1}$ )
CLC-1250	0.68	$-24.0$	37.5	53.8
PheLC-1250	0.79	$-20.2$	37.7	30.2
CLCE-635	0.43	$-41.5$	52.8	91.9
PheLCE-635	0.53	$-45.5$	51.2	52.6
CLCE-650	0.24	$-41.5$	53.0	90.2
PheLCE-650	0.29	$-41.6$	47.4	46.4
PCL diol 1250	n.d.	$-54.6$	53.4	72.6
PEG 600	n.d.	n.d.	21.4	130.7
CE 635	n.d.	$-67.0$	52.0	98.1
CE 650	n.d.	$-67.7$	47.5	83.8

n.d., not determined.



flexibility (restriction of molecular motion) influencing  $T_g$  were noted by changing CDM with the more bulky Phe diester chain extender. The DSC scan of PUs also revealed a broad endotherm peak varying from 37 and 53°C related to the melting of the PCL crystals in the soft segment. The melting temperature ( $T_m$ ) of PCL based PUs is about 16°C lower than that for PCL diol, due to the presence of less perfect crystals in the polymer compared to the PCL oligomer.<sup>8</sup> The effect of connectivity between the hard and soft segments in influencing crystallization emerged from melting enthalpies ( $\Delta H$  values) analysis; these values were calculated taking into account the weight fraction of PCL in the PUs. A significant reduction in crystallinity was observed for PCL based PUs, as previously suggested by the melting point.  $\Delta H$  data related to PCL-PEG-PCL based polymers also showed that links with hard segment, especially using Phe diester as chain extender, make the phase separation process and crystallization more difficult. No evidence of hard segment crystallization was detected.

Generally, cells on a soft substrate rapidly re-orient themselves upon contact with a stiff substrate, with the cell edge that contacts the stiff substrate becoming the new leading edge. The cell then transiently accelerates and migrates onto the stiff substrate. On the contrary, when cells on a stiff substrate contact a soft substrate, they change their direction to avoid the soft substrate and move parallel to it. PUs family represents a natural frame to study adaptation of cells to gradient of elasticity, because their typical interconnection of hard and soft domains (Fig. 1). This interconnection was examined making use of the modulation force tool for AFM. Moreover, this study demonstrates that lipid layer is able to recognize gradients of elasticity and adhesion.

The cellular analysis pointed out that all the PUs prepared were not cytotoxic and significant alterations in their morphology and apoptotic process were not observed. Adhesion test on these materials was also performed seeding the fibroblasts on the scaffolds and evaluating the surface cell density with an imaging software developed in Matlab. The data obtained showed good adhesion and there is no change in the cell morphology. (Fig. 2).

After the encouraging preliminary results obtained, the microfabricated structures were implanted subcutaneously in Wistar rats and after 1, 3 and 6 months were removed. A PU film was also implanted to evaluate the difference of

cellular integration between a microstructure with a well defined topology and porosity and a flat film. The histological analysis showed that the film and the microstructures did not produce an inflammatory response and in particular the microstructures after 3 months were completely integrated by the surrounding tissue and completely absorbed by it.

Surface modification of PU film samples was performed by plasma activation. The dependence of the peroxide formation on the glow discharge plasma power and time was determined by WCA measurements. Plasma activation does not lead to significant changes in film surface topography as emerged by AFM analysis. Grafting of AA was performed by vaporization of liquid monomer on activated films or exposition *in situ* to the monomer vapors. Thin AA layer was obtained (nanometric scale) in order to prevent delamination.

No remarkable monomer decarboxylation occurs by plasma deposition at power levels of 50–200 W, as confirmed by FT-IR analysis of the carboxyl group band (1715  $\text{cm}^{-1}$ ). The occurrence of the grafting reaction was confirmed by ATR analysis and microscopy techniques. Albumin, gelatin and poly(L-lysine) were finally immobilized on polymer surfaces using a water-soluble carbodiimide as coupling agent. Coupling reaction was confirmed by studying physico-chemical and morphological changes on film surfaces and performing topographic and mechanical characterization by AFM. Adhesion test with different cell lines (NIH-3T3 mouse fibroblasts and S5Y5 neuroblastoma) to check the different cell response on specific substrates are under investigation.

Covalent functionalization of PU systems with the peptides of interest was confirmed by UV analysis (absorption of Pbf group at 260 nm) before deprotection. Polymer characterization was performed as for unmodified PUs. Adhesion test using different cell lines are in progress to display the different behavior in promoting cell adhesion and proliferation of functionalized PUs with respect to the unmodified ones and to show the effect of the spacer in promoting cell response. In fact it can be expected that the presence of spacer allow the peptide to have increased conformational mobility enhancing the interactions of the substrate with the integrin receptors on the cell surface.

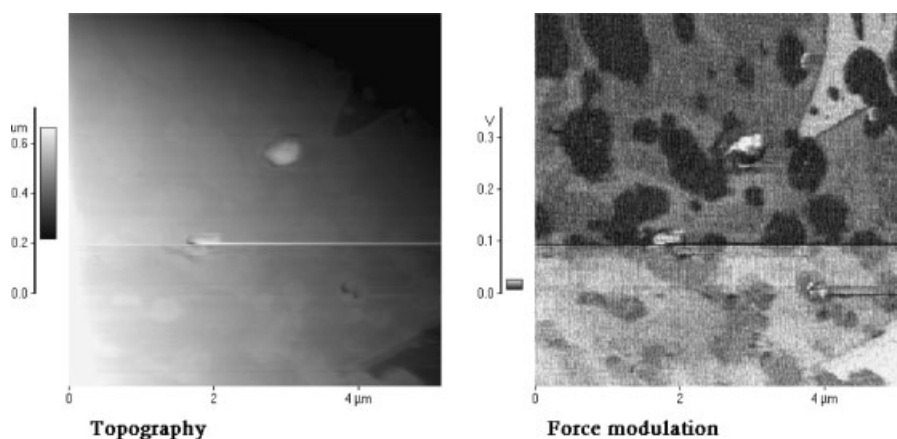
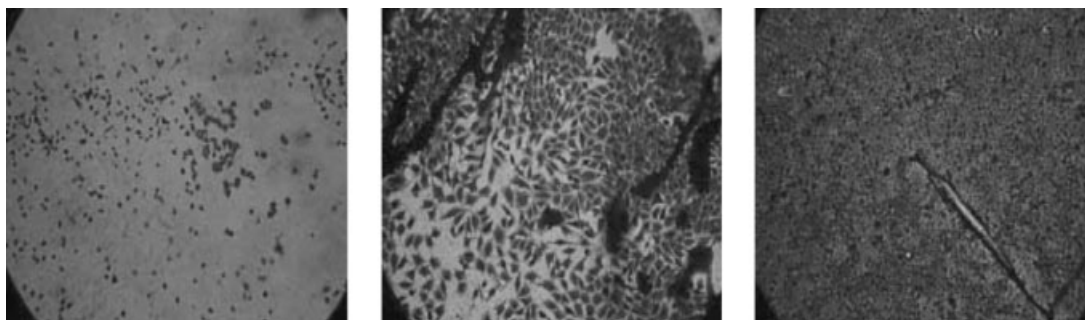


Figure 1. AFM and FMM images of a PU film sample.



**Figure 2.** NIH-3T3 mouse fibroblasts adhered on PU films at 4, 24 and 48 h after cell seeding.

## CONCLUSIONS

Biodegradable linear PUs were prepared and tested for applications in biomedical fields. Two different strategies were proposed in order to obtain synthetic biomaterials able to direct specific cell adhesion and proliferation mediated by biomolecular recognition.

## REFERENCES

1. Lambda NMK, Woodhouse KA, Cooper SL. *Polyurethanes in Biomedical Applications*. CRC Press: New York, 1998; 205–241.
2. Zdrahala RJ, Zdrahala IJ. *J. Biomater. Appl.* 1999; **14**: 67–90.
3. Guan J, Sacks MS, Beckman EJ, *et al.* *Biomaterials* 2005; **26**: 3961–3971.
4. Hersel U, Dahmen C, Kessler H. *Biomaterials* 2003; **24**: 4385–4415.
5. Poncin-Epaillard F, Legeay G. *J. Biomater. Sci. Polym. Edn* 2003; **14**(10): 1005–1028.
6. Ciardelli G, Rechichi A, Cerrai P, *et al.* *Macromol. Symp.* 2004; **218**: 261–271.
7. Van Bogart JWC, Lilaonitkul A, Cooper SL. *J. Macromol. Sci. Phys. B* 1980; **17**(2): 267–301.
8. Bogdanov B, Toncheva V, Schacht E, *et al.* *Polymer* 1999; **40**: 3171–3182.

## *APPENDIX C*

We report here the data of NMR analysis and Structure Calculations for some analogues of PTH(1-11).

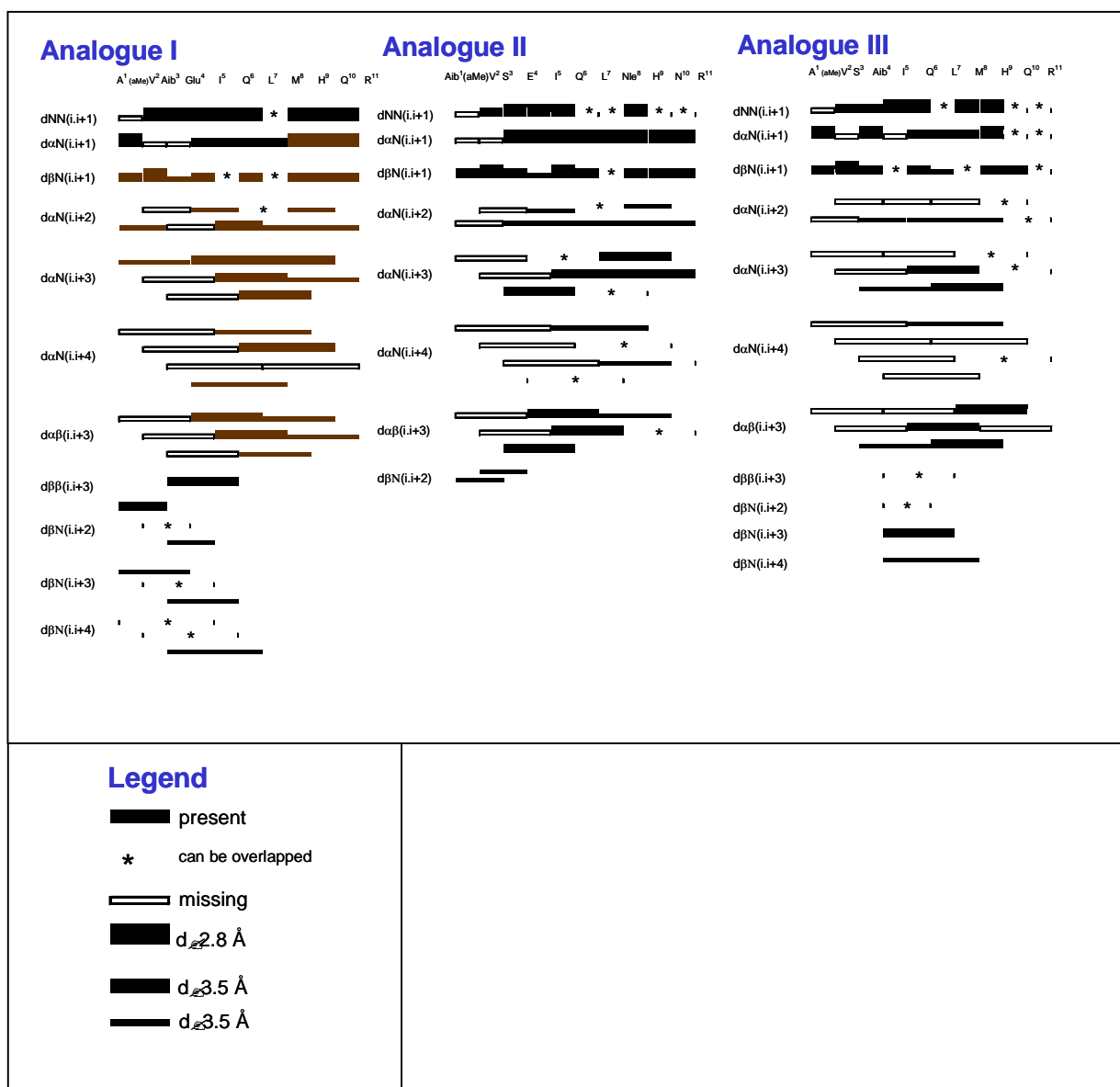
We can't report all analysis for all analogues synthesized because some work is still in progress. The data reported in this appendix are relative to PTH(1-11) analogues containing C<sup>α</sup>-tetra-substituted amino acids and peptidomimetic.

This part of the thesis is due to the hard work and effective collaboration with Dr Nereo Fiori.

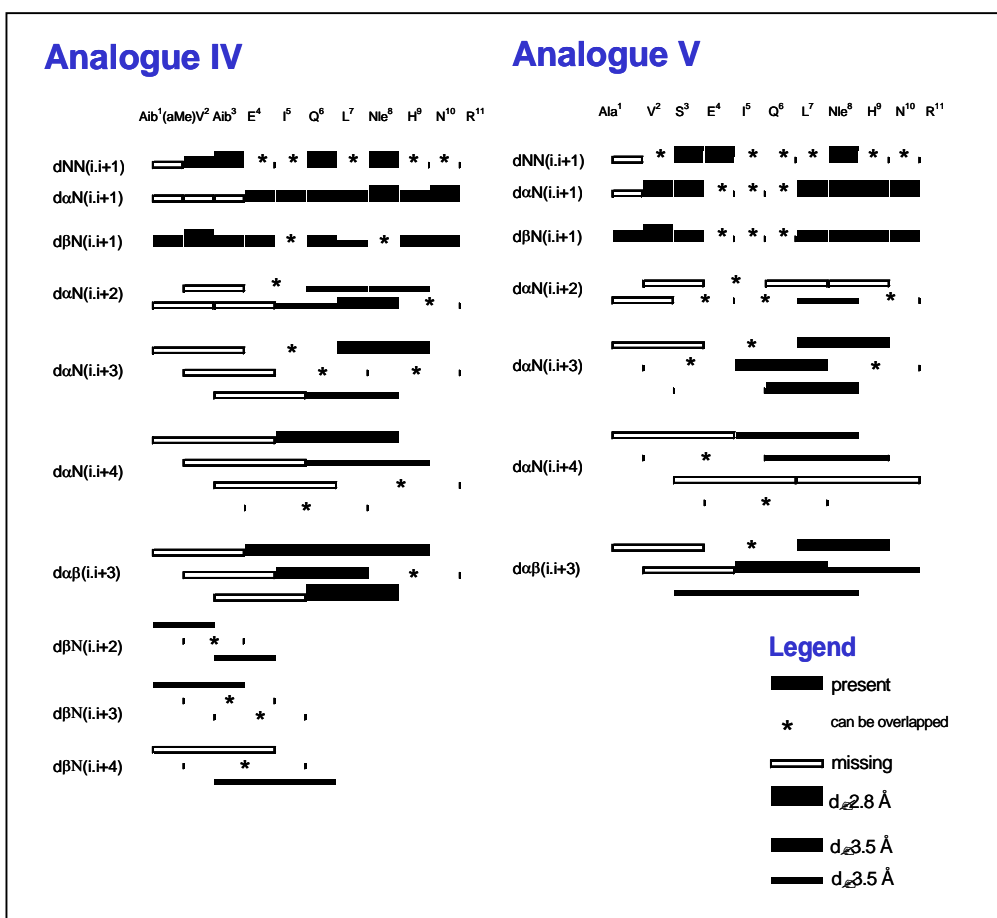
**C.1 PTH(1-11) analogues containing C<sup>α</sup>-tetra-substituted amino acids -  
αMeVal**

**Summary of ROESY connectivities of analogues I –V**

Name	Peptide Sequence
I	Ala-αMeVal-Aib-Glu-Ile-Gln-Leu-Nle-His-Gln-Arg-NH <sub>2</sub>
II	Aib-αMeVal-Ser-Glu-Ile-Gln-Leu-Nle-His-Gln-Arg-NH <sub>2</sub>
III	Ala-αMeVal-Ser-Aib-Ile-Gln-Leu-Nle-His-Gln-Arg-NH <sub>2</sub>
IV	Aib-αMeVal-Aib-Glu-Ile-Gln-Leu-Nle-His-Gln-Arg-NH <sub>2</sub>
V	Aib-Val-Aib-Glu-Ile-Gln-Leu-Nle-His-Gln-Arg-NH <sub>2</sub>





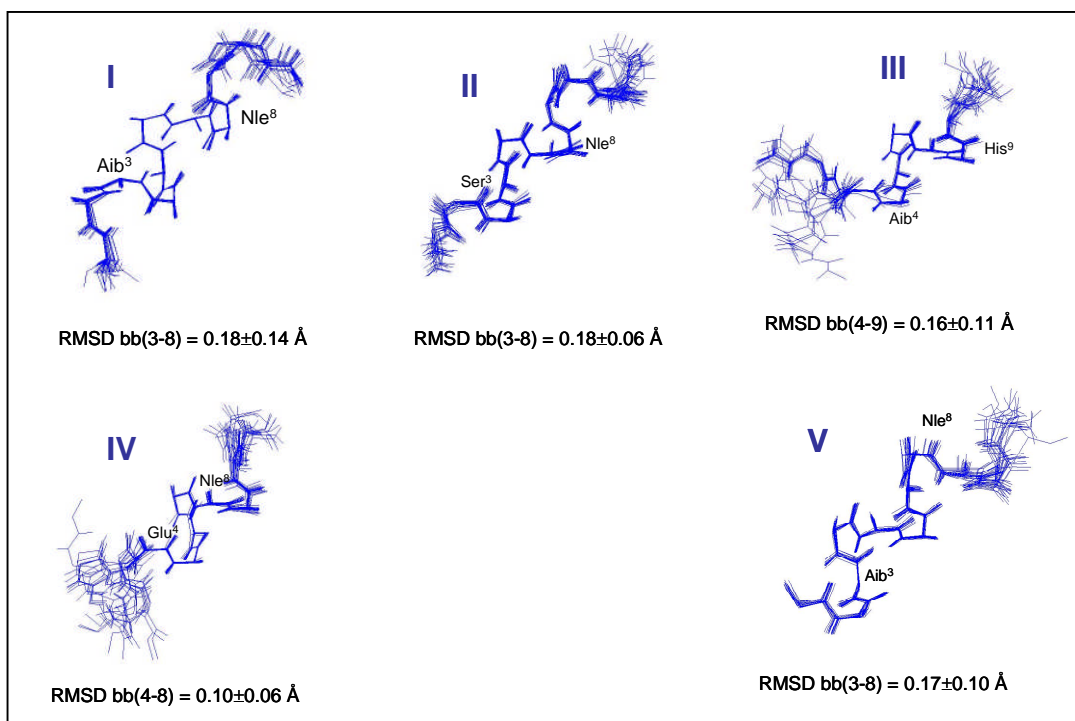


## Structure Calculations

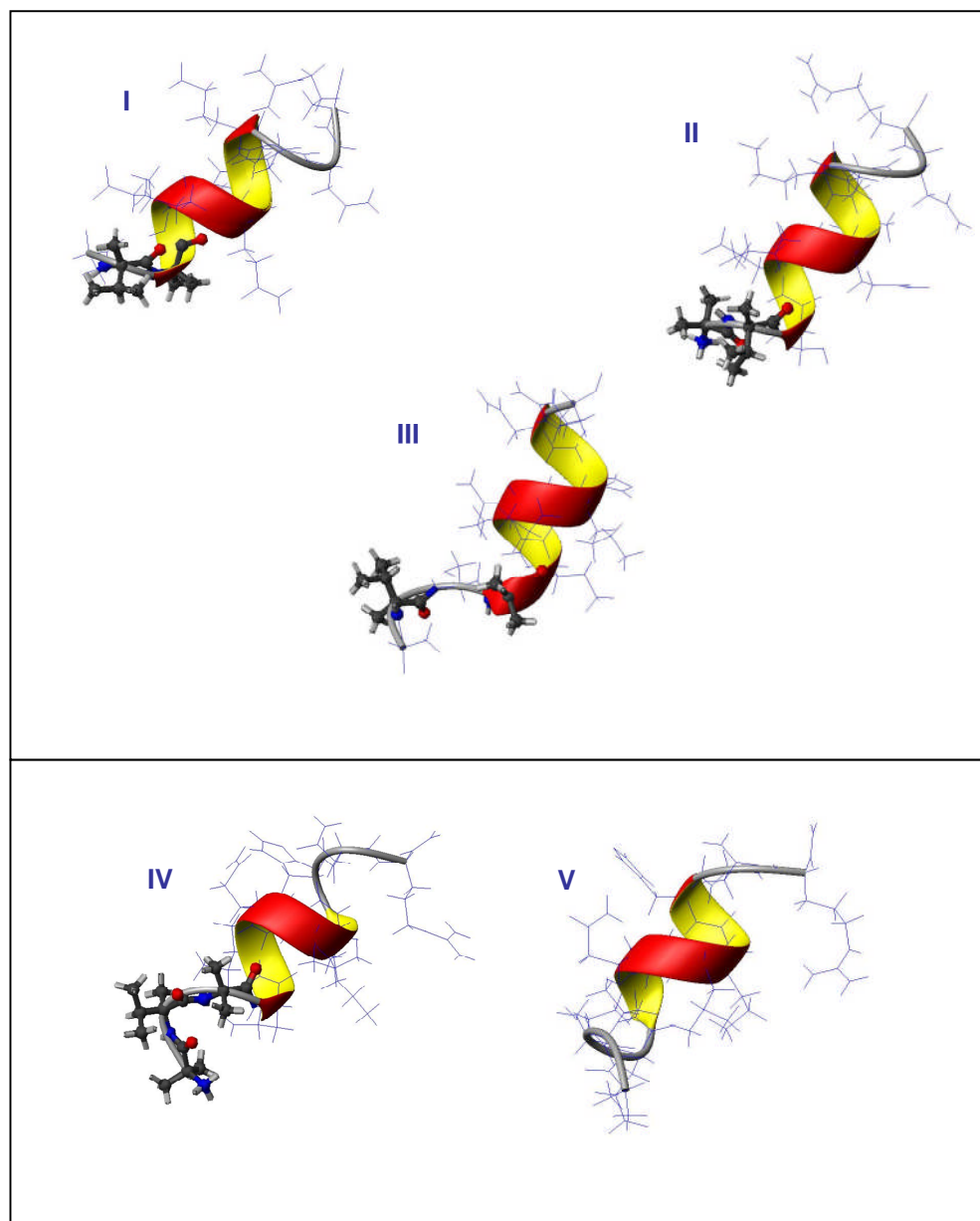
Interproton distances were experimentally determined by integration of ROESY cross peaks. Using these restraints, 150 structures were generated from simulated annealing MD calculations using the program XPLOR: 20 structures were chosen which fulfill the experimental restraints with violations lower than 0.5 Å and have the lowest energy values. *NMR Distance Restraints, Deviations from Idealized Geometry and Mean Energies for the NMR-based Structures after SA were refined with XPLOR.*

	Analogue I	Analogue II	Analogue III	Analogue IV	Analogue V
<b>Experimental NMR constraints</b>					
<i>Intraresidue</i> ( $i - j = 0$ )	32	47	40	34	37
<i>Sequential</i> ( $ i - j  = 1$ )	31	28	25	26	21
<i>Middle range</i> ( $2 \leq  i - j  \leq 4$ )	29	23	21	25	19
<i>Total</i>	87	98	86	85	77
<b>(RMSD) from experimental constraints (Å)</b>					
<i>distance</i>	$0.11 \pm 0.02$	$0.159 \pm 0.007$	$0.118 \pm 0.003$	$0.092 \pm 0.005$	$0.126 \pm 0.004$
<b>Atomic (RMSD) (Å)</b>					
<i>Backbone</i> (1-11)	$0.6 \pm 0.4$	$0.37 \pm 0.12$	$1.4 \pm 0.8$	$1.2 \pm 0.5$	$1.0 \pm 0.4$
<i>Heavy atoms</i> (1-11)	$1.5 \pm 0.5$	$1.3 \pm 0.2$	$2.4 \pm 0.8$	$2.1 \pm 0.5$	$1.9 \pm 0.5$
<b>Mean Energy (Kcal/mol)</b>					
$\bar{E}_{tot}$	$81 \pm 20$	$198 \pm 17$	$97 \pm 3$	$74 \pm 5$	$99 \pm 7$
$\bar{E}_{bonds}$	$4.0 \pm 1.4$	$13.7 \pm 1.1$	$6.1 \pm 1.0$	$3.9 \pm 0.3$	$7.6 \pm 0.6$
$\bar{E}_{angles}$	$19.7 \pm 1.0$	$44 \pm 4$	$24 \pm 2$	$27.8 \pm 1.5$	$24 \pm 3$
$\bar{E}_{NOE}$	$54 \pm 20$	$123 \pm 11$	$60 \pm 3$	$36 \pm 4$	$61 \pm 4$

Superimpositions of the ensembles of the lowest energy calculated structures of Analogues I-V.



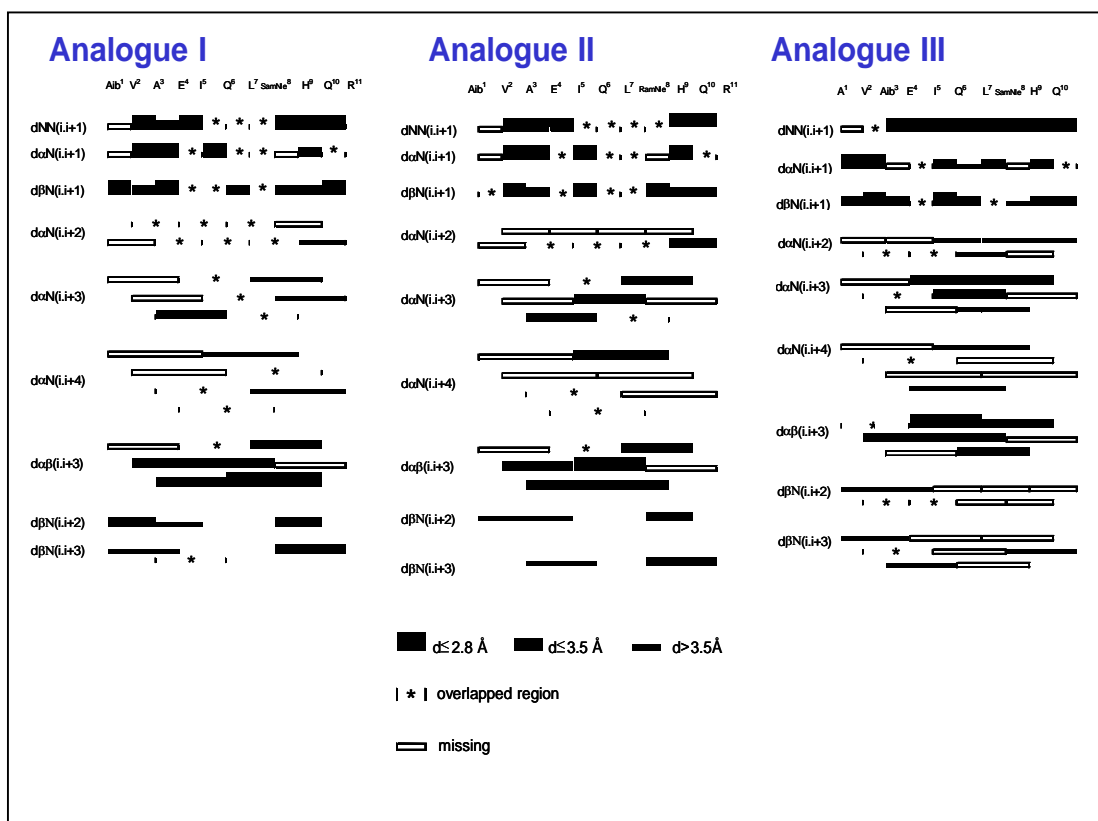
Schematic representation of one of the lowest energy structures of Analogues I-V

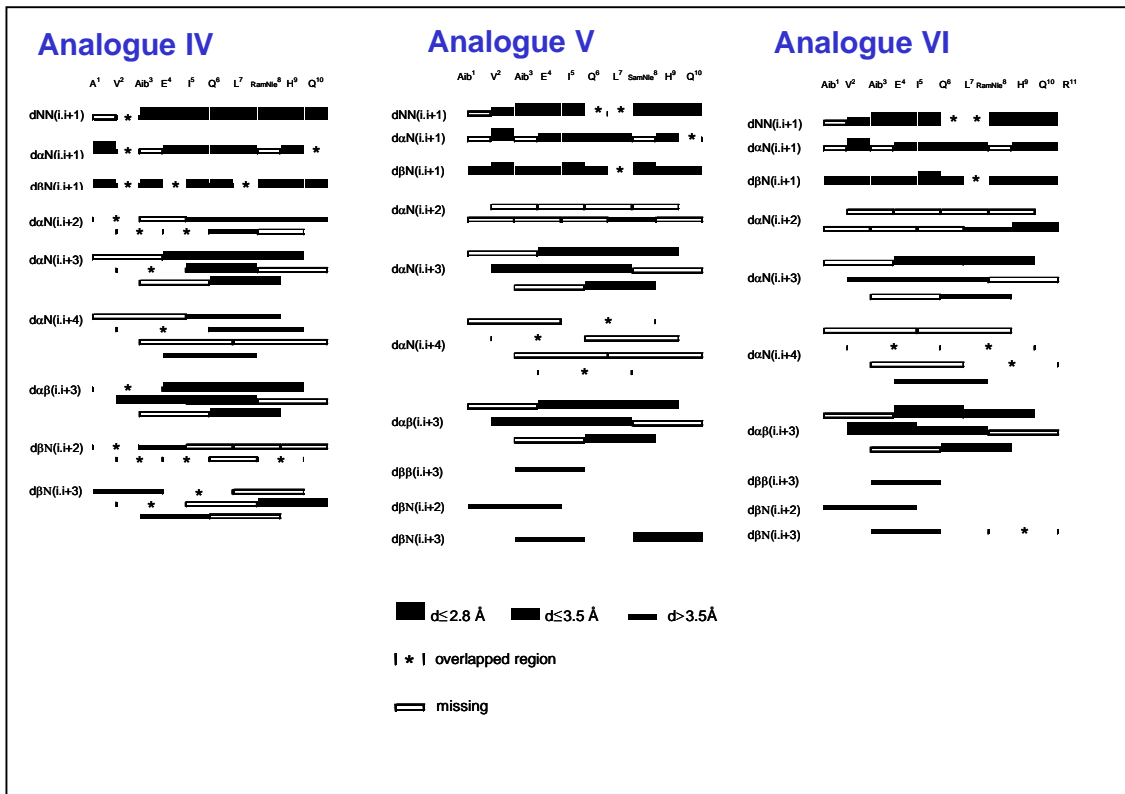


## C.2 PTH(1-11) analogues containing C<sup>α</sup>-tetra-substituted amino acids - αMeNle

### Summary of ROESY connectivities of analogues I – VI

Name	Peptide sequence
I	Aib-Val-Ala-Glu-Ile-Gln-Leu-L( <b>αMe</b> )Nle-His-Gln-Arg-NH <sub>2</sub>
II	Aib-Val-Ala-Glu-Ile-Gln-Leu-D( <b>αMe</b> )Nle-His-Gln-Arg-NH <sub>2</sub>
III	Ala-Val-Aib-Glu-Ile-Gln-Leu-L( <b>αMe</b> )Nle-His-Gln-Arg-NH <sub>2</sub>
IV	Ala-Val-Aib-Glu-Ile-Gln-Leu-D( <b>αMe</b> )Nle-His-Gln-Arg-NH <sub>2</sub>
V	Aib-Val-Aib-Glu-Ile-Gln-Leu-L( <b>αMe</b> )Nle-His-Gln-Arg-NH <sub>2</sub>
VI	Aib-Val-Aib-Glu-Ile-Gln-Leu-D( <b>αMe</b> )Nle-His-Gln-Arg-NH <sub>2</sub>

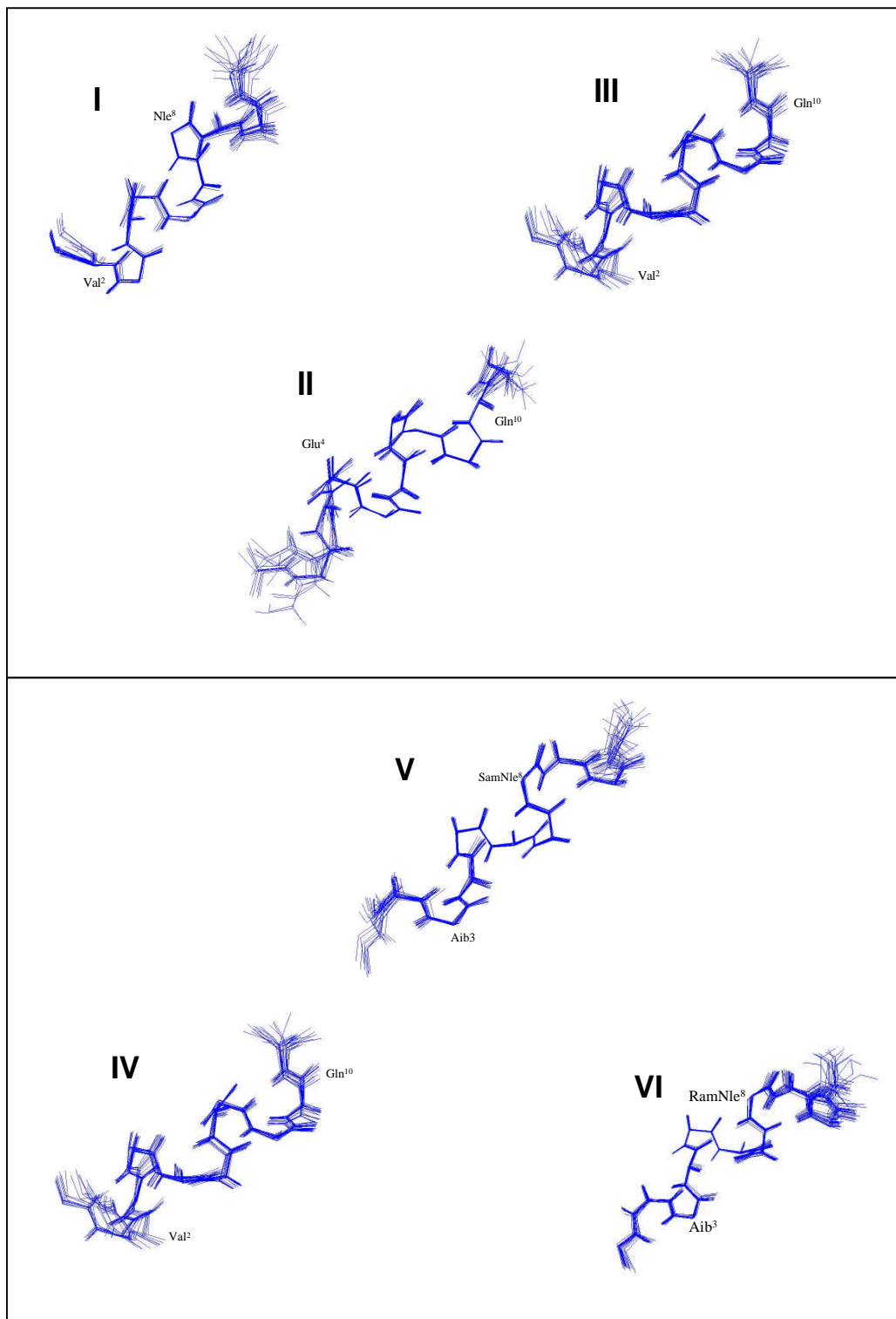




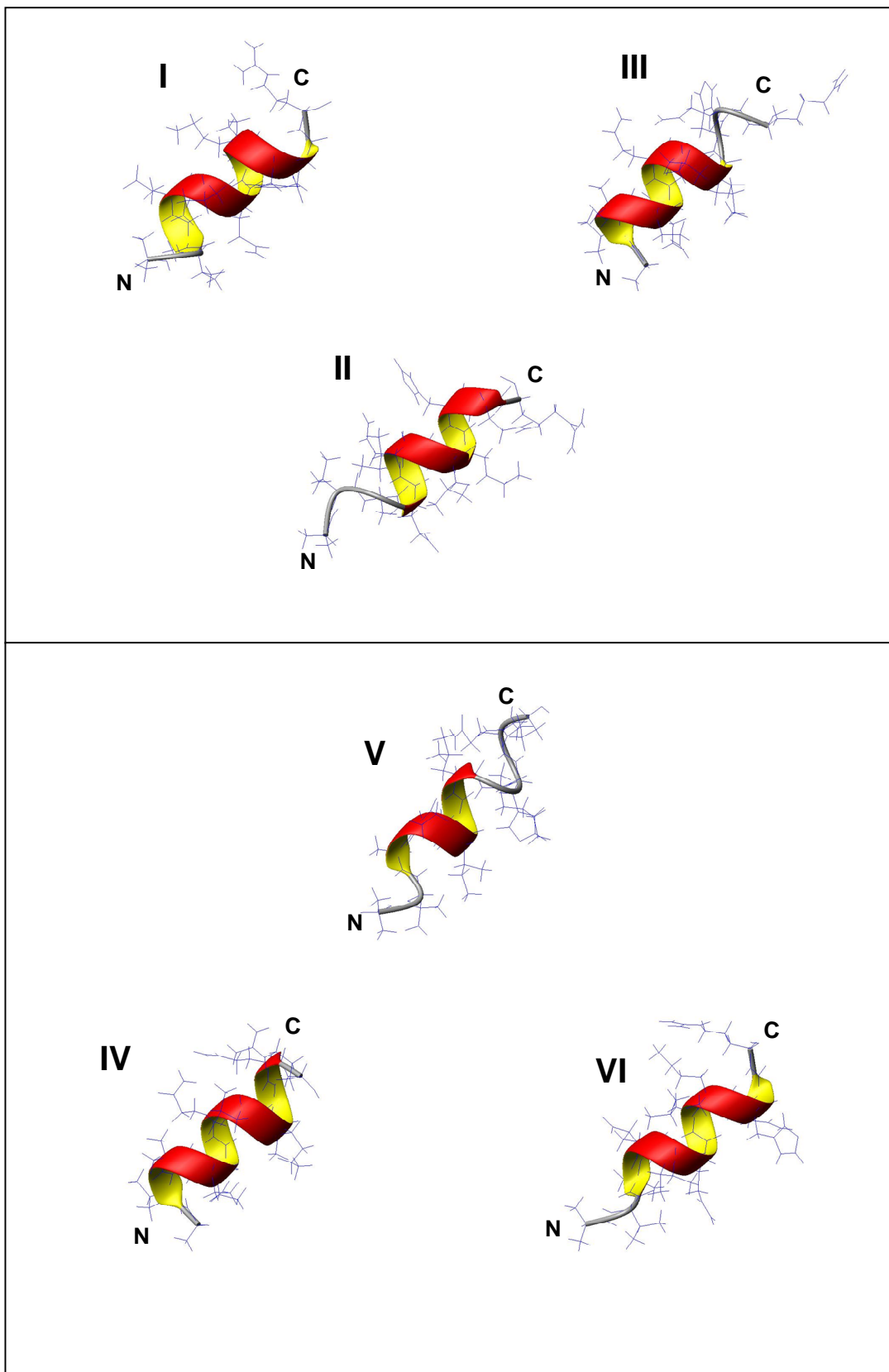
## Structure Calculations

	Analyse I	Analyse II	Analyse III	Analyse IV	Analyse V	Analyse VI
<b>Experimental NMR Constraints</b>						
<i>Intraresidue (i - j = 0)</i>	39	44	38	38	41	38
<i>Sequential ( i - j  = 1)</i>	19	23	26	25	24	28
<i>Middle Range (2 ≤  i - j  ≤ 4)</i>	19	19	28	26	17	24
<i>Total</i>	77	86	92	89	82	90
<b>(RMSD) from Experimental Constraints (Å)</b>						
<i>Distance</i>	0.099 ± 0.006	0.144 ± 0.003	0.117 ± 0.003	0.816 ± 0.002	0.829 ± 0.002	0.107 ± 0.002
<b>Atomic (RMSD) (Å)</b>						
<i>Backbone (1-11)</i>	0.7 ± 0.3	0.7 ± 0.3	0.41 ± 0.15	0.6 ± 0.3	0.6 ± 0.4	0.35 ± 0.15
<i>Heavy atoms (1-11)</i>	1.4 ± 0.3	1.5 ± 0.3	1.7 ± 0.4	1.4 ± 0.3	1.3 ± 0.2	1.4 ± 0.5
<b>Mean Energy (Kcal/mol)</b>						
<i>E<sub>tot</sub></i>	75 ± 7	139.8 ± 1.4	119 ± 4	69 ± 2	57 ± 2	93 ± 2
<i>E<sub>backb</sub></i>	4.1 ± 0.5	8.06 ± 0.15	4.8 ± 0.4	3.4 ± 0.2	3.9 ± 0.3	6.0 ± 0.2
<i>E<sub>angles</sub></i>	25 ± 2	32.9 ± 1.3	36.9 ± 1.6	26.0 ± 1.1	22.3 ± 0.8	27.5 ± 0.6
<i>E<sub>NDS</sub></i>	38 ± 5	89 ± 3	63 ± 3	30 ± 2	28.2 ± 1.4	51.7 ± 1.5

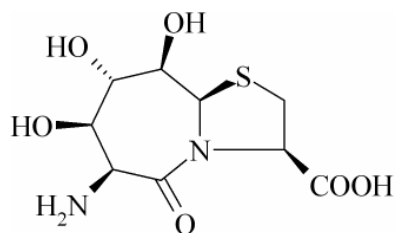
Superimpositions of the ensembles of the lowest energy calculated structures of Analogues I-VI



Schematic representation of one of the lowest energy structures of Analogues I-VI

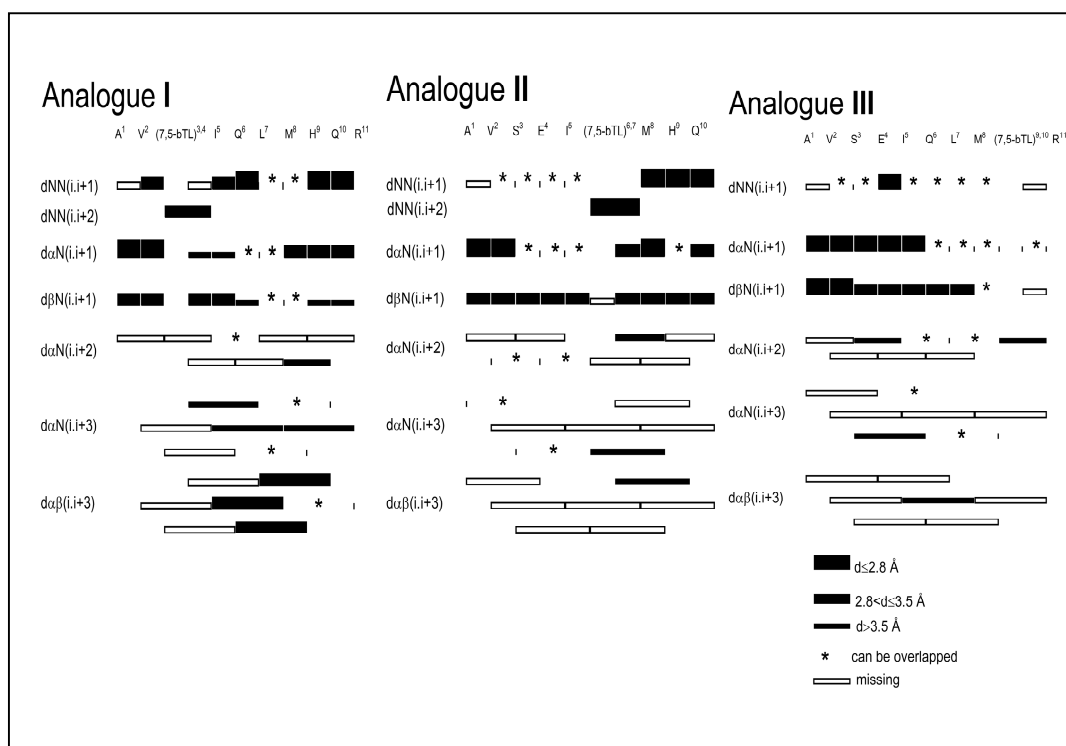


### C.3 PTH(1-11) analogues containing peptidomimetic – 7; 5 bTI



#### Summary of ROESY connectivities of analogues I – III

Name	Peptide sequence
I	[Ala <sup>1</sup> ,7,5-bTL <sup>3,4</sup> ,Nle <sup>8</sup> ,Arg <sup>11</sup> ]PTH(1-11)NH <sub>2</sub>
II	[Ala <sup>1</sup> ,7,5-bTL <sup>6,7</sup> ,Nle <sup>8</sup> ,Arg <sup>11</sup> ]PTH(1-11)NH <sub>2</sub>
III	[Ala <sup>1</sup> ,Nle <sup>8</sup> ,7,5-bTL <sup>9,10</sup> ,Arg <sup>11</sup> ]PTH(1-11)NH <sub>2</sub>

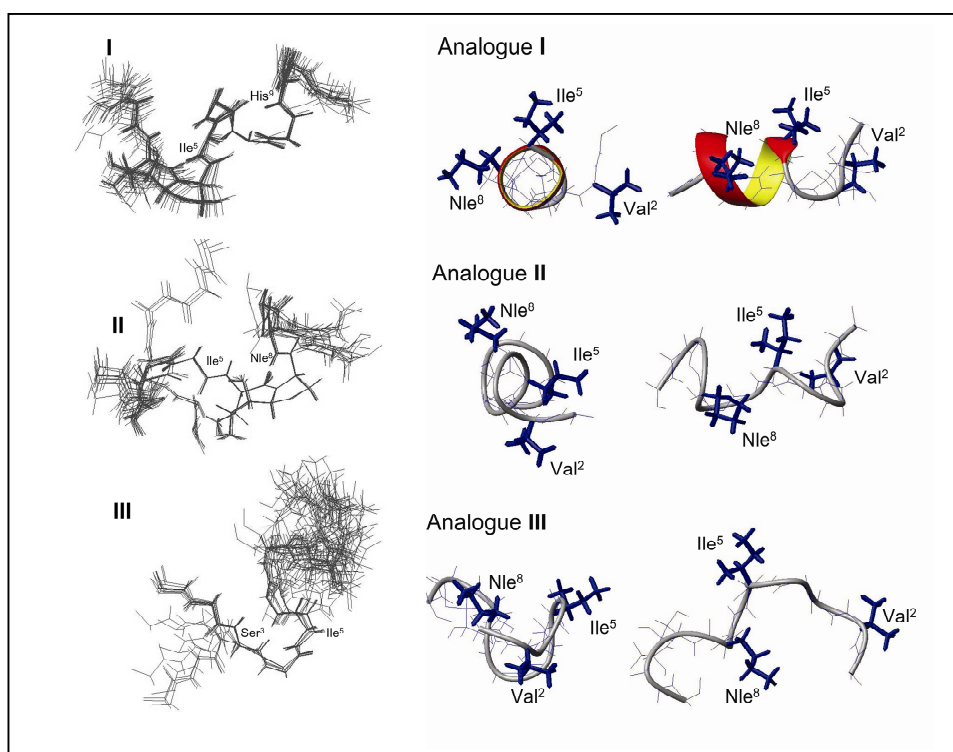




## Structural calculations

	Analogue I	Analogue II	Analogue III
<b>Experimental NMR constraints</b>			
<i>Intraresidue</i> ( $i - j = 0$ )	45	46	34
<i>Sequential</i> ( $ i - j  = 1$ )	32	20	20
<i>Middle Range</i> ( $2 \leq  i - j  \leq 4$ )	16	11	9
<i>Total</i>	95	77	63
<b>&lt;RMSD&gt; from experimental constraints (Å)</b>			
<i>distance</i>	0.088±0.010	0.116±0.002	0.116±0.004
<b>Atomic &lt;RMSD&gt; (Å)</b>			
<i>Backbone</i> (1-11)	0.7±0.3	2.0±1.1	1.4±0.6
<i>Heavy atoms</i> (1-11)	1.4±0.4	3.2±1.2	2.7±0.9
<b>Mean Energy (Kcal/mol)</b>			
$E_{tot}$	72±10	95±3	83±3
$E_{bonds}$	3.3±0.4	6.0±0.3	4.4±0.4
$E_{angles}$	25.5±1.1	27.9±1.3	28±2
$E_{NOE}$	37±8	51.3±1.7	43±3

Superimpositions of the ensembles of the lowest energy calculated structures and schematic representation of one of the lowest energy structures for Analogues I-III





## RINGRAZIAMENTI

Arrivati al termine di questa tormentata vicenda che è stato il mio dottorato sono doverosi una serie lunga di ringraziamenti.

Il primo grande grazie va al Prof. Evaristo Peggion, mio mentore e supervisore, che fin da subito ha creduto, sostenuto, incitato ed incoraggiato il sottoscritto in questo lavoro e nella mia attività di ricerca, dimostrandomi incondizionata fiducia e lasciandomi una rara libertà sia nella linea di ricerca sia nello sviluppare tutta una serie di filoni di attività parallele. Lo ringrazio ancora delle occasioni concessemi nel corso di questi "quattro anni" di dottorato, dalla partecipazione a congressi internazionali, alla possibilità di allacciare relazioni con altri docenti e gruppi di ricerca.

Il secondo grazie va al mio gruppo di ricerca, che mi ha sopportato e sostenuto: grazie perciò a Betty ed a Stefano.

Un secondo grazie va anche ai compagni di avventure: ancora presenti, Lisa e Lorenzo (tenete duro.....) e agli assenti (si spera per non molto!) Michele a cui va un grazie speciale per l'amicizia critica, sincera ed intellettualmente onesta che ci lega, e a Massimo, al "Divus Maximus" dimostratosi spesso persona di rara sensibilità.

Un sentito ed affettuoso grazie va a Barbara, collega di sintesi in fase solida ma soprattutto confidente, amica e compagna dei miei momenti sì e no (forse quest'ultimi un po' più frequenti!).

Ringraziamenti per tutte le chiacchierate chimiche e non, vanno a Fernando, Ale ed a Cristina.

Non dimentico di ringraziare i miei due prof. a cui sono ancora legato da profonda stima, la Prof.ssa Laura Biondi e il Prof. Fernando Filira. Infine voglio ringraziare ancora la Prof. Marina Gobbo e il Prof. Franco Marcuzzi, che, comunque, mi sono stati vicini in tutti questi anni e, "Last but not least", il prof. Claudio Toniolo che mi ha un po' adottato nel suo gruppo!

Un altro grazie per tutte le fatiche NMR a cui l'ho sottoposta va a Ile.

Non posso dimenticare i miei tre gruppi adottivi per antonomasia:

Il gruppo del Prof. G. Bandoli nelle persone di F. Tisato e soprattutto in Cristina Bolzati, amica e confidente.

Il gruppo dislocato del Prof. G. Ciardelli (GL!) che mi ha introdotto in un mondo nuovo della chimica, i polimeri, ed ad Alf e Susy, amiche e colleghe di "sventura RGD".

Meinem deutsche Forschungsgruppe bei Chiara Cabrale, che ancora ringrazio per avermi concesso di lavorare da lei, per l'aiuto "amministrativo" e per avermi "regalato" 8 mesi stipendi.

E dopo aver ringraziato i miei compagni di lavoro un pensiero va agli amici lontani: Pino (:)), Fabio, Beppe e Franz con cui ho condiviso uno dei periodi più belli della mia vita ed a cui mi lega una amicizia ancora giovane ma sentita e profonda (si spera)!

Un grazie affettuoso va ad Elena, l'amica di sempre, la confidente e la persona sempre presente nella mia vita, sostenitrice a latere di questa mia avventura.

Ed infine a tutti gli altri: Emi, Chiara, Franco, Alessio, Marta, Laura, Maksym, Damir, Louai, Laura, Ming Hong... E tutte le persone che inevitabilmente sto dimenticando.

A Onorio che se ancora adesso mi diverto a studiare lo devo un po' anche a lui.

Infine, come dice sempre il prof. Peggion, l'unico vero grazie va ai miei genitori, Ube e Rocco, che mi hanno sostenuto finanziariamente, moralmente e spiritualmente, nonostante le difficoltà e i problemi che in questi anni si sono avvicinati. Come sempre questi lavori sono monumenti alla abnegazione e al sacrificio delle famiglie, ancora grazie per tutto l'affetto e la fiducia che mi avete accordato e mi accordate anche in scelte impopolari o non remunerative.

Un pensiero affettuoso per il sostegno morale e la stima a Rosanna e Raffaele.

Infine un ultimo pensiero a chi non c'è più per gioire: Licia Scialpi Collavini.

